I wish to acknowledge the paper by Dr. I. ASIMOV, entitled 'THE ENDOCHRONIC PROPERTIES OF RESUBLIMATED THIOTIMOLINE: which has proved a source of inspiration throughout my work.

ON-LINE MEASUREMENT OF RANDOM WAVEFORMS: WITH PARTICULAR REFERENCE TO NATURAL CHARGE TRANSPORT IN n-HEXANE.

C.J.BUFFAM

Thesis presented for the degree of
Doctor of Philosophy
of the City University, London.

December 1976

ABSTRACT

The descriptions of the author's studies in this Thesis relate to the design and realization of a new instrument and its application to some specific measurements on the behaviour of natural particles in the dielectric liquid n-hexane.

Connection of a Biomation 8100 transient recorder to an on-line laboratory computer has provided a solution to the problems associated with capturing, storing and processing large numbers of waveforms of random origin. The novel application of a waveform recognition system has meant that the captured transients can be sorted into groups defined by the presence or absence of declared features in the waveshape.

The instrument formed by the union of the transient recorder and the computer has enabled a unique series of measurements to be undertaken. Confirmation of the findings of earlier workers relating to the potential of a natural impurity particle in the dielectric liquid came from the present author's initial measurements. In later experiments the motion of natural particles was monitored with the aid of a photomultiplier, and the first completely objective proof that natural particles in the liquid individually transferred charges in the order of a few femto Coulombs was established. Subsequently, measurements were carried out on the apparent dwell time of particles at an electrode.

An off-line study of the large pico Coulomb charge pulses has been performed and results are reported.

The on-line transient recorder has proved effective in solving

measurement problems arising in other fields where randomly occurring events need to be captured and processed. The measurements pertaining to the propagation of cracks in metal specimens is just one example of such measurements successfully performed.

CONTENTS

CONTENTS

LIST OF PRINCIPAL SYMBOLS

List of Principal symbols

d	minimum distance between electrodes
e	charge on an electron
E	electric stress
ε_o	permittivity of free space
ε_p	relative permittivity of particle
∇	Gradient (Grad)
i	current
η	viscosity
q	charge on particle (classical value)
q'	particle charge (limited value)
r	particle radius
R	electrode radius
S	particle density
t	time
T	particle transit time
$U[t-T]$	Unit step function at time T
μ	mobility
V	voltage across electrodes
V_o	particle potential
ω	angular frequency

SECTION 1

Introduction.

1.1 General Introduction

The measurement of transient phenomena was until the advent of the digital transient recorder to a large extent impossible. This is particularly true in the field of liquid dielectrics which has been, for a number of years, a subject of research in the Department of Electrical and Electronic Engineering at the City University.

The aim of the research into liquid dielectrics is to increase the understanding of the mechanisms of conduction and breakdown. The liquid state is probably the least known state of matter and has, in the past, necessitated the development of complex measurement tools; many of which have found applications in other areas of research.

The liquid studied by past workers in the author's group was the 'puriss' grade of n-hexane which contains a minimum of 99% pure n-hexane on arrival from the manufacturers. This liquid is one of the main constituents of transformer oil and is studied in the hope that understanding the effects in the pure liquid will throw some light on the processes in the oil used in industry. Thus to enable comparisons with the results of earlier workers this grade of n-hexane was studied by the author.

The present study follows on from the work of Rhodes (see Section 7) who performed measurements with the aid of a pulse height analyser that he had interfaced to a Ferranti FM1600B computer. The results from some of Rhodes' experiments indicated that a method of capturing and storing a large number of charge transients would allow a more detailed study of the charge transfer process to be made. Thus for this purpose a high speed digital transient recorder (Biomation 8100) was obtained with a Science

Research Council award.

This recorder is capable of capturing and retaining the section of a signal that occurs prior to the event which triggers it. The transient recorder is on its own a very powerful device. However, in conjunction with an on-line laboratory computer, such as the FM1600B, it becomes one of the most powerful aids to signal processing available at the time of writing. A complete philosophy regarding the transient recorder and its link to the computer, together with a basic waveform recognition system has been built up to cater for the study of transient events.

The computer used in the author's laboratory was provided by the University on the basis that its services would be available to other departments. The present author has performed several studies for other research groups in the University and some of these are given in Section 12 of this Thesis.

The reason for this Thesis possessing a dimerous structure is due to the nature of the research performed. The digital electronics, computer programming and pattern recognition techniques are, as subjects, far removed from the study of charge conveyance in dielectric liquids. Therefore Part I of this Thesis is confined to the author's measurement system whilst Part II contains details of the experiments performed, and the results obtained, with the aid of the on-line transient recorder. Although both Parts I and II contain a review section, a discussion and a theory section, the conclusions drawn from the present study are confined to Section 14. The appendices of this Thesis describe in detail the circuits and programs used in the on-line transient recorder system.

1.1

Throughout this Thesis waveforms plotted by the computer have been reproduced with a standard software package. This package generates a standard set of X and Y axes for all graphs and these are numbers for 0 to 10. The waveforms depicted are normalized within these limits. It is thus necessary on most of the graphs to include a calibration marker. It is this marker that defines the magnitude of the specified scale. On several waveforms no calibration is shown (see Section 5) as the waveforms are normalized and are dealt with only in relation to shape and not magnitude.

In several sections of this Thesis some words are used in quotes (i.e. 'intelligent' and 'knowledge'). This implies that the word in quotes is being used to convey an idea and is not employed in its strict form. The author is well aware that the 'intelligent' transient recorder is not intelligent!

Finally, the method chosen to reference other published material must be described. The technique reduces the title of a paper, or book, and the authors name to a group of mnemonics which are enclosed in square brackets thus:- [...]. Each reference may comprise two or three groups of letters. The last group refers to the name of the author, and the group or groups preceding relate to the title of the work. As an example the paper by Cookson and Wootton entitled, 'Particle Movement and Gas Breakdown in High Pressure Nitrogen and Sulphur Hexafluride' is referred to simply as [Part Gas Cook]. In Section 16 a list of authors together with the source of publication is given. The list is in alphabetical order with respect to the last group of letters in the brackets (i.e. the authors name). In the case of equipment manuals the name of the author is omitted.

1.1

Thus the service and instruction manual of the Biomation 8100 transient recorder is referred to as [Bio Man]. This is listed alphabetically as Man Bio. Some of the mnemonics are used repeatedly, such as 'Bd' for Breakdown, 'LD' for Liquid Dielectrics, 'To' for Transformer oil and 'Part' for Particle. A list of these commonly used mnemonics is also given in Section 16. This form of system is reported to be more convenient to both reader and author (see [Ref Ok]).

PART I

A Contribution to Random Waveform Measurement Techniques.

SECTION 2

Introduction. I.

2.1 Introduction to Part I

Part I of this Thesis contains details of the measurement techniques developed by the present author to analyse transient phenomena. A review of the field of transient recording is given followed by details of the author's approach to this problem. Technical details including circuit and waveform timing diagrams are presented together with the user's guide to the on-line transient recorder in Section 17. An outline of the system can be found in Section 4 in the form of a paper presented at the Conference entitled 'On-line Computers in Laboratory Use'.

During the course of a series of experiments prior to the 5th International Conference on Conduction and Breakdown in Dielectric Liquids it became apparent to the author that just to capture and store the transients (in the case of the femto Coulomb pulses of charge) was not sufficient. Too many of the captured transients were caused by phenomena other than the one of interest. For this reason a basic waveform classification system was implemented. This is described in Section 5, together with a brief explanation of the basic theories relating to pattern recognition.

To create an efficient software/hardware interface for an instrument such as the Biomation 8100 the designer must appreciate the constraints imposed at the various levels. This is important when considering the problems of the operating speed of the system, and the length of the controlling program. Great care has been taken to ensure flexibility within the computer system where ever possible. Liaison with member of Messrs. Ferranti Limited, throughout the present study, has enabled a new operating system to be commissioned. This system permitted the author to design and

implement the disc filing programs necessary for the management of captured waveforms.

The applications of the on-line transient recorder are described in Part II of this Thesis. In Section 10 the present author's own applications are described and Section 12 gives the use of the transient recorder in other fields. Some of the signal processing laws that must be understood when working with sampled signals are outlined in Section 8.

SECTION 3

Review.I.

3.1 Introduction

Transient recorders of the type used in this study had been available for some eight years at the commencement of this research and several papers have since been published regarding the connection of such devices to computer systems of varying complexity. These papers are reviewed in this section, and in the following section particular features described will be discussed in relation to the author's system.

Several papers relating to pattern recognition and its applications in waveform classification and feature extraction are reported at the end of this section.

3.2 The Structure of Transient Recorders

Although the digital version of the transient recorder is a relatively modern device it has a mechanical predecessor which is capable of monitoring pretrigger information and is still in use in the electrical supply industry for recording mains transients. The device called a disturbance recorder consists of a rotating cylindrical drum which is constantly being sprayed with ink. Situated just in front of the sprayer (in relation to the rotation of the drum) is a scribing nib which engraves the signal in the ink. Thus at any instant the drum carries a representation of the signal recorded during the immediately preceding revolution. Fresh ink is sprayed over the old recording just before the drum passes under the scriber (another version uses ink pens with a wiper to remove the ink). If the drum rotates 10 times in one second then the last 5 complete cycles of the 50 Hz signal will be stored on the drum. When a

3.2

mains transient occurs (e.g. a spike or lost half cycle) the recorder is 'triggered'. This causes the front of a roll of paper to be pressed against the drum just behind the ink sprayer. A copy of the information stored on the drum is now printed on the paper as both the drum and paper continue to rotate. The device will continue to record until it is reset. The paper will contain almost all of the information stored on the drum at the instant when the trigger event occurred and as much post trigger information as required. The disturbance recorders in use at the time of writing have 18 channels for relay timing signals, 3 current monitoring channels and 4 voltage monitoring channels; giving a total of 25 pens on each drum.

The above description demonstrates the need to store the incoming signal so that pretrigger information is available when required. A storage oscilloscope (or a camera coupled to an ordinary oscilloscope) containing a delay line is capable of capturing pretrigger information in transients containing only high frequencies (i.e. in the range over which the delay line is effective), but distortion due to the differing phase delays of the various frequency components is a disadvantage [Meas Inst Oli]. Such a device would prove useless at mains frequencies. Storage oscilloscopes have been used to capture transient events just by random arming coupled with automatic triggering but this method proves very unsatisfactory unless the repetition rate is high enough to set the probability of capture at a reasonable value.

The digital transient recorder is however, capable of capturing pretrigger information over a very wide range - typically several hours down to fractions of a microsecond. (See also Section 12.2

3.2

on the modified Video tape recorder). Fig. 3.2.1 shows comparisons of resolving time versus information content for several of the devices mentioned above.

Relative performance characteristics of different recording devices. Transient recorder A is an 8-bit, 2048-word, 10-ns device; B, a 6-bit, 256-word, 100-ns device; and C, an 8-bit, 1024-word, 500-ns device. Note that resolving time is defined as rise time, or the maximum sampling rate in the case of digital instrumentation. The writing rate of storage scopes requires smaller beam deflections for wider bandwidths, thus reducing information content; data is based on a writing rate of 5 cm/μs.

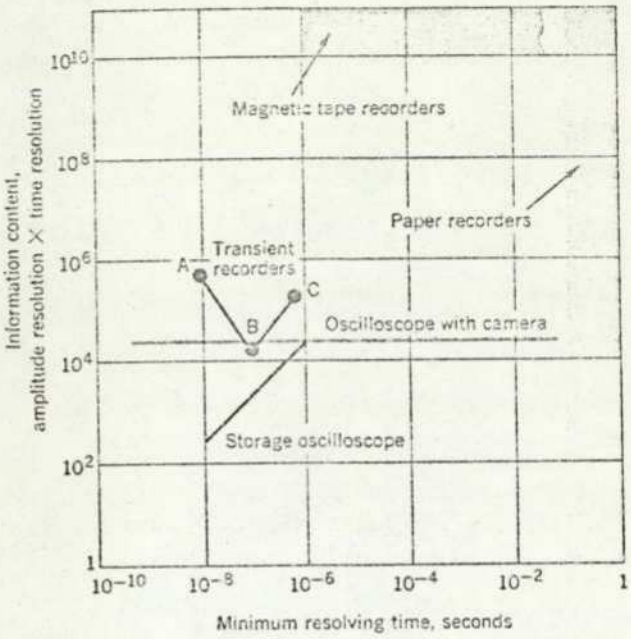

Fig. 3.2.1 (after Inst Elec).

The basic structure of the present generation of transient recorder (see Section 4.2) is common to all makes, but some differences occur in the options available [Tran Rec Fow, Tran Rec Say] e.g. the number of input channels, size of memory and range of sampling speeds.

Owing to their digital structure transient recorders can be easily provided with an interface suitable for connection to a digital computer. Some models offer a basic interface capable of transferring captured transients to the computer while others offer programmable functions and complete computer control.

One other device more recently available is the digitizing storage oscilloscope which is capable of pico-second time resolution of high speed transients. This device is similar to the oscilloscopes referred to earlier in this section except that

it operates at higher frequencies. Once the waveform has been captured the storage screen is scanned incrementally across the sweep and the height of the signal stored is quantized and fed to a digital memory housed in the oscilloscope. The data can then be transferred to a computer if the device is on-line. This instrument is designed for very high frequency work though it does extend the range over which transients can be captured.

3.3 Transient Recorder Interfaces

An early interface involving a digital transient recorder [Tran Comp Rat] was to a magnetic tape unit rather than direct to the laboratory computer, which made possible the storing of 70 transients on one reel of tape. This figure according to Ratcliffe is the average number of transients expected in one day of experiments The recorder, a Biomation, 802 was operated manually, although the interface could question some of the recorder settings and copy them onto the magnetic tape just in front of the waveform information. The total transfer time for one transient, including packing and formatting, is stated as being between 0.1 sec and 0.3 sec.

Once full, the magnetic tape unit was placed on-line to a PDP/8 or /15 mini-computer and the transients were transferred to the computer for analysis, each transfer taking approximately 1.0 sec.

Details of a transient recorder to CAMAC dataway interface module are described by Torok [Tran Cam Toro], the recorder used being a Biomation 8100. This interface allows the programming of

the front panel settings of the recorder (see Section 4.1) and packs two 8 bit bytes into a 16 bit word prior to transfer on the 16 bit dataway. Although the author of this paper [Tran Cam Toro] shows a system that can program the modes of the recorder, he states that to change the OUTPUT MODE from AUTO to EDIT [Bio Man] a wire link must be moved!

3.4 On-line Transient Recorder

Two papers are reviewed in this sub-section, though this is almost certainly not an indication of the actual number of transient recorders that have been interfaced to laboratory computers; for, owing to their area of application, such configurations often remain unpublished.

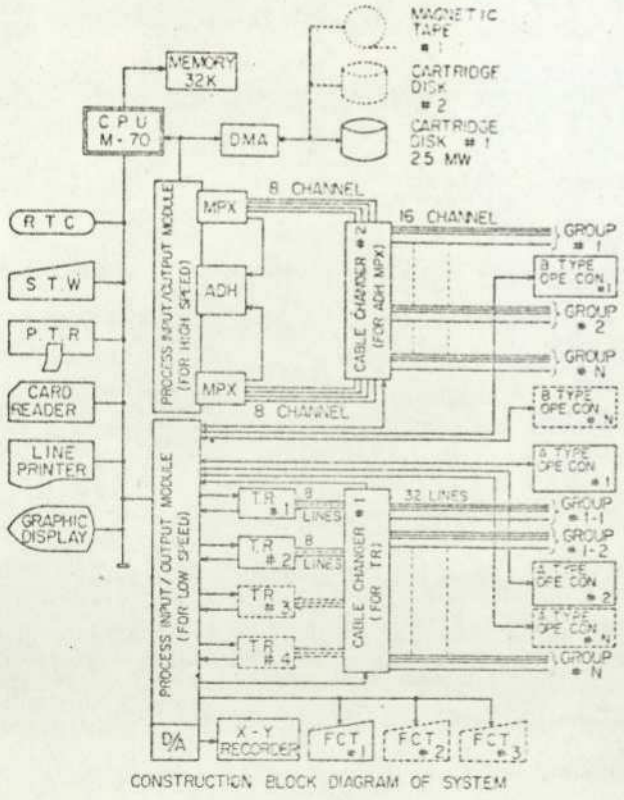

Block diagram of system.

Fig. 3.4.1 (after Tran Comp Miya).

The paper by Miyamoto et al [Tran Comp Miya] describes a mini-computer aided, real-time central data acquisition and analysis system in the High Voltage Laboratory at Mitsubishi Research. Fig. 3.4.1 shows the structure of their measurement system which comprises two Biomation 8100's (four are planned) a Melcom 70 mini-computer with 32 k words of core store, a 2.5 MW disc and a 16 channel multiplexed 100 kHz by 12 bit

3.4

analogue to digital converter. The transient recorders are programmed via a 'Type A' user panel which contains a duplicate set of recorder controls and some extra controls which allow communication with the C.P.U. of the computer. A system of programmable cable changers is used to switch the signals from a particular test area to the first available transient recorder via coaxial cables. The system time-shares the usage of the recorder to experimentors depending on their priority in the system.

One extra feature worth reporting is the facility for a user to view a transient before it is stored on disc and if the data are considered meaningless by the user, he can, by the 'Type A' control panel erase the waveform (cf. Visual Pattern Recognition section 5.3) so that it is not stored on disc.

A complex computer operating system governs the running of programs in a multi-task environment. Data aquisition takes priority in the foreground (core resident) whilst data analysis programs are run in the background mode (disc overlay), coming into core and running when time is available.

This system has been used to study the breakdown characteristics of SF_6 gas, liquid and solid dielectrics and vacuum. Long lengths of coaxial cable (up to 50 Metres) connect the measurement signals to the transient recorder. This may be a disadvantage with very high frequency transient events. Also microphonics in the cables could cause spurious signals. The authors have taken precautions regarding the screening of all cables and the central computer system. The earth point which was controlled by the computer could be transferred from one test area to another to improve the signal to noise ratio. The authors do not mention the total number of transients which can

3.4

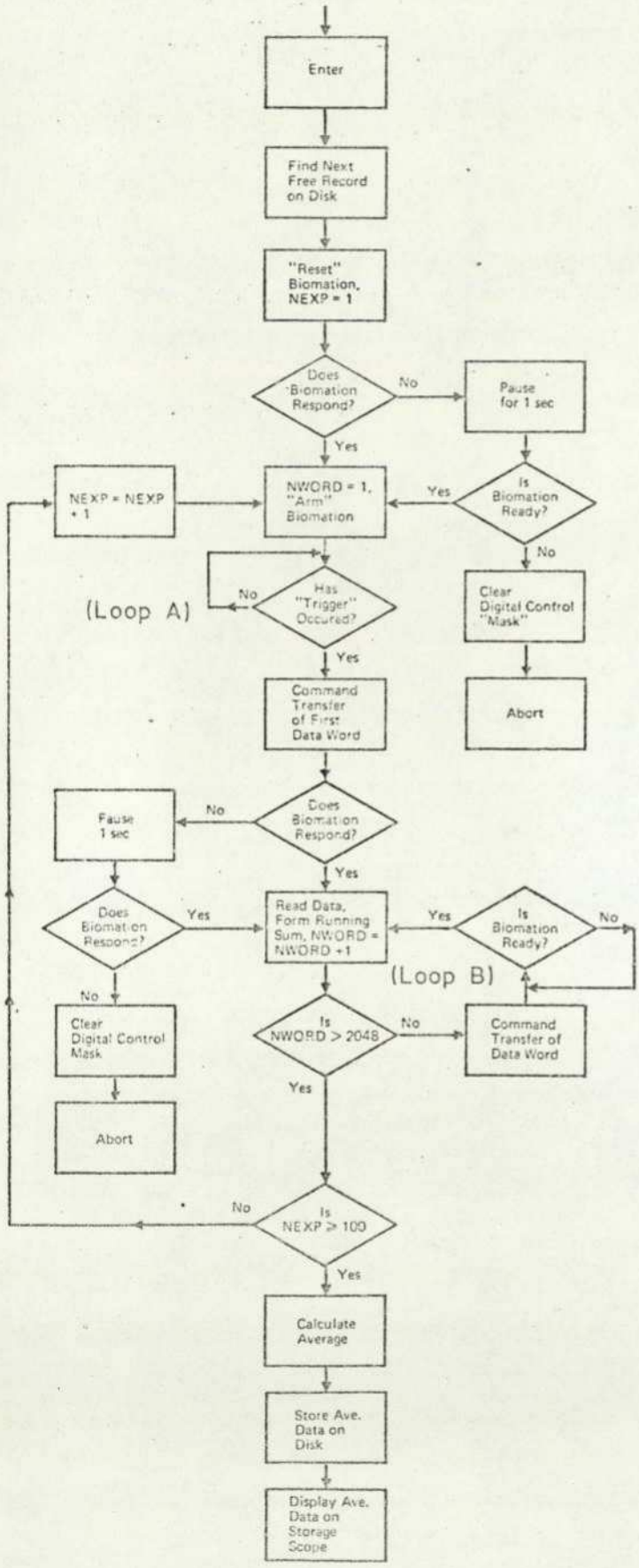

Flow chart of computer controlled transient experiment.

Fig. 3.4.2 (after Tran Therm Wied).

be stored on the disc; but assuming no packing overhead (which is unlikely) approximately 1220 transients could be stored on the disc cartridge.

The second paper [Tran Therm Wied] also concerns a Biomation 8100, in this case interfaced to an IBM System /7 computer. Unlike the CAMAC interface [Tran Cam Toro], which was mainly hardware with a little software, this system appears to have a simple hardware interface with a good deal of software to operate it. Fig. 3.4.2 shows several software loops which the program enters whilst awaiting the trigger event (loop A) and counting in the data transfers (loop B).

3.4

The software is designed in such a way that, should the recorder fail to respond, control is returned to the recorder and the experiment is abandoned. This system was used to study the dynamic magnetization of magneto-optic materials. The recorder was triggered by a pulse derived from the Laser Pulser which applied the write beam to the test sample and so the recorder was being used to capture a waveform whose occurrence was predictable, unlike most transient events which are random.

3.5 Pattern Recognition Techniques

Automatic computer-aided pattern recognition is now becoming common in many areas, from medical applications (such as continuous patient monitoring) to print inspection, colour quality checking for packaging plants and probably the largest area of all, character recognition. In some cases the decision making system will be simple [Comp Lab Ros] and run in a computer with other programs, while in other applications large amounts of core and processor time will be used. There are many papers pertaining to computer-aided decision-making and pattern recognition, but only a few are mentioned here, as the present author's system is limited by the availability of core store and is thus considerably less complex than the majority of the published systems.

One paper of engineering interest is an automatic transmission-line testing system. Bisignani [Pat Rec Bis] describes how impedance versus frequency plots are obtained for the line under test. Thirty two features are extracted from the impedance plot. These are values such as the frequency and impedance at maxima and minima in the plot, the impedance at two standard frequencies, the initial

slope of the graph etc. The system described could locate the position of a line fault and detect the failure of a load coil having previously measured the characteristics of a 'good' line. The author states that to perform this task a memory size of over 70,000 words would be required. In this application there were no time constraints imposed on the system, which allowed detailed calculations to be performed on the acquired data.

A different type of pattern recognition system is the waveform parsing variety. These systems divide a waveform into sections and then ascribe a shape to each section. Each shape is defined by a series of letters or words so that the parsed waveform can be represented by a syntactical structure. Such a system is described by Stockman et al [Pat Rec Sto]. This system is used to convert carotid pulse waves into a syntax structure. The authors used only linear and parabolic curve fitting to represent the waveform and report satisfactory results.

The parsing techniques used by other workers usually employ a large number of shapes which can be fitted to the measured wave-shape. In the medical field it is possible to store the typical shapes associated with a healthy patient and those relating to specific ailments. Such parsing systems have an optimum performance when they are tailored to analyse a limited range of shapes.

SECTION 4

The On-line Transient Recorder.

several thousand transients may be involved. It would appear that only one of the papers reviewed considered this to be important [Tran Comp Rat]. Tasks such as automatically decoding the data into two waveforms, each comprising 1024 words, when the computer has been 'told' that the recorder is in the dual channel mode become trivial in the present author's system. The computer can handle all the filing of transients on disc and carry out all the mundane 'housekeeping' associated with large amounts of data. As the computer effectively replaces the front panel of the recorder it should be at least as good as the original. It must be capable of warning the user of illegal or conflicting instructions (see Appendix I). The computer system, and especially the hardware interface, should be designed in such a way that the rate of capture is maximized. Some of the principles stated here can be summarized in the following three laws derived by the author in relation to the structure of the hardware software interface.

(1) Data are sacrosanct.

(2) The user's interface must be as simple as the First Law permits.

(3) The program's demands on the computer must be as small as the First and Second Laws allow.

The following section gives in further detail the structure of the hardware/software interface designed to link the Biomation 8100 to the FM1600B computer.

4.5 On-line Capture and Analysis of Random Phenomena

In this section is described the on-line system designed and constructed by the author, it takes the form of a paper published in On-Line Computing in the Laboratory. A brief mention of the pattern recognition techniques is made though these are treated in more depth in Section 5.

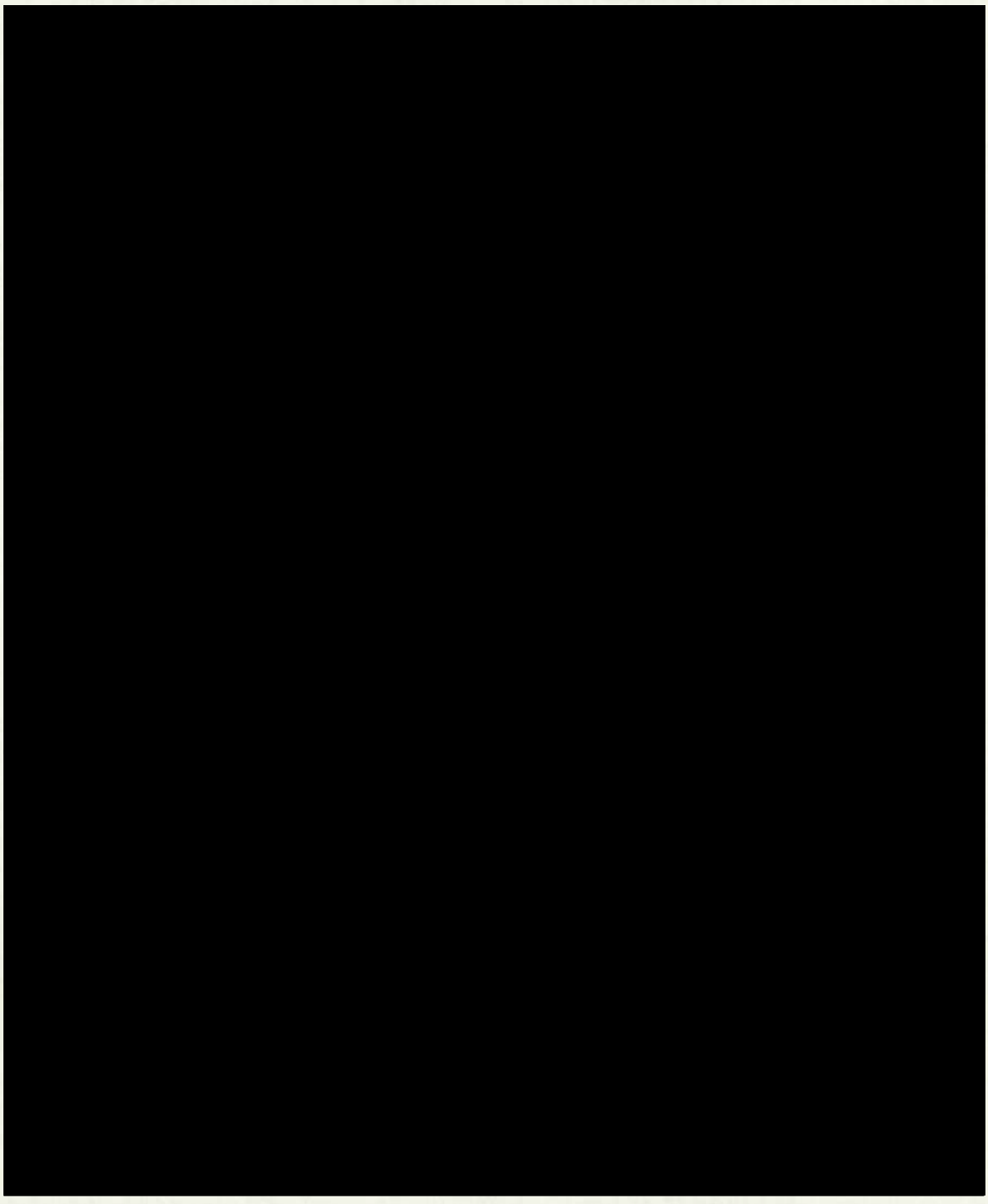

4.5

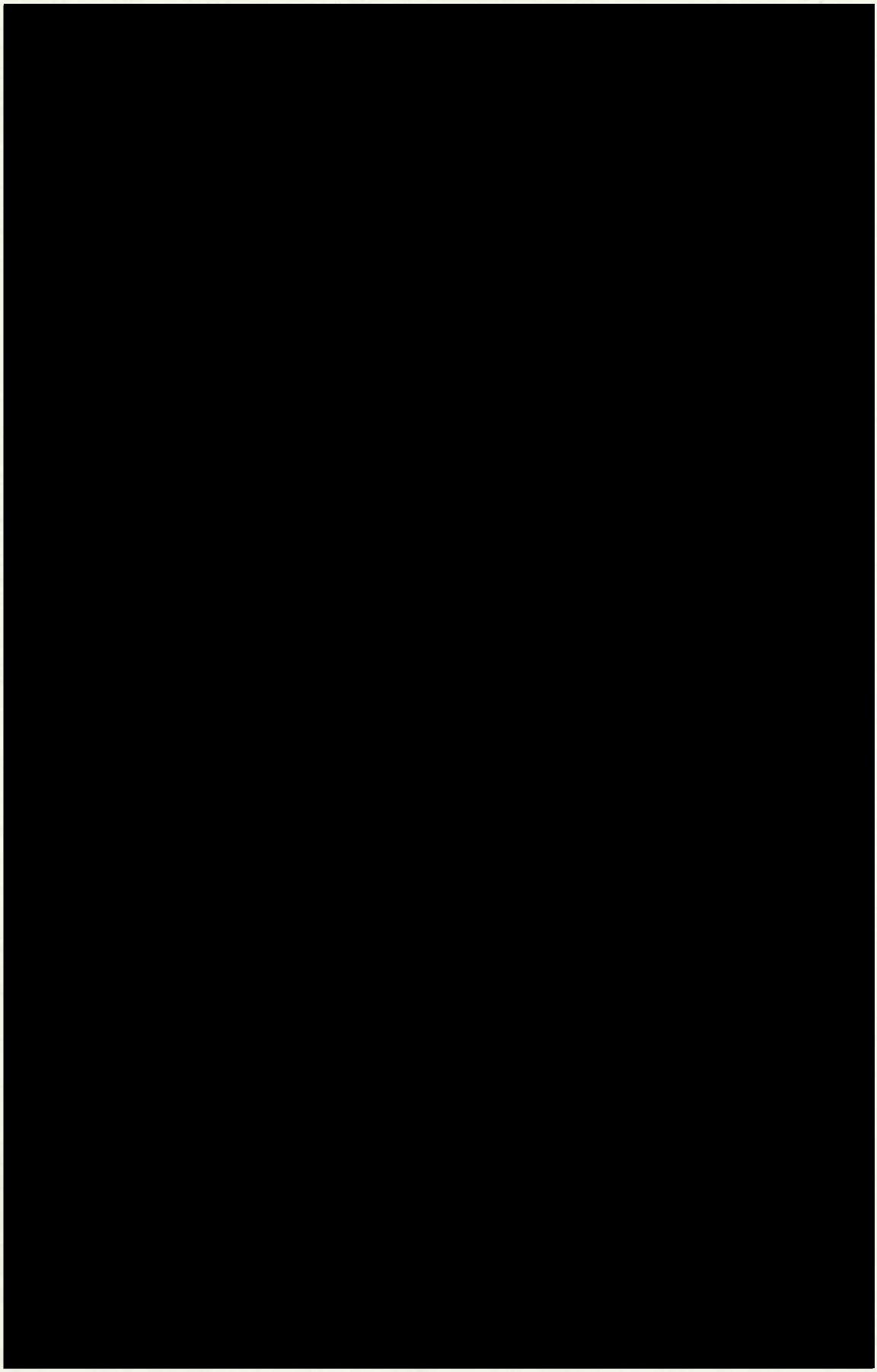

4.5

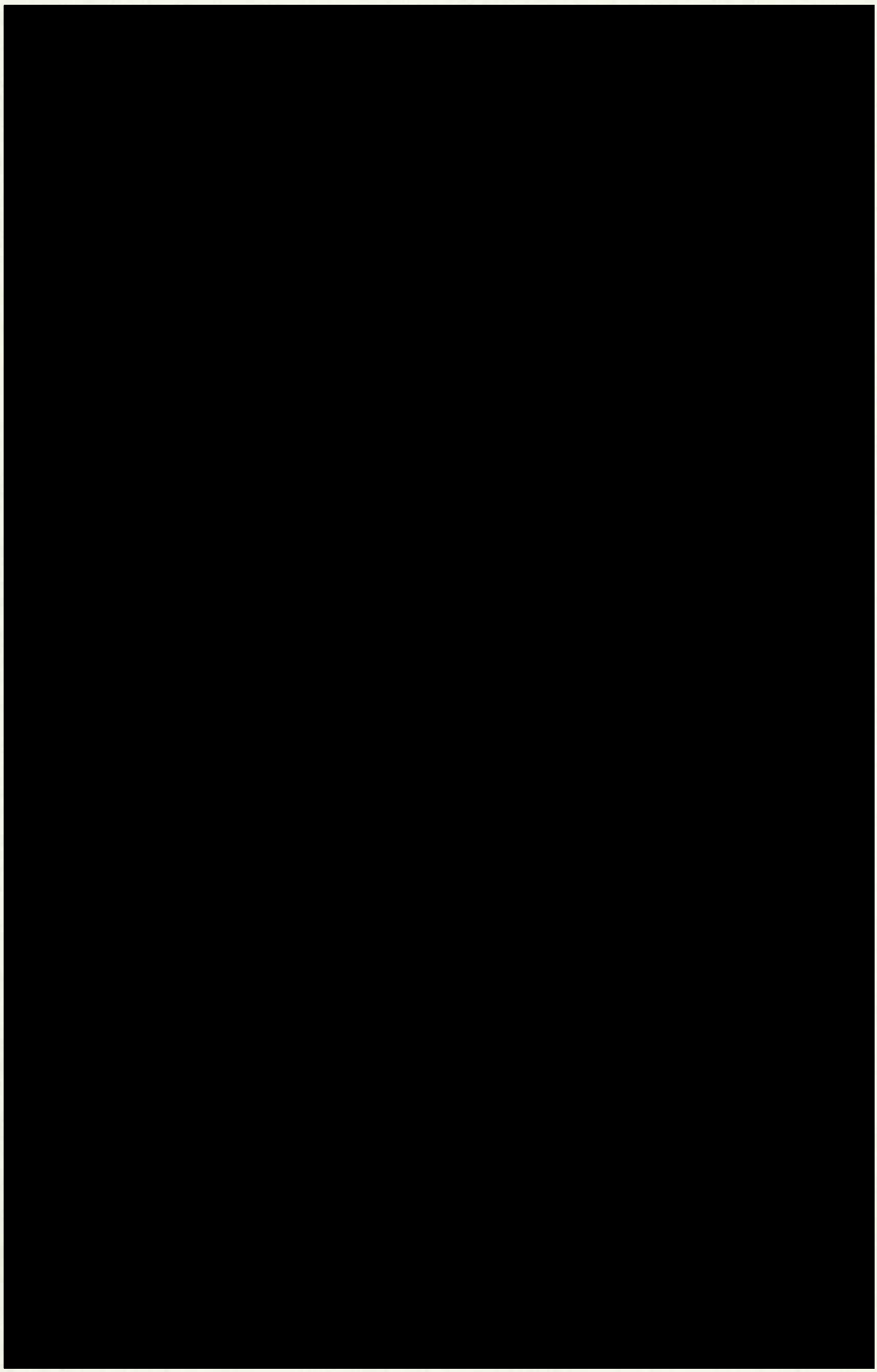

4.5

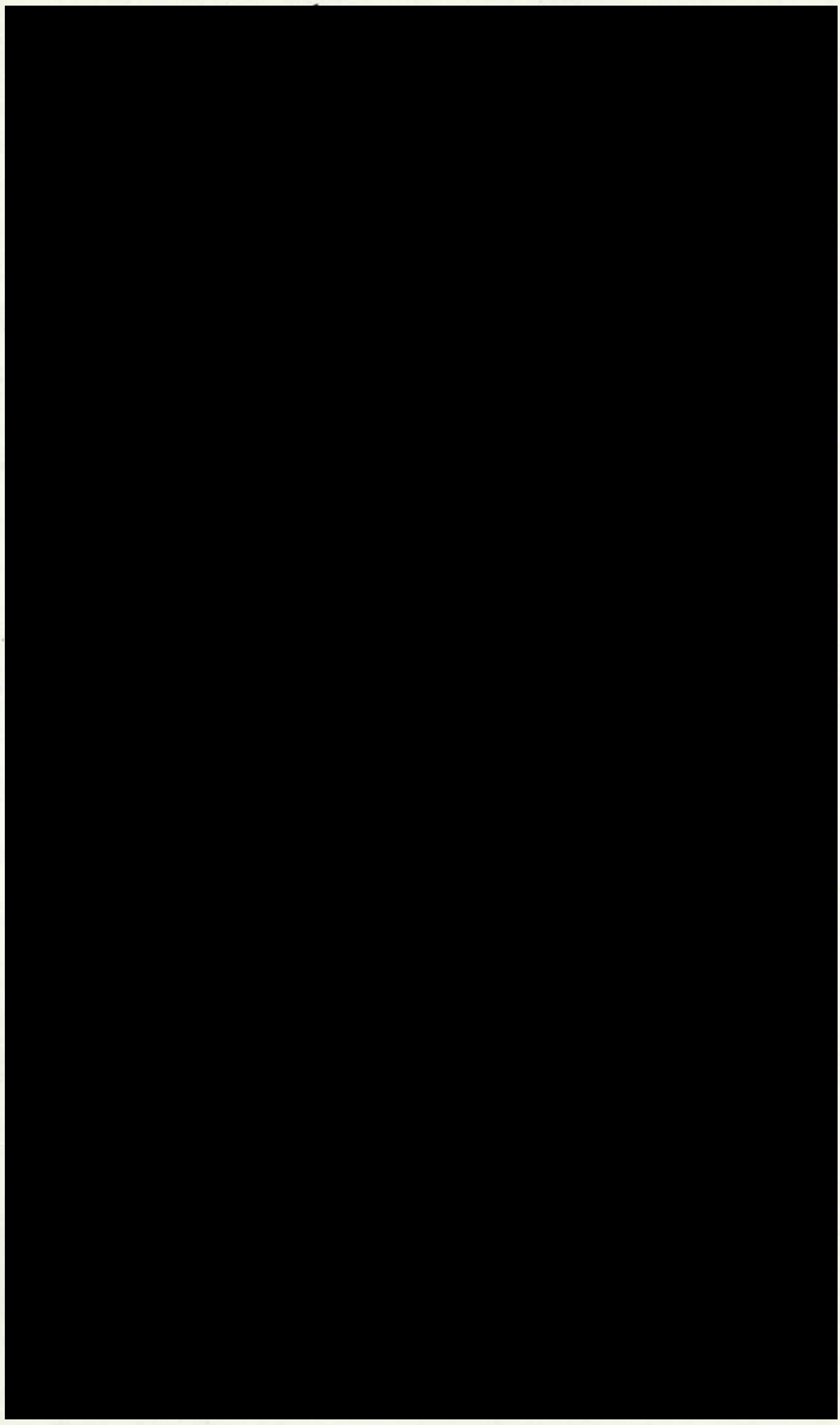

4.5

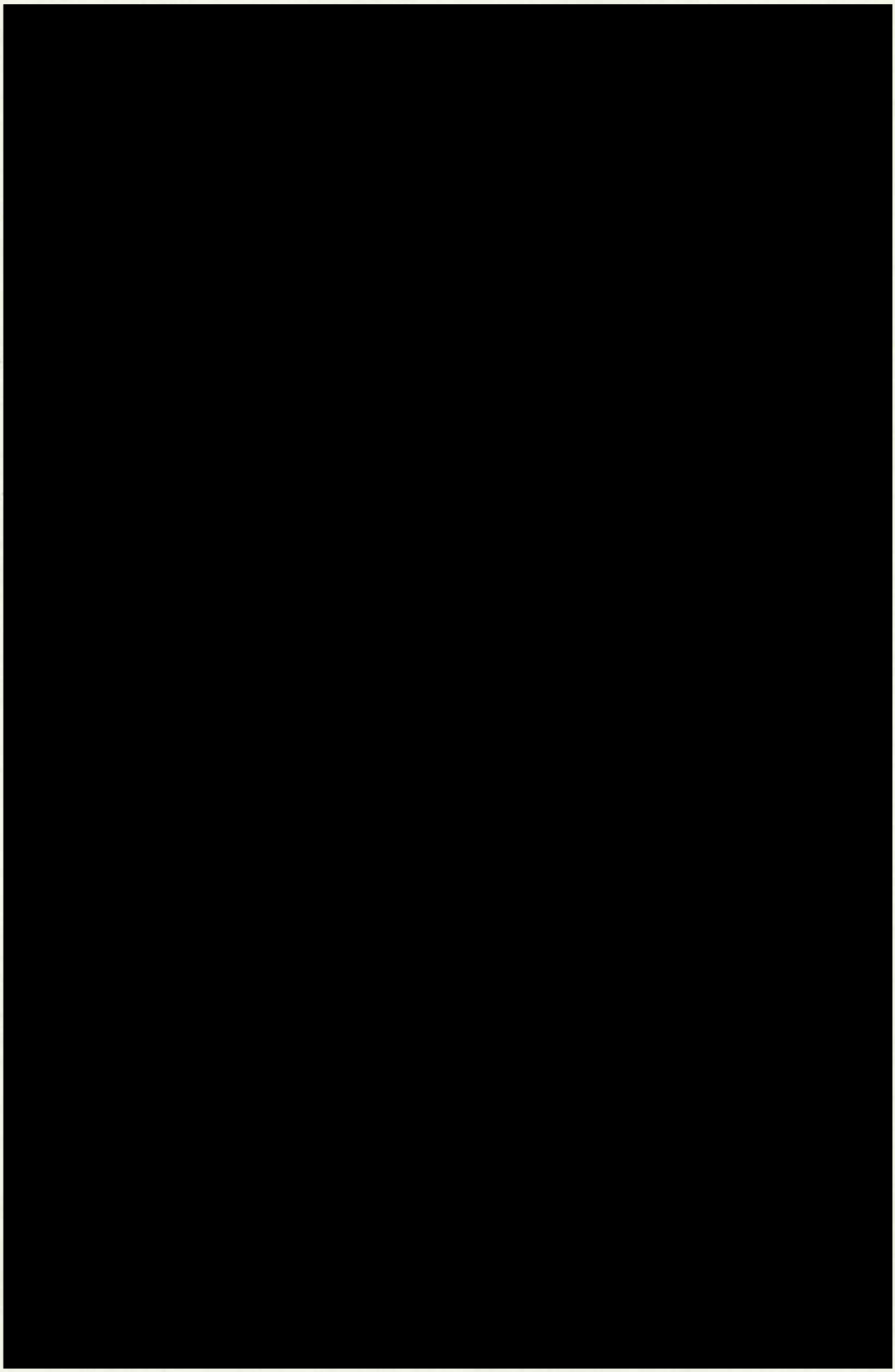

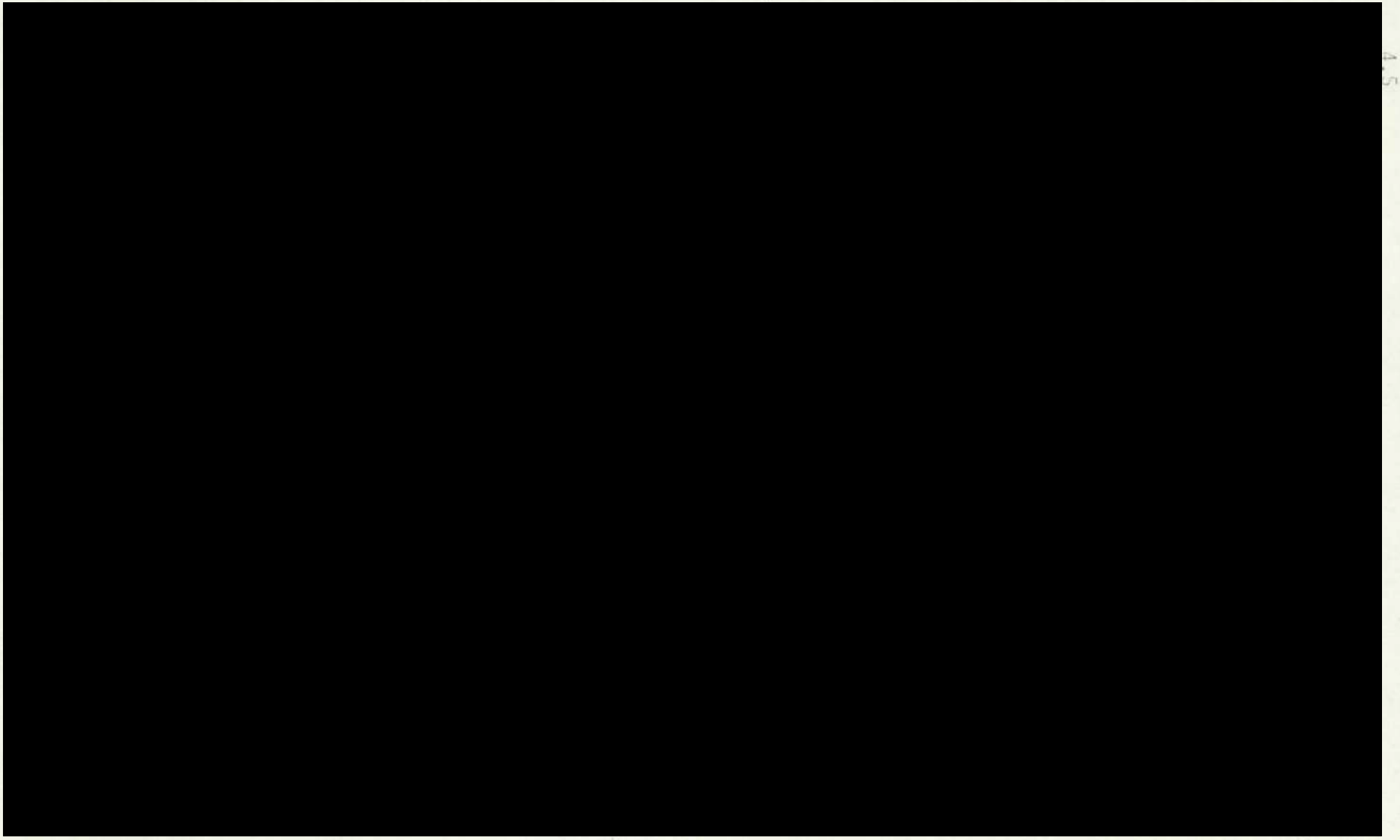

4.5

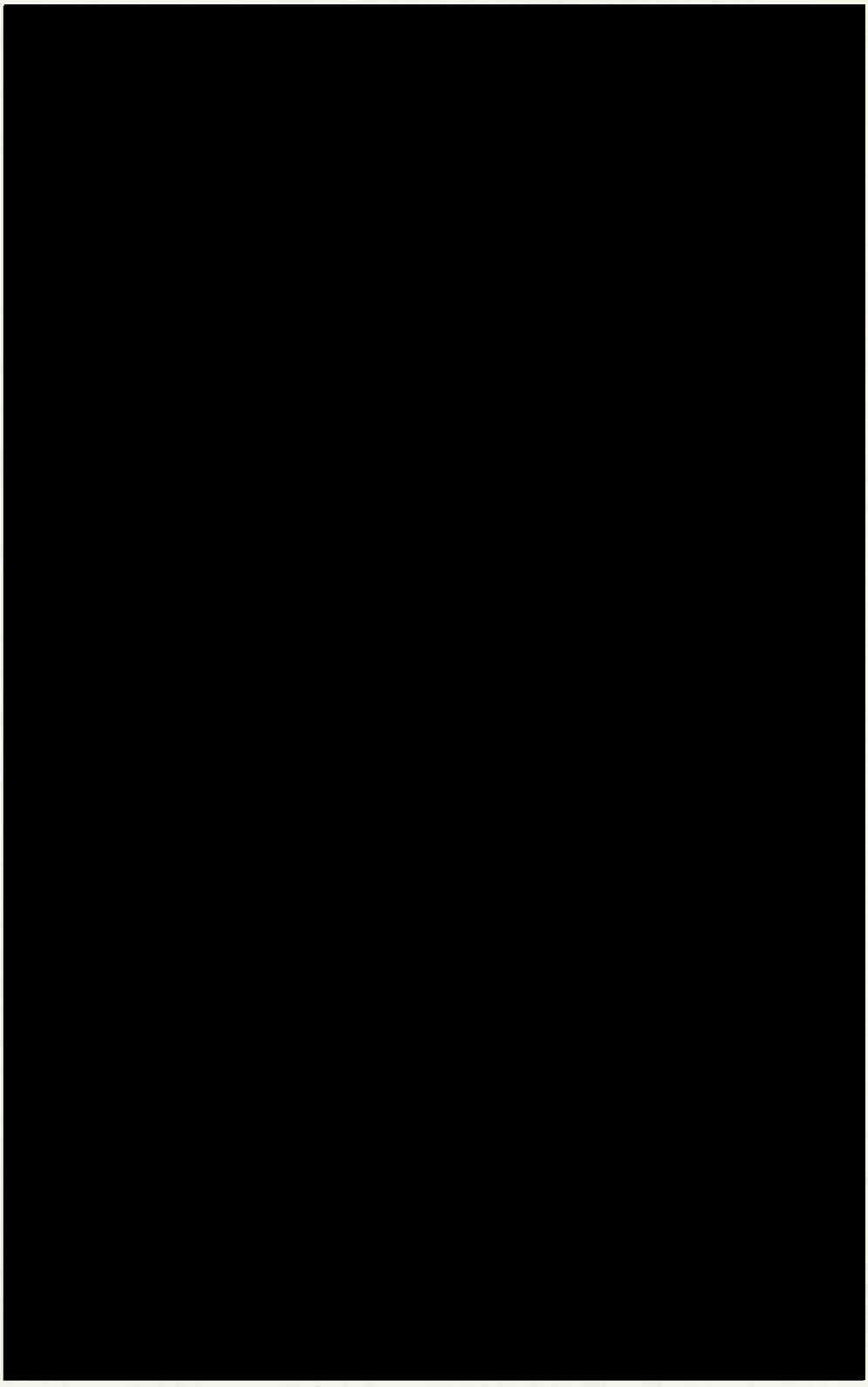

4.5

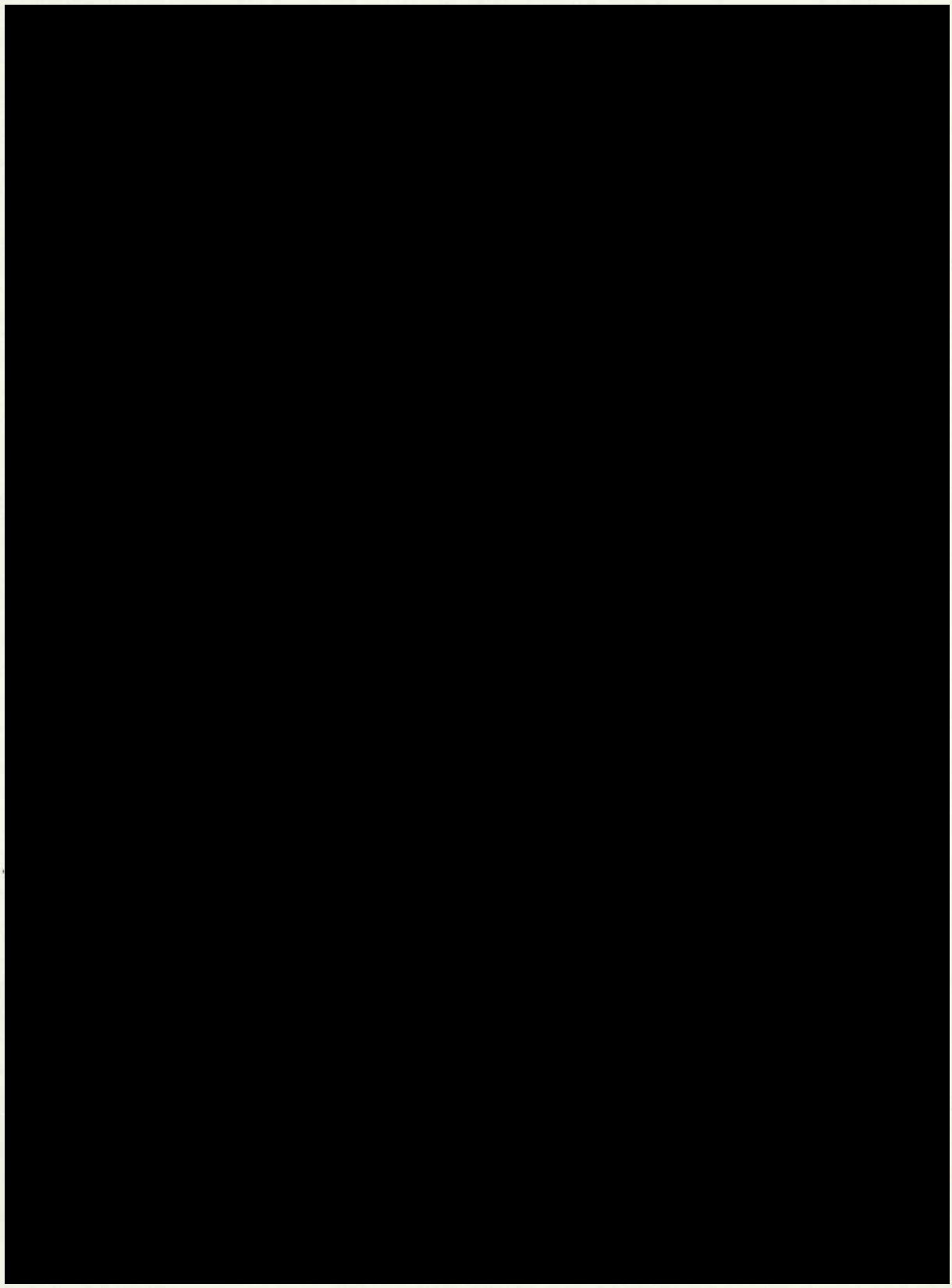

4.5

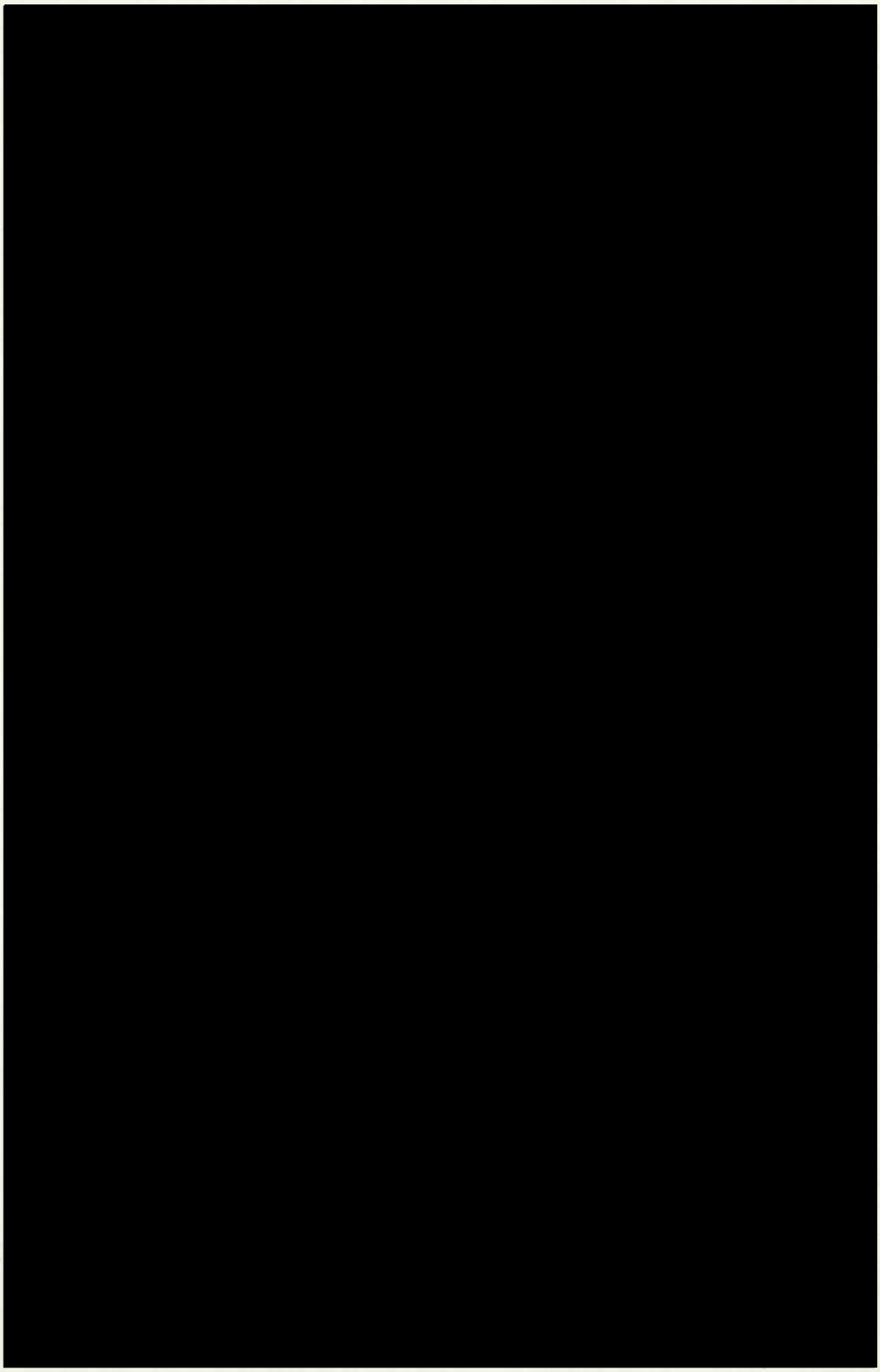

4.5

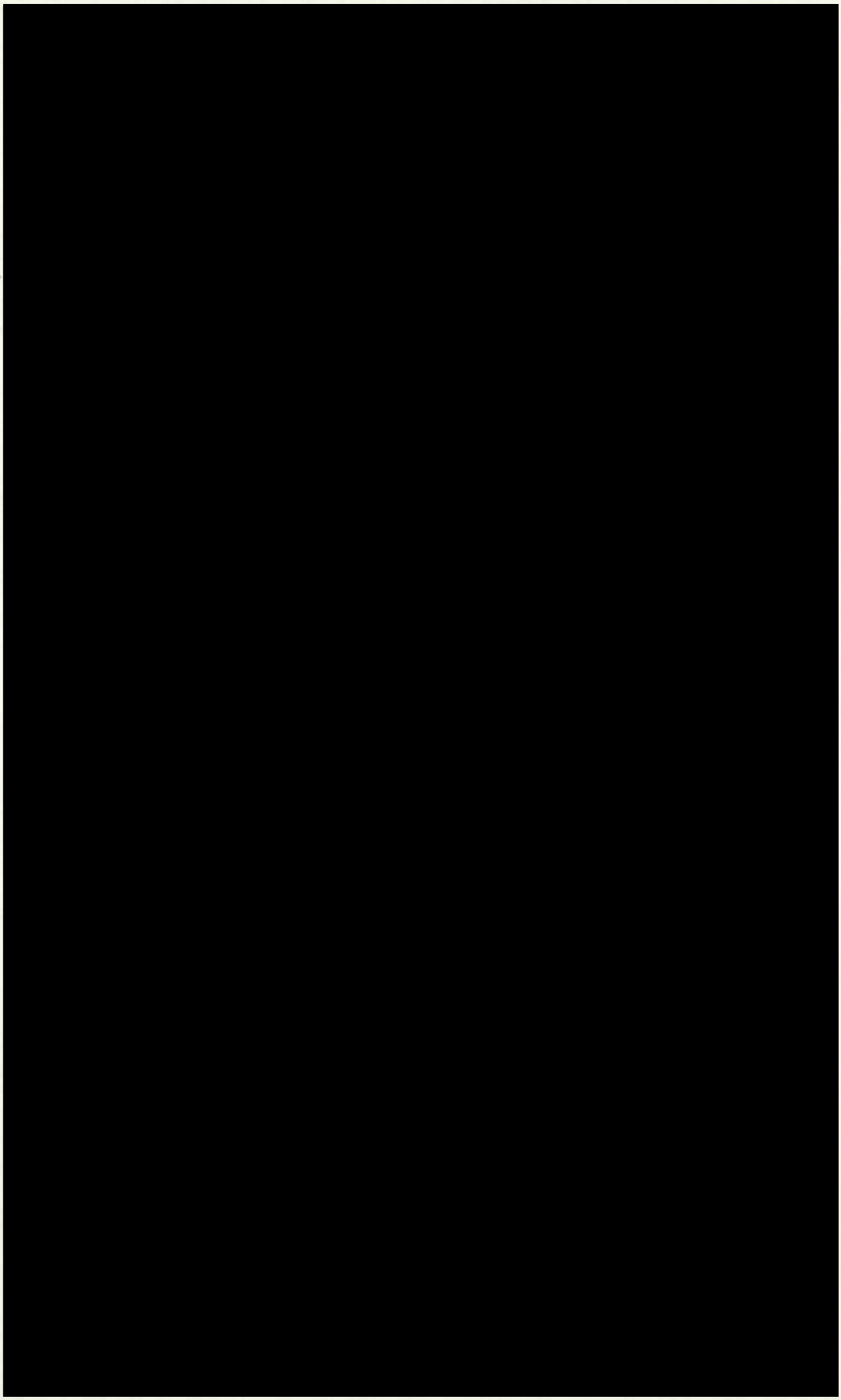

4.5

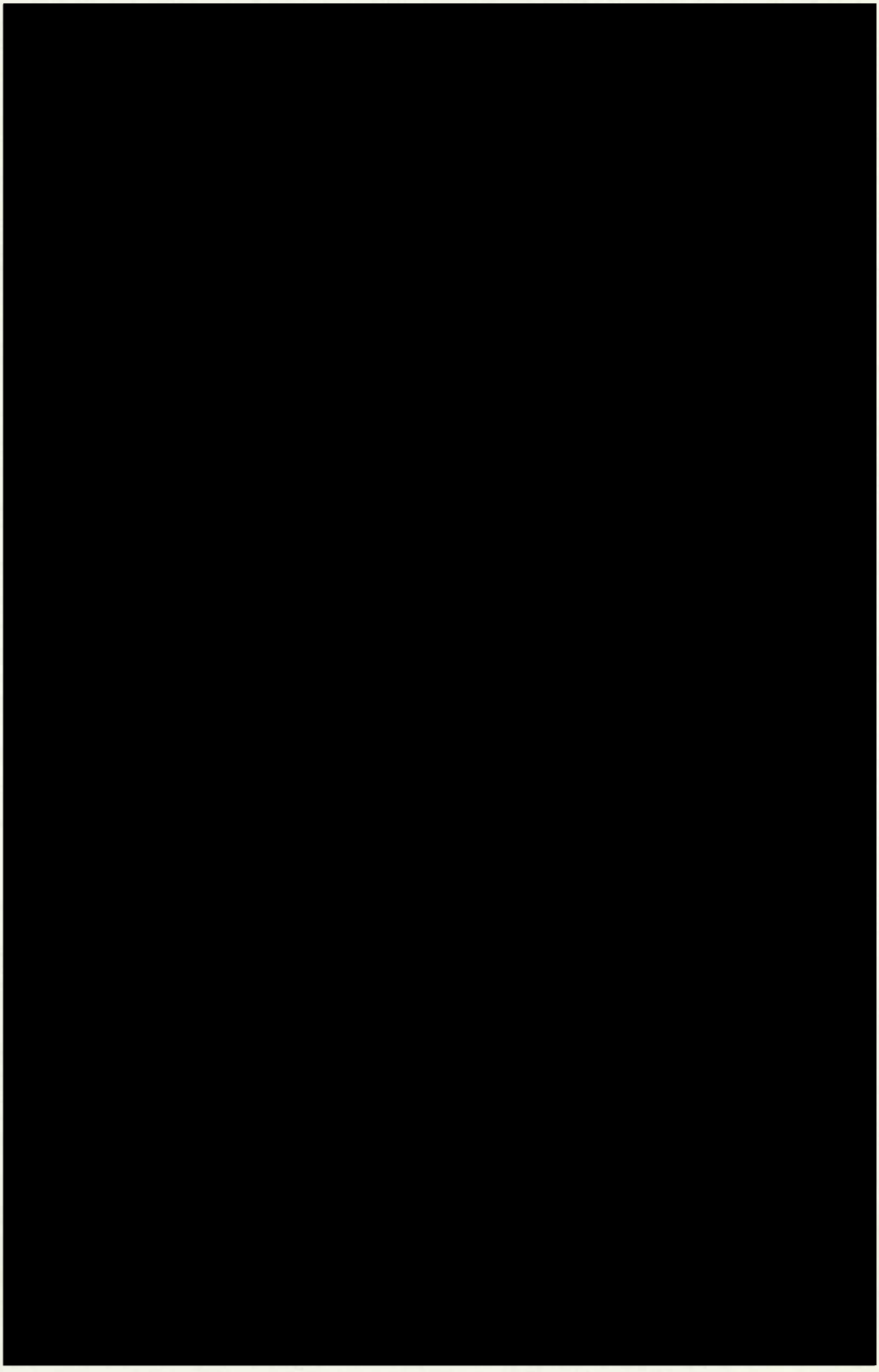

4.6 Discussion of the More Important Features of the System

Inspite of the specific requirements of the author (see Section 10) it was decided that the power and cost of the transient recorder demanded a comprehensive interface. Thus the hardware interface was designed to give the maximum flexibility at software level consistent with the one constraint of keeping the data transfer speed high (this rules out, for example, program controlled transfers as used by [Tran Therm Wied]). The software was arranged in such a way that it used the automatic facility of the transient recorder which transfers transients immediately after capture. It would be possible to wait until the status from the recorder indicated a waveform had been captured before initiating the data transfer to the computer. This, however, in most applications reduces the speed at which the system will operate and thus lowers the capture rate (for this reason the technique has not been implemented at software level). In comparison both the CAMAC [Tran Cam Toro] and IBM System /7 [Tran Therm Wied] designers have used program controlled transfers which tie up processor time and are thus wasteful. The author's system after arming the transient recorder (i.e. initiate a sampling scan) returns control to the user to allow further processing to be carried out until a transient is captured. By their nature transients are very unpredictable and oftern lapses may occur before an event is recorded; this demonstrates the disadvantage of the approach taken by Wieder [Tran Therm Wied] in program loop A in Fig. 3.4.2. In the author's implementation the user enquires by a call to the on-line Transient Recorder Control Program (Appendix I) if a waveform has been captured and transferred to store.

The approach taken by Ratcliffe in his recorder to magnetic tape

interface [Tran Comp Rat] has the advantage of extending the effective memory of the recorder to 70 transients, but, as will be demonstrated in later sections (5 and 10), in the recording of transient phenomena, events can be rare and can sometimes occur between other phenomena of no interest but of sufficient magnitude to trigger the recorder. This system [Tran Comp Rat] can perform no pre-processing, and so some of the magnetic tape storage may well be wasted on unwanted data which pre-processing could have filtered out (such pre-processing is described in Section 5.3)

The CAMAC interface [Tran Cam Toro] has two major disadvantages. One already mentioned is the program controlled data transfers; the author has, however, used the interface to pack two 8 bit data words into a 16 bit word before transfer on the CAMAC highway. This will double the potential word transfer rate from the transient recorder but increase the software which will have to decode the incoming data. The second (somewhat suspicious) disadvantage is the need to change a wire link in the CAMAC crate in order to program the recorder in the AUTO or EDIT output mode, which is clearly a restriction on the use of the recorder. Although in the software described in Appendix I the AUTO mode is enforced at software level, the hardware does accept the EDIT mode instruction which is used to enable the PLOT sequence via the digital interface.

In the system described by Miyamoto et al [Tran Comp Miya] the visual pre-processing of data by the experimenter (c.f. Visual Recognition Section 5.3) has been catered for, however there appears to be no communication of the front panel control settings of the transient recorders (loaded via the Type 'A' control panel) to the computer. Thus the transients, coming from up to four different

recorders, are stored on disc without documentation.

Referring now to the three laws stated at the end of Section 4.4. The first law is self evident: no data acquisition system should be allowed to corrupt data unnecessarily; though analogue to digital conversion is a form of corruption [Lab Comp Brig]. Owing to the requirements of the second law the software for the on-line transient recorder has been designed in such a way that the user need only familiarize himself with the specification of one program and all interaction with the recorder is via this program (Appendix I). The third law is demonstrated in several ways, as already described after arming the recorder the software returns control to the user to allow other processing to be carried out. Also a disc overlay of certain subroutines has been incorporated to reduce the overall length of the interface software. This overlay is controlled automatically by the interface software and is not apparent to the user. However all the code used by the recorder to capture and decode transients is core-resident to give the maximum speed possible. One limitation with any such system is the speed at which data are transferred to backing store (usually mechanical in structure and hence relatively slow). Thus the number of transients captured by the on-line transient recorder may be potentially high, but the disc will only be capable of storing a few waveforms every second. In the author's system the waveform transfer rate of the transient recorder is 20 per second as compared with the disc rate of 2 per second. If the repetition rate of transients is of the same order as the disc transfer rate then few transients will be lost. If, however, the rate is high, only a small fraction of the total will be captured. A buffer can be used in the computer to store several

transients and this can be useful if the events occur in groups or bursts, but the average rate will still be low. Even so, this is far faster than the off-line transient recorder in Section 4.4.

Thus speed of transfer, ease and flexibility of use are the features of the hardware/software package designed for the Biomation 8100 transient recorder. Full specifications of the Control Program and the Interface can be found in Appendices I and II. The versatility of the system is demonstrated in some of the other applications outlined in Section 12.

SECTION 5

Waveform Recognition.

5.1 Introduction

The problem of waveform recognition may be regarded as a one dimensional case of pattern recognition. In this section the subject of pattern recognition is summarised in relation to its realization in a basic waveform classification system for use with the on-line transient recorder. No attempt is made in this Thesis to include an indepth study of pattern recognition theory, but some of the basic concepts and principles of this extensive subject are described. The structure and modes of operation of the author's basic waveform classification system are explained with an example of the system capabilities. The constraints imposed by the FM1600B operating system are mentioned together with details of improvements which have been made. Programming techniques are outlined at the end of this section as they have played an important role in the rapid development of the measurement programs.

The need for a waveform classification system became apparent in the series of measurements made shortly after the transient recorder had been interfaced to the FM1600B computer. Figs. 5.1.1 a and b show two typical charge waveforms obtained from the test cell containing liquid n-hexane with an applied high voltage. Full details of these experiments are given in Part II of this Thesis. Fig. 5.1.1a was believed to be due to a charged particle moving between the two spherical electrodes under the influence of the applied field. Fig. 5.1.1b was a waveshape of a type frequently captured during the experiment and represents a large fluctuation of charge in the test cell.

The experiment required many of the waveshapes typified by that in Fig. 5.1.1a to be captured and various parameters to be extracted

5.1

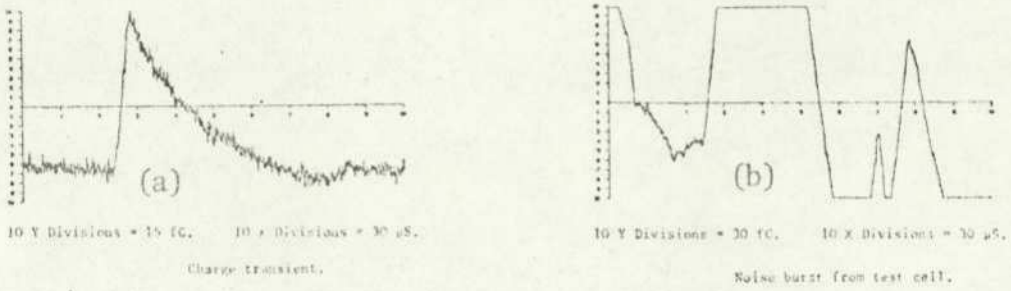

10 Y Divisions = 15 fC. 10 X Divisions = 30 μS.
Charge transient.

10 Y Divisions = 30 fC. 10 X Divisions = 30 μS.
Noise burst from test cell.

Fig. 5.1.1

from the shapes of the curves. With the aid of the transient recorder in the on-line configuration it was relatively easy to capture and store a large number of waveforms on the disc; but because of the large bursts of noise (defined as any unwanted signal), which would trigger the transient recorder owing to their greater magnitude, it was found that over 90% of the stored waveshapes were of the unwanted noise burst type. It was clear from this study that a system capable of making basic decisions as to whether a particular transient belonged to one group or another was essential if the on-line transient recorder system was to have any practical use. Just how necessary the waveshape classification system proved in the study of transient phenomena will be shown in Part II.

5.2 A Summary of Basic Pattern Recognition Theory

To enable an object or event to be assigned to a particular group, measurements of certain parameters or shapes must be made. The results of these measurements are used to determine to within which class a particular object falls. These tests are known as metrics and should be chosen so as to highlight the differences between two classes. Thus events or objects in the real world can be mapped, via a number of metrics, into numerical values. If the

metrics are correctly chosen then the numerical values obtained from testing similar events should form a cluster (metrics are usually chosen to be orthogonal, i.e. independent).

Fig. 5.2.1 shows the result of comparing two sets of samples A and B defined by two orthogonal metrics m_1 and m_2. Thus all the

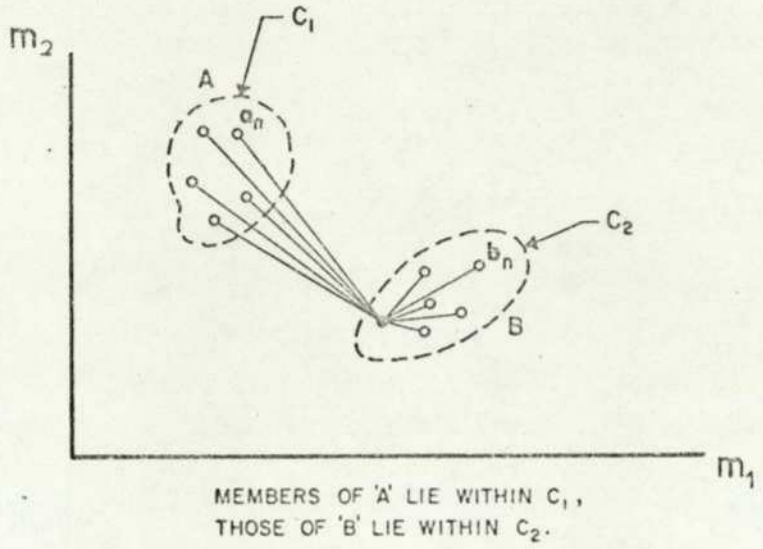

Fig. 5.2.1. Separation of classes (after Dec Pro Seb).

samples belonging to class B form a cluster within C_2 and all those in class A form a cluster within C_1. The metrics must be chosen to minimize the spread of the cluster whilst maximizing the 'distance' between the two clusters. The concept of the 'distance' between two points in the sample space indicating the similarities between two sets of events is the basis of pattern recognition theory [Dec Pro Seb].

Attempts may be made to improve the grouping of the cluster and thus increase the likelihood of correct decisions. Fig. 5.2.2 shows that by linearly transforming m_1 and m_2 to m_1' and m_2' an improved cluster is formed. Transforms can often be made before the metric is applied. This has been found most useful when dealing with transient waveshapes.

To measure the 'distance' between two clusters in the sample

5.2

space, a mean-square distance test is used. For Fig. 5.2.1 this is given by:-

$$D(a, b) = \frac{1}{N} \sum_{n=1}^{N} (a_n - b_n)^2 \qquad \text{Eq. 5.2.1}$$

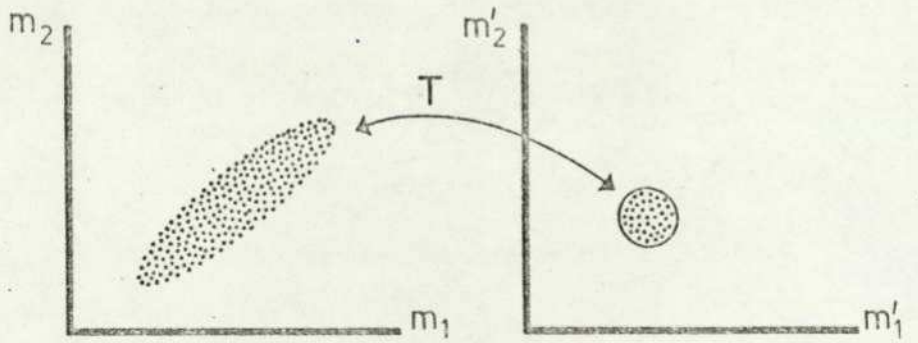

Fig. 5.2.2. Clustering by transformation (after Dec Pro Seb).

It is interesting to note that this formula is also used as a metric for comparing the shapes of two transients, which can be considered as a series of points in a bounded two dimensional space.

Certain advantages accrue from the limitation of the recognition system to temporal waveforms. These waveforms are continuous over their finite length and bounded in their maximum and minimum values. Although an event can be shifted in the time domain (relative to the start of the waveform) rotation about a fixed point is impossible, unlike information presented in optical form e.g. hand written characters. Another advantage is that there already exist many standard operations which can be applied to a signal in the form of metrics or transforms e.g. Fourier Transforms and Digital Filters. All these factors greatly reduce the need for complexity in the recognition system.

In early typed-character recognizing systems, templates or masks were often used to classify characters. Ullman [Pat Rec Tech

5.2

Ul1] describes several mask matching systems. In one such system for recognizing numerals, the mask was like a stencil or photographic negative of the numeral it characterized. When a numeral (positive image) was projected on to each mask in turn, the mask which caused the minimum of light to be transmitted indicated the numeral being 'read'. The transmitted light was monitored by a photo cell. The numeral was recognized as the one whose mask it matched, the match being indicated by the photo cell output falling below a set limit.

The principle of the template or mask is convenient for time waveforms, especially when the 'distance' between two groups is large. A template waveform can be stored in the author's recognition system and compared with incoming signals with the aid of equation 5.2.1, a zero resultant indicating identical signals.

A weighting function is a particular form of transform which may be of use in separating the characteristics of two groups. Such functions can be applied to the time waveforms to amplify features of interest and attenuate sections containing little or no information.

'Learning' is another important part of the subject of pattern recognition. A system applies its metrics to a set of test data of known classification and estimates the decision boundaries (i.e. C_1 and C_2 in Fig. 5.2.1) for each group. Systems can also be made adaptive in such a way that they 'learn' whilst performing classifications; these systems are, however, large and complex.

One other important and widely used technique, especially when analysing temporal signals, is that of parsing. A given signal is divided into sections and each section is considered separately. This technique has proved very efficient in the medical field where

rhythmic waveforms, for example heart beats, can be parsed and each section analysed in detail. Some systems even diagnose complaints after analysing the shape of each section of the waveform (see Section 3.5). This process of parsing is only convenient for well defined shapes where small irregularities are to be observed. Waveforms such as that in Fig. 12.2.4a cannot be easily recognised by a parsing system.

Statistics forms the major part of pattern recognition theory and such approaches are well adapted to classifying events which have a known distribution (likelihood ratios are dealt with in detail in many books on pattern recognition [Dec Pro Seb]). The learning process often becomes a matter of calculating a probability of an event.

These statistical methods prove satisfactory when there are no time or storage constraints. For the author's system such methods were considered impractical particularly when analysing such processes as those in liquid dielectrics, which are often stochastic.

5.3 The Implementation of the Pattern Recognition System

The method chosen to sort waveshapes into groups is now outlined. A detailed description of the subroutines used and the modes of operation is given in Appendix III.

The system has been designed to accept up to 24 metrics (supplied by the user) which will be applied to each waveform input to the system. The results of each test is a number normalized

between 0 and +0.9999; this number is called the Match Factor. If the resultant Match Factor is nearly +0.9999 then the test indicates the occurrence of some characteristic sought for by the metric or a similarity between the input waveform and a template.

Supplied to the system with each metric subroutine are a pair of numbers called the Upper and Lower Decision Levels and the location on disc of a template waveform if required by the metric.

The values of the Upper and Lower Decision Levels are used to predetermine the acceptable range of a given metric to identify a specific characteristic in a waveform. These two levels can be set by the operator according to need, or in the case of the Upper Decision Level, calculated automatically. The 3 possible relationships of the Match Factor to the two Decision Levels are defined in Fig. 5.3.1. The Matched and Unmatched cases represent the success or failure of a particular test. The third case, a Mismatch represents the failure of the metric to define whether or

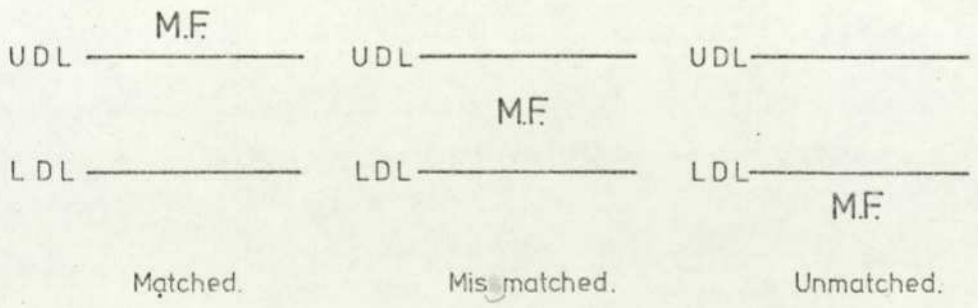

Fig. 5.3.1. The three possible outcomes for each test.

not a characteristic is present; that is, it indicates an uncertainty condition. The system is designed in such a way that the occurrence of an uncertainty in any test forces the waveform to be placed in a class reserved for these waveforms. The user may

then visually scan these transients (another facility of the classification system) and classify them appropriately.

The results from the comparison of the Match Factors with their respective decision levels are used to build up a binary pattern (of up to 24 bits, depending on the number of metrics) which represents the attributes of a particular class. Ten different classes can be specified by the user who supplies the bit patterns to be associated with each class. The bit pattern derived for each waveform is exclusively ORed with each of the 10 groups until a zero result is obtained; the transient is then assigned to the class defined by the pattern. Should no zero result occur the transient is put into another class defined as the 'rubbish' class.

Fig. 5.3.2 shows the effect of the decision levels in the case of 2 metrics. Three types of waveshape a, b and c are shown in this

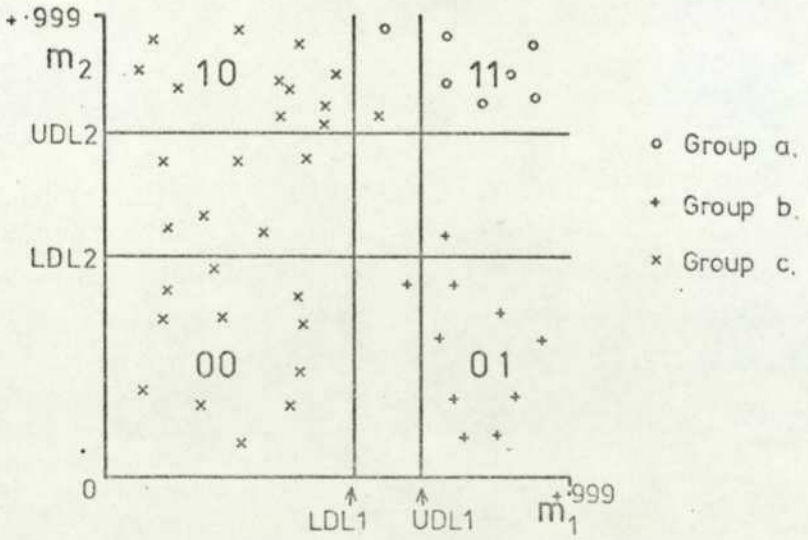

Fig. 5.3.2. An example of the decision levels operating with two metrics.

diagram. Two metrics are used to separate the three groups. All the waveforms in the top righthand box will be represented by binary 11, i.e. success in both tests. The type b waveshapes are defined

by the success of metric 1 and the failure of metric 2. Note: the fact that a particular feature is not indicated as present may also be used to make a decision. The third group of waveforms represent unwanted data. It can be seen in Fig. 5.3.2 that if UDL1 is lowered slightly (i.e. moved to the left) then one of the class c waveshapes will be placed erroniously in the class that should only hold type a waveforms. This demonstrates one of the problems that can arise in pattern recognition when the metrics do not separate the groups sufficiently. There is then a trade-off between the number of waveforms rejected and the number which are incorrectly classified. These two numbers tend to be inversely proportional [Pat Rec Tech Ull] (see Ullman on reject/substitution errors). Thus, providing the metric used separates the groups as much as possible, the linear grouping using decision levels is an adequate means of classification. The inclusion of the Lower Decision Level allows the user to look at waveshapes the system fails to classify.

The classification of transient waveforms can be performed either at the time of capture (before the transient is written to the disc) or at a later time after the completion of the data acquisition period, when all the captured transients are on disc. There are several advantages and disadvantages to both run-time and post run-time modes.

The run-time mode has the advantage of prefiltering the data so that waveforms classified as rubbish are not stored on disc, thereby allowing more space for valid data (unclassified transients are also written to disc). This method lowers the turn round time between capture and the re-arming of the recorder if the percentage of

'rubbish' is small. The main disadvantage is the risk of discarding valid data owing to a poor choice of decision levels or metrics.

The post run-time mode has the advantage that all the captured data can be repeatedly classified with different metrics and decision levels until the optimum classifications have been made. The system stores the Match Factors generated for each waveform on another disc file and on successive re-classifications uses these values with the updated decision levels as opposed to re-calculating the Match Factors every time.

The run-time approach was used to filter out the large 'noise' bursts mentioned at the start of this section (see Fig. 5.1.1 a and b). A simple metric was used (this helps keep the capture rate as high as possible) to detect overflow in the waveform. Only transients within the limits of the input amplifier of the recorder were loaded on to the disc.

The system is capable of automatically calculating the Upper Decision Level when given a set of waveforms whose class is defined. This is a crude form of learning as mentioned earlier in the section. The system simply sets the Upper Decision Level to the lowest value necessary to classify all the waveforms in the training set into their specified class.

An example of a transformation prior to classification is the approach used with the acoustic waves emitted from a propagating crack (this study is described in Section 12). A software envelope detector was used to transform the captured waveform. The envelope obtained was compared with a template to classify the waveform as an acoustic emission or a transient caused by tape

noise (see Figs. 12.2.4a and 12.2.5).

To demonstrate the capabilities of the pattern recognition system six waveforms are shown in Fig. 5.3.3. These waveforms were captured in conditions similar to those mentioned in Section 5.1 except that the electric stress on the liquid was lower (in a region where large noise bursts are rare). No scaling is shown on these waveforms as the pattern recognition system deals with waveforms containing 2048 points whose range has been normalized to be +0.9999 and -0.9999 (the normalizing factors are stored and are available if required). Waveform A was used as a template for the first metric as it resembled the required waveshape (designated class 1). The second of the two metrics used was simply a check that the waveform was within range. On two successive scans of 162 waveforms the effect of raising the Upper Decision Level (for the template comparison test) from + .97 to .974 moved waveform B from class 1 to the uncertainty class (defined as class 0) and placed waveform D into class 11 (the rubbish class) from class 0; waveform F also moved from class 1 to class 0. Thus two waveforms considered by the operator to be unsuitable (D and E) were not in class 1 but waveform B (which was suitable) was put into class 0. This demonstrates the usefulness of the visual recognition system which can be used to scan class 0 and allow the operator to define the class of the waveform. On the first scan, 124 of the total 162 transients were defined as class 1, 26 as class 0 and 11 as class 11, as compared with the second scan where 121 transients were placed in class 1, 13 in class 0 and 29 in class 11. The increase in the number of class 11 transients in the second scan was caused by the raising of the Lower Decision Level for metric 1 from + .84 to + .94

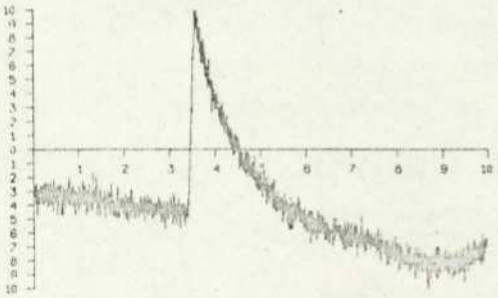

A. Comparison waveform.

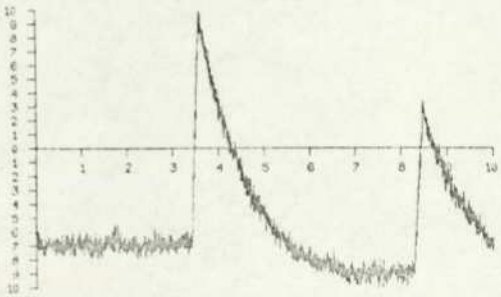

B. Scan 1- Class 1.
2- Class 0.

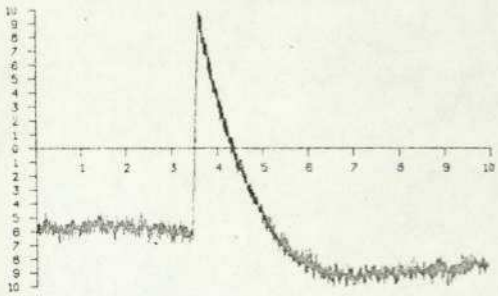

C. Scan 1- Class 1.
2- Class 1.

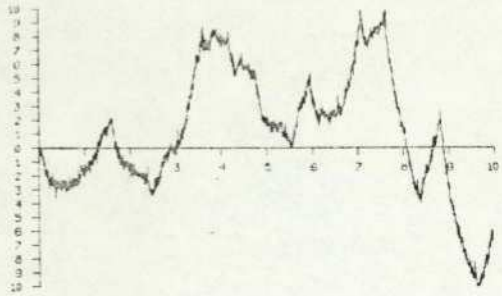

D. Scan 1- Class 0.
2- Class 11.

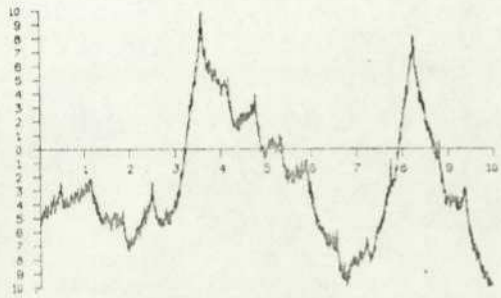

E. Scan 1- Class 0.
2- Class 0.

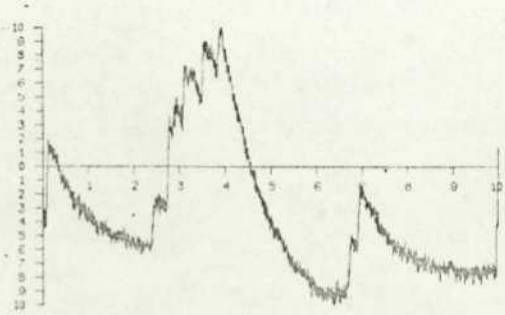

F. Scan 1- Class 1.
2- Class 0.

Fig. 5.3.3. An example of the capabilities of the waveform classification system (see text).

thus narrowing the uncertainty band. This demonstrates that with care the number of uncertainties that occur in the classification process can be reduced to a low enough level to allow visual classification to be practicable. Up to 500 transients have been classified in one scan with only 37 class 0 transients remaining to be visually classified.

5.4 Constraints of the Operating System

There is an extreme danger in the field of computer aided measurement that a measurement program will be rendered useless by a sophisticated [Lab Com Brig p207] operating system or supervisor.

This was found to be the case with the operating system supplied with the FM1600B after the disc drive had been incorporated into the computer system. This operating system treated disc files as reels of 8 bit paper tape, which forced a large software overhead on all disc transfers caused by packing, unpacking and formating data to be stored on disc. A period of over 30 min was required to reach the 1500th transient. This system clearly stifled the power of the classification system. With the aid of Messrs. Ferranti Ltd. a second method of disc accessing was implemented. This treated each file as a reel of magnetic tape with its associated block structure. This structure has proved successful in the efficient packing of transients and has improved the access time by a factor of 6 to 10. This is still not up to the maximum capability of the disc (150 mS access, worst case) but is a worthwhile improvement (details are given in Appendix III and in the User's Guide to the Magtape Simulator CJB).

5.5 Program Development

The technique used to develop the measurement system which performed most of the on-line measurements described in Part II of this Thesis is slightly unusual and thus is felt worthy of mention.

The measurement program comprises the on-line transient recorder programs, pattern recognition programs, on-line EHT program and standard system software; and was over 21 k words long when fully assembled. Over 6,900 words of this system were written by the author (this figure excludes blank data areas). The estimated figure for software development in industry is 1 k words per man year including development and documentation. The technique that permitted the system to be made operational in less than 18 months was the use of the author's on-line machine code editor. This program removed the need for repeated re-compilation and assemblies every time a few errors were discovered by allowing instructions to be 'patched' into the existing program as necessary. When a set of edits was complete the whole program was copied to disc and used as the starting point for the next de-bugging session. This updating process continued until the program ran correctly. Corrections were then made to the assembler code and a re-compilation was carried out (this usually occurred every 4 months as it takes several days to update source tapes, re-compile and assemble a new system). Details of the machine code editor now expanded by other workers in the computer engineering group are given in Appendix IV.

PART II

Applications to the Problem of Natural Charge Transport in n-Hexane.

SECTION 6

Introduction.II.

6.1 Introduction to Part II

Part II of this Thesis relates to the measurements performed by the author with the aid of the instrumentation and waveform recognition techniques described in Part I.

The present study of natural impurity particles in liquid n-hexane follows on from the work of Rhodes who used an on-line pulse height analyser to measure the contribution made by the femto Coulomb and the pico Coulomb pulses to the conduction current. The use of an audio visual technique enabled Rhodes to correlate the motion of one or two particles with the occurrence of the small femto Coulomb pulses for low values of electric stress.

In the present study the instrumentation described has, together with an electro-optic device, been applied to the correlation of the movement of natural impurities and the passage of a femto Coulomb packet of charge.

Section 7 contains a review of published work relating to the author's study. Some theoretical considerations of the motion of a charge particle in a stressed liquid dielectric are given in Section 8. The measurement apparatus (excluding the on-line transient recorder) is outlined in Section 9. The experiments performed with this equipment are featured together with the results in Section 10. A discussion of the author's findings in relation to the published literature comprises Section 11. Other measurements performed by the author are related in Section 12. Section 13 contains suggestions for future work following the results of the present study. Section 14 contains conclusions drawn from the present author's findings.

Throughout this part of the Thesis the charge signals derived

6.1

from the test cell are referred to as 'charge pulses'. In fact the term 'pulse' is not strictly true. Each event is a pulse of current which is a discrete quantity of charge. The term pulse is suffered as the amplifier which monitors the charge has a built in decay, to prevent charge build up, which converts the step waveform to a step followed by an exponential decay (see Section 9.6.2). Thus the transit of a charge is represented by a pulse.

SECTION 7

Review. II.

7.1 Introduction

This review covers some of the published work which relates to the effects of impurity particles under the influence of high electric fields. General reviews covering the various aspects of liquid dielectrics are available in the proceedings of conferences organized by groups such as the Institution of Electrical Engineers and the Institute of Electrical and Electronics Engineers. There are also the proceedings from the International Conferences on Dielectric Liquids. There have been five conferences in the series during the last seventeen years, a list of these is now given.

1959 Philadelphia USA (individual papers)

1963 Durham England (individual papers)

1968 Grenoble France (Pub. C.R.N.S.)

1972 Dublin Ireland (Pub. Typografia Hiberniae)

1975 Delft Holland (Pub. Delft University Press).

There are also the general reviews of the subject such as Adamczewski's 'Ionization Conductivity and Breakdown in Dielectric Liquids' [Cond Bd Adam], Conduction and Breakdown in Mineral Oil by Zaky and Hawley [Cond Bd ZaHa] and most recently of all Simple Dielectric Liquids by Gallagher [Si Dl Gall].

The summary of published work relating to particle contamination is divided into 3 groups; the action of particles in high fields, the conduction phenomena that have been attributed to particles and the breakdown of insulating systems due to particulate contamination.

7.1

The existence of impurity particles in high voltage insulation has been recognized for many years but the effects of these impurities in various vacuum, gaseous and liquid systems is still a topic of research in many laboratories. Even in good laboratory controlled conditions the preparation of liquid or gas samples without any particles is practically impossible. Harper [Cont Elec Harp] states that dust that settles on a surface is often so firmly attached that it can not be removed by a flowing liquid. When a liquid is used to clean a surface, it may contain suspended particles which can become attached to the surface being flushed.

An analysis of the number and size of particles found in a typical liquid dielectric test cell was made by Krasucki [Part Imp Kras], see Fig. 7.1.1, following a series of runs in an ultrasonic cleaner.

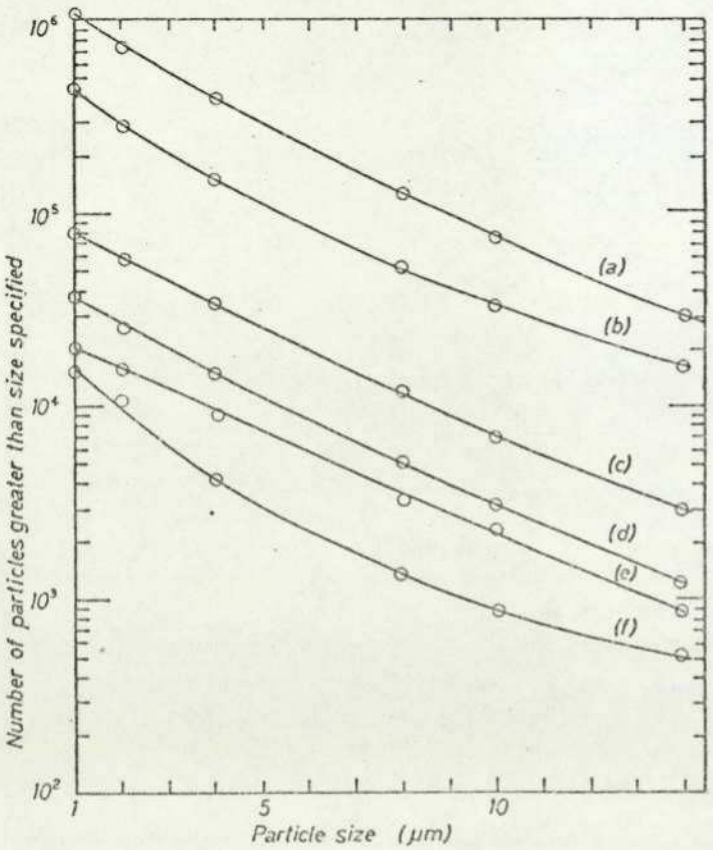

Distribution of the size, and number, of particles removed from a typical test cell in six successive ultrasonic cleaning operations.

Fig. 7.1.1 (after Part Imp Kras).

Gallagher [Si Di Gall], however, considers that the cavitation effects associated with this form of cleaning may have eroded surfaces such as glass, perspex and aluminium, which are common materials in such cells.

The present author has found that even with care in preparation and recycling the liquid through the cell (see

7.1

Section 9.3.2) the electrode gap will contain several particles in the order of 1 μm diameter shortly after the application of the electric stress.

Useful comparisons between the roles of particulate contamination in gaseous, vacuum and liquid insulating systems can be made, so some of the more recent findings in these other environments are mentioned.

7.2 The Action of Particles in High Fields

The motion of particles subjected to high electric stresses has been observed by many workers in the dielectrics field. In early years particle motion in oil was studied but only in the last 10 years (at the time of writing) has the action of particles in 'pure' liquids been investigated.

Gosling [Thes Gos] and others [Dis Gas Noss, Cond Puls Huq, Thes Slet] have reported particles oscillating between the electrodes of a test cell containing transformer oil. Gosling mentions a 'conditioning' process in which during a period of 2 to 3 hours the particles leave the inter electrode gap under the influence of the constant applied field. He also found that should a particle bridge form it usually caused a breakdown. The oscillation of particles between electrodes was noted by Stannet [Cond Part Sta] who added aluminium particles to transformer oil (see Section 7.3). Sletten and Lewis [Dis Gas Slet] found 1 μm size particles in their test cell. These were found to oscillate between the electrodes by a reduced amount when oxygen was added to the n-hexane under test. For

increased levels of oxygen particles were expelled from the gap. This was assumed to be due to oxygen molecules adhering to particles to change their effective permittivity thus reversing the dielectrophoretic force on the particle.

Goswami et al [Imp Part Gosw] reported three types of particle motion. One along the field lines between the electrodes, (oscillations) the second a random motion over the surface of an electrode and the third for gaps greater than 150 μm and frequencies of applied stress between 150 Hz and 300 Hz a circular motion was seen.

Cookson and Wootton, and Cookson and Farish [Part Gas Cook, Part Bd Cook] report the motion of fibres in compressed SF_6 and nitrogen. Under alternating voltage conditions fibres and particles moved from the bottom electrode into the gap and returned or oscillated between the electrodes; taking many cycles of the applied voltage to make the transition. These authors found the particles considerably more active when the stress remained constant. Fig. 7.2.1 shows their plot of the distance moved by a particle or fibre from the bottom electrode as a function of the applied stress, both alternating and direct.

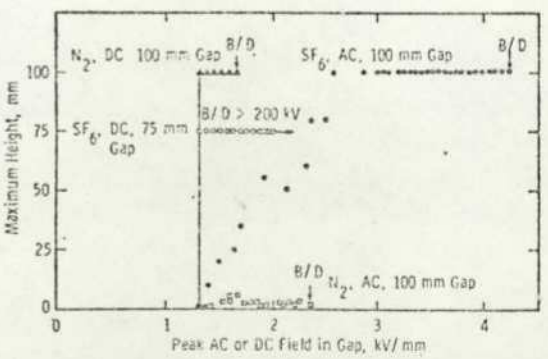

Maximum height moved by particle off bottom electrode as function of applied field for AC and DC voltages in nitrogen and SF_6, pressure 0.44 MN/m^2, particle 0.4 mm diameter, 6.4 mm long; B/D is breakdown

Fig. 7.2.1 (after Part Gas Cook).

Gray [Part Cont Gray] comments that particle initiated, or enhanced, discharges have been reported at high and low pressures in relay contacts. Particle sizes range from a few hundred angstroms to several millimeters and in every case the presence of particles was detrimental to the operating strength of the device.

7.2

Several workers in the field of liquid dielectrics have analysed the forces acting on a particle immersed in a liquid and subjected to an electric stress.

Kao [Elec Mech Kao] uses the principle of minimum energy to derive an expression for the force on a spherical particle of radius r and permittivity ε_2 in a dielectric medium of permittivity ε_1 in an electric field of strength E. This is given as:-

$$F_d = 2\pi r^3 \varepsilon_1 \left(\frac{\varepsilon_2 - \varepsilon_1}{2\varepsilon_1 + \varepsilon_2} \right) \nabla E^2 \qquad \text{Eq. 7.2.1}$$

An identical result was obtained by Viviani [Ed Imp Viv] who considered the field distortion due to an impurity in the liquid. Pohl [Die Phor Pohl] discussed some of the uses of dielectrophoresis in separating powder mixtures into their components, the purification of liquids and the separation of living and dead cells. In the studies performed on 'pure' liquid dielectrics the dielectrophoretic force acts so as to bring particles whose permittivity is higher than that of the liquid (this includes conducting particles) into the high stress region and to force those whose permittivity is lower than that of the liquid away from the high stress areas.

After 1965 there appears to be an increase in the interest taken in the effects of impurity particles and their relationship to conduction phenomena.

Felsenthal and Vonnegut [Part Cond Fel] studied the motion of conducting particles in Freon 113 (trichlorotrifluorethane, a precision cleaning agent) in a test cell with large plane parallel electrodes, and the usual oscillations were noted. Rhodes [Thes Rho]

reports that the oscillating motion of natural impurities was present and noted that the particles spent a long time on the electrodes compared with the transit time, this was also noted by Birlasekaran and Darveniza [Part Mov Bir].

Gzowski et al [Lum Dl Gzo] analysed the light-flashes output from a cell filled with hexane containing traces of anthracene (known to exhibit luminescence when subjected to an electric stress above 50 MV m^{-1}). The light output was assumed to be due to the increasing of the electric field near an electrode as a charged particle approached, which caused the anthracene to glow (in the absence of anthracene no light pulses were observed). It is also stated that the light output increased with the applied stress and was related to the current flowing. A step voltage was repeatedly applied to the cell and the voltage and light output signal (measured via a photomultiplier) were observed on a dual beam oscilloscope. Only the first 100 μS after the application of stress were considered. The time at which the first and second light pulses occurred were noted for each application of the voltage; this was assumed to be the time it took the first two particles to become charged and travel across the gap. The authors deduced that the transit time of a particle across a 100 μm gap at a stress of 43 MV m^{-1} is about 60 μS (giving a mobility of 4×10^{-8} m^2 V^{-1} s^{-1}).

Rhodes [Part Cond Rho] observed particles being ejected from the gap (in a sperical electrode configuration) during periods of increased conduction. Krasucki [Part Imp Kras] derives an expression for the radius at which a spherical particle oscillating between sphere/plane electrodes is stable (i.e. does not change its distance from the axis of the electrodes). This is said to occur when the dielectrophoretic

and the centrifugal forces acting on the particle are equal. Krasucki states that the dielectrophoretic force is approximated by

$$F_d = - r^3 Ex \frac{dEx}{dx} \qquad \text{Eq. 7.2.2}$$

Comparison with equation 7.2.1 suggests that the permittivity term has been omitted from the above formula though the calculated curve has been made to fix the measured data.

The experimental observations of Birlasekaran and Darveniza [Part Mov Bir] are worth mentioning, unlike Felsenthal and Vonnegut [Cond Part Fel] who state that it was necessary for particles to touch the electrode for charge transfer to occur. Birlasekaran and Darveniza found that a 0.4 mm radius steel ball supported by a glass or plastic tube at stresses between 0.7 and 1.4 MV m^{-1} did not contact the electrode but stopped short on each excursion. Four possible causes of this effect could be that the ball was not carrying a charge but was moved by liquid motion; small impurities may have transferred the charge from the ball to the electrode, the ball discharged by ionic conduction or more likely space charge was present at the surface of the glass or plastic support near the electrode and aided the neutralizing and recharging of the ball. Fig. 7.2.2 shows the current waveform recorded during the transition of the ball between the electrodes. It

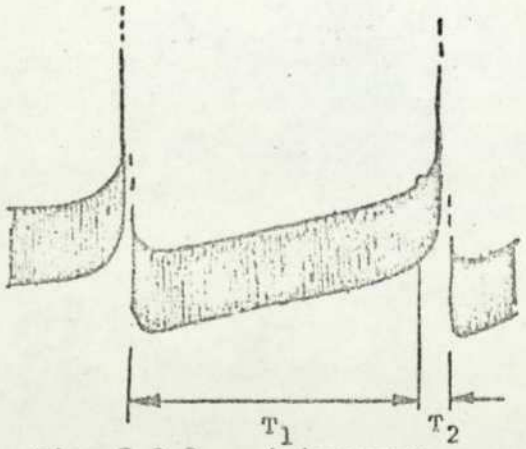

Fig. 7.2.2. A 'current pulse recorded at the cathode'. The shaded area is reported to be r.f. ripple from the power supply oscillator (after Part Mov Bir).

is a little difficult to explain the shape of the trace although the pulse, of duration T_2 may be a micro discharge between the particle and the electrode as observed by Gosling and others [Thes Gos, Lum Dl Gzo] (see also Section 8.5). During the period T_1 a steady level of current would be expected as the ball transfers charge across the gap. Shammas et al [Puls Gen Sha] have used a similar cell structure to utilize the microdischarge each time the ball nears an electrode to obtain a nanosecond pulse.

Spitzer [Bd To Spit] comments that particle activity is greatly reduced in a test cell with needle electrodes. This is probably due to the very non-uniform fields close to the electrodes and the resultant high value of dielectrophoretic force (note this force is proportional to the gradient of the applied field). Gallagher [Mag Fie Gall] in studying the effects of magnetic fields on the breakdown strength of n-hexane comments that particle oscillations were not greatly affected by the magnetic field. However in some cases the application of the magnetic field apparently caused a few particles to leave the central region of the gap. Any particle within the magnetic field will experience a force acting in the same direction for each transit of the gap.

Rhodes [Thes Rho] reported that if the stress remained at a constant level for a period of time the particle motion would subside and eventually all particles would adhere to one electrode or the other. The particle motion would recommence if the stress was raised. The gap clearing process in oil [Thes Gos] was not apparent in n-hexane at lower levels of stress but at high stresses a rapid clearing of the gap was reported. This often occurred just before breakdown.

7.2

Zaky and Hawley [Cond Bd ZaHa] in their review described some of the effects of particles, in particular the formation of bridges which in the case of oils containing free water droplets together with solid impurities may lead to breakdown.

Some authors have put forward models to describe the action of particles in high fields. Krasucki [Cond LD Kras] derives equations for the current due to the presence of particles which are presumed to convey charge within the liquid. Birlasekaran and Darveniza [Part Calc Bir] apply Krasucki's equation to find the 'average conduction current and discrete pulse characteristic' which they relate to their observations [Part Mor Bir]. A more detailed model of low field conduction has been considered by Denegri et al [Imp Part Den]. The model takes into account the electrophoretic, dielectrophoretic and gravitational forces and torque acting on a particle. A sphere plane electrode system is assumed and the parameters relating to the liquid and the particle are supplied to the model. A digital computer calculated the trajectories of a particle under the applied conditions, Fig. 7.2.3 shows four paths

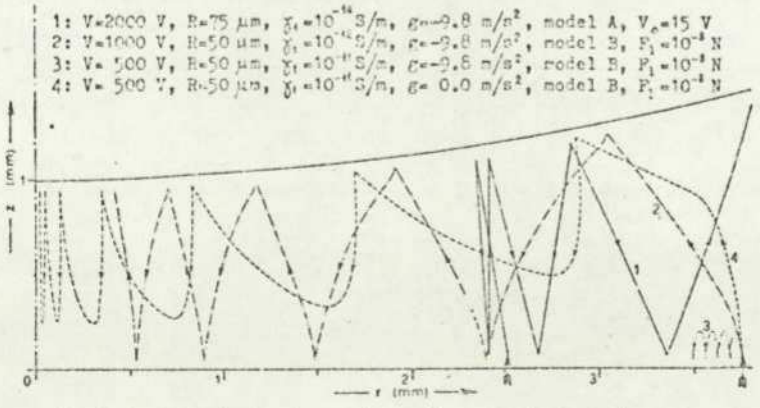

Particle trajectories in a sphere-plane electrode system.

Parameter values defined in Sec. 4. - V, applied voltage - R, particle radius - g, gravitational field component parallel to the vertical axis - V_0, Felsenthal-Vonnegut potential - F_1, limiting adherence force - $\frac{1}{n}$, starting points.

Fig. 7.2.3 (after Imp Part Den).

generated by the model. The model can be programmed to assume various hypotheses; for example the dwell time of a particle may be defined as zero or set to a defined value also the charge acquired may be calculated from Maxwells formula [Elec Mag Max] (model A) or the limited value proposed by Felsenthal and Vonnegut [Cond Part Fel] (model B); the model assumes no interaction between particles.

To verify this model the authors designed a test cell with the following specifications; sphere/plane electrodes, sphere diameter 15 mm and a 1 mm gap containing metallic particles with diameters between 130 μm and 150 μm. The liquid used was n-hexane. The following parameters were supplied to the computer model, together with preceding cell specifications, liquid density 0.663 g/cm^3, viscosity .312 centipoise, relative permittivities of 1.89 (liquid) and 1.00 (particle). The computed trajectory of one particle in the cell when a step of 2000 volts is applied is shown in Fig. 7.2.4. The particle oscillated to and fro in the gap until it gains

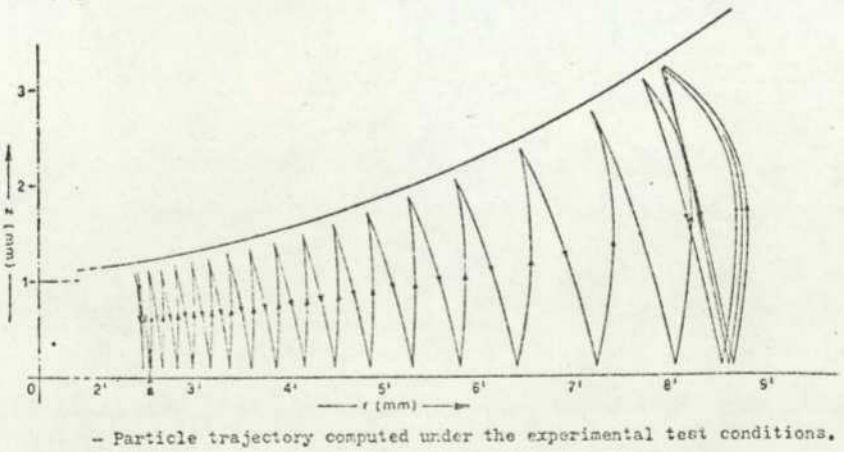

– Particle trajectory computed under the experimental test conditions.

Fig. 7.2.4 (after Imp Part Den).

an equilibrium position. To obtain this curve a model between A and B was used. The chosen parameters gave a result which agreed well with the experimental results. It is, however, interesting to note that the relative permittivity of the particle was chosen to be equal to 1.00 (for a conductor a value of infinity is a better approximation).

This is less than the relative permittivity of the liquid and would imply a dielectrophoretic force, from Eq. 7.2.1, acting out of the gap. It is not unreasonable to question why the model predicted that the particle would remain in the gap. It may be due to the assumption of zero dwell time and that the particle/electrode collisions were elastic.

7.3 Conduction Phenomena Attributed to Particles

It is in this area that the published results indicate a wide variety of observations and hypotheses. At one time or another particles have been prescribed as the cause of almost every observed phenomena in the field of liquid dielectrics. Zaky and Hawley [Cond Bd ZaHa] quote Gosling's observations, which were confirmed by Huq and Tropper, in that at those stresses where visual observation of the gap through a microscope showed violent particle activity when the conduction current pulses were at a minimum. As the stress was raised the particles left the gap and the current fluctuations increased. It was concluded that no correlation existed between random current pulses and visible particle activity. However in Gallagher's [Si Dl Gall] review the results of Megahed and Tropper are said to be supported by the work by Nelson and McGrath, in that large current pulses are related to particle movement whereas small current pulses are attributed to the ionization of microscopic gas bubbles by electrons from the cathode. These two extracts indicate the disagreement between results but as Gallagher points out direct comparisons between results are difficult when investigators use different conditioning procedures and differently prepared liquids.

7.3

It is also doubtful whether the instrumentation available to the authors would lend much support to their conjectures.

The effects of particles with respect to reducing the resistivity of dielectric liquids can be divided into two main areas. These are the particle as a charge conveyor and the particle as an enhancer of emission at the electrode surface. Stannet [Cond Part Sta] measured the change in conductance of transformer oil before and after the addition of aluminium particles, he found that conductivity increased in proportion to the number of aluminium particles present in the cell. Each of these two topics is dealt with separately in the next two subsections.

7.3.1 Particles as Conveyors of Charge

Several authors have attempted to explain the published conduction curves as the result of a number of particles (size and quantity are usually calculated) oscillating between the electrodes and thus conveying a charge. Krasucki [Cond LD Kras] calculated that the conduction curve obtained by House [Thes Hou] could be explained (to a good approximation) by one particle of 188 nm radius or 646 particles of 1.88 nm radius. Fig. 7.3.1.1 shows the results of similar calculations as made by Birlasekaran and Darveniza [Part Calc Bir]. The statement made by Morant (published in the proceedings of the Grenoble conference) is relevant not only to the work of Krasucki (to which he refers) but also the later work in [Part Calc Bir]. Morant states that the two sizes of particles considered by Krasuki (0.188 μm and 0.0188 μm) would be too small to be seen even with the aid of a

7.3.1

Liquid	Investigator	Filter pore size (μm)	Particles postulated Number	Radius (μm)
n-hexane at a 50 μm gap	Goodwin and MacFadyen (1953)	–	33 or 2	0.12 or 0.3
	House (1957)	5 to 10	11	0.04
	Sletten and Lewis (1963)	1	3	0.04
	Zaky *et al.* (1963)	1	6	0.06
Transformer oil at a 1000 μm gap	Zein El-Dine *et al.* (1965)	1	460	0.5
	Sugita *et al.* (1960)	–	153	0.5

Fig. 7.3.1.1. Number and size of carbon particles to give the best fit between calculated and experimental current-field curves (after Part Calc Bir).

microscope and scattered light. However reproducibility is considered to be the significant point. If the current is carried by particles Morant felt it reasonable to assume that workers would obtain different current/stress plots owing to the inevitable variation of contamination. Reproducibility had been obtained by many experimenters. Gallagher [Si D1 Gall] states that in his work on liquid argon (which he considered to be more contaminated than dielectric liquids at room temperature) a steady current of no greater than 10^{-14} A was recorded. He concludes that either particles of any size were practically non existent, which he considers most unlikely, or charge transported by particles is insignificant in argon. The work of Rhodes [Thes Rho] confirms this view. Rhodes measured the charge believed to be carried by particles and obtained values of the order of a few femto Coulombs. At values of stress up to 25 MV m^{-1} Rhodes used an audio visual technique to establish a link between the small femto Coulomb pulses and the motion of a particle. The signal from the charge sensitive amplifier was fed to a loudspeaker via an audio amplifier so that the small charge pulses could be heard as discrete 'clicks'. Rhodes reports that

7.3.1

direct observation of the gap whilst listening to the loudspeaker showed that when one of the larger particles (seenas a point of scattered light) oscillated between the electrodes a series of clicks was heard. The value of the total current as compared with the impulsive current (assumed to be due to impurities) is shown in Fig. 7.3.1.2.

The work presented in [Cond Part Fel] does not substantiate a model in which the main charge transfer mechanism is due to particles. They suggested that although the charge gained by a particle in contact with an electrode obtained the value defined by classical

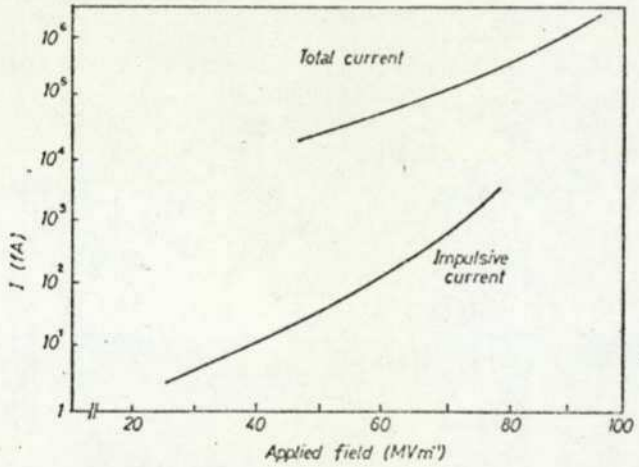

The dependence on applied field of the total conduction current, and of the amount of current due to pulses.

Fig. 7.3.1.2 (after Part Cond Rho).

electrostatics theory, as the particle leaves the electrode the charge becomes shielded by the fluid or some excess charge is lost to the liquid. This results in a charge proportional to the radius of the particle. The value of current, using this assumption of a constant potential on the particle, gives an expression in which the conduction current is proportional to the square of the applied stress. This agrees with the measurements made by Stannet [Cond Part Sta] with aluminium particles in transformer oil. Rhodes [Part Cond Rho] was able with the aid of a charge sensitive amplifier to measure directly

the charge transferred and applying Felsenthal and Vonnegut's hypothesis, calculated the potential on the impurities in his cell to be 12 V. This value compares favourably with that given in [Cond Part Fel] of 16 V for liquid Freon.

Coelho and Gosse [Bd LD Coel] mention ways in which a particle suspended in a liquid may become charged by trapping ions or by the presence of an electrochemical potential (between the particle and the liquid). They state that no particle may carry a charge greater than $\frac{r^2}{10}$ (where r is the radius of the particle) as the field at the surface of such a particle would cause discharging by field emission.

The role of sub-micron size particles has been examined by Mirza et al [Liq Mot Mir] at low values of stress (0.5 MV m^{-1}). Fig. 7.3.1.3 shows the conduction current in n-hexane, both maximum

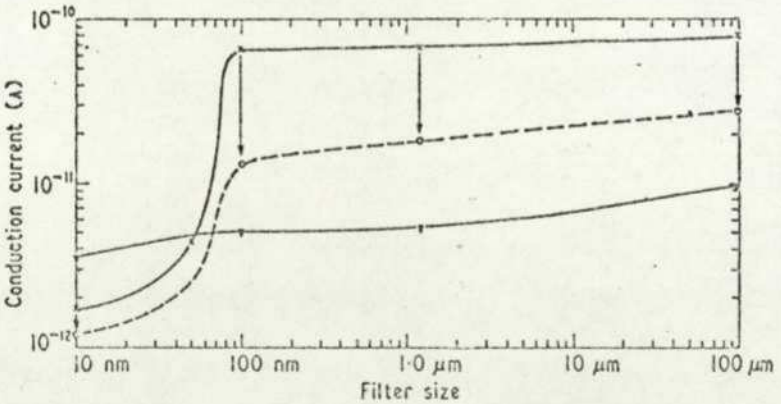

Effect of filtering *n*-hexane and transformer oil on conduction current. × maximum conduction current in *n*-hexane; ○ value of conduction current near equilibrium after several hours; ▽ conduction current in transformer oil.

Fig. 7.3.1.3 (after Liq Mot Mir).

and steady state values, for varying degrees of filtration. This graph shows that a decrease in the level of current by a factor of 20 occurred when particles whose diameters were less than 0.1 μm were removed from the liquid. The removal of particles in the range 0.1 μm to 100 μm had little effect on the conduction current. The change for transformer oil is small compared with n-hexane. This

graph also highlights one of the other effects attributed to particles, that is the initial peaking and decaying of the conduction current to a steady level following the sudden application of a constant stress. Fig. 7.3.2.3a shows this effect as seen by Hesketh and Lewis [Cros Wir Hes] where, after each increase in stress the current reaches a peak and returns to a new constant level (their experiment is described in further detail in Section 7.3.2). This effect was thought to be due to sub-microscopic (less 0.1 μm) particles suspended in the fluid. Fig. 7.3.1.3 shows a decrease in the difference between the maximum and the average current as the size of particles present is reduced. Further evidence to support this theory is given by Matuszewski et al [Rot Cond Mat 1, 2]. In this work test cells were designed and constructed for use with a high speed centrifuge capable of rotating at up to 16,000 revolutions per minute (r.p.m.) Fig. 7.3.1.4 shows the change in the conductivity of

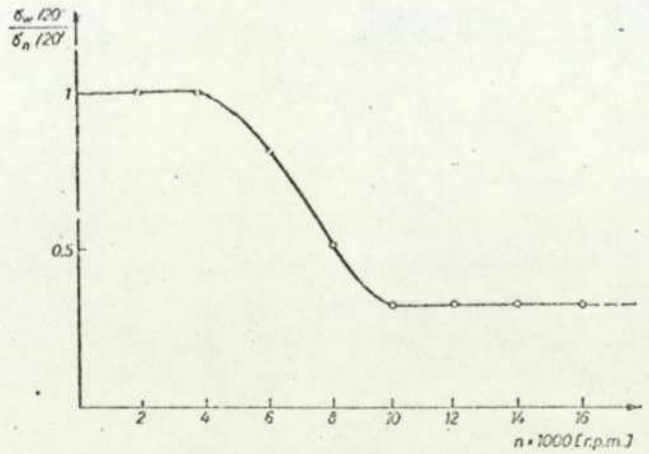

The ratio of the intrinsic conductivity after and before rotation as a rotation frequency function (Chamber I; cyclo-hexane: E = 425 V/cm; t = 15 min)

Fig. 7.3.1.4 (after Rot Cond Mat2).

the sample as the rotational speed of the centrifuge is increased. Thus as the sub-microscopic particles are forced into the capture region (i.e. away from the conductivity test area) of the cell they have less effect on the conductivity of the liquid. At speeds above

10,000 r.p.m. there is little change and it must be assumed that all the solid impurities are clear of the measuring area. The specimen was centrifuged for 15 minutes before each reading was taken. Fig. 7.3.1.5 shows the effect on the current decay with and without rotation.

Pohl [Fie Eff Pohl] has also calculated the effects of suspended particles in a coaxial test cell and shows that the initial attraction

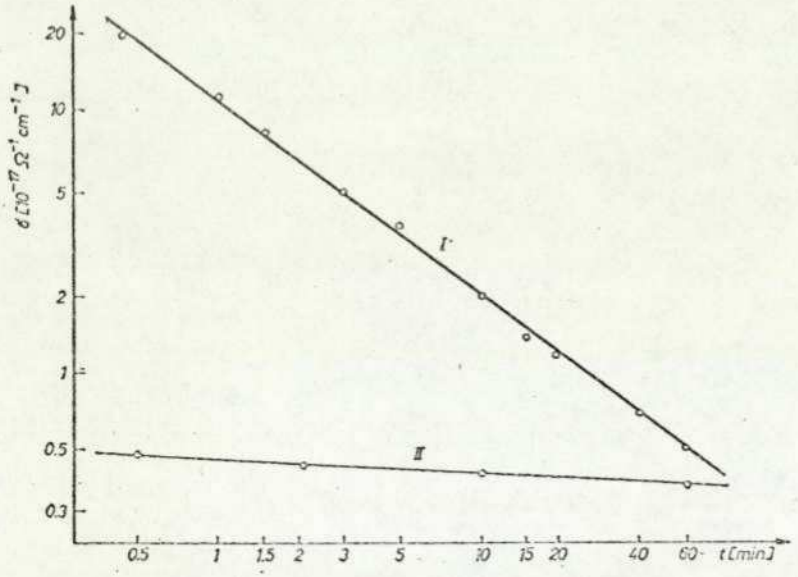

Background time dependence before and after rotation (Chamber I; cyclo-hexane: E = 425 V/cm; n = 16500 r.p.m.; t = 15 min)

Fig. 7.3.1.5 (after Rot Cond Mat2).

of particles to the central electrode due to the dielectrophoretic force is gradually overcome by the repulsive effects of the charge accumulated on the particle due to ionic conduction in the liquid.

7.3.2 The Role of the Particle in Increasing Field Emission

Cantril and Pohl [Ind Cond Can] found that the presence of insulating particles in a coaxial test cell arrangement increased the conduction current considerably. The authors state that in most cases the current was increased by a factor of 3 when particles were

present. To account for such a large factor by the effective enlargement of the central electrode as if by a conducting layer, (which it was not) the authors estimated an increase in the electrode diameter of 10.5 times would be required. As the impurities were insulators this simple model was dismissed. The suggestion put forward to explain the increase in current was that field intensification at the edge of the particle (when resting on the electrode) causedenhanced electron emission. The particles are pulled dielectrophoretically into the region of highest field intensity where they tend to locally intensify the field even further. Fig. 7.3.2.1 demonstrates this effect. The consequence of the presence of the particle on the electrode and the resultant increase in field was calculated and shown to be in good agreement with the values obtained in practice. Fig. 7.3.2.2 shows the current obtained with liquid toluene with PVC particles added. The increased values of current with particles present is clear. The authors concluded that their theory of insulating particles adhering to the inner electrode and increasing the field emission of electrons was valid. Young [Cond To You] comments that layers of carbon particles particularly on the cathode may be a contributory factor in increasing the conduction current in his system.

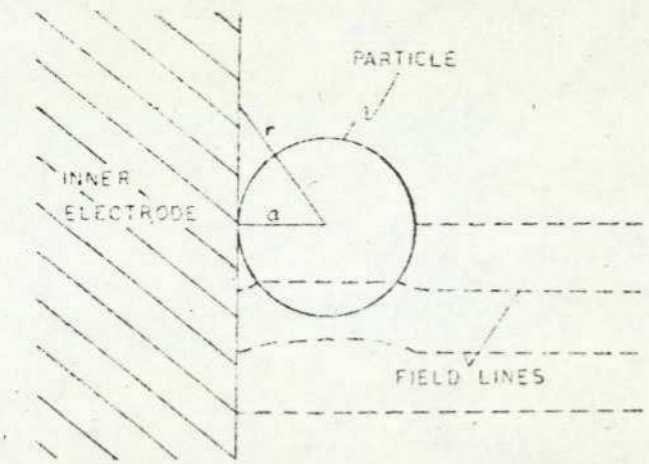

Sketch of particle at center electrode showing field intensification.

Fig. 7.3.2.1 (after Ind Cond Can).

7.3.2

The work of Hesketh and Lewis [Cros Wir Hes] has already been referred to with regard to current decay. In their unusual test cell they were able to analyse the effects of a small drop (less than 10^{-9} m^3) of liquid under stresses of up to 80 MV m^{-1}. The test cell comprised two crossed wires the distance between which (at their point of intersection) could be adjusted down to about 3 μm. The droplet was held between the crossed wires by its own surface tension and the authors were able to obtain droplets with no visible particulate contamination. Fig. 7.3.2.3a shows the current waveform after four increases in the

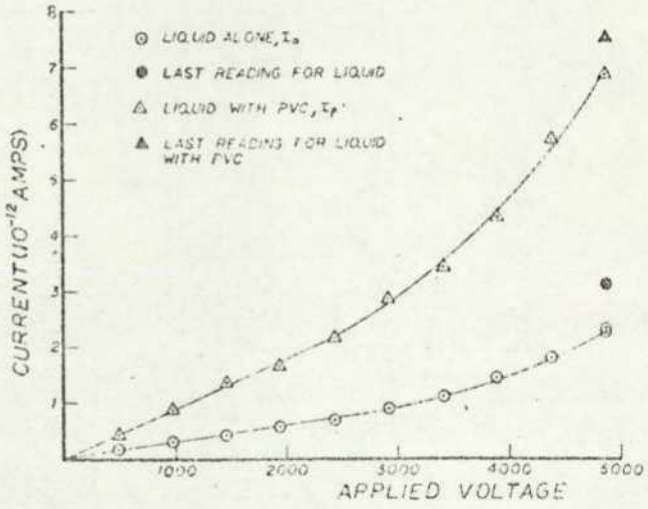

Current vs. voltage curves for liquid alone and liquid with 80-100 mesh size PVC

Fig. 7.3.2.2 (after Ind Cond Can).

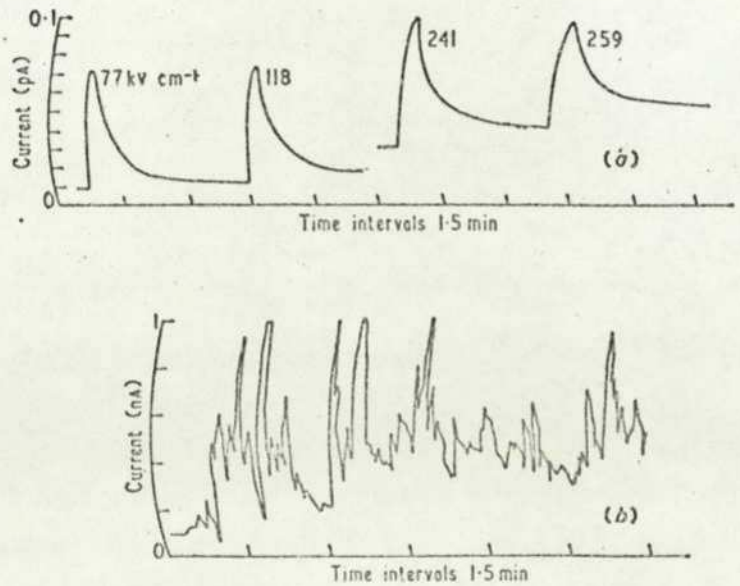

Current-time curves. (*a*) Current through droplet of *n*-hexane showing relaxation phenomena after each stress change. Final currents are highly stable. (*b*) Current fluctuations when cell is completely filled with *n*-decane at a stress of 81 kv cm^{-1}.

Fig. 7.3.2.3 (after Cros Wir Hes).

stress level. Fig. 7.3.2.3b depicts the current waveform obtained when the cell was completely filled (and thus containing particle impurities) with n-decane at a stress of 8.1 MV m^{-1}. This waveform has the characteristic current pulses described by many authors (for example Goodwin and MacFadyen [Cond Bd Good]).

In transformer oil Huq and Tropper [Cond Puls Huq] (mentioned earlier) state that the fluctuating current occurred after the impurity particles had left the inter electrode region. However Sletten and Lewis [Dis Gas Slet] noticed that on occasions the current bursts would start when a big particle arrived at the cathode.

Gosling [Thes Gos] observed that when a cluster of a large particle became attached to the anode, a slight blue glow appeared at its tip with an area of light on the cathode just opposite the particle.

7.4 Dielectric Breakdown Attributed to Particles

In covering the published work relevant to this sub-section it is again apparent that there is a wide variation of opinions and results as to whether particles are the main cause of breakdown. The results for transformer oil with high particle concentrations are more consistent where for both alternating and direct voltages the presence of particles lowers the breakdown strength. Fig. 7.4.1 shows the fall in the alternating voltage strength, as measured by Darveniza [Part To Dar], of transformer oil containing carbon particles in various electrode configurations (the NSB or non-sustained breakdown voltage refers to microdischarges that did not

7.4

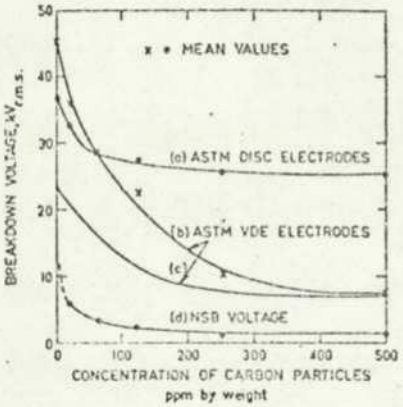

The Electric Strength of Transformer Oil containing Carbon Impurities.

(a) Determined according to ASTM D877-64 at 2 kV/sec.
(b) Determined according to ASTM D1816-60T at ½ kV/sec.
(c) The lower limit of breakdown voltages recorded during tests with VDE electrodes.
(d) Average non-sustained breakdown voltage during 1-kV 1-min. step tests with disc and VDE electrodes.

Fig. 7.4.1 (after Part To Dar).

cause complete breakdown). In this work the formation of a dense cloud of particles between the electrodes usually led to breakdown at a low level without the formation of a bridge. Breakdown at higher values of stress occurred when particles were dispersed in the liquid. The particle velocity is calculated by the authors as a maximum of 0.1 ms^{-1} (a discussion of the possible effects of various particle velocities is given later, see Section 11.4). Bridge formation has been postulated by Kok et al [Bd Liq Kok] as one mechanism which may lead to breakdown, however work in simple liquids by Sletten and Lewis [Dis Gas Slet] and Rhodes [Thes Rho] showed that bridge formation occurred without causing breakdown. A study of bridge formation in transformer oil was carried out by Goswami et al [Imp Part Gosw]. Fig. 7.4.2 shows their results for bridge formation, gap clearing, breakdown, and the critical stress (above which bridges will not form) for various values of stress and frequency.

7.4

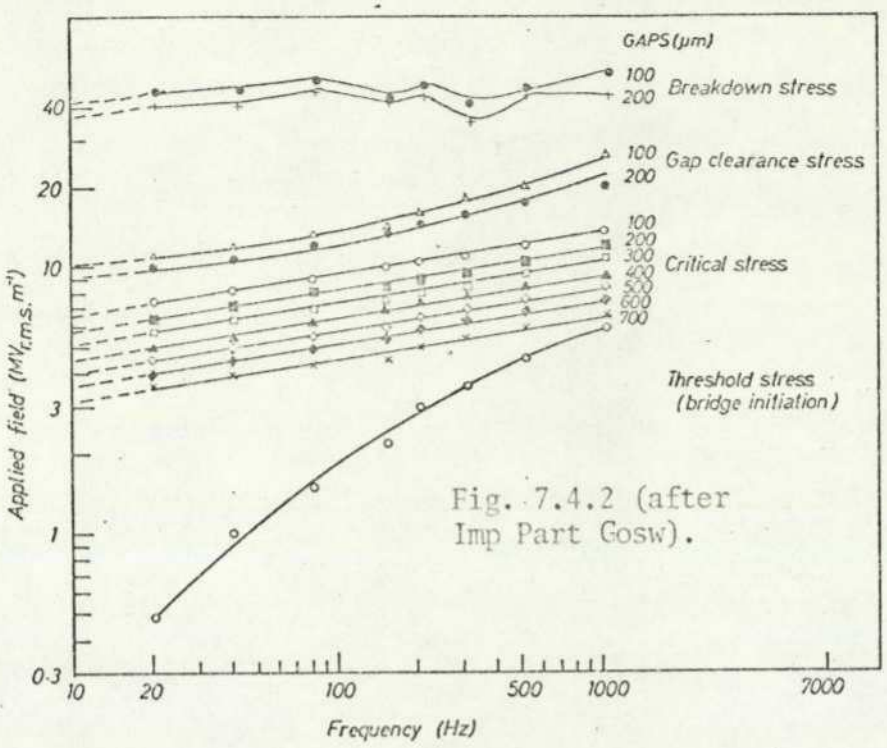

Fig. 7.4.2 (after Imp Part Gosw).

Bridge formation as a function of frequency in transformer oil. containing selenium or silicon particles of sizes ≤ 45 μm.

Young [Cond To You] also working with transformer oil (heavily contaminated) comments that there may be a link between the low voltage resistance and the particle number. Earlier work by this author [Cont To You] showed that the alternating (50 Hz) strength of the liquid stabilized when the particle contamination reached a constant level. The levelling off of the quantity of contamination was thought to be an effect of the agitation produced by the switch and the dispersal of particles into the bulk of the liquid.

The use of liquid motion to clear particles from the high stress region tends to confirm the effects of particles on breakdown values. Abgrall and Cardon [Imp To Abg] found that the strength of transformer oil could be increased if the liquid was filtered after each breakdown. The more prolonged the cyclic filtering the greater the increase in strength. The authors conclude that the particles caused by one breakdown can reduce the subsequent breakdown strength by a factor of 2. They also found that the reduction in strength due

to conducting particles was more pronounced than that due to non-conducting ones (provided the latter was dried). This 'memory' effect has been studied by Bommeli et al [Mem Dis Bom] who use an on-line computer to operate a high voltage high current source, and apply pulses to a series of concentric electrodes in the form of a pseudo random sequence. The computer records the breakdown voltage and its location and then processes the data for plotting. Although some uncertainty is expressed by the authors regarding the interpretation of the initial results and how to overcome effects caused by their cell geometry. Fig. 7.4.3 shows a decrease in the electric strength of paraffin oil with the increase in the level of contamination.

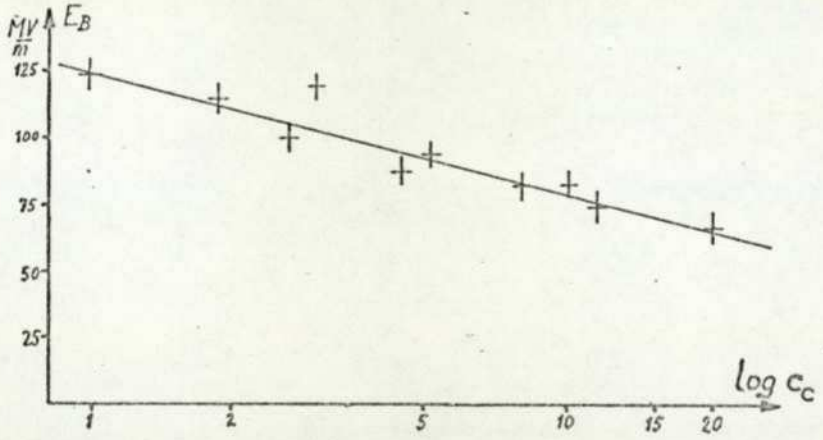

Fig. 7.4.3. The breakdown strength (E_B) of paraffin oil as a function of the concentration of contamination (C_c) in relative units (after Mem Dis Bom).

The effects of moving the liquid through the high stress region have also been studied by Boone and Vermeer [Liq Cir Boo]. Spherical electrodes 1.27 cm in diameter were placed 76 μm apart and a circulating pump was used to force liquid between the electrodes at a speed of 0.4 ms^{-1}; the liquid was recycled through a 1 μm filter. An image of the gap was projected onto a screen so that any

particles moving in the gap could be observed. The strengths of four liquids were tested and it was found that, in each case, the strength when the liquid was being cycled was greater than the stationary strength. The authors observed that particles which started to cross between the electrodes (under the action of the electrophoretic force) were carried out of the gap by the circulating liquid. Boone and Vermeer considered the combination of electric stress and liquid motion to be an ideal way of cleaning electrodes. Fig. 7.4.4 shows a plot of the applied alternating stress to the stationary liquid versus the maximum value of stress obtained for the circulating liquid (these values were obtained by finding the breakdown voltage of the circulating liquid, stopping circulation and measuring the breakdown value of the static liquid). The authors conclude that there is a relationship between the maximum stress applied to the moving liquid and the breakdown stress in the stationary liquid. For values of Em below 1 MV m^{-1} there appears to be no pre-stressing effect, but above this level the two values become equal. This is believed to be due to particles being increasingly removed from the gap when the stress exceeds critical level of 1 MV m^{-1}. Nelson et al [Larg Elec Nel] made similar findings with transformer oil in a cell

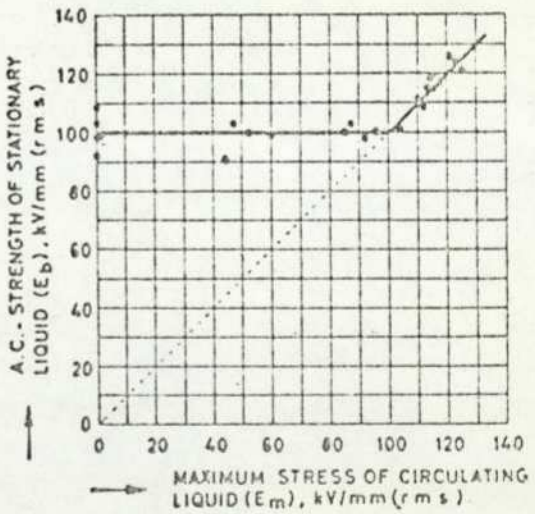

A.C - STRENGTH OF STATIONARY LIQUID AS A FUNCTION OF MAXIMUM STRESS OF CIRCULATING LIQUID.

Fig. 7.4.4 (after Liq Cir Boo).

with a large electrode area. Figs. 7.4.5a,b show the increase in breakdown value when the liquid is circulated. These two graphs also show that the breakdown distribution for the static fluid is an extreme value distribution while the one for the circulating liquid is normal. Boone and Vermeer confirm this result [Liq Cir Boo] for alternating stress conditions and Centurioni et al [Flo Liq Cen] for both alternating and direct stresses.

Gallagher [Mag Fie Gal1] posits that the increase in breakdown strength (in the presence of a magnetic field) may be partly due to the removal of particles from the high field region (in this case under the action of the Lorentz force).

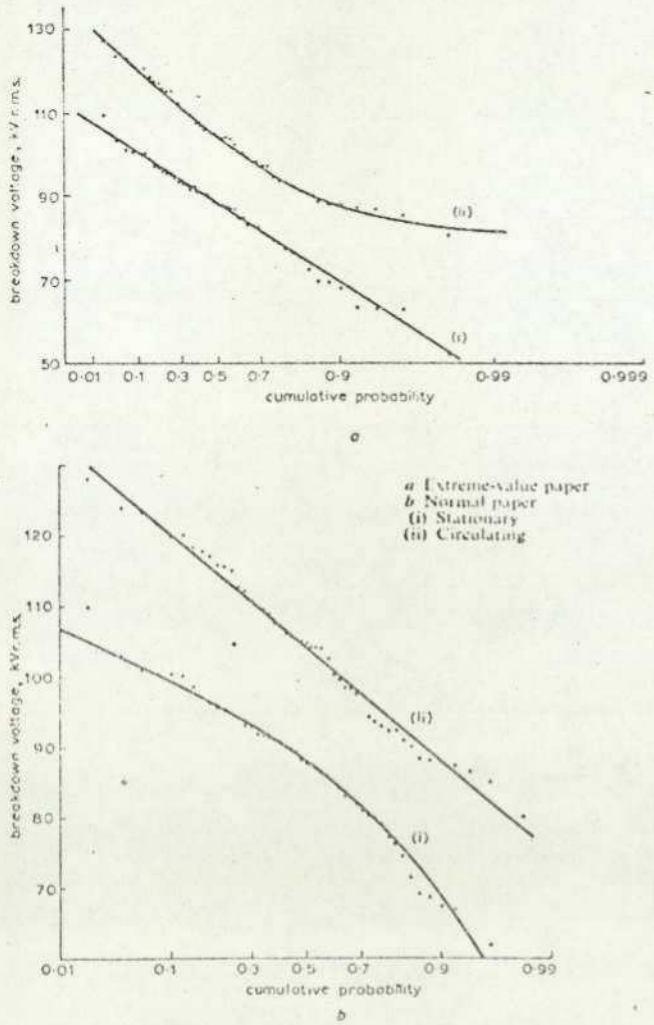

Fig. 7.4.5. Cumulative probability for stationary and circulating oil samples (after Lang Elec Nel).

Some effects of particles in gas insulating systems will now be discussed. Mulcahy [Part Air Mul] studied the effects of the presence of insulating and conducting particles and fibres on the breakdown strength of air at atmospheric pressure. He reports the oscillatory motion of fibres, between the electrodes, along the field lines. Insulating particles had little effect on the breakdown voltage, but conducting particles and fibres (insulating and conducting) reduced the

breakdown strength by as much as 40%. Wet fibres are reported to oscillate out of the gap. The reduction in strength is believed to be due to effective gap shortening by the presence of fibres and increased field emission at the tips of fibres and particles.

With respect to a vacuum insulating system containing carbon particles, Gray [Carb Part Gray] considers what happens when a charged particle approaches one of the electrodes. He calculates that a typical discharge started by the approach of a charged particle (1 μm in diameter) will neutralize the charge on the particle in 10^{-15} seconds. He therefore rules out the approach of particles as the major cause of breakdowns in his system.

The effect of adding small copper wires was demonstrated by Cookson and Farish [Part Bd Cook]. Their results for 150/250 mm coaxial electrode cell containing compressed SF_6 with 0.4 mm particles is shown in Fig. 7.4.6. At a given pressure increasing the size of the particle lowers the breakdown strength.

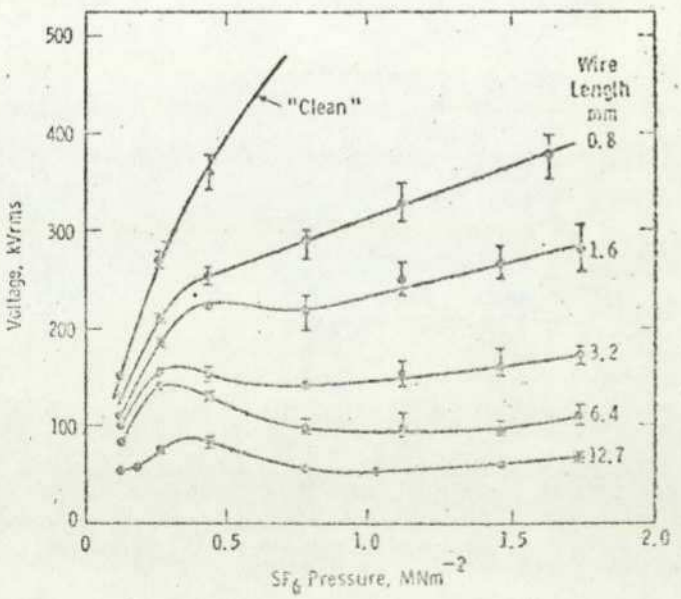

Breakdown initiated by free copper wire particles in 150 mm/250 mm coaxial electrode system: wire dia. 0.4 mm

Fig. 7.4.6 (after Part Bd Cook).

These authors worked with particles both fixed to the electrode and free to move. The authors state that whether particles are able to cross the gap or not, free conducting particles do not behave like particles fixed on an electrode (i.e. breakdown is not simply

due to field enhancement). Microdischarges occurring between fibres and the electrode are thought to be the mechanism causing breakdowns.

Finally, to conclude this section relating to breakdown, the work of Thomas and Forster [Cond Bd Tho, Mol Stru Tho] is reported. These authors have developed a high speed schlieren photographic system which can take one picture at a predefined time after the stress has been applied to the cell. Using a variable delay between the over-volting of the gap and the firing of the laser pulse (used to expose the photographic film) they have obtained pictures of the breakdown and pre-breakdown events in a plane/plane electrode configuration.

In view of the present authors study one result of Thomas and Forster's work is of particular relevance. Fig. 7.4.7 shows the initiation of a streamer from a suspended particle in liquid

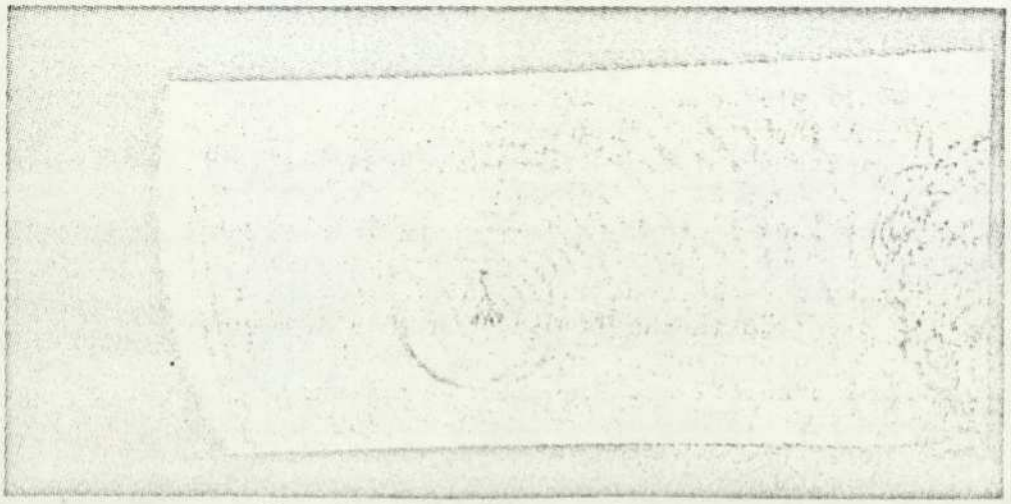

Fig. 7.4.7. Laser schlieren photograph in toluene (after Mol Stru Tho).

toluene. The main breakdown arc, due to the rapid over-volting of the gap, occurs at the right hand side of this figure. The authors consider that this streamer may be evidence for the initiation

breakdown in the liquid as opposed to at the electrode liquid interface. In this study the over-volting technique was thought to be more likely to cause a rapid breakdown initiated at the cathode, than the slower streamer initiated breakdown starting from a suspended particle. Their photographs show that prior to the breakdown there is a period of plasma growth (from asperities) at the cathode. One of these plasma regions is reported to extend across the gap and cause a breakdown. This process was put forward by Chadband and Wright [Pre Phen Chad] who monitored the growth of a plasma from a point electrode until it caused breakdown. In [Cond Bd Tho] the asperities are said to be irregularities in the cathode surface where electron emission is preferred. This plasma growth may well be what Krasucki [Bd LD Kras] observed as 'dark regions' growing from the electrode. He reports that when particles were visible on the electrode the 'dark region$\overset{s}{\wedge}$' occur preferentially at the particles.

SECTION 8

Theoretical Considerations.

8.1 Introduction

This section contains a variety of theorems and formulae which relate to both Part I and Part II of this Thesis. In Section 8.2 the laws governing the acquisition of data and the manipulation of quantized variables are outlined, together with several examples of how features and parameters have been extracted from captured transients.

Section 8.3 contains a resumé of the Felsenthal and Vonnegut hypothesis, while Section 8.4 gives consideration to a simple model of the forces acting on an ideal particle moving between two spherical electrodes under the influence of an applied field. The current caused by a moving charge is defined in Section 8.5.

8.2 Theoretical Considerations Pertaining to Signal Processing

As waveforms are represented in this work by a sequence of discrete integers, it is necessary to understand the effects of sampling and quantization on a waveform. In the case of the Biomation transient recorder each waveform is represented by 2048 integers each of which can be between -128 and +127, giving 256 levels.

The most important law which must be considered when a signal is converted into a series of discrete numbers is the sampling theorem. This theorem states that the rate at which a signal has to be sampled must be at least twice the value of the highest frequency component present. Thus if frequencies in a signal of up to 1 MHz are to be represented, then the sampling frequency must be at least 2 MHz. It is more usual with waveform analysis to ensure a high enough sampling speed so that the waveform is represented

with as much detail as possible. Failure to obey the sampling theorem leads to the aliasing of some of the frequencies present in the waveform. This is explained with the aid of Fig. 8.2.1 which shows the frequency spectrum of a periodic waveform. If the wave-

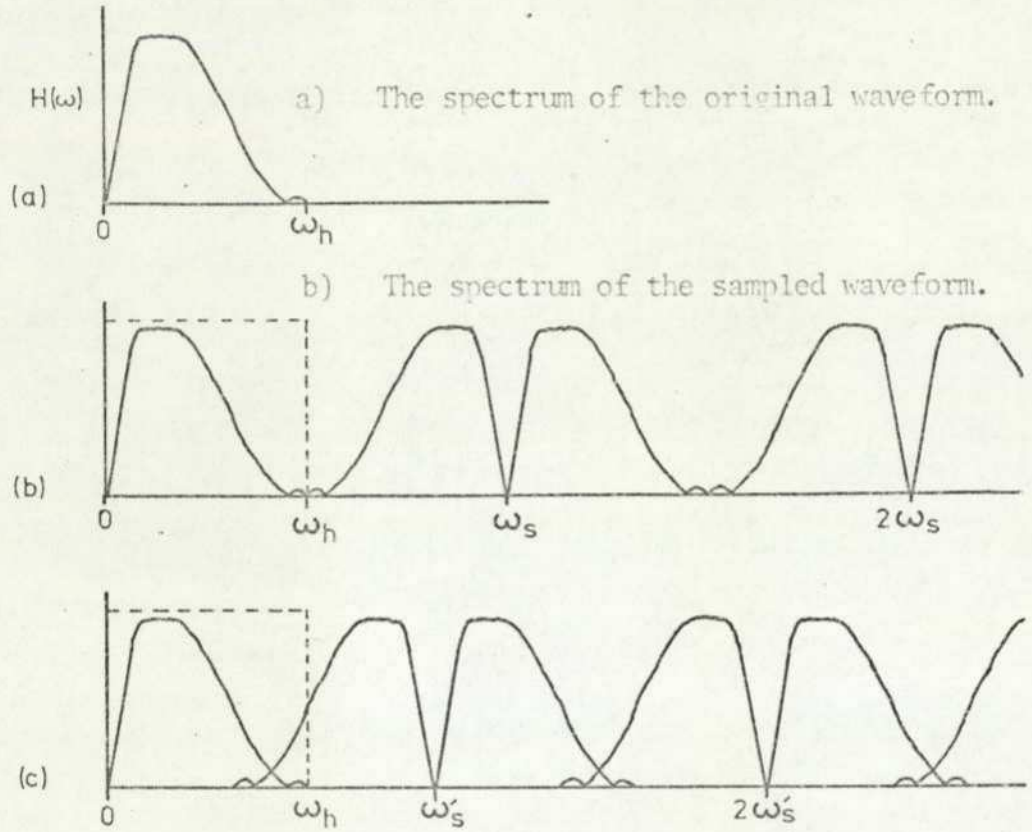

a) The spectrum of the original waveform.

b) The spectrum of the sampled waveform.

c) Aliasing: the effect caused by reducing ω_s to ω_s'. The dotted line represents the filter response necessary to restore the original waveform.

Fig. 8.2.1

form is sampled at an angular frequency ω_s such that $\omega_s \geq 2\,\omega_h$ (where ω_h is the highest frequency present) then the amplitude spectrum of the sampled wave is given by Fig. 8.2.1.b. Each harmonic of ω_s is bounded by the spectrum of the original signal and its image. Should ω_s be reduced, the image frequencies in the region below ω_s' would merge with the frequencies below ω_h. The result is demonstrated in Fig. 8.2.1c. In the region of overlap the frequencies belonging

to the original amplitude spectrum and those of the image of the first harmonic of ω_s' are indistinguishable. In this case low-pass filtering (cut off at ω_h) of the sampled signal would not restore the original waveform but instead present a distorted one.

One precaution which will prevent aliasing of a sampled signal is to filter the signal before it is sampled and to limit the highest frequency in the signal to half the value of the sampling frequency.

The next problem to be considered in signal sampling is the effect of quantization. This is a non-linear process and is represented in Fig. 8.2.2 which shows the transfer characteristic of

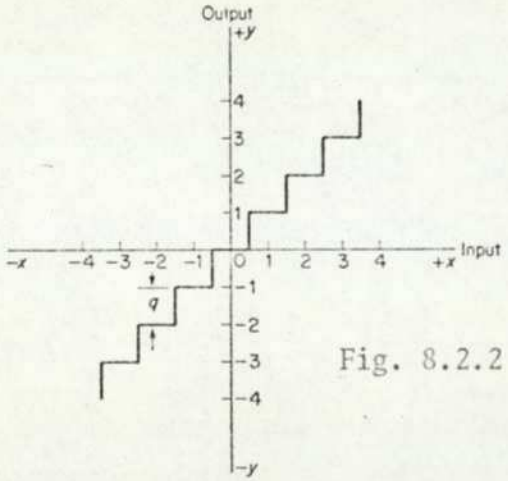

Quantiser transfer characteristic.

Fig. 8.2.2 (after Sig Pro Beau).

a quantizer [Sig Pro Beau]. When a signal is quantized, each sample of the signal must be assigned an integer value. This value is not the actual value of the signal at the sampling point, but one which is an approximation. Thus there is a discrepancy between the value of the actual signal and the integer representation; this is termed the quantization error. The quantization of a signal with the associated error may be represented by

$$q(t) = x(t) + n(t) \qquad \text{Eq. 8.2.1}$$

where x(t) is the original signal, q(t) is the quantized result and n(t) is the difference between these two. Beauchamp [Sig Pro Beau] calculated that for 256 levels of quantization (i.e. 8 bits) the minimum signal to noise ratio is approximately 60 decibels. It is important to recognize the presence of quantization noise when performing any signal processing as operations such as differentiation will amplify the noise component.

One further effect of the analysis of waveforms in a digital manner which must be mentioned is the effect of time limiting a waveform. This occurs when a sampled waveform has a finite number of samples (in the case of the Biomation 8100 transient recorder this number is 2048 or 1024). The consequence of time limiting a signal is to convolve the signal with an oscillating sinc function in the frequency domain (see Fig. 8.2.3a). The principal effect according to

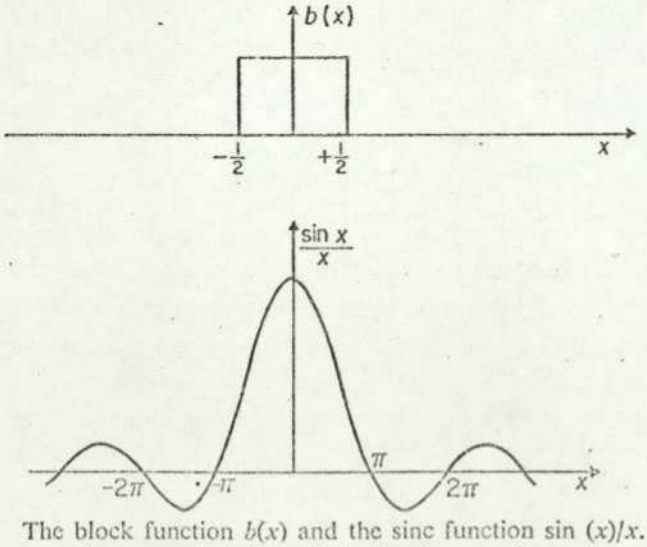

The block function $b(x)$ and the sinc function $\sin(x)/x$. The most important Fourier pair in signal processing

Fig. 8.2.3a (after Lab Comp Brig).

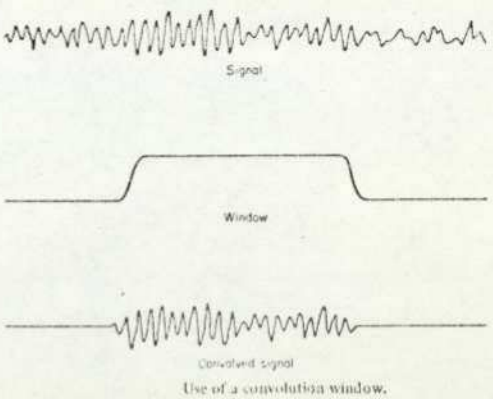

Fig. 8.2.3b. The use of a convolution window (after Sig Pro Beau).

[Lab Comp Brig] is a leakage of energy from each isolated component of the source signal into adjacent frequencies and the consequent introduction of irrelevant minor lobes in the spectrum. To minimize this effect, a convolution window may be used. Fig. 8.2.3b

demonstrates the use of such a window. This window obviates the injection of high frequency transients into the data which arise from the abrupt beginning and end of the waveform. Such windows can be applied to the waveform in the computer before a frequency analysis is performed. Thus in the present analysis transients were considered cyclic about their block length. An example of this is the re-registration that was found necessary on some waveforms (see Section 10.2.3), which had to be shifted forward or backwards relative to a fixed point. The only allowable method under the constraint mentioned above was a cyclic shift which gives the effect that the waveform is periodic about its block length.

The measurement of parameters in the work undertaken usually required specialized software for each feature. As an example the methods of finding two features are described. The charge transferred and the charge transit time are the two measurements considered. Figs. 8.2.4a and b show a typical charge waveform (trace a) and a more detailed view of the leading edge of such a transient (trace b).

The estimate of the charge transferred is obtained by measuring the height of the waveform. The program that finds this parameter firstly locates the peak of the waveform by finding the maximum value of all the data words in the waveform. The value of the peak is copied to the remainder of the transient (starting at the peak) to blank out the exponential decay (this is indicated by the dotted line between F and H in Figs. 8.2.4a and b). The minimum value of the waveform is now located, this will lie somewhere between A and B. The difference between the maximum and minimum values represents to a good approximation the amount of charge transferred. The program

8.2

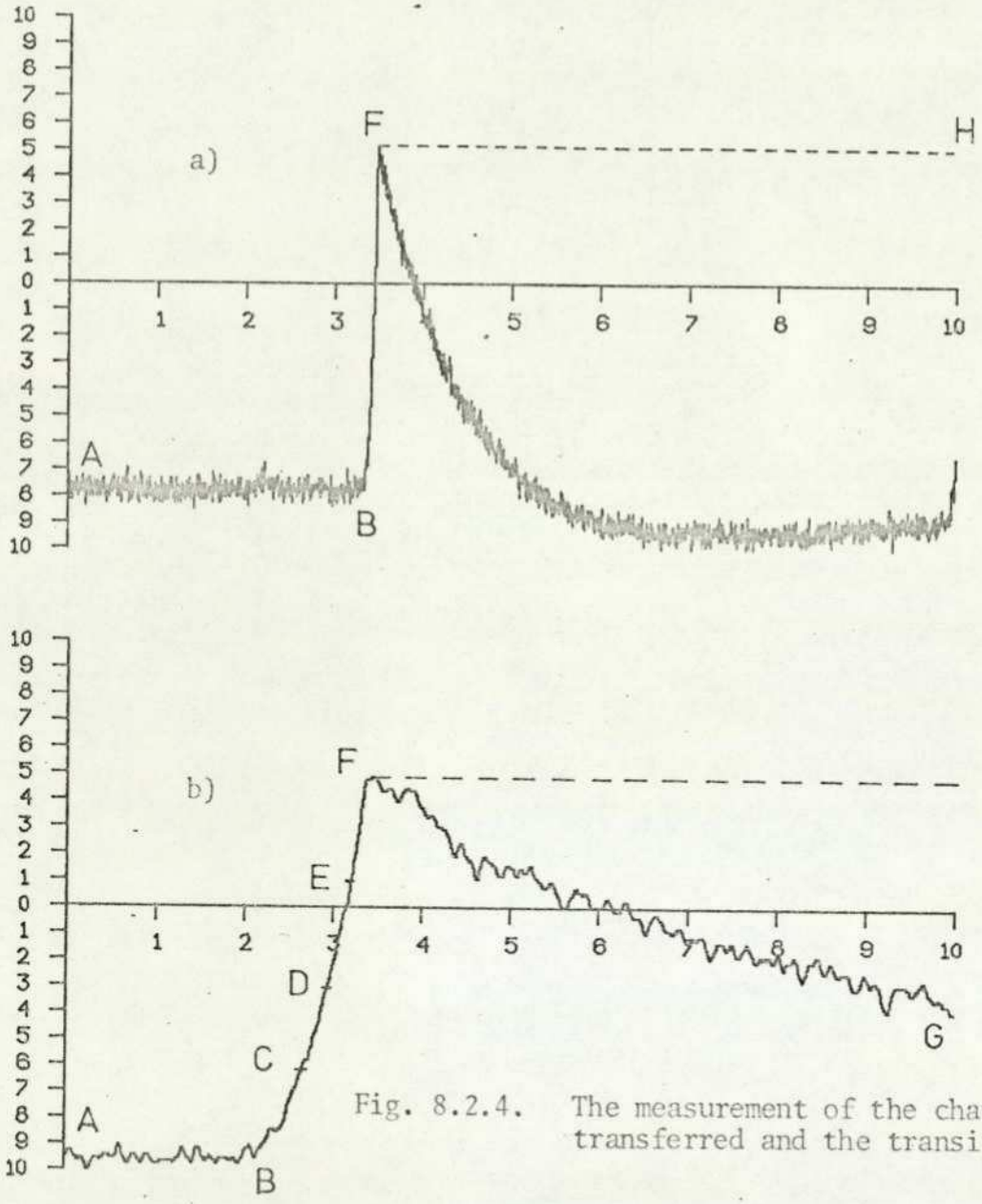

Fig. 8.2.4. The measurement of the charge transferred and the transit time.

can convert the integer value representing the height of the transient into terms of charge by extracting the input range of the transient recorder (which is located in the control program for the recorder, see Appendix I) and using a preset calibration factor.

The method by which the transit time is estimated is now outlined with the aid of Fig. 8.2.4. Each value of the original transient is divided by 129 to convert the integer values to fractions. As before, the peak is located and its value copied to

the remainder of the waveform. The waveform is normalized with respect to its height. This is accomplished by dividing the data by a factor of 2 (to prevent overflow) and finding the new maximum and minimum values. The distance of the mid point (in height) from zero is calculated and the waveform is shifted vertically to make the midpoint value zero. The waveform is now divided by the difference between the maximum and minimum values (i.e. the range of the waveform) which makes the maximum value + 1 and the minimum value - 1. In practice it is arranged so that the maximum is + 0.9999 and minimum is - 0.9999 as the data must remain in fractional form. In Fig. 8.2.4b the normalization described above would lead to point F being + 1, D being + 0 and B being - 1. The program now scans from F backwards through the data area (i.e. towards E) and finds the location whose value is nearest to + 0.5 (E). The location is noted and the program continues to scan until the location of the value closest to + 0.0 is found (D) and similarly for the - 0.5 value (C). The difference between CD and DE is checked to make sure that the leading edge is approximately linear and therefore the assumption that 2 x CE is a reasonable estimate of the transit time. Estimations of the transit times are within 10% and usually better than 5% but this depends on the amount of noise and the shape of the leading edge of the pulse (assumed linear). Fig. 8.2.4b shows in detail a curved leading edge, which is probably due to a particle crossing the gap some distance from the gap centre and thus travelling in a non uniform field. The sample interval setting of the transient recorder is stored in the control software and so can be used to convert the number of store locations which form the leading edge of the pulse, to the value of transit time in seconds.

8.2

One important signal processing technique employed during the measurement of charge transported by impurity particles was that of cumulative averaging. This method of averaging is used to calculate the average of a given number of waveforms (each containing a fixed number of points) without the need to store all the waveforms separately. Only the total average already calculated and the next block to be averaged need be stored in the computer. The following formula defines this operation and is applied to each point in the waveform.

$$y_{(i+1)} = \frac{M+1}{M} y_{(i-1)} + \frac{1}{M} y_{(i)} \qquad \text{Eq. 8.2.2}$$

where:-

$y_{(i-1)}$ is the average of M - 1 waveforms

$y_{(i+1)}$ is the average of M waveforms

$y_{(i)}$ is the waveform to be incorporated in the average.

A good example of this process can be found in [Lab Comp Brig pg 278].

8.3 A Résumé of the Theory of Felsenthal and Vonnegut

As the theory put forward by Felsenthal and Vonnegut [Cond Part Fel] features strongly in Part II of this Thesis, a summary of the formulae they derived is now given.

These authors postulate that the charge obtained by a conducting particle of radius r in contact with an electrode, may be expressed as

$$q = \frac{2}{3} \pi^3 \varepsilon_o \varepsilon_1 r^2 E \qquad \text{Eq. 8.3.1}$$

but the effective charge transported is given by

$$q' = 4 \pi \varepsilon_o \varepsilon_l r V_o \qquad \text{Eq. 8.3.2}$$

where q is the classically predicted charge, q' is the limited charge, V_o is the potential on the particle, ε_l is the relative permittivity of the liquid, E is the electric field. This latter equation indicates that the ratio $\frac{q'}{r}$ is a constant since V_o is defined as a constant.

As the velocity of particles in the experiments performed by Felsenthal and Vonnegut were observed to be constant, a balance between the electrophoretic and viscous forces was assumed. This gives, for a spherical particle

$$q'E = 6 \pi \eta r v \qquad \text{Eq. 8.3.3}$$

where η is the viscosity of the liquid, v is the velocity of the particle.

For a pair of plane parallel electrodes a distance d apart and an applied voltage V, the expression for the electric stress in the gap (assuming no space charge is present) is

$$E = \frac{V}{d} \qquad \text{Eq. 8.3.4}$$

Also for the particle velocity

$$v = \frac{d}{T} \qquad \text{Eq. 8.3.5}$$

8.3

where T is the particle transit time.

Substituting Eq. 8.3.4 into Eq. 8.3.3 gives

$$\frac{q'V}{d} = 6\pi\eta r v \qquad \text{Eq. 8.3.6}$$

substituting, for q' in Eq. 8.3.2 into Eq. 8.3.6 produces

$$v = \frac{2\varepsilon_o\varepsilon_1 V_o V}{3\eta d} \qquad \text{Eq. 8.3.7}$$

This equation shows that the velocity of the particle is proportional to the applied voltage.

Rearranging Eq. 8.3.6 and substituting in Eq. 8.3.5 gives the particle radius as

$$r = \frac{q' T V}{6\pi d^2 \eta} \qquad \text{Eq. 8.3.8}$$

This allows the particle radius to be determined from the charge transferred (q') and the transit time (T). The potential to which the particle is charged can be calculated from Eq. 8.3.2.

8.4 The Forces on a Moving Particle

Some simple analyses of the forces acting on a spherical particle moving in a stationary fluid have been undertaken by the present author in an attempt to link the observed phenomena with theory. Little success has been achieved in this attempt for reasons which are

8.4

stated. Some of the work is produced below as it may be of use to other workers in the field.

Fig. 8.4.1 indicates the forces acting on a spherical particle as it crosses between two spherical electrodes.

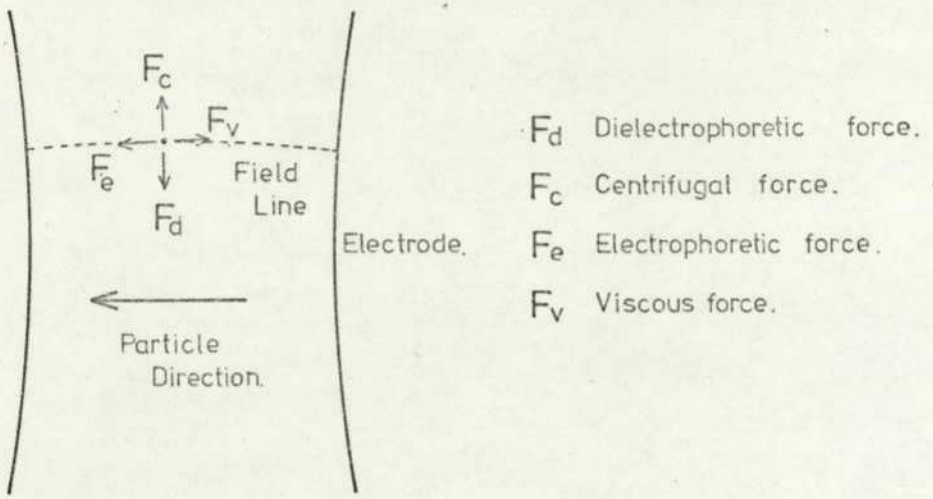

Fig. 8.4.1. The forces on a charged spherical particle in motion between two electrodes.

Four main forces are considered in the simple model, these are the electrophoretic (F_e), viscous (F_v), dielectrophoretic (F_d), and centrifugal (F_c) forces. As the particle travels between the electrodes at a linear speed [Part Cond Fel] the electrophoretic and viscous forces are assumed to be equal and opposite in magnitude. The distance that a particle will oscillate from the centre of the gap depends on the values of F_c and F_d, which act in opposition. Unfortunately F_d is difficult to evaluate owing to the need to assign a value to the permittivity of the particle (see Eq. 7.2.1).

It was decided to consider the ratio of the centrifugal and dielectrophoretic forces to establish their relation. Thus for a particle of density S, radius r, mobility μ, relative permittivity ε_p describing a curve of radius r_F the ratio of F_c to F_d is given

8.4

by

$$\frac{F_c}{F_d} = \frac{(4/3)\pi r^3 3\mu^2 E^2}{r_F 4\pi \varepsilon_1 \left(\frac{\varepsilon_p - \varepsilon_1}{2\varepsilon_1 + \varepsilon_p}\right) r^3 E \nabla E} \qquad \text{Eq. 8.4.1}$$

which reduces to

$$\frac{3\mu^2 E}{3 r_F \varepsilon_1 \left(\frac{\varepsilon_p - \varepsilon_1}{2\varepsilon_1 + \varepsilon_p}\right) \nabla E} \qquad \text{Eq. 8.4.2a}$$

then separating out the constants for a given particle and liquid gives

$$\frac{3\mu^2}{3 \varepsilon_1 \left(\frac{\varepsilon_p - \varepsilon_1}{2\varepsilon_1 + \varepsilon_p}\right)} \cdot \frac{E}{r_F \nabla E} \qquad \text{Eq. 8.4.2b}$$

The dimensionless quantity $E(r_F \nabla E)^{-1}$ is intrinsic to the spherical electrode system. Values of the electric field at various points in the gap have been calculated by Thwaites [Elec Fie Th]. More recently Garton [Dis Pot Gar] derives an expression which produces an approximation to the value of stress along the central plane of the gap. It is this latter expression which is now used to evaluate the function $E(r_F \nabla E)^{-1}$.

The field along the central plane of the gap a distance X from the centre of the gap is given by

$$E_x = E\left(1 + \frac{x^2}{Rd} + \frac{x^4}{12R^3 d}\right)^{-1} \qquad \text{Eq. 8.4.3}$$

where E is the applied voltage divided by the minimum gap distance (d) and R is the radius of the electrodes.

Differentiating Eq. 8.4.3 to obtain ∇E_x produces

$$\nabla E = -E\left(1+\frac{x^2}{Rd}+\frac{x^4}{12R^3d}\right)^{-2}\left(\frac{2x}{Rd}+\frac{4x^3}{12R^3d}\right) \qquad \text{Eq. 8.4.4}$$

To evaluate r_F the radius of the arc described by the particle as it crosses between the electrodes Fig. 8.4.2 has been included to demonstrate the geometrical proof that r_F can be written as

$$r_F = \frac{R(1-\cos\phi)+d/2}{\sin\phi} \qquad \text{Eq. 8.4.5}$$

This can be simply converted to the variables employed in Garton's equations:

$$r_F = \left(\frac{x}{2}+\frac{Rd}{2x}+\frac{xd}{8R}\right) \qquad \text{Eq. 8.4.6}$$

Substituting Eq. 8.4.4 and Eq. 8.4.6 into $E(r_F\nabla E)^{-1}$ produces the following result.

$$\frac{E_x}{r_F\nabla E_x} = -\frac{1+\frac{x^2}{Rd}+\frac{x^4}{12R^3d}}{1+\frac{x^2}{Rd}\left(1+\frac{5R}{12d}\right)+\frac{x^4}{12R^3d}\left(2+\frac{R}{2d}\right)} \qquad \text{Eq. 8.4.7}$$

8.4

Note that the term E disappears which proves that the ratio is only dependent on the electrode geometry.

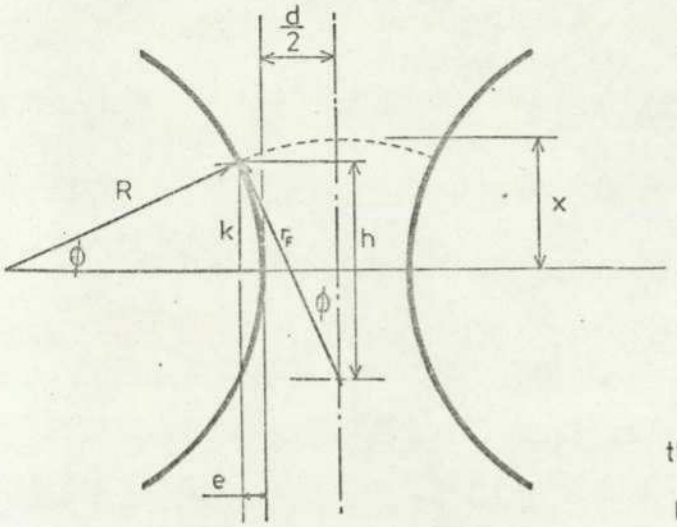

Since

$$\phi = \sin^{-1}\frac{k}{R} \quad ,$$

$$e = R(1-\cos\phi)$$

and

$$\sin\phi = \frac{e + d/2}{r_F}$$

therefore

$$r_F = \frac{R(1-\cos\phi) + d/2}{\sin\phi} \quad .$$

The distance x is given by

$$x = r_F - h + k \quad = \quad r_F - r_F\cos\phi + k$$

substituting for r_F gives $k + \dfrac{(R(1-\cos\phi) + d/2)(1-\cos\phi)}{\sin\phi}$.

Fig. 3.4.2. The proof of the relationship between the radius of curvature of a field line and the distance (k) the field line is from the centre of the gap at its point of contact with the electrode.

The values of 0.005 m for the electrode radius and 100 x 10^{-6} m for the minimum electrode spacing when substituted into Eq. 8.4.7 gave the following results for five values of X .

X μM	$E(r_F \nabla E)^{-1}$
0	1.0
10	0.99999833
50	0.99995803
100	0.99982871
200	0.99926364
400	0.99643110

8.4

The ratio of the dielectrophoretic and centrifugal forces is thus largely dependent on the value of the constant term in which δ and ε_p are unknown.

$$\frac{\delta\mu}{3\varepsilon_1\left(\frac{\varepsilon_p - \varepsilon_1}{2\varepsilon_1 + \varepsilon_p}\right)} \qquad \text{Eq. 8.4.8}$$

It should be noted that the approximation of the field by Garton is not sufficiently accurate for this analysis, especially when it is divided by its derivative which will be an even less accurate approximation to the gradient of the field.

The ratio $E(r_F \nabla E)^{-1}$ is none the less an important one and the use of a large computer to evaluate Thwaites' expressions for the field components may be a more worthwhile approach to this problem.

8.5 The Current Contributed by a Moving Charged Particle

It is important to recognize that the current caused by a charged impurity particle moving between two electrodes is dependent on the velocity of the particle. In the presence or absence of a space charge the current is given by

$$i = \frac{q'v}{\tau} \qquad \text{Eq. 8.5.1}$$

Where q' is the charge transported, v the velocity of the particle and τ the transit time.

8.5

In the case of spherical electrodes a particle will give a higher current if it traverses the gap at its shortest point than if it moves along a longer path away from the centre of the gap. Note that the current flows the whole time the particle is in motion.

The current in a non-uniform gap is given by the Shockley-Ramo Theorem [Mov Char Sho, Elec Mot Ram] which includes a geometric factor determined by the position in the given geometry. In this case the geometric factor is numerically the field factor tabulated by Thwaites.

SECTION 9

Apparatus.

9.1 Introduction

This section contains the more important details of the apparatus utilized in the measurements described in Section 10, together with comments on the liquid tested and the methods of purification.

As an optical technique was developed to detect particle impurities in motion, Section 9.7 contains details of the photo-multiplier, the light source and other auxil ary devices.

9.2 The Dielectric Liquid

The liquid studied throughout the present author's work was the 'puriss' grade of n-hexane produced by Koch-Light Laboratories Limited. Figs. 9.2.1 a and b give details of the composition and properties of the liquid as stated by the manufacturers, together with the chromatogram obtained by Kahan and Morant [Che Pur Ka] for this grade of liquid. The 'puriss' grade according to [Che Pur Ka] contains far less chemical contaminants, even prior to purification, than the 'special for spectroscopy' grade used by many of the earlier workers (Kahan and Morant found only 77% n-hexane in this liquid).

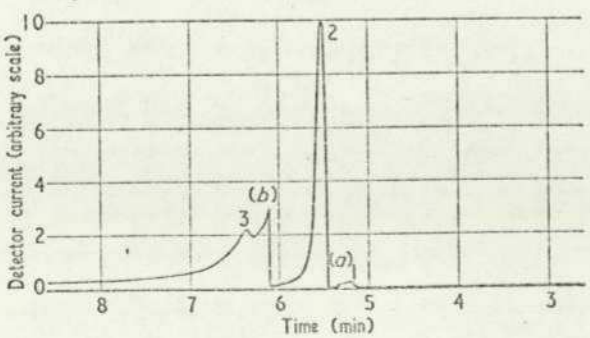

Chromatogram of 99% pure *n*-hexane. (The vertical sensitivity was reduced by 33 times between (*a*) and (*b*).)

Fig. 9.2.1a (after Che Pur Ka).

9.3

Composition		Properties	
2,4 Dimethyl pentane	0.07%	Molecular weight	86.18
2- Methyl pentane	0.2%	Freezing point	-95.5°C
3- Methyl pentane	0.3%	Boiling point	67-71°C
Methylcyclopentane	0.2%	Specific gravity 20/4°C	0.660
Benzene	0.015%	Non-volatile matter	0.005 g/100mL
Hexane	99.2%		

Fig. 9.2.1b (after Thes Rho).

9.3 The Purification of the Liquid

The liquid is initially filtered and distilled in apparatus developed by previous researchers in the author's laboratory before being passed to the closed loop filtering system which incorporates the modified version of Rhodes' [Thes Rho] test cell.

9.3.1 The Distillation Process

The distillation plant is featured diagrammatically in Fig. 9.3.1.1 and also in Plate 9.3.1.1 (with the author's cyclic filtering system connected).

Following comments by Hewish (private communication), who found the effects of the existing silica-gel column and molecular sieve to be deleterious to the liquids the n-hexane was poured directly into the 500 mL flask located just below tap J (see Fig. 9.3.1.1). The process proceeds as follows. With the system evacuated to better than 10^{-6} Torr (the section to the left of the valve G) valve F is closed and the temperature of the distillation flask is lowered to around -80°C. A thermos filled with a mixture of methyl alcohol and liquid nitrogen controls the temperature of the flask. This is achieved by raising or lowering the vessel which increases or decreases the amount of cold fluid in contact with the glass wall of the flask (see Fig. 9.3.1.1). Valve G is opened slightly; this draws the liquid through

HEXANE PURIFICATION PLANT

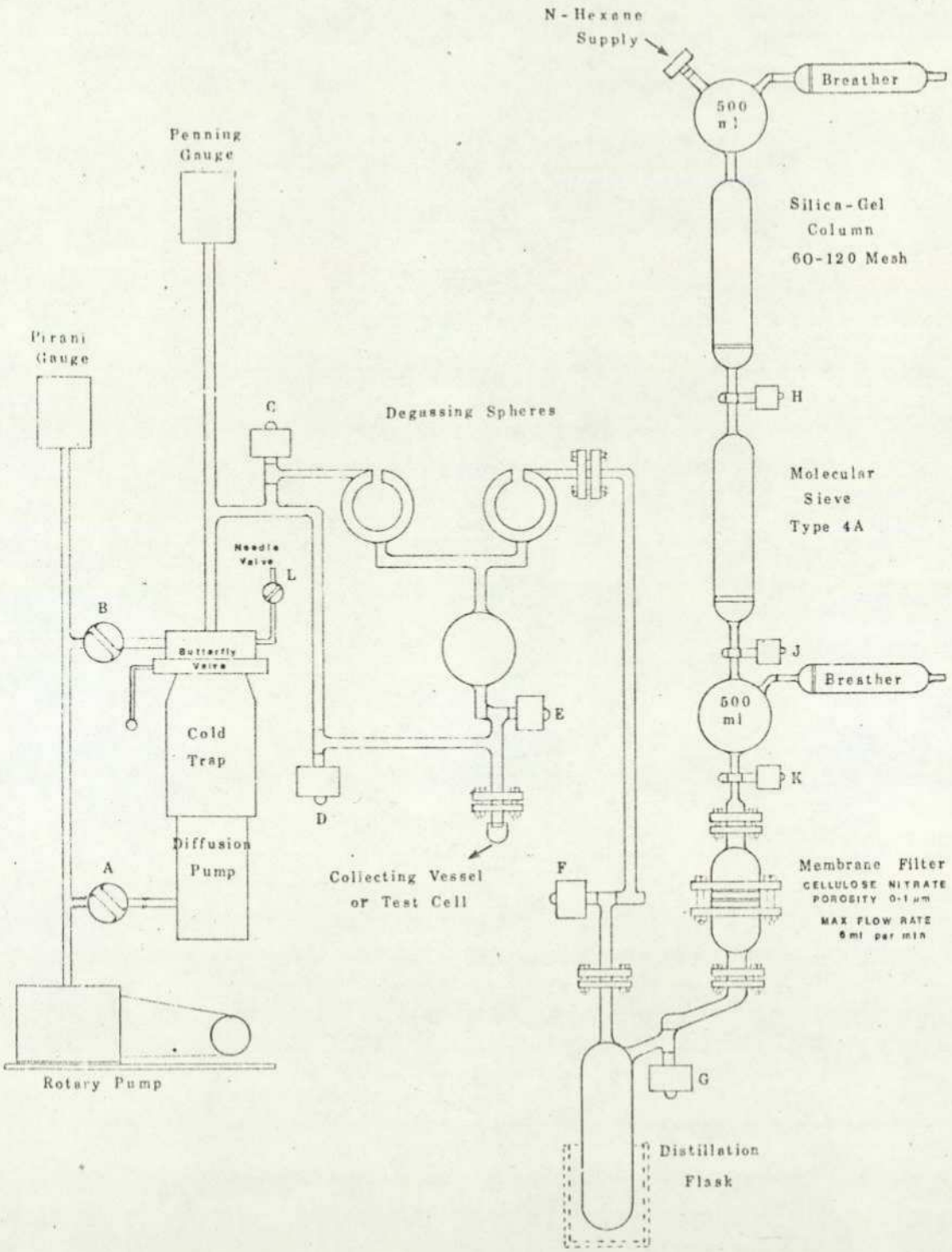

Fig. 9.3.1.1

9.3.1

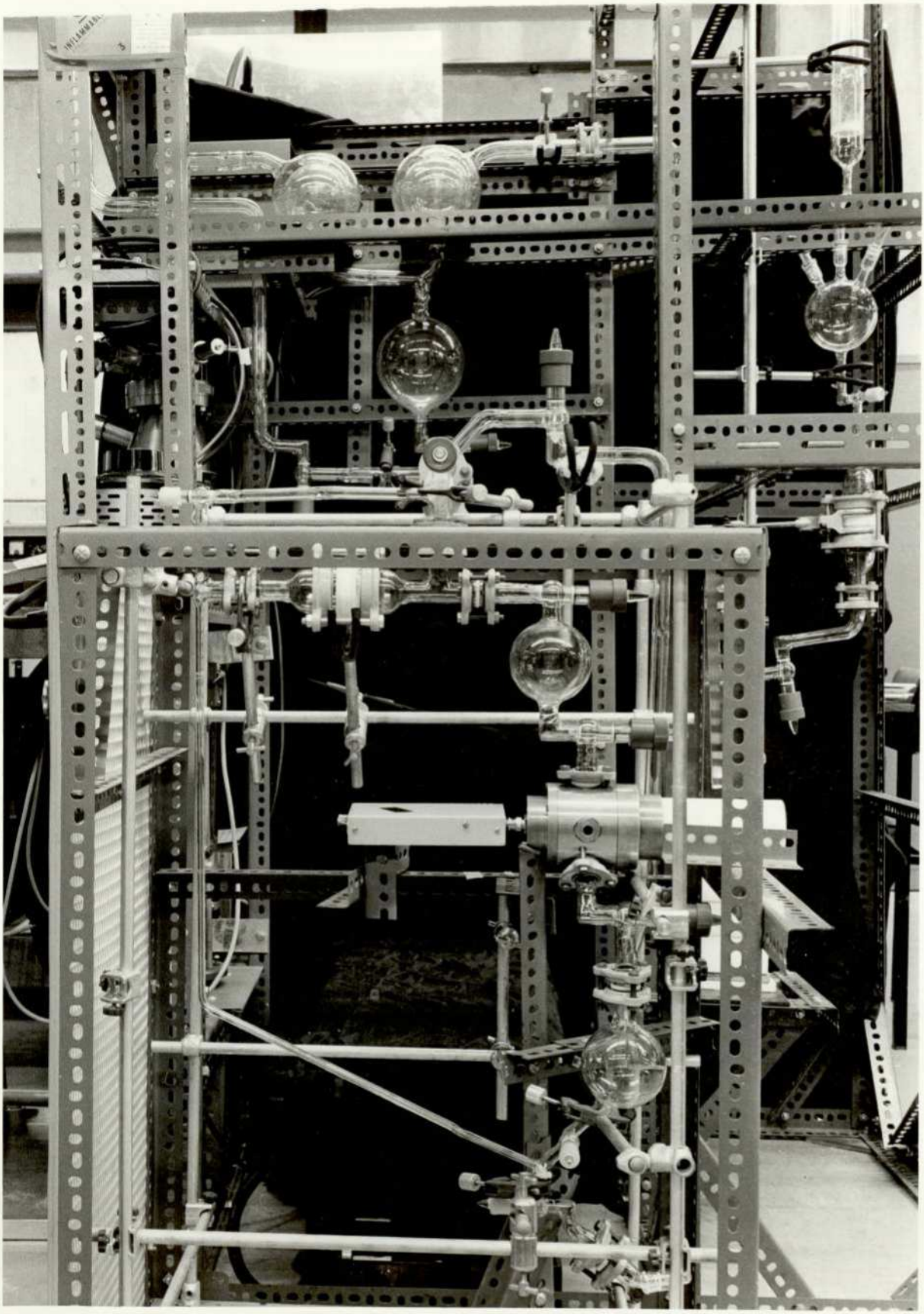

Plate 9.3.1.1

9.3.1

the 0.1 μm porosity filter into the distillation flask. Valve G is closed when sufficient liquid has entered the flask. Note that a liquid head is maintained above valve G to ensure that air cannot enter the flask. The degassing spheres are cooled with liquid nitrogen. Valve F is now opened and the liquid is allowed to distil at a pressure of less than 10^{-5} Torr. The vapour rises and solidifies on the spheres. The rate of distillation is governed by the temperature of the distillation flask (which controls the temperature gradient between the flask and the cooled spheres).

The rate of distillation is important as for high flow rates the larger number of molecules in motion (which will have velocities of sonic magnitude [Thes Brig]) may be capable of forcing solid impurities through the system. At low flow rates although the molecular velocities are as high the number of molecules is reduced and so is the likelihood of impurities being swept up in the flow. To overcome this problem Brignell used a more elaborate system to control the rate of molecular flow.

Once the liquid has been frozen onto the degassing spheres valve F is closed and the distillation ceases. A residual is left in the flask which will contain small solid impurities and heavy chemical contaminants. The degassing spheres are allowed to warm and the hexane melts and collects in the vessel below the spheres. Tests have shown that n-hexane from the bottle contains approximately 250 ppm (vol) of water before, but less than 1 ppm (vol) after distillation.

The author's test cell housed in the particle extracting system can be connected to the distillation rig and with taps C and E closed and D open may be thoroughly dried out. If tap D is then closed and tap E opened the purified n-hexane will flow into the test cell

9.3.1

(see details of cyclic filtering system given below).

9.3.2 The Closed Loop Particle Extracting System

This system was developed to shorten the period of time taken for the particle content of the test cell to be reduced to a low level suitable for the desired measurements to be made. Although Sletten [Thes Slet] doubts the usefulness of flushing a small electrode gap to remove particles, the system described here has been found partly successful. The particle extracting system has proved useful for removing fibres and larger particles that may enter the cell during the assembly process, in spite of the precautions taken (see Section 9.4.1).

Fig. 9.3.2.1 shows the layout of the system, also featured in Plate 9.3.2.1. The system is constructed from pyrex glass with QVF flange joints. The glassware is supported by retort clamps mounted on a tubular aluminium alloy frame. This frame is bolted to a plywood base which is located in a Dexian frame; this enables the rig to be transported between the distillation systems and the screened room in which the experiments are performed. The system was cleaned prior to assembly. A 0.1 μm porosity membrane filter was used in the filter chamber and was supported by a sintered glass support. This filter is made by sandwiching two PTFE support flanges on either side of the membrane and clamping this sandwich between two 4 cm diameter QVF flange joints. This produces an excellent seal, and overcomes the problems of earlier filter holders (this unit is based on an idea of Rhodes who experienced difficulty with filter supports [Thes Rho]). The test cell can be removed (together with

9.3.2

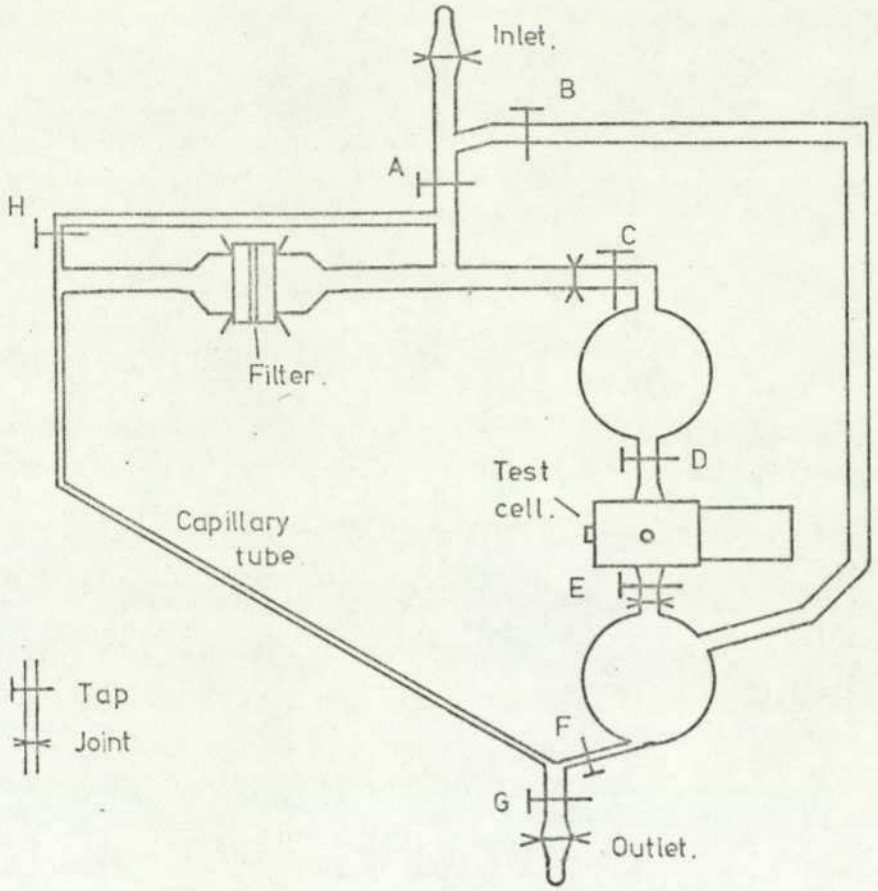

Fig. 9.3.2.1. The closed loop particle extracting system.

the 250 mL reservoir) from the system by disconnecting two of the flange joints; when removed the cell and the reservoir are isolated from the atmosphere by two taps, C and E. Below tap E is a second reservoir used to hold the liquid before it is drawn, via tap F, up the capillary tube to the filter chamber. The liquid can either be drawn up the capillary tube by lowering the pressure on the right hand side of the filter (with tap H closed) or by pumping dried nitrogen through tap B (with taps A and E closed), which increases the pressure in the lower reservoir and pushes the liquid up the small bore tube. The former technique was found to be the most effective. The liquid, after passing through the filter chamber flows into the upper reservoir where it can be stored prior to re-filling the test cell. One problem arises in this system

9.3.2

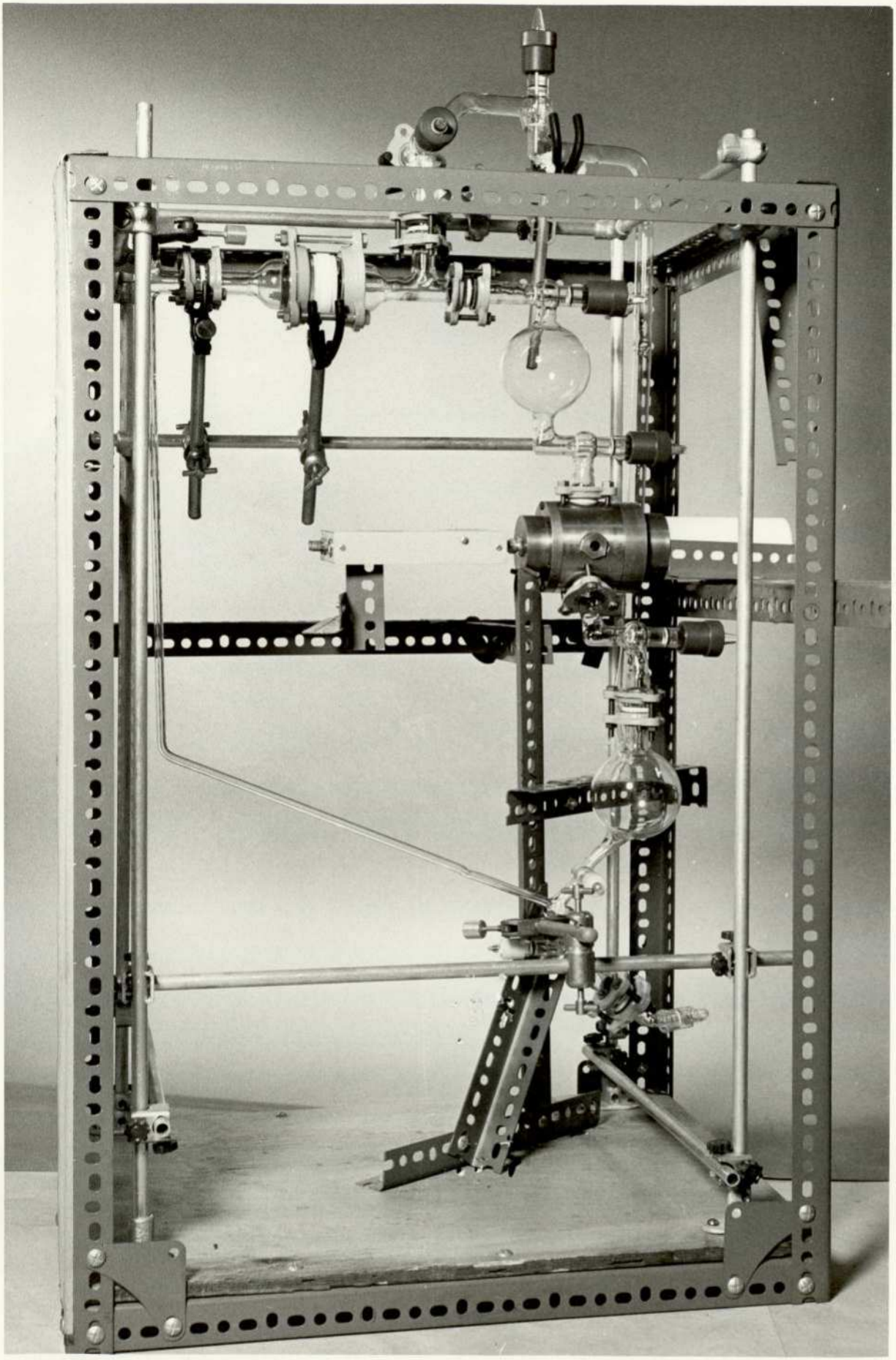

Plate 9.3.2.1

9.3.2

when the n-hexane is drained from the test cell to be recycled, a drop of liquid held by its own surface tension remains between the electrodes. Any attempt to flush particles from the gap will fail whilst this drop is present. It is therefore necessary to remove the drop of n-hexane. This can be achieved by closing taps F, D and A, and opening taps E and B, the cell may then be pumped down by a roughing pump. This causes the liquid in the drop to evaporate and thus leave the electrodes clear for flushing. The lower reservoir must be empty to avoid excess pumping on the liquid which would contaminate the oil in the pump. If taps E and B are closed when tap D is open liquid will be drawn into the cell. Experimentation by the author has indicated that if nitrogen is used to pressurise the top reservoir then the n-hexane is forced in with enough pressure to liberate some of the small particles from the electrode. An approximate decrease of 30% in the particle population in the gap was observed on several occasions when the cell had been in use for a long period and the particle population was high (i.e. sufficient to cause particle bridges to form). Examination of the filter paper before and after one series of tests showed that the particles were being successfully transferred from the cell to the filter paper.

Before the particle extracting system was filled with n-hexane it was connected to the diffusion pump of the distillation system for several days in order to dry it out. This process was employed to remove traces of oxygen, water and other cleaning fluids (n-hexane and acetone). Tap H serves as a filter bypass circuit. This circuit allows a low pumping resistance path to both sides of the filter, as the filter and capillary tube form a virtual leak. This

system proved very effective in the early stages of cleaning out the test cell, which Rhodes [Thes Rho] reports as a tedious process taking several months. However, whenever the electrodes became heavily contaminated the cell was dismounted and the electrodes changed (see Section 9.4.2).

9.4 The Test Cell and Electrodes

9.4.1 The Test Cell

The cell used for the studies described in Section 10 was designed by Rhodes [Thes Rho] for use in his measurements of the conduction currents in n-hexane.

The modifications made to this test cell are now described. Fig. 9.4.1.1 shows the cell as used by the author. The inlet and outlet ports have been adapted to connect to a standard ground glass QVF flange mounting joint (see Plate 9.4.1.1 which shows the test cell and the upper reservoir). This type of joint has the advantage

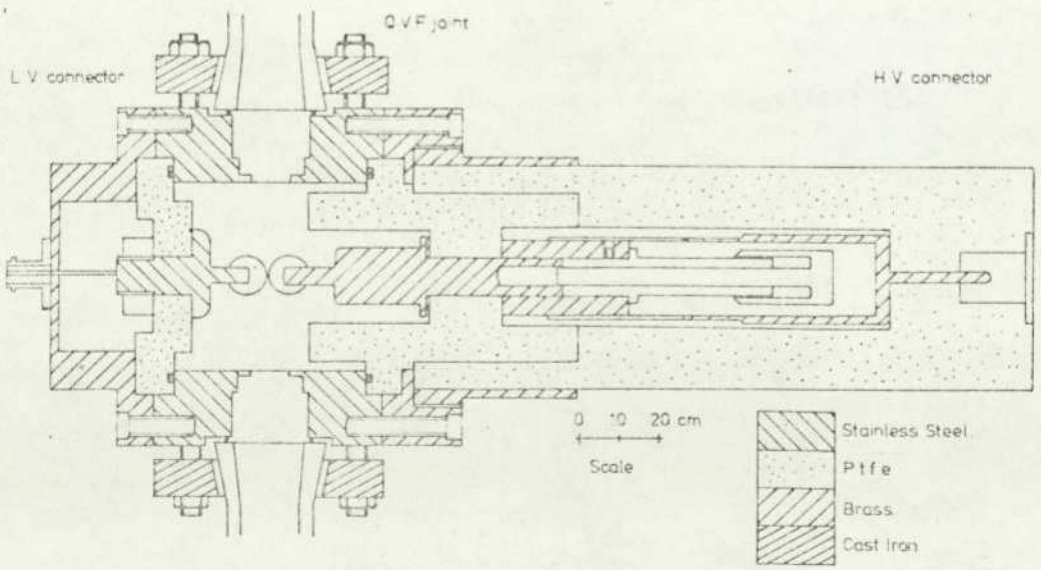

Fig. 9.4.1.1. The Rhodes' test cell as modified for the present study.

9.4.1

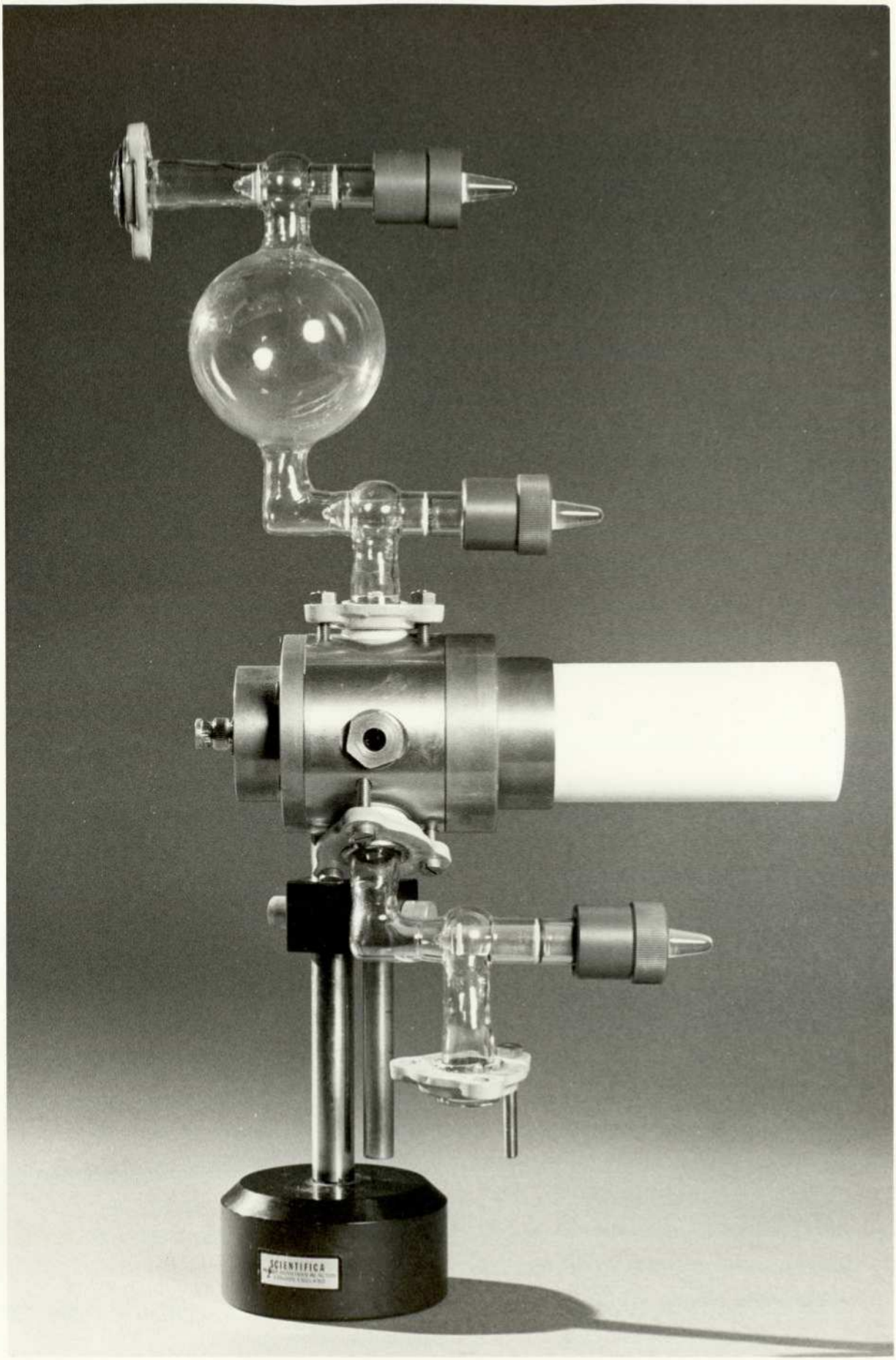

Plate 9.4.1.1

of forming a much better vacuum seal than the original PTFE tapered joint.

The bellows system allowing an adjustable inter electrode gap had to be replaced at short notice (prior to a series of experiments to be presented at the 5th International Conference on Dielectric Liquids, see Section 10.2.1). A fixed brass high voltage mount was used. The gap size is set by adjusting the position of the high voltage electrode (see Section 9.4.2) on the 2 BA thread at the end of the brass mount. The cell is assembled and the gap examined through a microscope with a calibrated optical grating. The cell is then partly dismantled and the position of the electrode adjusted to improve gap setting. This trial and error method proved to be of little bother as experience allowed the gap size to be set to within 20 - 30 μm after several attempts. The high voltage electrode was locked in place with the aid of a brass 2 BA lock nut (whose sharp edges had been removed). Care was taken not to handle the electrodes and to avoid contaminating the cell; which was only opened in the clean air room that houses the disc drive for the FM1600B computer. The air in this room is filtered to 1.0 μm. All parts of the cell were washed in n-hexane prior to assembly. An ultrasonic cleaner containing a detergent was used only when the cell was first brought out of storage, as for several years it had been dismantled. The cell has three quartz windows. The positions of the windows are shown in Fig. 10.2.3.1. The ports are used to view the inter electrode gap and illuminate the natural impurity particles in the gap (see Section 10.2.3).

9.4.2 The Electrodes

The electrodes in the present author's studies on liquid n-hexane have been stainless steel spheres of 0.005 m radius (1 cm diameter). For the purpose of mounting, each sphere is drilled and tapped with a 2 BA thread.

The main reasons for choosing spherical electrodes to approximate to plane electrodes are firstly the problems of polishing and alignment, secondly to keep the probability of breakdown low it is necessary to reduce the stressed area as much as possible (see Section 10.2.1) and thirdly the relative ease with which ball bearings can be obtained and converted. Preparation is carried out by polishing the surface of the electrode with increasingly finer grades of diamond polishing paste. Grade No. 6 is used for poor surfaces to remove deep scratches, grade No. 1 smooths the surface and removes shallow scratches and inclusions, whilst grade No. $\frac{1}{4}$ gives the final highly polished finish that is required. The surface is inspected under a microscope using various magnification factors to ensure that all surface irregularities are removed. Each electrode is frequently flushed with n-hexane and wiped with a lens cleaning tissue in accordance with [Cont Elec Harp] to remove surface debris which could further score the electrode during polishing. Care is taken to ensure that the electrodes are not touched by hand during or after the cleaning process. A nylon tube is used to grip the electrode when it is transferred from the polishing mount to the test cell. The electrodes are mounted in the cell, which is then assembled and evacuated in order to reduce the effects (noticed by many workers) caused by oxygen molecules becoming adsorbed on to the electrode. However, the high temperature encountered during polishing will cause

some impurity gases to be retained on the electrode surface.

9.5 EHT Supplies

9.5.1 The High Voltage Power Supply

A Brandenburg 807R supply (of the Alpha range) was used to provide the high voltage for the test cell. This supply is capable of producing voltages up to 25 kV at 1 mA with a stability against a +10% to -7% mains variation of 0.01%. The supply is fitted with a current trip set at the specified limit of the unit. A 4½ inch scale meter gives the output voltage to ±2%. The unit contains a 33 kHz power oscillator which feeds a step up or multiplier circuit. The high voltage is fed to the output connecter via a low pass filter with a time constant of 45.0 mS.

Two 807R high voltage supplies were modified by Rhodes [Thes Rho] for use with the high stability low voltage digital control unit [Hi Volt Re]. The digital controller has since been superceded by the advent of an on-line link to the FM1600B computer [Bd Phen Mear]. This on-line interface is described in the next section.

The high voltage electrode was connected to the EHT (Extra High Tension) supply via a resistor chain (50 MΩ). As on most occasions, breakdowns were unlikely a current diverter was not connected. The majority of measurements were made with this off-line EHT supply.

9.5.2 The Computer Controlled High Voltage Power Supply

On several occasions very high stress levels (near to dielectric breakdown) were obtained from the on-line EHT supply. This peripheral is mentioned briefly in Section 4.5. The system was designed by one of the author's co-workers [Bd Phen Mear] and operates one of the modified 807R supplies (described in the previous section). The computer generates a 12 bit digital number that is output to the EHT Control Unit where a digital to analogue converter produces a voltage. This voltage is fed to the EHT supply control circuitry and sets the value of the high voltage produced. A 12 bit word to control the voltage as opposed to the 8 bits in [Hi Volt Re] results in an incremental step of 6 volts as compared with 96 volts. Thus the on-line supply permits a finer control over the level of the applied voltage. Apart from the resistive link between the supply and the cell, two methods of protection are employed to reduce damage to the electrodes at breakdown. The first method is a bypass thyratron (Mullard XH25-500) triggered by an amplified version of the breakdown current pulse from the test cell, which diverts the breakdown current within 0.5 μS. To zero the voltage from the EHT the second protective measure, a computer interrupt, is generated by the breakdown pulse. This pulse causes the interface hardware to zero the EHT voltage and inform the user program that a breakdown has occurred. The removal of the voltage usually occurs within 100 μS.

This peripheral allows the experimenter in his program to request the status of the EHT Control Unit and, when a breakdown event is indicated, extract the voltage at which dielectric failure occurred.

9.5.2

The EHT controller when linked with the real time clock in the computer is capable of generating voltage ramps (which, with such small incremental steps, approximate to linear ramps) that can last over several seconds, minutes, hours or even days! The bypass thyratron circuit and filter circuit are those described by Rhodes [Thes Rho] and are shown in Fig. 9.5.2.1 together with the on-line EHT supply and its connections to the test cell.

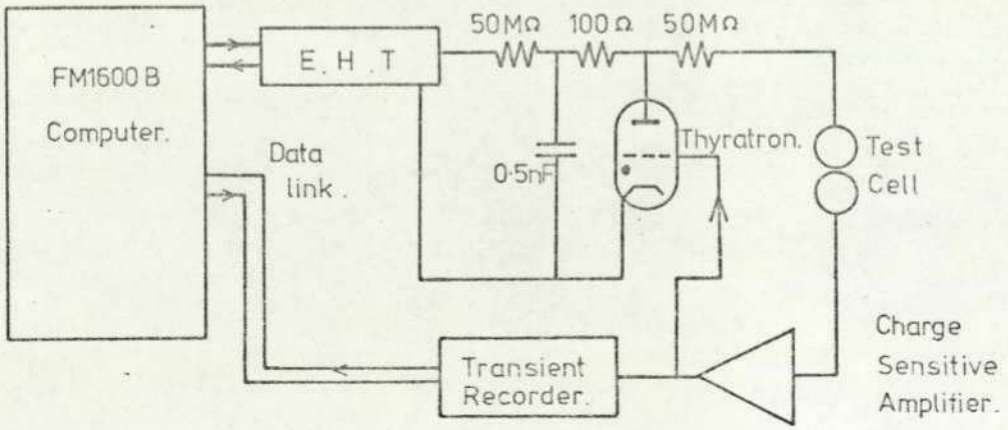

Fig. 9.5.2.1. The on-line EHT with the thyraton diverter.

9.6 The Charge Sensitive Amplifier and Ancillary Devices

9.6.1. Introduction

The charge sensitive amplifier is described in the following subsection with the aid of a mathematical analysis of the effect of the protective circuit which prevents charge pile up in the amplifier. The other devices which amplify and filter the signals monitored are mentioned in Sections 9.6.3 and 9.6.4.

9.6.2 The Charge Sensitive Amplifier

It was Rhodes [Thes Rho] who first measured the charge transferred between two electrodes with this amplifier. In his Thesis

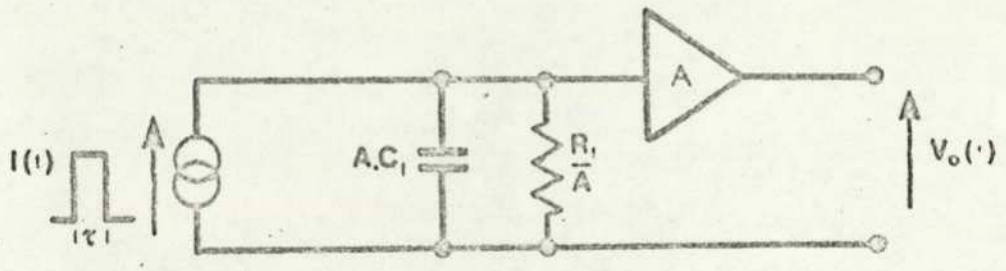

$R_f = 500\ M\Omega$, $C_f = 1\ pF$, $A = 10000$

Equivalent circuit of the charge sensitive amplifier.

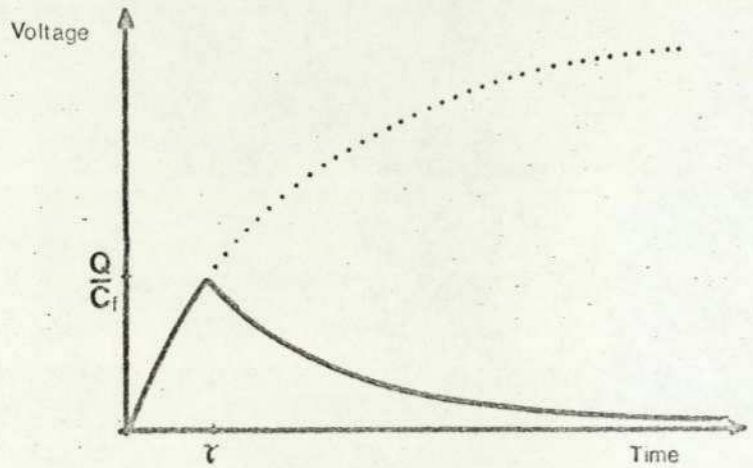

Sketch of the output voltage waveform.

Fig. 9.6.2.1. (after Thes Rho).

Rhodes analysed the effect of a short current pulse (see Figs. 9.6.2.1 a and b) i(t) applied to the input of the charge sensitive amplifier. Such a pulse can be represented by

$$i(t) = \frac{q}{T}\,(U[t] - U[t-T]) \qquad \text{Eq. 9.6.2.1}$$

where U(t) is the unit step function at zero time.

9.6.2

The output of the amplifier is given by

$$V_o[t] = \frac{qR_f}{T}\left\{(1-e^{-t/C_fR_f})U[t] - (1-e^{(t-T)/C_fR_f})U[t-T]\right\} \quad \text{Eq. 9.6.2.2}$$

for $t \leq T$, $U[t] = 1$ and $U[t-T] = 0$, so the above expression becomes

$$V_o[t] = \frac{qR_f}{T}\left\{1 - (1 - \frac{t}{R_fC_f} + \text{higher terms in } \frac{t}{R_fC_f})\right\} \quad \text{Eq. 9.6.2.3}$$

$$\approx \frac{q}{C}\cdot\frac{t}{T} \quad \text{Eq. 9.6.2.4}$$

when $t = T$,

$$V_o[T] = \frac{q}{C_f} \quad \text{Eq. 9.6.2.5}$$

Thus for C_f equal to 1 pico Farad, an output voltage of 1 mV represents a charge of 1 femto Coulomb. This analysis does not take into account the effect of the 50 μS decay, which is built into the charge sensitive amplifier to prevent it from saturating. This can be caused by a charge piling up at the input of the amplifier.

To consider the decay the charge sensitive amplifier may be represented by two buffered circuits. The first is an approximate integrator with a time constant of 500 μS, and gives the relation between input charge and output voltage as described previously. The second is a differentiating circuit which causes the 50 μS time constant decay. As these two elements are buffered, their responses to any stimulus may be considered separately. The use of the Laplacian

9.6.2

operator allows the responses of the equivalent integrating and differentiating circuits to be found as follows:

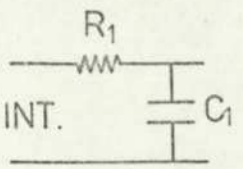

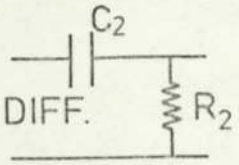

$$H(s) = \frac{\frac{1}{sC_1}}{R_1 + \frac{1}{sC_1}} \qquad H(s) = \frac{R_2}{R_2 + \frac{1}{sC_2}}$$

$$= \frac{\frac{1}{R_1C_1}}{s + \frac{1}{R_1C_1}} \qquad = \frac{s}{s + \frac{1}{R_2C_2}}$$

where $R_1C_1 = 500\mu S.$ where $R_2C_2 = 50\,\mu S.$

multiplying these two responses and substituting T_1 for R_1C_1 and T_2 for R_2C_2 gives

$$H(s) = \frac{s/T_1}{(s + 1/T_1)(s + 1/T_2)} \qquad \text{Eq. 9.6.2.6}$$

Splitting this expression by the method of partial fractions produces,

$$H(s) = -\frac{\frac{T_2}{T_1(T_1 - T_2)}}{(s + 1/T_1)} + \frac{\frac{1}{(T_1 - T_2)}}{(s + 1/T_2)} \qquad \text{Eq. 9.6.2.7}$$

This is the impulse response of the cascaded circuits. If Eq. 9.6.2.7 is mapped into the time domain and integrated the result will be the output voltage when a current step is applied at the input.

9.6.2

The inverse Laplace transform of Eq. 9.6.2.7 is

$$-\frac{T_2}{T_1}\frac{1}{(T_1-T_2)}\cdot e^{-t/T_1} + \frac{1}{(T_1-T_2)}\cdot e^{-t/T_2} \qquad \text{Eq. 9.6.2.8}$$

Integrating this result (to obtain the step response) between 0 and τ proceeds as follows:-

let A & B represent the two constant multipliers,

then $$\int_0^{\tau} -Ae^{-t/T_1} + Be^{-t/T_2}\, dt \qquad \text{Eq. 9.6.2.9}$$

$$= \left[-T_2Be^{-t/T_2}\right]_0^{\tau} - \left[-T_1Ae^{-t/T_1}\right]_0^{\tau} \qquad \text{Eq. 9.6.2.10}$$

$$= (-T_2B + T_2Be^{-\tau/T_2}) - (-T_1A + T_1Ae^{-\tau/T_1}) \qquad \text{Eq. 9.6.2.11}$$

$$= -T_2B(1 - e^{-\tau/T_2}) + T_1A(1 - e^{-\tau/T_1}) \qquad \text{Eq. 9.6.2.12}$$

$$= -\frac{T_2}{(T_1-T_2)}(1 - e^{-\tau/T_2}) - \frac{T_2}{(T_1\ T_2)}(1 - e^{-\tau/T_1}) \qquad \text{Eq. 9.6.2.13}$$

$$= -\frac{T_2}{(T_1-T_2)}(2 - e^{-\tau/T_2} - e^{-\tau/T_1}) \qquad \text{Eq. 9.6.2.14}$$

The exponential term $e^{-\tau/500\times10^{-6}}$ approximates to a linear function for values of τ which are less than 20 µS but the error due to the 50 µS decay is found to increase with τ.

Replacing the exponential terms in Eq. 9.6.2.14 with their series expansion but including only the zero and first order terms results in,

$$-\frac{T_2}{(T_1-T_2)}\left(\frac{\tau}{T_2} + \frac{\tau}{T_1}\right) \qquad \text{Eq. 9.6.2.15}$$

The difference between Eq. 9.6.2.14 and 9.6.2.15 is the error in the amplitude caused by choice of an exponential function to represent a linear one and the use of a charge pile up protection circuit. Tabulated values of the percentage error in the height of the output voltage at a time τ after the application of a current step are given below.

τ µS	Percentage error in output voltage
1	0.9
2	1.8
4	3.7
6	5.5
8	7.5
10	9.4
15	14.2
20	19.27

From these tabulated values it is apparent that the longer the charge transit time the less accurate is the estimate of the charge transferred. As the measurements of the present author were performed with computer programs that could only estimate the charge transferred to within ± 10% no corrections were made in the computer. If, however, the transit time of the charge could be measured more accurately the value of the charge could be adjusted accordingly to correct for the effect of the 50 µS decay. Methods of deconvolving the charge waveform with the impulse response of the charge sensitive amplifier have been studied by a colleague of the present author (Pocknell private communication). The results obtained during the course of the present research are not considered to be sufficiently accurate to be included in this work.

The amplifier was mounted directly on to the test cell via a 50 Ω BNC connector; its position can be seen in Plate 9.3.2.1, just to the left of the test cell. The only modification to this amplifier was a pair of zener diodes placed back to back across the input of the device. These diodes direct the large breakdown

9.6.2

currents away from the FET input of the amplifier.

9.6.3 Preamplifiers

The output from the charge sensitive amplifier was suited to direct connection to the transient recorder when the large pico Coulomb pulses were being studied. However, for analysis of the femto Coulomb charge transits further amplification was necessary. Two amplifiers were available for this purpose. These were an Advance Instruments Modules (AIM) low noise amplifier (type LNA 133A) and a Nuclear Enterprises NE4603 amplifier.

The AIM amplifier has its lower and upper -3 dB points at 1 Hz and 200 kHz respectively, with a maximum gain of 100. The output impedance of the device is 50 Ω which matches that of the transient recorder.

The NE4603 pulse-shaping amplifier was set with its integrating time constant at the minimum value of 0.1 μS and the differentiating time constant at maximum. In this way the pulse shaping effects of the amplifier were reduced to their minimum. The amplifier has a gain ranging from 16 times, increasing by multiples of 2, up to 1024 times.

9.6.4 The Active Filter

A Kemo VBF/1 dual variable active filter eliminated some of the high frequency noise from the photomultiplier signal (see Section 9.7.2). The unit has two filters which can be used separately as high or low pass filters, or in parallel to form a band pass or band stop filter.

9.6.4

Channel 1 has a gain of 1, 3, 10, 30 or 100 whilst channel 2 has unity gain. The maximum bandwidth of the filter is 0Hz to 200 kHz. Each channel comprises a 4 stage Butterworth filter giving a 24 dB/octave attenuation. Channel 1 has an input resistance of 1 MΩ shunted by 40 pF (D.C. coupled) and channel 2 has a 200 kΩ input shunted by 40 pF; the output impedance is quoted as 51 Ω for both channels.

9.6.5 The Oscilloscope

A Tektronix 475 200 MHz dual channel oscilloscope located inside the screened enclosure monitored the signals from the charge sensitive amplifier and the photomultiplier tube before they were fed to the transient recorder. This device had the advantages of being small and of not generating a great deal of heat, which was important in the confined area within the screened room. Also the range controls were illuminated and could thus be read even in the darkened room.

9.7 Apparatus Relating to Optical Observations

9.7.1 Introduction

The following subsections describe the optical method of monitoring the motion of natural particles in the test cell. Section 9.7.2 describes the photomultiplier used and some of the noise problems associated with such devices. Sections 9.7.3 and 9.7.4 deal with the ancillary apparatus that made possible the work described in Section 10.2.3 and 10.2.5.2.

9.7.1

9.7.2 The Photomultiplier

Light scattered from impurity particles in the test liquid was monitored by a Mullard photomultiplier type 56 AVP, containing 14 dynodes and giving an overall gain of 10^8 (for a supply value of 2240 V). The circuit configuration is given in Fig. 9.7.2.1; the energy storage capacitors are omitted as the device was not operated in a pulse detecting mode.

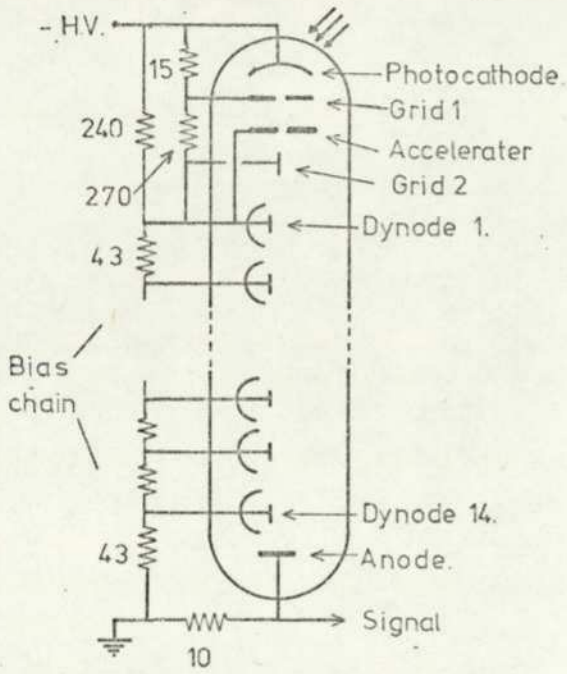

Fig. 9.7.2.1. The Mullard 56AVP photomultiplier with biasing components.

The tube has an S11 spectral response with a peak in the visible 'blue' region. The tube was mounted in a light proof metal box. Light was allowed into the box through a small tube so that a small area of the photocathode would be illuminated (see Section 10.2.3). The photomultiplier was operated in complete

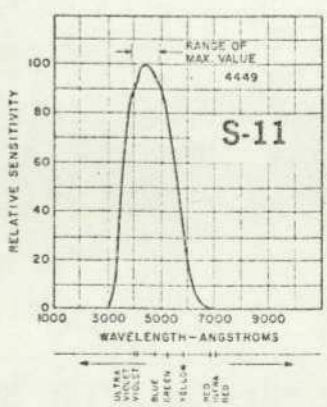

Fig. 9.7.2.2. The S11 response.

9.7.2

darkness for at least one hour to allow the dark current to subside.

The main noise source, apart from Johnson noise generated in the load resistor, is shot noise. This noise is caused by the quantized nature of the light falling on the photocathode and the secondary emitted electrons from the dynodes; shot noise is multiplied by the gain of the photomultiplier. The waveform in Fig. 10.2.3.4 was frequently captured during the experiment and was probably caused by energetic particles of naturally occurring radiation producing photons in the window of the tube either by the Cerenkov effect [Mod Phys Be] or by fluorescence. According to Dance [Photo Dev Dan] this source of dark current produces fairly large pulses.

The tube was driven by a 0 to -2.5 kV Brandenburg high voltage supply and was normally operated at its maximum voltage (- 2.24 kV). A typical photomultiplier signal is illustrated in Fig. 10.2.3.3 (upper trace).

9.7.3 The Light Source

The illumination for the observation of particles in the test cell (by scattered light) was obtained from a Rank Taylor Hobson 150 W cold light source. The unit contains a powerful projector bulb with a built in reflector. The element in the bulb is rated at 150 W at 21.5 V (i.e. 6.9 A). A transformer is used to drive the bulb. The voltage across the bulb is controlled by a switch, which changes the number of turns in the secondary coil of the transformer; this varies the brightness of the bulb. It was found that the use of the switch increased the likelihood of the element in the bulb

failing; owing to current surges during switching. The bulb was protected by placing a thermistor in series with the primary coil of the transformer and setting the switch to maximum intensity before switching on the mains supply. The current was found to take approximately $\frac{1}{2}$S to reach its maximum and so the bulb suffered no rapid changes in current. This form of thermistor protection was found very effective in increasing the life of the projector bulbs used during the measurements on particles.

9.7.4 The Light Bench Apparatus

The light from the projector bulb was passed through a set of condensing lenses on to an iris. The image of the iris was collimated and transmitted via two surface coated optically flat plates of glass, operating as a periscope, to a 25 cm focal length lens. This lens focussed the parallel beam on to the inter electrode gap. The coating which had been vacuum deposited on to the glass was aluminium.

The image of the inter electrode gap was magnified 100 times by a microscope containing a projection eye piece. The projected image was reflected through 90^{o} (into the horizontal plane) and passed through a mask on to the photocathode of the photomultiplier. After a relatively short period of exposure the aluminium coating would degrade and the mirrors would then be cleaned and a new layer of metal deposited. For stability all the optical apparatus was mounted in retort clamps to the frame of the particle extraction system (see Section 9.3.2) or placed on an optical bench.

9.8 Accessories for the Transient Recorder

In the description of the Biomation 8100 transient recorder in Section 4.2 mention was made of the analogue output channel which reconstructs the stored waveform for plotting or displaying. The author found the Hewlett Packard 1300A X-Y Display the most convenient means of presenting the transient stored in the recorder. The display receives the X, Y and Z (blanking) signals from the transient recorder and is mounted on top of the recorder (this is shown in Plate 4.4.1). Careful adjustment of the X and Y amplifier gains allows the waveform to be expanded to fill the full width of the calibrated screen, thus making estimations of the duration of an event possible.

Hard copies of a stored waveform, acquired when the recorder was off-line, were plotted on a Hewlett Packard YT Plotter with plug in amplifiers and sweep generators.

The low impedance (50 Ω) of the inputs to the amplifiers of the recorder occasionally proved inconvenient when monitoring a high impedance source. Two Hewlett Packard 1124 A high voltage high impedance probes were obtained as accessories to the recorder. The probes were of the active type and obtained their supply from outlets on the recorders front panel. Each probe has an input resistance of 10 MΩ shunted by 10 pF. Within these devices field effect transistors (FET's) provide a bandwidth of 0-100 MHz (a rise time of less than 3.5 nS is quoted by the manufacturers). The probes were calibrated, in accordance with the manufacturers guide, at regular intervals.

9.9 The Screened Room

Throughout the studies made on charge transport by particle impurities in highly stressed n-hexane it has been found necessary to perform all measurements in an electrically screened enclosure in order to reduce extraneous signals to a minimum.

Fig. 9.9.1 shows the screened room containing the high voltage power supply (the off-line version is shown), the test cell, charge sensitive amplifier, the preamplifier and the photomultiplier with its power supply.

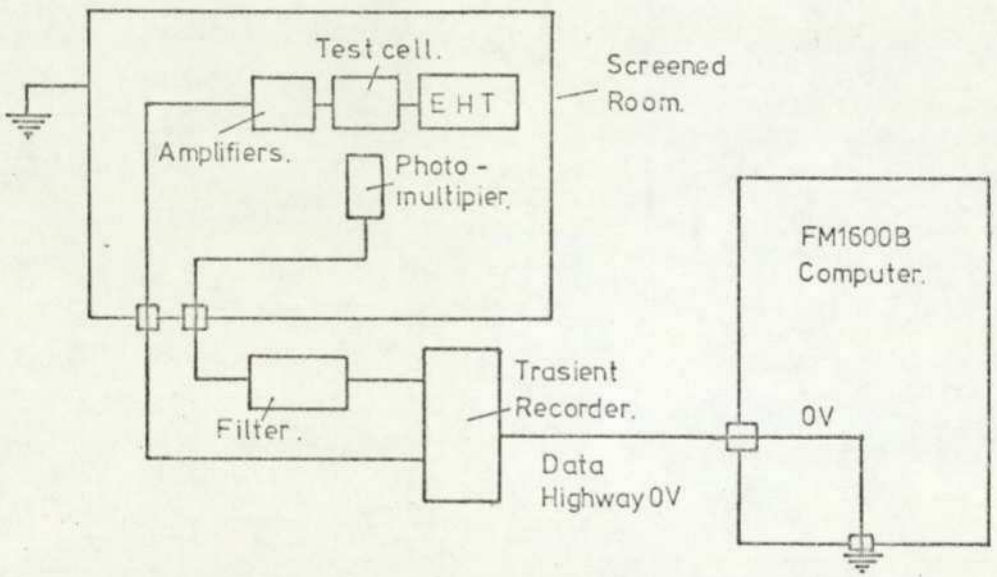

Fig. 9.9.1. 0V and earth connections to the screened room and computer to prevent earth loops.

The wall of the room is connected to a local earth point while the equipment inside is earthed to the central earth point in the computer. While on-line measurements are carried out the apparatus in the screened room is isolated from its metal wall of the room. For off-line measurements, in which the data highway of the recorder is disconnected, the apparatus is linked electrically with the wall of the screened room. The screened room and the computer share a common mains supply, which enters the room via a balanced filter.

9.9

Various combinations of earthing were examined but that shown in Fig. 9.9.1 was found to give the greatest noise immunity.

The signals from the photomultiplier and charge sensitive amplifier were carried by coaxial cables through the wall of the screened room to the recorder situated outside (note: all amplifiers were fed from isolated supplies). The recorder is itself a source of noise as it contains a 200 MHz oscillator and a large amount of digital switching circuitry. It is, therefore, kept outside the screened enclosure. A tolerable amount of noise was generated by the high voltage power supplies which use radio frequency oscillators to generate the EHT.

The worst earth loop encountered was associated with the on-line EHT (see Section 9.5.2), which closed a loop comprising the OV data highway lines of the EHT controller and the transient recorder. Optical isolation in the data highway would be a convenient way of overcoming this particular problem.

Modifications to make the screened room serve as a darkened enclosure proved to be relatively easy. Heavy tarred paper was placed over the two grids in the wall and the extracter fan was fitted with a light proof baffle, which permitted air to circulate freely.

Inside the room, blackout cloth was used to shield the light from the projector bulb along its path to the test cell. Black PVC tape covered front panel bulbs on the power supplies.

SECTION 10

Methods and Results.

10.1 Introduction

This section comprises a description of the experimental methods used by the author to measure various phenomena occurring in highly stressed liquid n-hexane and the results obtained. Section 10.2 deals with the work relating to the small charge pulses (having a charge in the order of femto Coulombs, fC) believed by Rhodes [Part Cond Rho] to be caused by particle carriers. In view of Rhodes' hypothesis, a more intensive study was made of the fC pulses and these results are given in the form of a paper published by the present author in the proceedings of the 5th International Conference on Dielectric Liquids. Some of the work leading to the conclusive proof that the femto Coulomb pulses are due to charge transportation by particulate contamination is then described and summarised in the form of a letter to the Editor of Nature. Measurements of the apparent dwell time of particles oscillating between the electrodes are also reported.

A brief off-line study of the large charge pulses was made and the initial results are given. Some observations and comments relating to breakdown and conditioning end this Section.

10.2 The femto Coulomb Charge Transits

The studies by Rhodes [Thes Rho] of femto Coulomb pulses (see Section 7.3.1) appears to substantiate the work of Felsenthal and Vonnegut [Cond Part Fel] for the few values obtained. An initial aim of the present author's investigations was, assuming that the femto Coulomb pulses were in fact due to natural impurity

particles, to perform measurements of the charge transported and the transit time over a wider range of stresses than was previously possible.

10.2.1 The Initial Studies of femto Coulomb Pulses

The use of the on-line transient recorder (see Part I) permitted transits to be recorded at stress levels above 40 MVm^{-1}. In this region the large pico Coulomb charge pulses are likely and until this present work have made isolated measurements of the small pulses difficult. Sections 5.1 and 5.3 refer to the problem of the noise bursts and how, with the aid of the run-time waveform classification system, all transients whose amplitudes exceeded the input amplifier range were ignored. It must be stated that this technique set an upper limit to the amplitude measurements that were made, but care was taken to ensure a sensible input range. The lower limit of the pulse height is set by the trigger level, which was kept just above the nominal noise level so that even the smallest of pulses would be captured (i.e. down to approximately 1 fC) several hundred waveforms were captured for this initial study; the methods used to measure the transit time and the amount of charge transferred are described in Section 8.2. The experimental procedure and results of the initial studies are now related in the following paper.

10.2.1

This paper was presented at the 5th International Conference on Dielectric Liquids held at Noordwijkerhout, Holland in 1975.

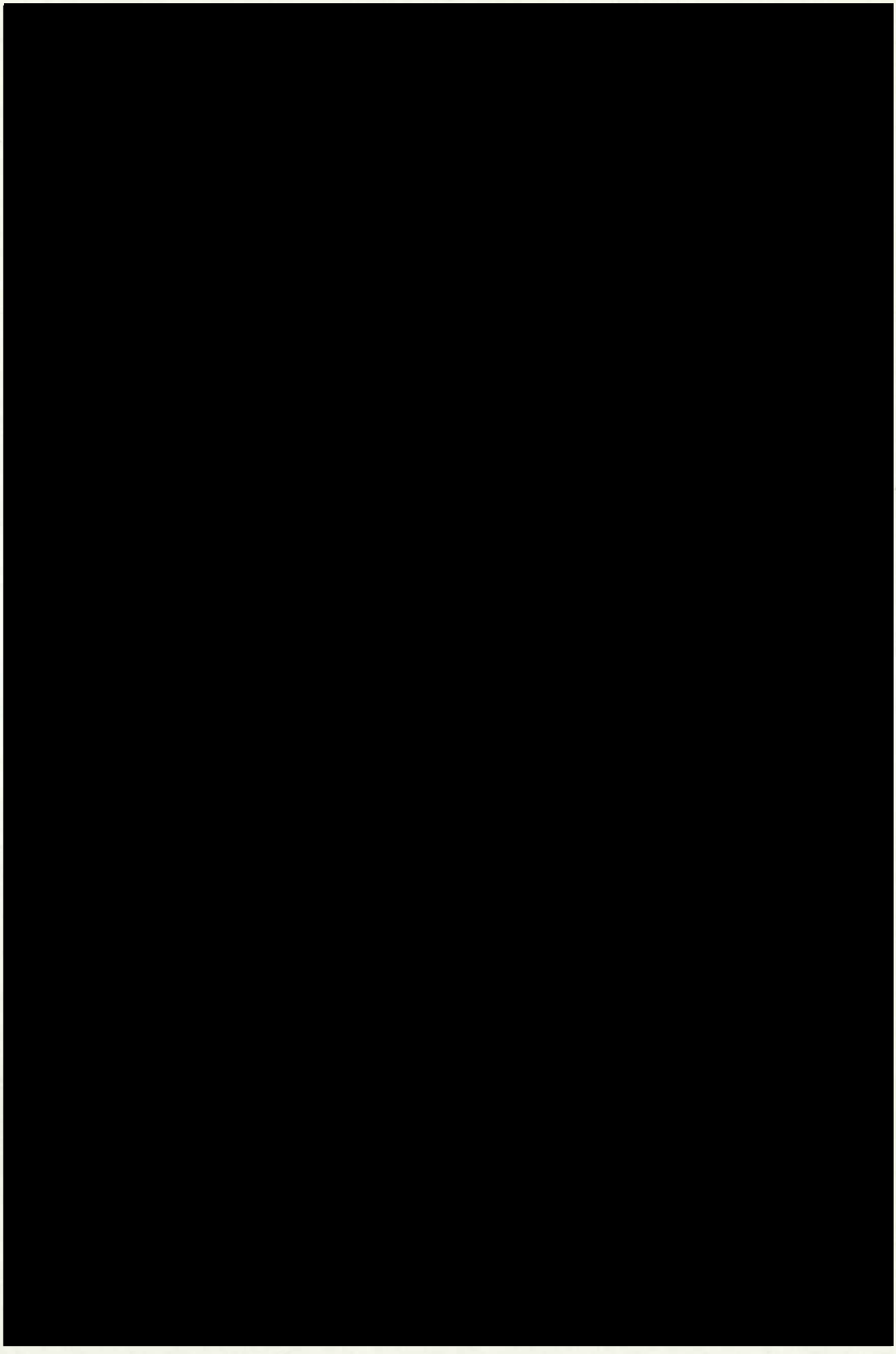

10.2.1

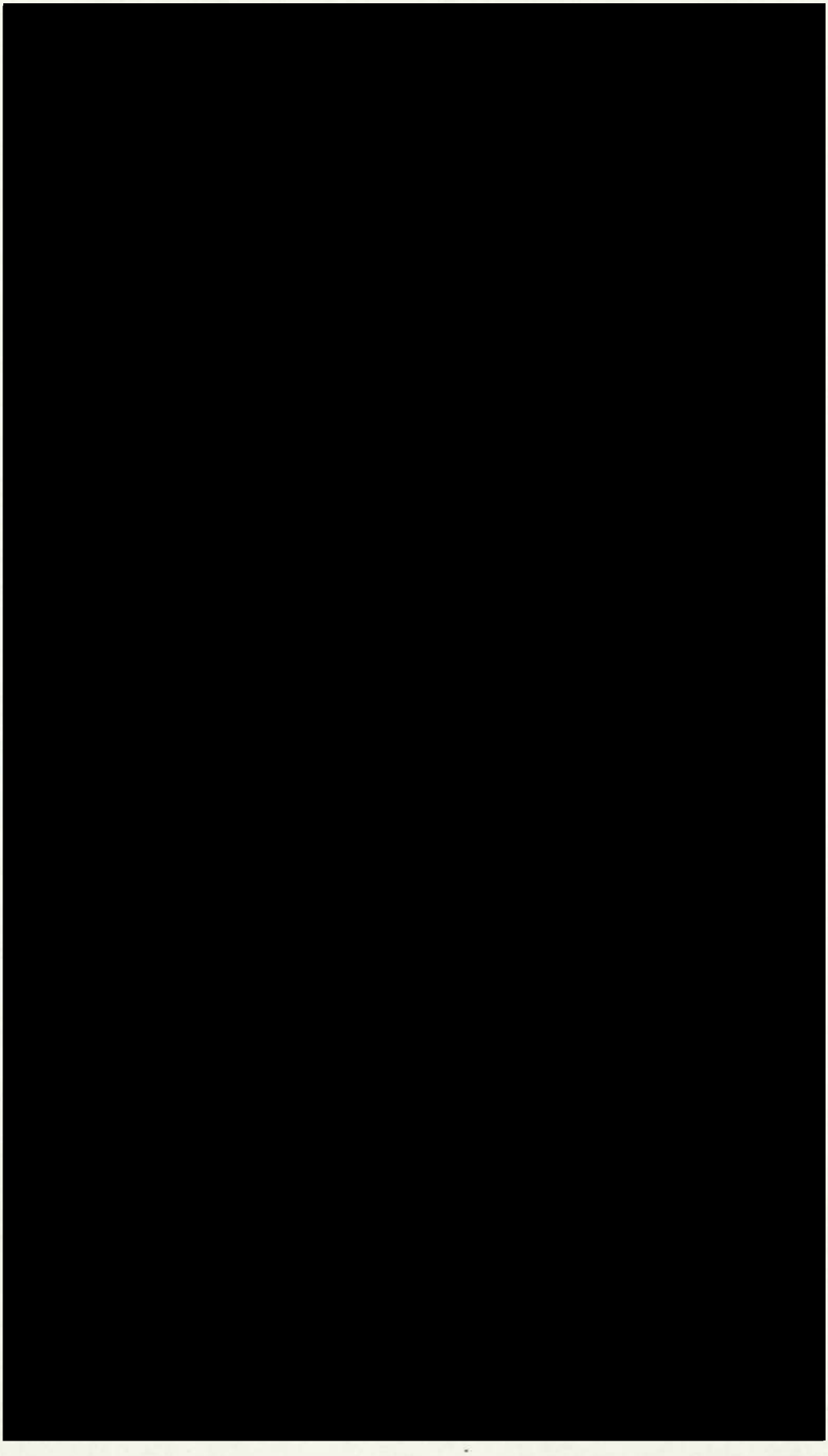

10.2.1

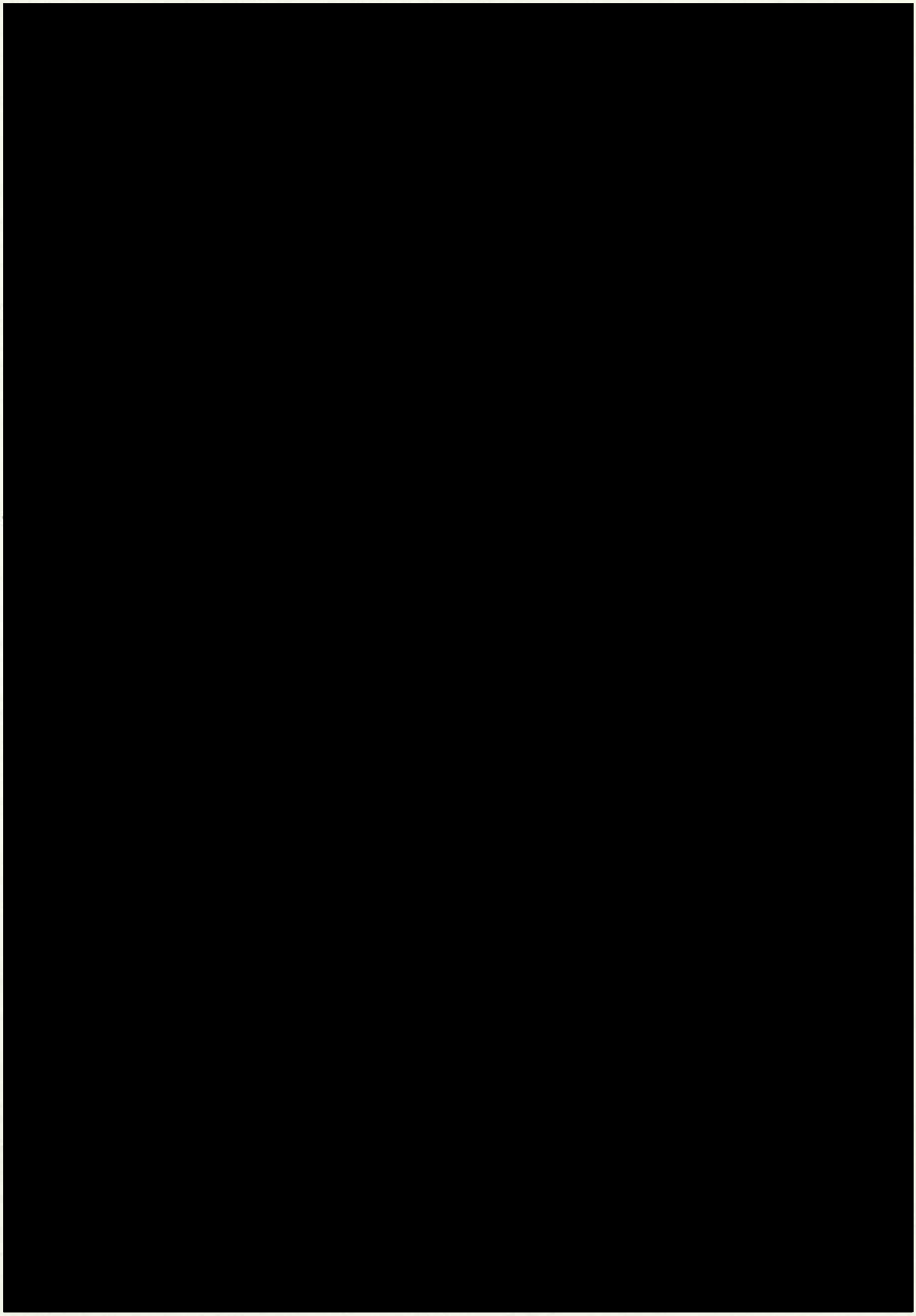

10.2.1

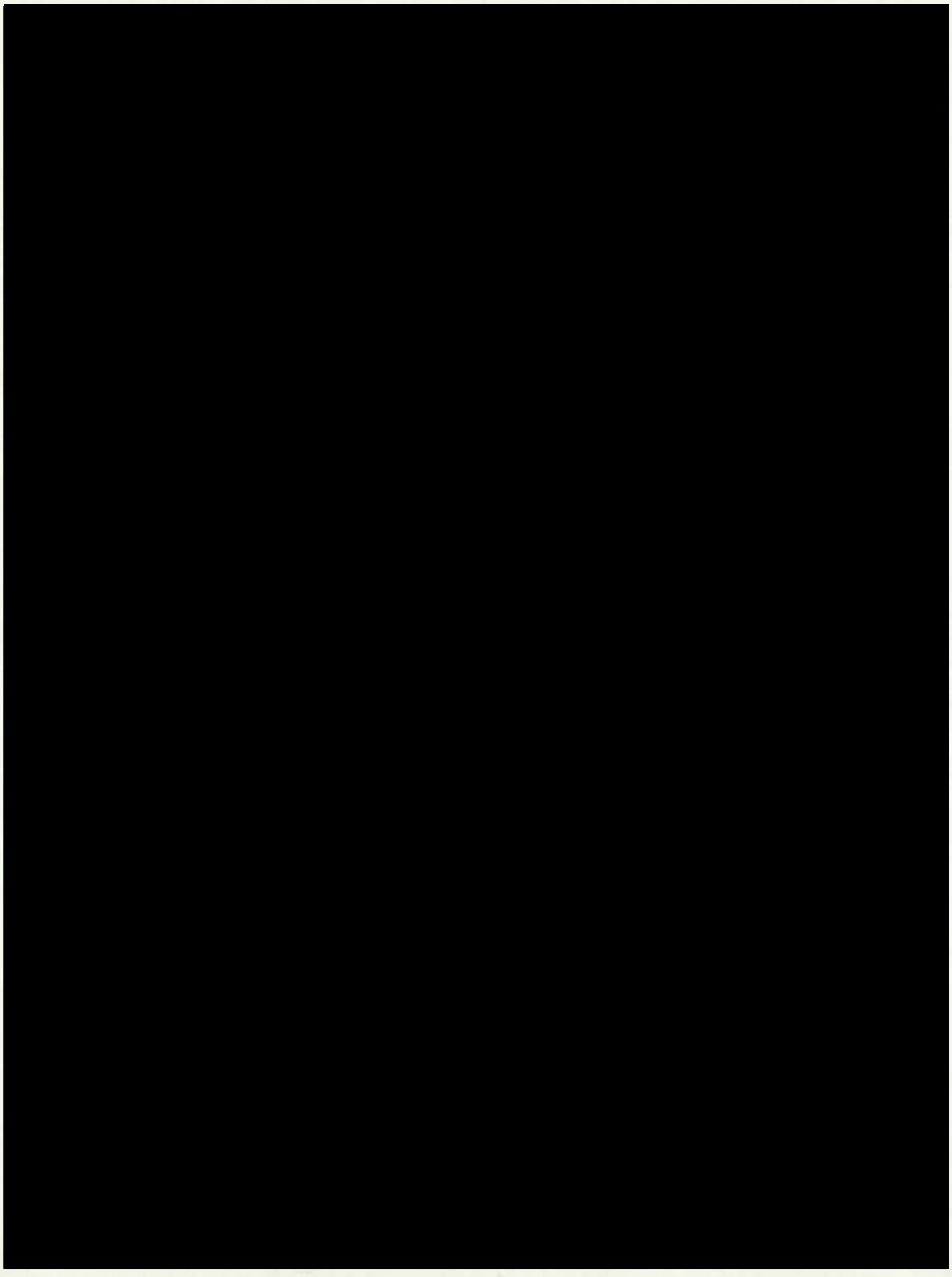

10.2.2 Further Results from the Initial Study

In a set of measurements presented at the conference in Holland, but not included in the paper, sufficient waveforms were captured to permit a distribution of the voltage V_o (the potential on a particle [Cond Part Fel]) associated with each particle to be plotted. Fig. 10.2.2.1 shows this distribution. The average voltage for this

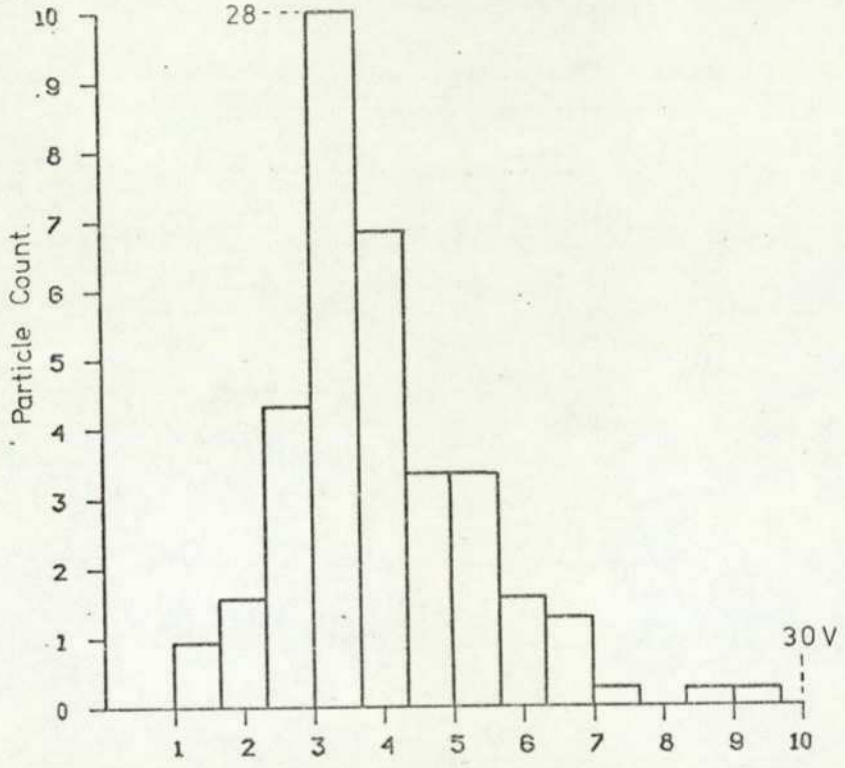

Fig. 10.2.2.1

set of results is 11.1 volts, which is in agreement with the earlier results of the present author and those of Rhodes [Part Cond Rho].

10.2.3 Attribution of the femto Coulomb Transits to Particle Motion

In an attempt to prove conclusively that the small femto Coulomb (fC) pulses had their origin in the movement of particles between the two electrodes in the cell, an electronic method of 'viewing' the particles was developed. The experiment used a 150 watt projector bulb to illuminate the inter electrode gap and act as a

light source for scattering by microscopic particles in the cell. A high gain photomultiplier (see Section 9.7.2) was used to detect the light scattered from a particle in the gap. Fig. 10.2.3.1 shows the relationship of the light source the electrode gap and the photomultiplier. The light from the projector bulb was condensed

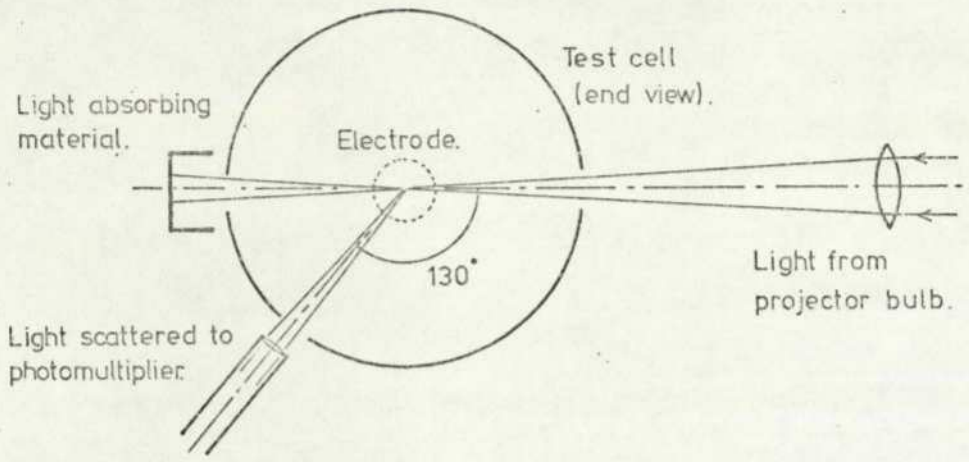

Fig. 10.2.3.1. The relative positions of the light source and photomultiplier with respect to the 3 windows of the test cell.

and focused onto an iris (2 mm dia.). Light from the iris was transmitted by two surface coated mirrors to a point where it was focussed onto the gap between the electrodes and the electrode surface in this region. A long focal length lens was used to focus the light onto the gap so as to keep the solid angle of the beam small. The beam passed through the quartz window in the front of the cell between the electrodes and out of the cell by the rear window. This ensured that the amount of light that was scattered inside the stainless steel test cell was kept to a minimum. The effect of scattered light was to reduce the signal to noise ratio of the photomultiplier output.

The image of the gap was projected onto the photomultiplier cathode with the aid of a microscope by means of a projection eye-piece; the magnification obtained was in the order of X 100. The

light reached the photomultiplier via a tube of diameter 3 mm and length 5 cm giving the photomultiplier an angle of view of approximately 2^{o}. The effective area of view with a magnification of 100 times is $.706 \times 10^{-9}$ m^2 (this is equivalent to a square of side 26.5 μm). Fig. 10.2.3.2 shows the area covered by the photomultiplier. The biasing of the photomultiplier was initially

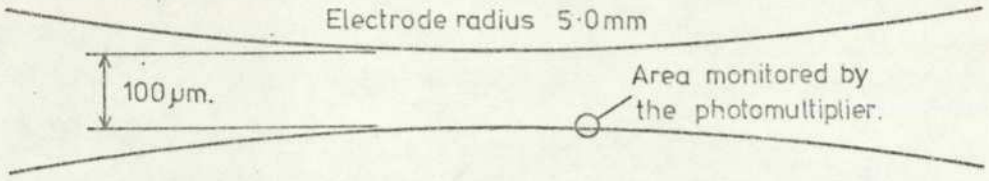

Fig. 10.2.3.2. The field of view of the masked photocathode.

arranged in such a way that light pulses of 10 μs duration would be amplified without drawing energy from the bias chain of the photomultiplier. The 10 μS limit was imposed so that the photomultiplier would be able to monitor particles in transit. Experimentation indicated that the intensity of scattered light coupled with the high speed of the particle in the centre of the gap produced a signal that was insufficient, compared to the noise level, to indicate the passage of a particle. It was found, however, that the light scattered from a particle resting on the electrode was sufficient to change the current flowing through the photomultiplier tube. Presumably, owing to diffraction effects, there is a concentration of light at the electrode surface. This arrangement made possible the detection of particles a few micrometres in diameter resting on an electrode. So despite the fact that a particle could not be 'seen' crossing the gap its arrival or departure from the electrode could be noted by a change in the level of the photomultiplier

signal.

Considerable time was needed to set up the optics and align the photomuliplier tube with the image of the electrode liquid interface. The illumination of the gap was found to be critical to the achievement of sufficient signal amplitude from the photomultiplier. It was necessary for the author to spend half an hour in the completely blacked out screened room before the required visual sensitivity enabled adjustments to be made. Once the 150 watt projector lamp was switched on the light escaping from the blackout blanket (surrounding the lamp, the optics and the cell) was found sufficient to dimly illuminate the room. The photomultiplier was screened from this stray light.

Fig. 10.2.3.3 shows the output from the photomultiplier for a particle arriving (negative going edge) and leaving (positive going edge) the electrode (upper trace). The associated charge waveform (lower trace) shows a number of fC pulses. A drop in the output of the photomultiplier represents an increase in light level (as the

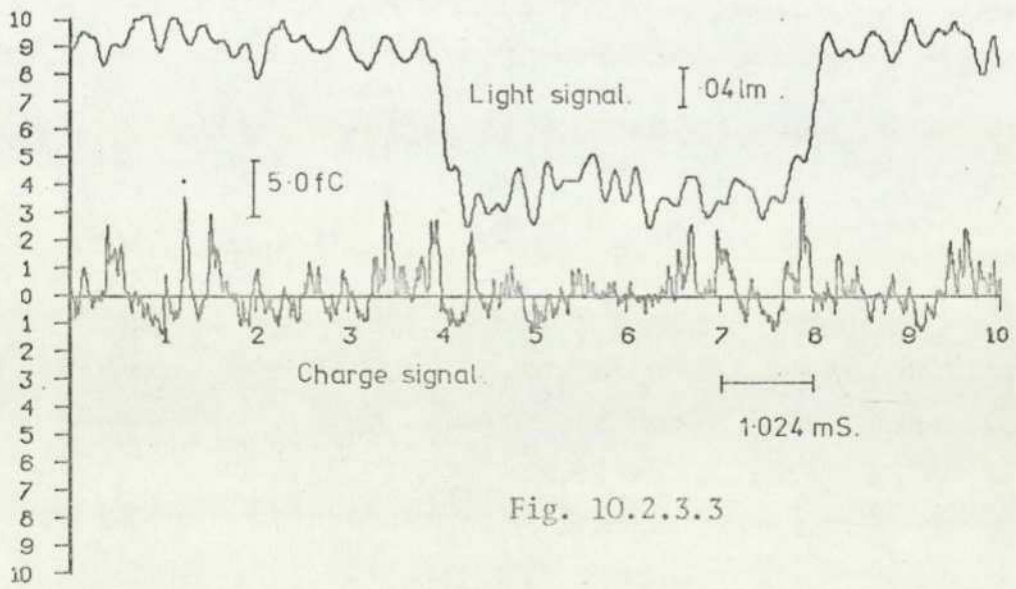

Fig. 10.2.3.3

tube is negatively biased). The charge waveform demonstrates part of the problem posed to the author. Two of the charge transients appear to occur just prior to the changes in the light signal (the photomultiplier signal is heavily low pass filtered, this accounts for the delay) but, with so many fC pulses present the assumption that there is a correspondence between the signals appears to be very tenuous. On the whole more fC pulses than light pulses would be expected, as the charge sensitive amplifier measures all charge transferred (i.e. all particles crossing the gap if they are charge conveyors) whereas the photomultiplier is only 'viewing' a small percentage of the total gap. It is also possible, however, for particles to move along the electrode surface without crossing the gap (see comments in Section 7.2 on [Imp Part Gosw]) thus causing a change in the light signal but with no corresponding charge transfer; subsequent investigations suggested that this latter variety form only 10% of the total captured.

Many pairs of waveforms similar to those in Fig. 10.2.3.3 were captured by the off-line transient recorder, but the subjective correlation of the transition of the photomultiplier from one level to another and the occurrence of a charge pulse was not always clear. The method employed to establish conclusively a correlation between the change in light level with the arrival or depature of a particle demonstrates the unique capabilities of the computer measurement system described in Part I of this Thesis. Indeed, without this system it is hard to imagine how the correlation could have been positively established. The experimental technique is now described.

The two signals, one from the photomultiplier and the other from the charge sensitive amplifier, were fed to the two input channels of

the on-line transient recorder. The light signal was used to trigger the recorder on negative edges (i.e. an increase in light intensity). The computer was set up to capture and store on disc several hundred of the light and charge waveform pairs. A stress was applied to the cell, and each time the photomultiplier voltage fell sufficiently the recorder was triggered and the data passed to disc. The photomultiplier signal was actively filtered to remove some high frequency noise present in the signal, though one characteristic type of photomultiplier noise that was not removed (see Section 9.7.2) generates a waveform typified by that in Fig. 10.2.3.4. These waveforms would trigger the transient recorder and get stored on disc

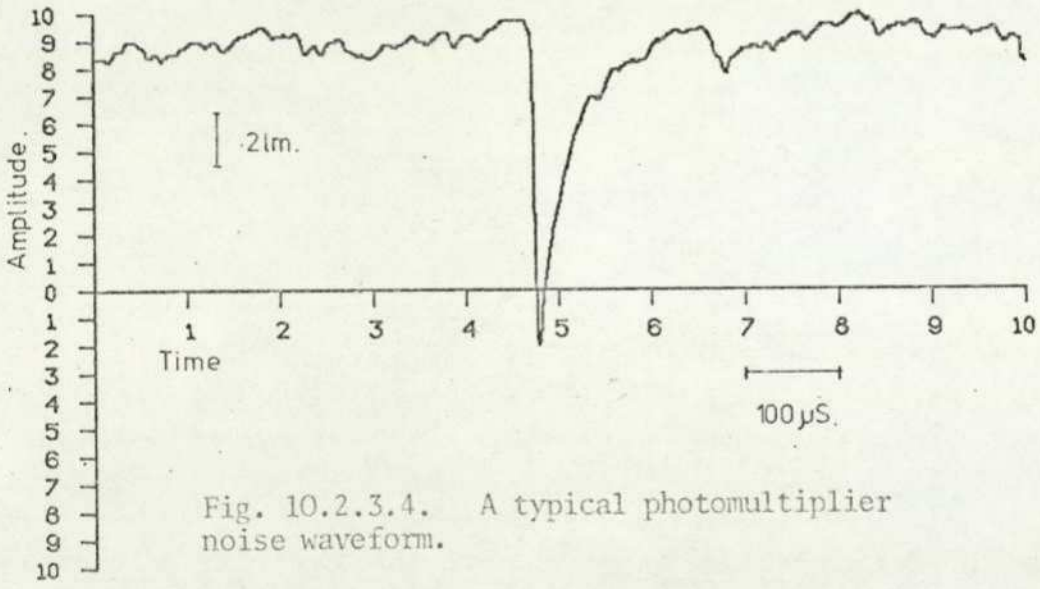

Fig. 10.2.3.4. A typical photomultiplier noise waveform.

with the accompanying charge waveform. After the completion of one experiment about 30% of the light waveforms were found to be due to this photomultiplier noise.

The post run-time pattern recognition software was used to separate the photomultiplier signal into classes representing particles arriving at the electrode (similar to that in Fig. 10.2.3.5a) and noise waveforms. Two metrics were found sufficient for this

task. The first was a template comparison and the second a check that the waveform only crossed the zero level once (this is half the height of the waveform after normalization). The waveforms classified as representing a particle arriving were placed in class 1.

To examine the correlation between the light and charge waveforms it was decided to average cumulatively all the charge waveforms associated with light waveforms in class 1. Owing to the unfiltered noise on the light waveform, the negative edge of the photomultiplier signal was often shifted, in the time domain, to the left or right of a central position. Thus if any of the fC pulses were associated with the increase in light entering the photomultiplier they would also be shifted relative to the central point. This mis-registration had to be taken into consideration if the cumulative average was to be of any help. It was therefore necessary after reading down a pair of class 1 waveforms to measure the amount the negative edge of the light waveform was shifted from a fixed reference point. This point was chosen as the centre of the waveform (i.e. 512 words from the beginning of the 1024 word transient) whose value was zero with respect to the normalized waveform value. Thus any photomultiplier transients whose 512th datum word was zero would need no re-registration; a transient whose 522nd word was zero would need to be shifted to the right by 10 words. Once the amount of shift had been measured the charge waveform (unnormalized) was cyclicly shifted to the left or right by the measured number of words (see Section 8.2). The charge waveform was then cumulatively averaged with the preceding charge transients. The waveforms in Fig. 10.2.3.5 demonstrate the measurement described and the effect of re-registration on the

10.2.3

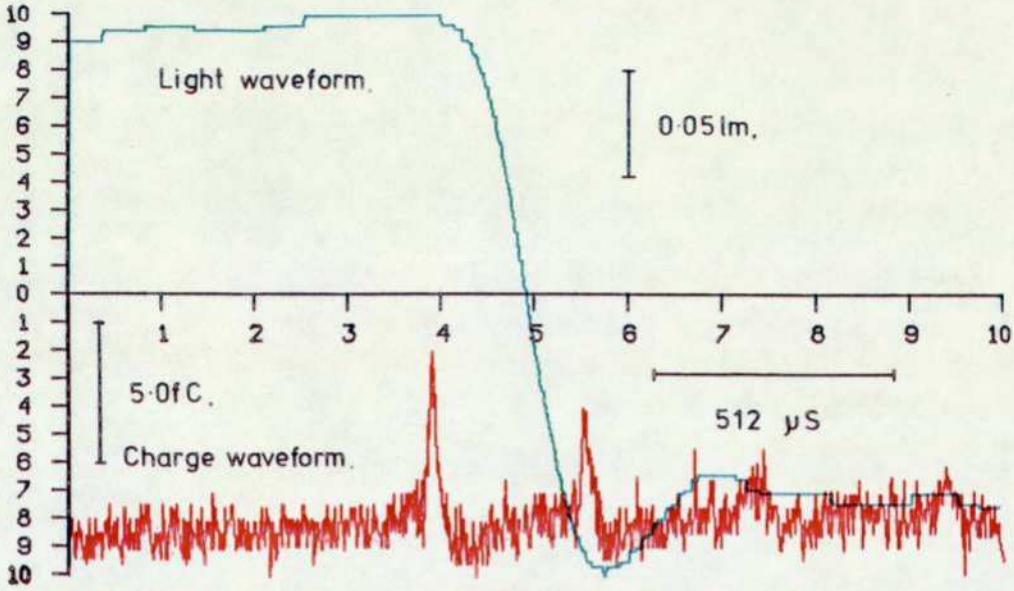

Fig. 10.2.3.5a

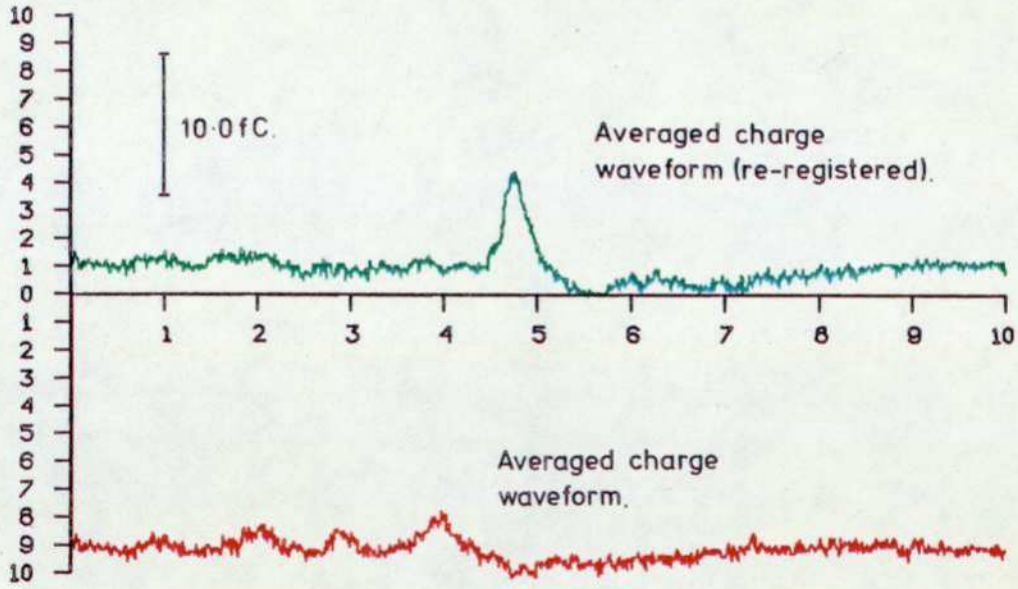

Fig. 10.2.3.5b

cumulative average. In Fig. 10.2.3.5a the green waveform shows a typical photomultiplier signal caused by a particle arriving at the electrode. The red trace shows the charge waveform captured by the second channel of the transient recorder. The delay between the first pulse of charge in the red waveform and the drop in the photomultiplier is caused (as mentioned earlier) by the filtering of the light signal. Fig. 10.2.3.5b shows the result of averaging 42 charge waveforms, classified as belonging to class 1 (by the shape of their associated photomultiplier waveform). The curve drawn in green was obtained by re-registering the charge waveform before averaging and clearly shows a pulse similar in shape to a charge transient. The result of averaging the charge waveforms without re-registering is shown in the red trace in Fig. 10.2.3.5b; the effect of re-registration is clear from these two traces.

The average charge waveform in Fig. 10.2.3.5b (green trace) represents conclusive evidence for the statement that the femto Coulomb charge pulses are conveyed between the electrodes by micro scopic particles. The waveforms in Figs. 10.2.3.5a and b were obtained from the test cell with a 100 μm gap and a voltage of 1 kV (i.e. a stress of 10 MV m^{-1}). In subsequent experiments with a stress level of 46 MV m^{-1}, 120 charge waveforms were averaged. The result is shown in Fig. 10.2.3.6b. Fig. 10.2.3.6 a shows a typical photomultiplier

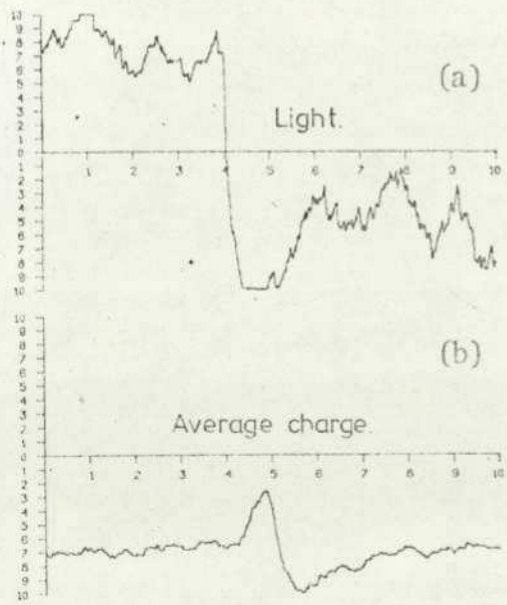

Fig. 10.2.3.6

waveform obtained at this high level of electric stress. This level is well above that at which Rhodes [Thes Rho] was able to use his audio visual correlation technique. The results from this series of measurements are summarized in Section 10.2.4 in the form of a letter to the Editor of Nature. This experiment underlines the power of the on-line transient recorder system working in combination with the pattern recognition software.

10.2.4 Letter to the Editor of Nature

The following letter contains a summary of the results described in the previous section. This letter also contains a diagramatic layout of the apparatus used in this work.

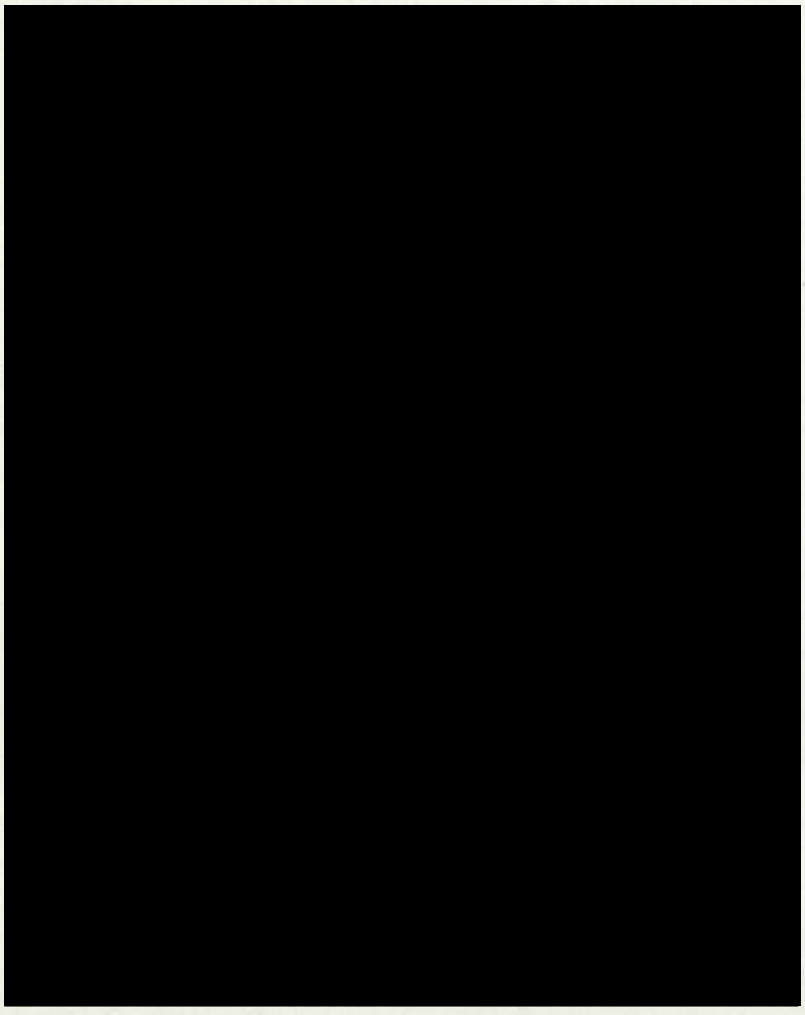

10.2.4

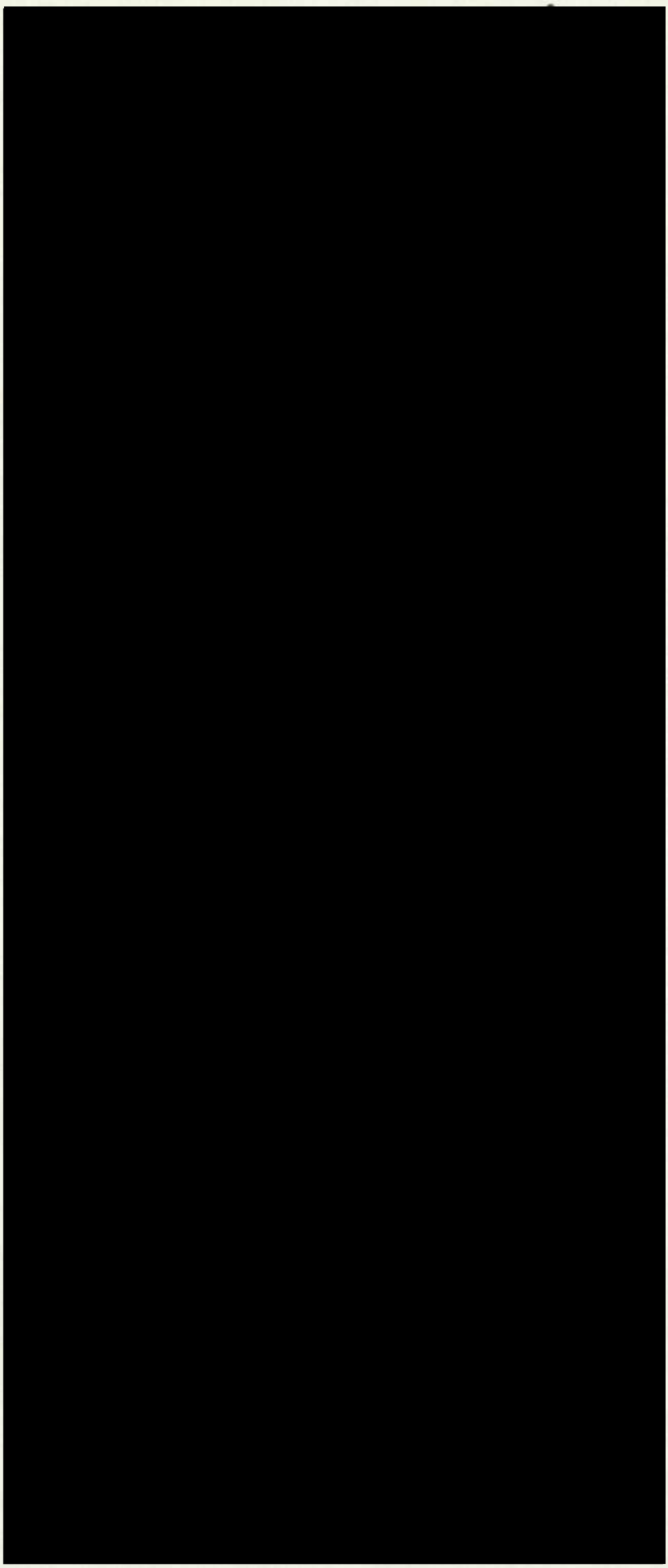

10.2.4

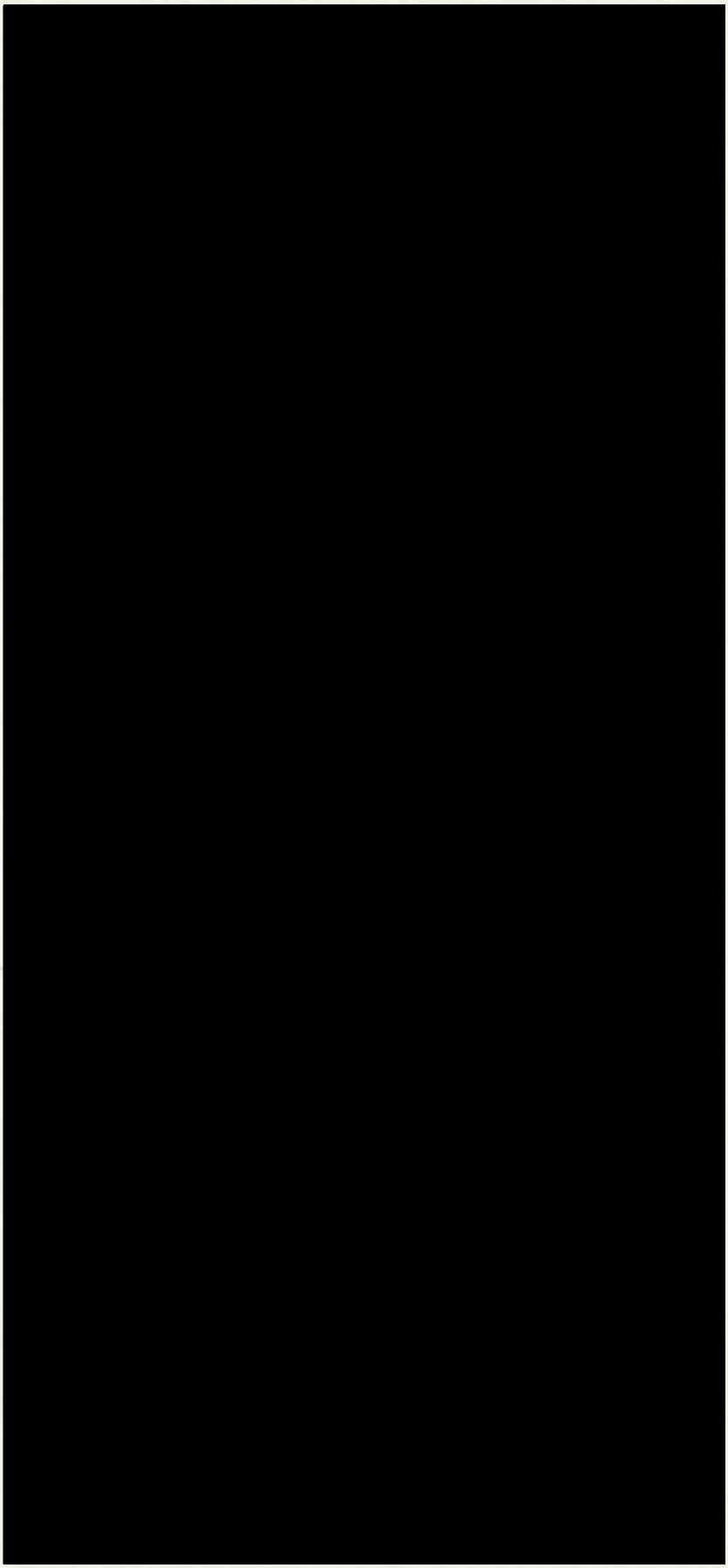

10.2.4

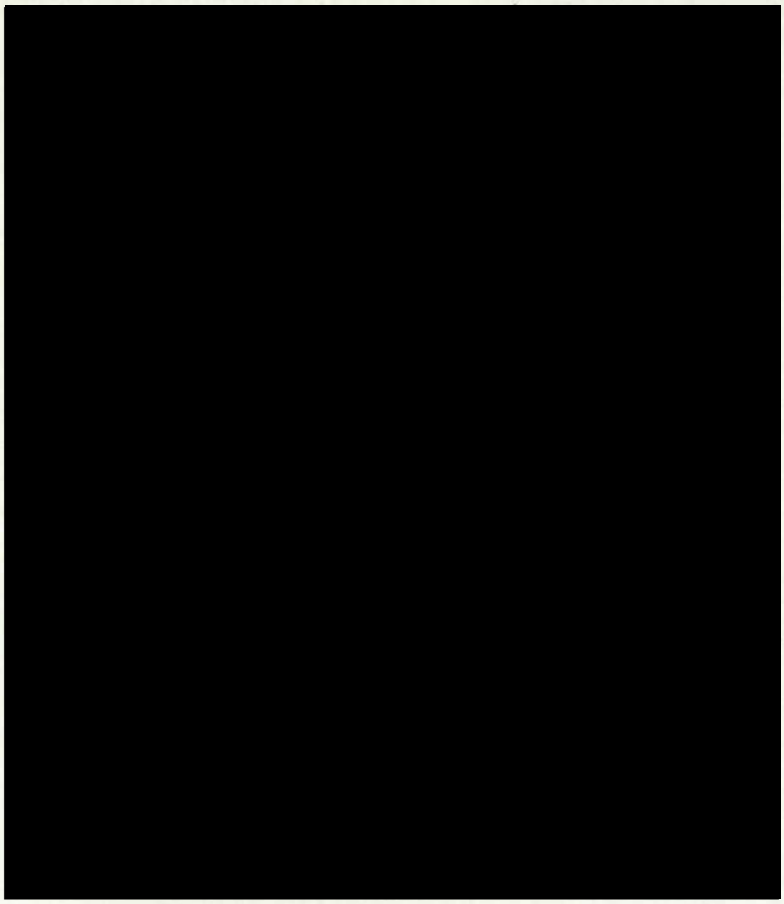

10.2.5 Particle Transit and Apparent Dwell Time Measurements

Two other important measurements have been made possible with the apparatus used in the previous experiment. Firstly the charge sensitive amplifier and the on-line transient recorder have been utilized to find the distribution of particle transit times at various stresses. Secondly the photomultiplier has been employed to measure the apparent particle dwell time at various stresses. This latter measurement was performed with the recorder off-line.

10.2.5.1 The Measurement of Particle Transit Times

The signal from the charge sensitive amplifier was further amplified and fed to the transient recorder. The measuring system captured several hundred transients at each of four different stresses and with the aid of a template and a check on waveform overflow, the classification program removed any waveform defined as unmeaningful. The classified charge waveforms for a particular level of stress were then read from disc and the transit time, between the electrodes, was estimated (see Section 8.2) The values of all the estimated transit times for a given value of stress were then punched onto paper tape and read into another program. This program was used to plot histograms from the supplied data (Mears private communication).

Fig. 10.2.5.1.1 shows four transit time distributions obtained at 20 MV m^{-1}, 26.6 MV m^{-1}, 33.3 MV m^{-1} and 40 MV m^{-1}. These graphs show that at low values of the applied stress the transit times are more spread out than at higher stresses; also the mean transit time decreases with stress (Fig. 3 in the paper in Section 10.2.1 shows that

10.2.5.1

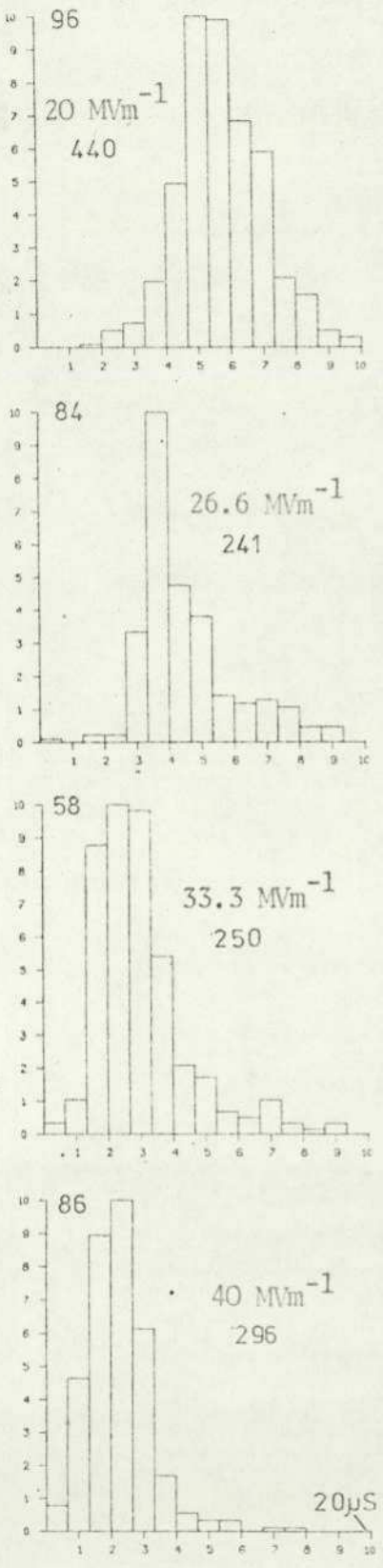

Distributions of particle transit times.

Fig. 10.2.5.1.1

the velocity is proportional to the applied stress). The results from the four graphs in Fig. 10.2.5.1.1 are in good agreement with those of Fig. 3 Section 10.2.1. The narrowing of the distribution as the stress increases is probably due to the inverse relationship between the transit time and the stress, but particles being confined to the more central region of the gap where the field is highest and the gap is narrowest may also effect the spread of the distribution.

10.2.5.2 The Measurement of Apparent Particle Dwell Times

This measurement was carried out using the transient recorder in the off-line mode owing to a shortage of sufficient computer time to develop the necessary measurement programs. The upper trace of Fig. 10.2.3.3 shows the photomultiplier waveform for a particle arriving at and leaving the electrode. It must be stated that it may not be the same particle that leaves as arrives, but the likelihood of it being a different particle is low; for this reason the

10.2.5.2

measured parameter (the width of such negative pulses) is referred to as the effective or apparent particle dwell time.

In one day over 350 measurements were taken at three stress levels. The distributions obtained are shown in Fig. 10.2.5.2.1. Distribution b has only seven bars as only 50 values were obtained at this stress. The other distributions each comprise over 130 values.

The shortest apparent charging time for the particle is at 53.3 MV m^{-1} and is 200 µS ± 10%. The mean value of the effective charging time over the measured range appears from Fig. 10.2.5.2.2 to be inversely proportional to the applied stress, values of skew indicate that the apparent dwell times become bunched at higher stresses.

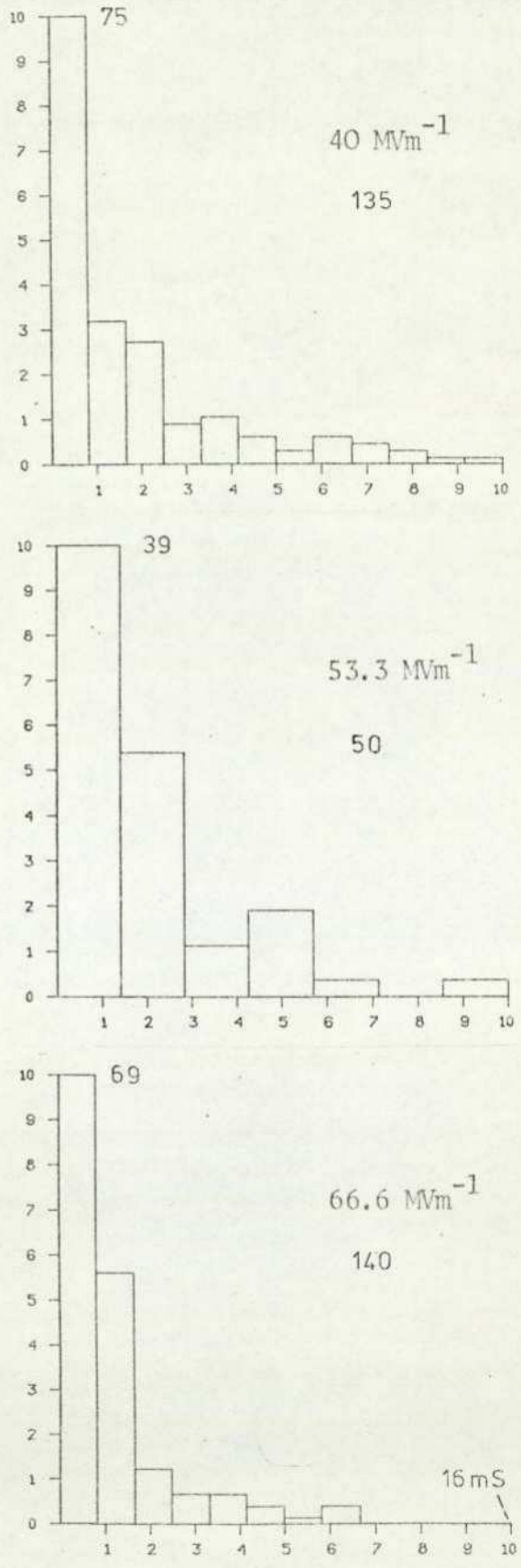

Distribution of apparent particle dwell time.

Fig. 10.2.5.2.1

10.2.5.2

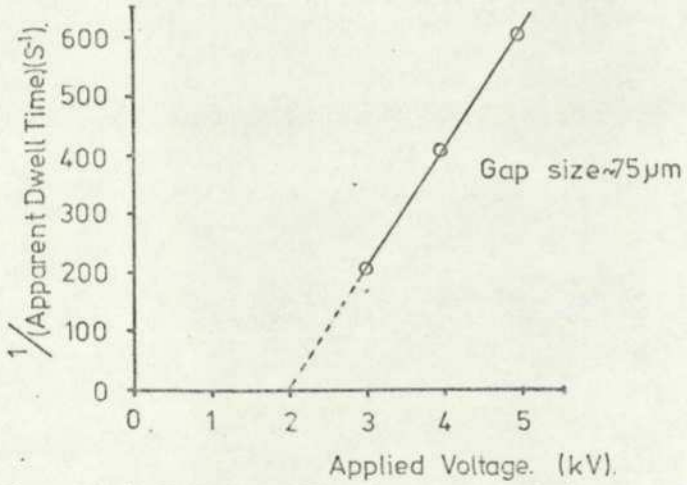

Fig. 10.2.5.2.2. The inverse of the mean apparent particle dwell time versus the applied voltage.

The measurements of transit time and apparent dwell time prove that the latter is at least two orders of magnitude greater than the former, which substantiates the statements of Rhodes [Part Cond Rho] and Birlasekaran and Darveniza [Part Mov Bir].

10.3 The Pico Coulomb Conduction Charges

A short study of the large pico Coulomb charge pulses was undertaken in the later stages of this research. The work was performed in the off-line configuration and measurements were made on the XY display (see Section 9.8) coupled to the transient recorder.

10.3.1 The pico Coulomb Charge Bursts and Their Relation to the Direct Current

In the course of liquid dielectrics research many workers have commented on the random nature of the conduction current (see Section 7.3). Fig. 10.3.1.1 gives an example of the charge bursts over a

period of ten seconds. It has also been stated by Rhodes [Thes Rho]

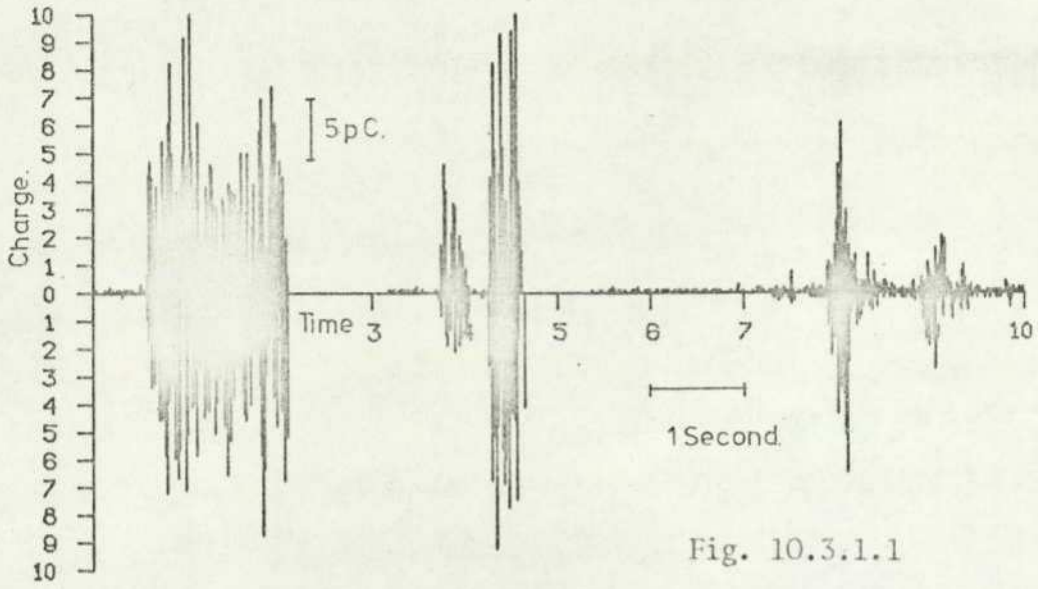

Fig. 10.3.1.1

that such bursts became less frequent if a constant stress is maintained; an observation confirmed by the present author. A check was made on the relationship between the pico Coulomb conduction pulses and the direct current flowing through the cell.

The direct current was measured by placing a 1.5 MΩ resistor in parallel with the charge sensitive amplifier and measuring the voltage across the resistor with a high impedance probe (see Section 9.8). The current and charge waveforms were fed to the transient recorder for comparison. Fig. 10.3.1.2 shows clearly the relationship between the two quantities.

The short current pulses correspond to a short burst of the pico Coulomb pulses and the fluctuation in direct current corresponds to larger bursts. The measurement showed that the larger and higher the frequency of the bursts, the greater was the level of conduction current. Bursts of charge only occur at stresses above approximately 40 MV m^{-1} (which is in agreement with [Thes Rho]). It will be seen

10.3.1

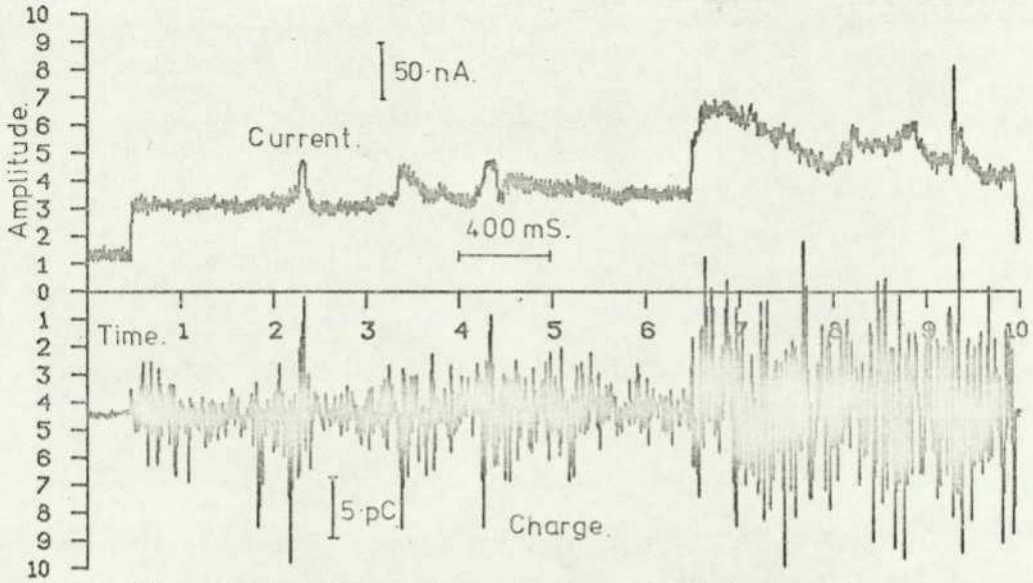

Fig. 10.3.1.2. The relationship between the current and charge waveforms.

that the pico Coulomb charge bursts make a substantial contribution to the apparent low frequency fluctuation of the high field conduction current.

10.3.2 Some Features of the pico Coulomb Pulses

During the brief study of pico Coulomb pulses certain features about the shape and regularity of the waveforms captured became apparent.

Rhodes [Thes Rho] stated he saw shapes similar to those of the femto Coulomb pulses but having a charge of tens of pico Coulombs. Figs. 10.3.2.1a to e show just some of the shapes obtained: waveform a is very similar to the shape of a particle transient and is undoubtedly what Rhodes observed.

Some general comments may be made about the basic shape of the pC pulses. Although they appear at first sight to be different, they

10.3.2

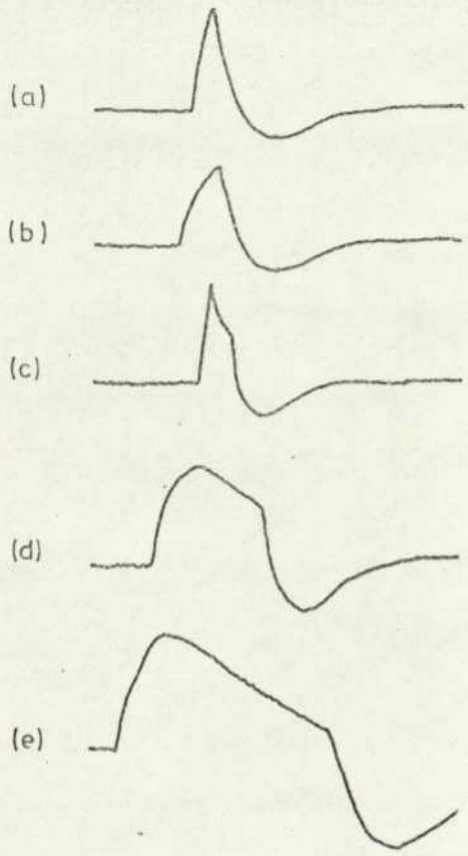

Fig. 10.3.2.1. Five typical pico Coulomb pulse shapes. Note that (a) is similar in shape to the femto Coulomb pulses caused by particles.

are in the author's opinion variations on a basic shape. Fig. 10.3.2.2 shows a typical pico Coulomb waveform.

The first section of the waveform, A B is common to all these shapes and it has an exponential shape. The section from B to C is the most variable part of the basic shape. It is sometimes not present at all, its absence giving rise to a pulse similar to the femto Coulomb type. When section B C is present it usually has a gradually decreasing shape with noise superimposed on it. Section C D is the 50 μS decay of the charge sensitive amplifier and section D to E is a decay caused by the pulse shaping

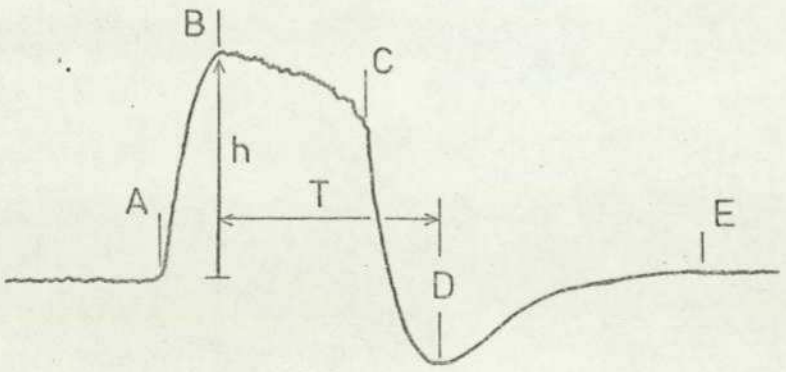

Fig. 10.3.2.2. The features of the basic pico Coulomb pulse.

10.3.2

amplifier (see Section 9.6.3) and has a time constant of 200 μS.

An analysis of some of these shapes was carried out and the results are presented below.

The features were measured from fifty waveforms recorded at four different levels of stress. The height of the pulse (h) was measured at B (see Fig. 10.3.2.2) and the time interval (T) between this peak and the end of the 50 μS decay at D. The results were punched on paper tape and distributions of h and T were generated with the aid of the histogram plotting program (mentioned earlier). Fig. 10.3.2.3 shows the distributions of T at 55.5 MV m^{-1}, 60.0 MV m^{-1}, 65.5 MV m^{-1} and 70.0 MV m^{-1}. As the stress is increased the mean value of T is found to decrease. The distribution associated with the h feature showed little variation over the range of stresses already mentioned. Rhodes [Thes Rho] using a pulse height analyser found the distribution of the pico Coulomb pulses to be basically

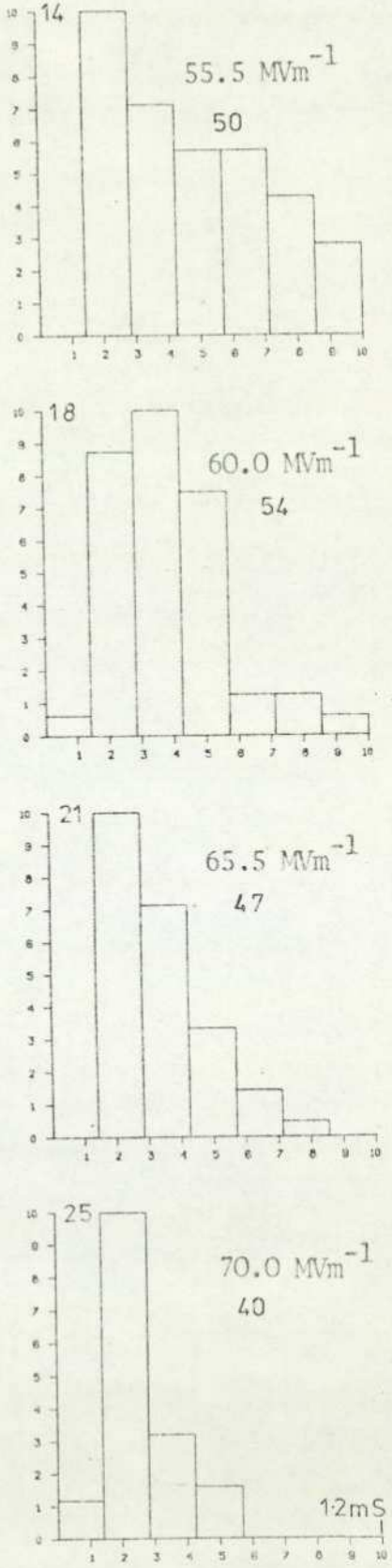

Fig. 10.3.2.3. Distributions of T at various levels of stress.

exponential but exhibiting an excess of large pulses. Megahead and Tropper [Cond Puls Meg] found the large current pulses in transformer oil to be exponentially distributed but as their graphs are uncalibrated comparisons with the work of Rhodes cannot be attempted It is felt that more data would be required before any positive comments could be made about the variation of h with stress.

Checks were made to ensure that these shapes were not caused by the EHT supply or the charge sensitive amplifier (though the 50 μS decay from C to D in Fig. 10.3.2.2 is known to be an amplifier effect). The EHT supply was monitored, via a capacitor, by the transient recorder and no disturbance was associated with the occurrence of pico Coulomb pulses. A scatter diagram of h versus T for each 50 values was plotted to test for amplifier effects and no correlation was apparent.

10.4 Observations on Breakdowns

Throughout these preceding measurements breakdowns were avoided as much as possible, but inevitably some would always occur. When, after one series of measurements near breakdown, the cell was well contaminated (i.e. with at least 1 particle bridge) it was decided to attempt to capture the charge waveform prior to breakdown. Rhodes [Thes Rho] states that breakdown usually occurred during an intense burst of pico Coulomb pulses but occasionally occurring during a 'quiet' period. The transient recorder was set up to trigger only when the breakdown occurred. The output from the charge sensitive amplifier was amplified and fed to the input of the recorder. In over three hundred breakdowns (obtained by leaving the stress at a constant level until conditioning forced this value

to be raised) only two waveforms such as that in Fig. 10.4.1a were captured; all others occurred during a noise burst and so were out of the input range of the recorder. The breakdown occurred at x = 6.75 on the normalized time axis; just prior to this a small increase in charge is indicated. Expansion of the waveform over the region of interest gives the waveform in Fig. 10.4.1b. Despite quantization, the rise at the end of the trace indicates a charge of

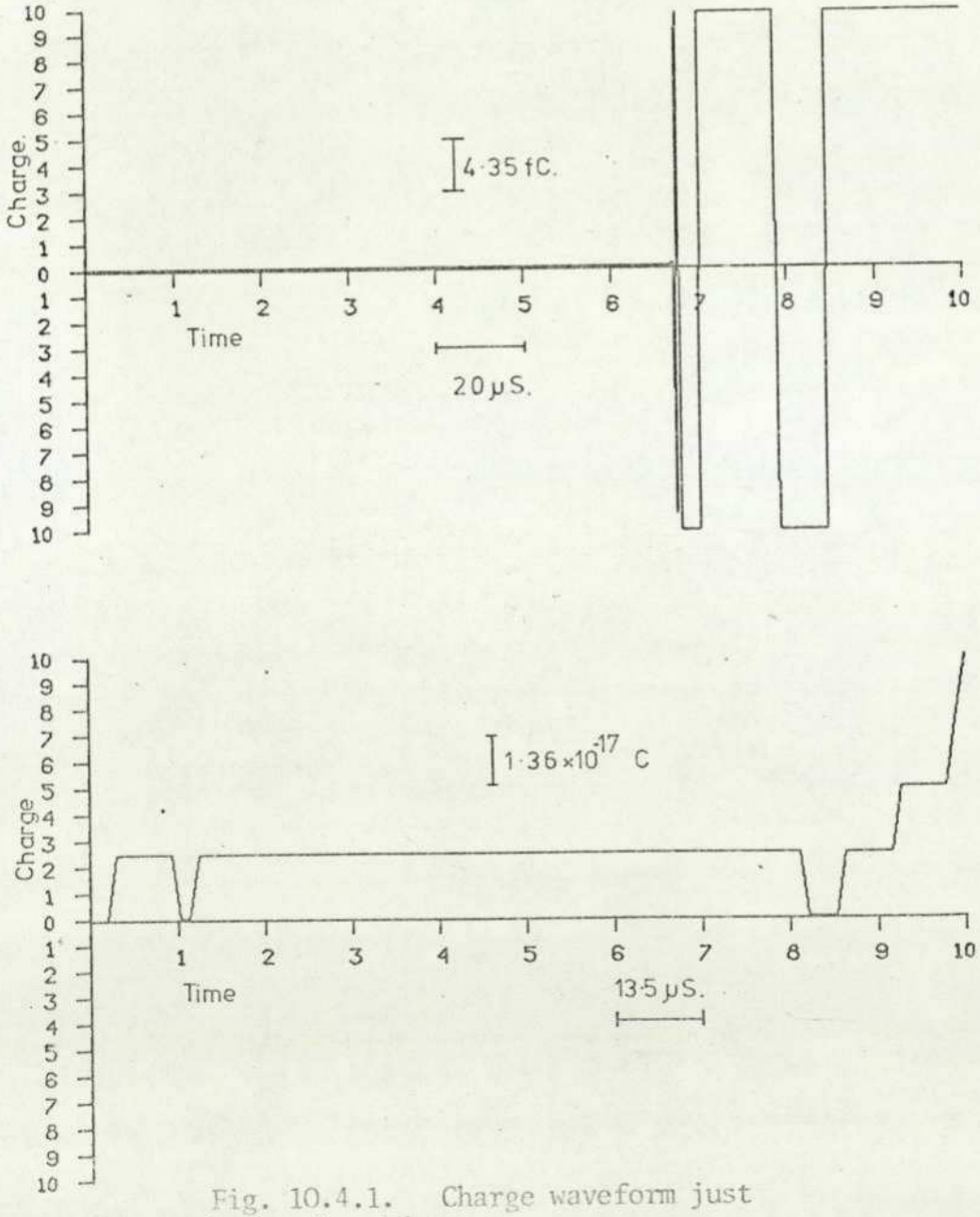

Fig. 10.4.1. Charge waveform just before breakdown.

10.4

6.8×10^{-17} Coulombs moving between the electrodes at a speed of 62 ms^{-1} (this could also be a constant current of approximately 42×10^{-12} amps flowing for 1.6 μS). This increase just prior to breakdown is unlikely to be caused by a particle crossing the gap as only a very small charge is conveyed. Further measurements will be necessary before any conclusions can be drawn.

10.5 Comments on Conditioning

Although no detailed analysis of the conditioning process (in the liquid/test cell system) has been performed (during the course of the present work) some of the present author's observations are considered sufficiently important to be included.

The observations stem from the operation of the particle extracting system (see Section 9.3.2). This system allows liquid to be removed from the test cell, filtered and subsequently returned to the cell. Approximately twice the total volume of liquid necessary to fill the test cell was present in the system at any time. It was possible that during the recycling process liquids conditioned to varying degrees could become mixed. When a small quantity of liquid was drained from the cell and replaced with filtered n-hexane a distinct increase in the rate of pico Coulomb pulses was observed and the breakdown strength was noticeably lower. It was not even necessary for the electrodes to be exposed to vapour for the effect to occur. Even when, following a series of breakdown measurements the cell contained a few particle bridges, after the liquid was recycled a conditioning process was observed. It is possible that the presence

10.5

of some previous unstressed n-hexane may be the cause of this effect.

SECTION 11

Discussion.

11.1 Introduction

This section commences with a summary of the more important results of the present author's work described in Section 10. Some of the features of the on-line transient recorder are discussed in Section 11.3. In section 11.4 an attempt is made to relate the main results of this work to some of the main points considered in Section 7.

11.2 Summary of Results

The seven diagrams in Fig. 11.2.1 form a compendium of the results described in Section 10. Fig. 11.2.1a shows a typical charge transient caused by the motion of a discrete quantity of charge crossing between the electrodes (assumed to be conveyed by a natural impurity). Computer analyses of large numbers of these transients (made possible by the on-line transient recorder described in Section 4), permitted the relationships to be established between particle charge and particle radius, which are shown in Fig. 11.2.1b, and also between particle velocity and applied stress, shown in Fig. 11.2.1c. The captured waveforms enabled a distribution of the potential associated with each particle (V_o see [Cond Part Fe1]) to be generated. This is shown in Fig. 11.2.1d. The capability of 'seeing' a particle arrive and leave an electrode whilst simultaneously monitoring the charge transferred is demonstrated by the two waveforms in Fig. 11.2.1e. The first completely objective correlation between the charge transported and the motion of particles between the electrodes is given in Fig. 11.2.1f. The use of the photomultiplier signal alone enabled the analysis of the effective dwell times of particles at an electrode to be made. The result that

11.2

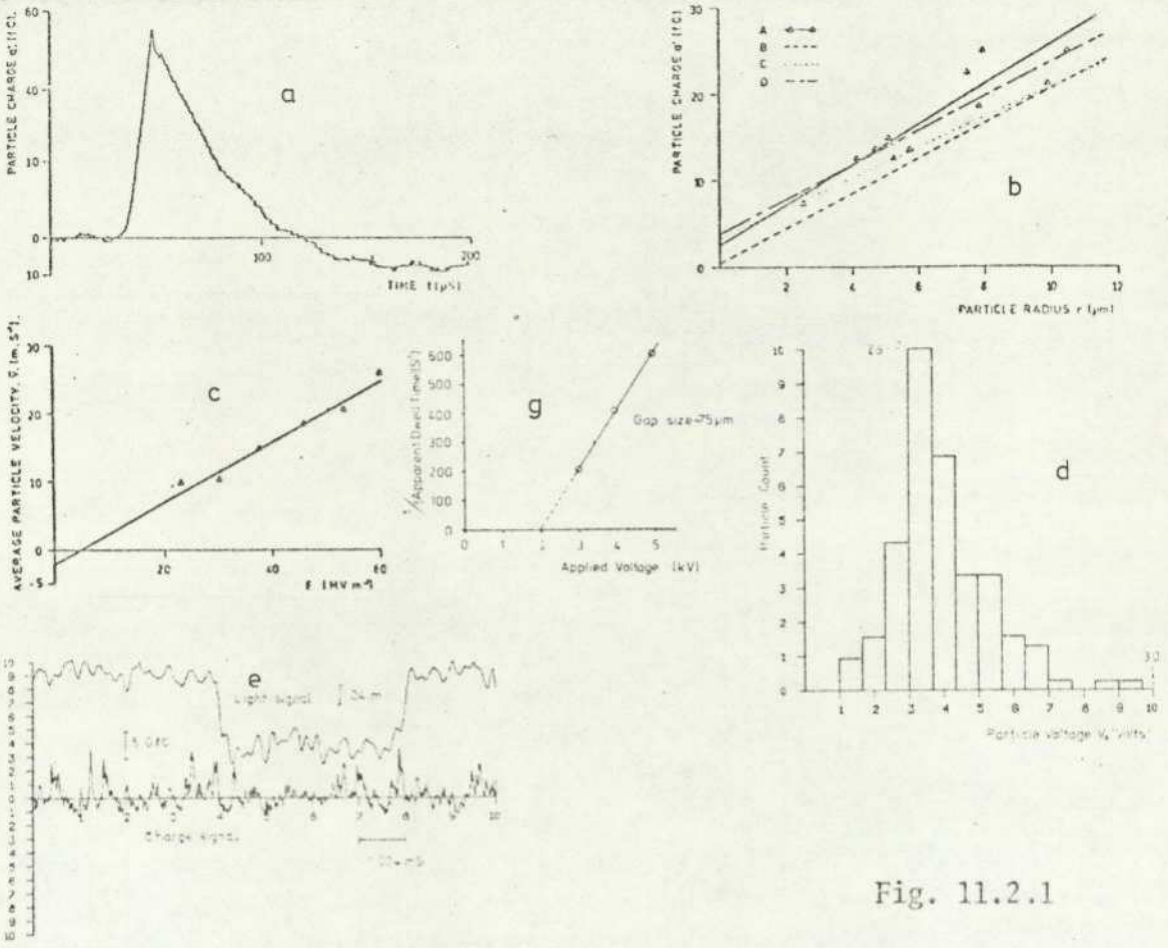
a
b
c
d
e
g
PARTICLE CHARGE q (fC)
PARTICLE RADIUS r (μm)
AVERAGE PARTICLE VELOCITY, v (m.s⁻¹)
Gap size=75μm
Applied Voltage (kV)
Particle Count
Particle voltage V, volts

Fig. 11.2.1

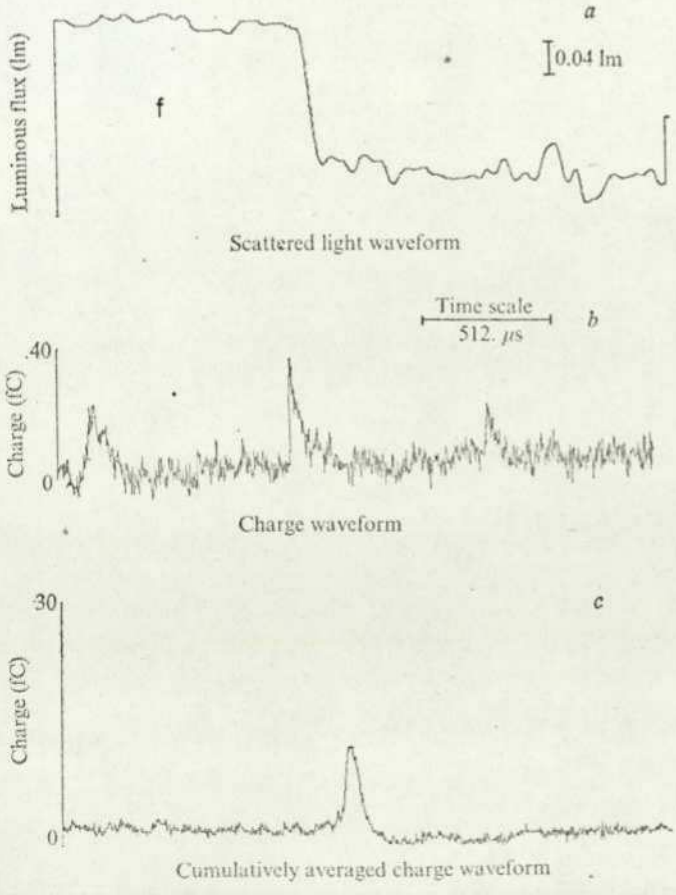
a
0.04 lm
f
Luminous flux (lm)
Scattered light waveform
Time scale
512. μs
b
Charge (fC)
.40
0
Charge waveform
c
30
Charge (fC)
0
Cumulatively averaged charge waveform

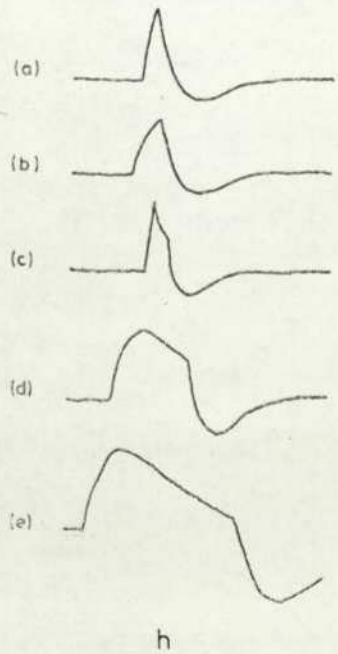
(a)
(b)
(c)
(d)
(e)
h

11.2

the effective dwell time is inversely proportional to stress over the measured range is shown in Fig. 11.2.1g. Fig. 11.2.1h features some of the large pico Coulomb pulses believedto be variations of a basic shape.

11.3 Capture and Processing of Transients

In Part I of this Thesis the structure of the author's on-line transient recorder system was described together with the methods of waveform recognition for the classification of captured transients. In Section 8 various constraints and common sources of errors which are encountered when working in the discrete time domain are featured.

The detailed descriptions of the programs and circuits required to control the transient recorder and organize the storage of transients on the disc are to be found in Section 17. These documents indicate the considerable time required to design and build the on-line transient recorder system.

Fig. 11.2.1a shows a charge transient as captured by the on-line recorder and plotted by the incremental plotter. This waveform gives directly the amount of charge transferred and the time taken for the charge to cross the gap; it is a good example of the accuracy with which waveforms can be represented digitally.

The establishment of a positive correlation between the femto Coulomb conduction pulses and the motion of a particle (see Section 10.2.3) represents a difficult measurement which the 'intelligent' transient recorder was able to perform with relative ease. Neither the transient recorder nor the on-line computer could have individually tackled this task. The necessity for a high capture rate is also apparent, since at higher stresses the large

pico Coulomb pulses tend to swamp the system, and in order to capture a few femto Coulomb pulses a large number of waveforms must be processed. The application of the waveform recognition system to this problem enabled the recorder to be immediately re-armed if the captured waveform was out of range.

The disc filing system in spite of its inefficiencies (see Section 5.3) has proven a vital aid to the on-line transient recorder. The experiment described in Section 10.2.3 was particularly difficult to set up. Thus the capability of storing data for later processing allowed the re-registration program to be developed on the original set of waveforms without the time overhead of operating the apparatus and instrumentation. Another advantage of having the captured waveforms stored and documented is that further waveform parameters or statistics can be easily obtained should they be required.

Section 12 contains examples of other studies made during the course of the present research.

11.4 Present Results in Relation to the Previous Work

Prior to the discussion of the motion and effects of natural particles in liquid dielectrics consideration of the role of the test cell in the measurements performed is worthwhile. In the light of the work by Krasucki [Part Imp Kras] and subsequent comments by Gallagher [Si Dl Gall] on the cleaning techniques used in preparing a test cell, the construction and cleaning of the cell utilized (see Section 9.4.1) in the present study is of considerable importance. The majority of the metal in contact with the liquid is stainless steel, the fixed high voltage electrode mount being

brass. The insulating sections of the cell are made entirely from PTFE. Ultrasonic cleaning was only employed when the cell was first reconstructed after a long period of disuse. Subsequent flushing of the cell with n-hexane and wiping with lens-cleaning tissues was used [Cont Elec Harp]. The implementation of a cyclic filtering system operating with the cell in a closed loop has been found to be advantageous in reducing the impurity content of 1 um size particles and very effective with larger particles and fibres. The importance of the effect of test cell material on conduction studies was pointed out by Morant [Pola Dl Mor] who found evidence of charge storage on the insulating surfaces of his test cell. The coaxial construction of Rhodes' cell with both electrodes enclosed by a grounded stainless steel tube will reduce the effect of charge storage. Though there may be some charge storage on the PTFE insulation in the cell it is, however, remote from the electrode gap. The amount of PTFE in contact with the liquid was reduced by the modifications made by the present author to the inlet and outlet ports.

The motion of impurities in high fields is seen from Section 7 to be similar for gases vacuum and liquids; in the three phases the oscillating motion is reported, although some of the other particle effects are peculiar to the given system (such as particle vapourization due to impact [Carb Part Gray]). In the majority of the literature surveyed this oscillating motion has been assumed to be caused by the particle acquiring a charge on an electrode and being forced by the electrophoretic force (qE) to move to the other electrode; once there it gives up its charge and gains one of the opposite sign and thus returns to the first electrode.

11.4

Much of the work on particles has been carried out in viscous liquids or at low values of electric stress where the particles have velocities which are much lower than in simple liquids under high stress conditions. The speeds obtained in [Cond Part Fel] are under 0.15 ms^{-1}. This made measurements considerably easier than those of Rhodes [Thes Rho] or the present author. Rhodes was able to obtain a few femto Coulomb pulses at various stresses to substantiate the claims made in [Cond Part Fel] that the particle velocity was linearly related to the applied stress. Fig. 11.2.1c shows the results of the present author; each point is the average of several particle velocities obtained at each level of stress. The six points represent over 70 transients. The value of mobility obtained, 0.45×10^{-6} m^2 V^{-1} S^{-1}, agrees well with the value estimated by Rhodes [Part Cond Rho]. It is interesting to note that Felsenthal and Vonnegut were unable to reproduce their results in transformer oil or n-hexane.

Fig. 11.2.1b is a graph of particle charge versus particle radius. This justifies the hypothesis that the particle charge is effectively lower than would be predicted by the model of a conducting sphere in contact with a plane, and that the ratio of particle charge to effective particle radius is a constant. In the case of natural particles in n-hexane some spreading of the results occurred; Fig. 11.2.1d shows the distribution of the potential (V_o see [Cond Part Fel]) associated with 106 particles. This spread of values may be due to variations in the shape of particles and the condition of the electrodes. This may also be an indication of the variations noted by Felsenthal and Vonnegut in n-hexane. It must be emphasized that the natural particles studied by the author are not in fact ideal spherical particles in contact with a perfectly smooth

electrode but more likely resemble 'a rock in a ploughed field'. Therefore, it is in some ways surprising that the present author's findings agree so well with the work by earlier workers who used controlled quantities of particles in more viscous liquids.

Measurements by Rhodes indicate that in n-hexane the dwell time was much longer than the transit time. Before this observation most researchers had assumed a zero dwell time. In viscous liquids, where the particle velocities are low, the assumption that the dwell time is zero may be a good approximation. If the transit time is in the order of 1S a dwell time of 500 μS will not be apparent to an observer. It would appear that the dwell time on most of the reviewed papers was finite but short, and so may have gone unnoticed. Measurements in the present author's system indicate that the dwell time may be as short as 200 μS (apparent dwell time is a better description of the actual quantity measured, see Section 10.2.5.2). Birlasekaran and Darveniza [Part Mov Bir] quote transit times in the order of tens of milliseconds, but make no direct reference to dwell times when their ball made contact with the electrode (elastic collisions may mask the actual charging time).

In Fig. 11.2.1g inverse apparent dwell time is plotted versus stress. The value at which the line crosses the stress axis agrees approximately with the value below which particles remain stationary and do not cross the inter electrode gap. In practice this threshold level for particle movement is not fixed, but appears to be affected by the conditioning process.

11.4

Section 10.2.3 considers the role of particles as conveyors of charge. The experimental results reported conclusively prove that the natural microscopic particles carry a charge of the order of femto Coulombs. This thus substantiates the previous work of Rhodes at lower stresses and the theory put forward by Felsenthal and Vonnegut.

The results obtained by Birlasekaran and Darveniza [Part Mov Bir] have been reviewed by Gallagher [Si Dl Gall] who considers that their findingsfavour the [Cond Part Fel] theory. In fact, taking the 6 results given in [Part Mov Bir] and assuming the not unreasonable value of 0.1 P for the viscosity of the transformer oil used applying equation 8.3.8 gives particle radii ranging from 0.47 mm to 0.39 mm and an average value of 0.43 mm. The actual size of the steel ball used was 0.4 mm radius. These measurements must add great weight to the statement made by Rhodes that the contribution of current caused by what has now been proved to be particulate contamination was less than 1% of the total conduction current.

The theory of Felsenthal and Vonnegut suggests that the effective charge on the particle as it crosses between electrodes is shielded from the liquid. Evidence for ionic attachment has been put forward by Sletten and Lewis [Dis Gas Slet] who thought that oxygen molecules were becoming attached to particles and thus changing their effective permittivity (see also [Dis Gas Noss]). In the case of the present author's system it seems likely that such a shielding layer could originate from ions from a space charge at the electrode surface. The evidence for space charge in this system is quite strong. Use of the Kerr electro-optic effect by several authors [Spa Cha Good, Spa Cha Cas] and mathematical models with experimental comparisons

11.4

[Spa Cha Cal] indicate that at both anode and cathode, under high field conditions, a space charge of opposite polarity to that of the electrode will exist. Further evidence that the transfer of charge from the liquid to the metal is not an efficient process is indicated by the findings of Hughes and Secker [Char Coll Hug]. They experienced difficulty in collecting charge from a moving stream of liquid in measurements to evaluate the possibility of making a high voltage electrostatic generator using a liquid to convey the charge. It is possible that a particle in contact with an electrode once it gains sufficient charge to overcome the binding forces leaves the electrode but carries with it a shielding layer formed by ions from the electrode space charge.

The inefficiency of the charge transfer mechanism observed by Hughes and Secker is evident in the case of natural particles in n-hexane, and in studies involving charge conveyed by particles, by the dwell time of the particles on the electrode. The rate at which particles obtain and lose charge at the electrode will depend on the surface conditions. The build up of wax deposits on the electrodes following breakdowns in the liquid is reported by many authors; this insulating layer will certainly tend to inhibit the transfer of charge. An oxide layer together with adsorbed gas present on all electrodes may have a similar effect. In a test cell where few breakdowns have occurred and therefore the electrodes are in a good condition (assuming that the usual cleaning and polishing techniques have been employed) the charging time of a particle may be expected to be shorter than in a cell with heavy wax deposits. The experiments made by Gzowski et al [Lum Dl Gzo] would appear to substantiate this idea (see Section 7.2). They measured the time of the first two particles

to cross the gap after the rapid application of a voltage and found it to be 60 μS. This 60 μS must be the time taken for the particle to gain its charge and cross the 100 μm gap. The transit time for these authors' conditions (similar to those in the present study) would give a particle transit time of 10 μS at the stress of 43 MV m^{-1} used in the experiment. Thus the charging time would appear to be in the order of 50 μS. In the study on apparent dwell time the test cell had suffered enough breakdowns to give the electrode a covering of wax and this may explain the difference in the longer charging time in the present authors study. Gzowski et al use the figure of 60 μS to calculate the mobility of the particle. This gives an erronious result as the charging time has not been deducted from the transit time.

It is more difficult to account for the motion along the surface of an electrode than between the transit across the inter-electrode gap; and, incidentally, for the tendency of particles under some conditions to leave the gap completely. The early workers using oil suggest that this gap clearing may be the cause of the observed conditioning process [Thes Gos]. The effect seen by Rhodes [Thes Rho] in n-hexane was not quite the same, in the case of oil the particles left the gap completely; in n-hexane they returned after a short period of time, or immediately if the stress was reduced or removed. Rhodes reported that the expulsion of particles from the gap appeared to coincide with an increase in the impulsive charge (i.e. an increase in the pico Coulomb pulses see Section 10.3.1). Rhodes postulated that if a large amount of charge was injected into the liquid its effective permittivity would increase and thus cause a

reversal of the dielectrophoretic force which would then tend to remove particles from the gap until the charge had dispersed or re-combined. The origin of conditioning in oil could be that water impurities present in the oil were attracted into the inter electrode gap. According to the argument put forward by Rhodes this would change the effective permittivity of the liquid and reverse the dielectrophoretic force or oxygen impurities becoming attached to particles would have the same effect. Owing to the low mobility of ions in oil, these processes could take several hours [Dis Gas Noss]. In the case of an air insulating system Mulcahy [Part Air Mul] reports that wet fibres oscillate out of the high field region. This result is contrary to the preceding discussion as the fibres would have an increased permittivity and would thus expect to be pulled into the gap. It may be in this case that the centrifugal force was greater than the dielectrophoretic force for wet fibres but less than it for dry ones (on the assumption that the wet fibres can carry more charge) and so wet fibres would oscillate out of the gap.

The magnitude and balance of forces acting on a spherical particle (see Section 8.4) in transformer oil and in n-hexane are considerably different owing to the difference in viscosities of the liquids. In oil the particles will move slowly (many earlier observers report seeing particles crossing between the electrodes) whilst in liquid n-hexane the particles can only be seen on the electrode, their passage between the electrodes being too fast to observe. This variation in speed will alter the centrifugal force acting on the particle, as this force is proportional to the square of the velocity. It seems likely that, ~~although~~ in the pure liquid the

centrifugal force is greater than the dielectrophoretic force and will cause particles to leave the gap; in oil the centrifugal force will be in proportion very much smaller and thus have less effect on the motion of the particles. Owing to the uneven contours of natural particles in oil or n-hexane, the simple model of forces acting on the particle (see Section 8.4) is grossly inadequate. The electrophoretic and frictional forces, which are typically 3 to 4 orders of magnitude greater than the centrifugal or dielectrophoretic forces, may have minor components at right angles to the direction of motion of the particle along a field line. Liquid motion is yet another factor which may affect the course of a particle, more so in oil which has a high viscosity. Evidence for liquid motion between spherical electrodes is given by Smith and Calderwood [Bd Dl Smi] who show how a jet of coloured hexane flowing between the electrodes was disturbed in the presence of an electric field; though the electrohydrodynamic stability of the liquid will be lower if some liquid motion is already present.

The experiments of Mirza, Matuszewski and Hesketh and Lewis [Liq Mot Mir, Rot Cond Mat, Cros Wir Hes] strongly suggest that the decay component of current following the application of stress is due to nanometre size impurities, but the work of Morant [Pola Dl Mor] may indicate that this effect is partly due to charge storage on insulating sections of the test cell; PTFE, nylon and glass are common insulating materials which may hold a surface charge.

The work of Hesketh and Lewis [Cros Wir Hes] supports the view that the fluctuating component of conduction current can be caused by the presence of particulate impurities, (enhanced field emission being

the suspected mechanism). The work of Cantril and Pohl [Ind Cond Can] provides further evidence for particles increasing the conduction by enhancing the field at the cathode. Though, as Gallagher [Si Dl Gall] points out, in test cells where breakdown increases the particle content, the effect of the increase may be countered by the build up of wax deposits on the electrodes, which would hinder the charge transfer process. For a spherical electrode system subjected to a large number of breakdowns, the present author has observed that the wax layer forms a ring around the central region where breakdowns occur. Thus particles in the central regions may still be able to raise the field; though the very nature of the breakdown craters is a more likely cause of enhanced field emission.

The observations of Huq and Tropper [Cond Puls Huq] lead them to state that the current fluctuations were lowest when the particles were in motion and highest when only a few particles remained in the gap. This corresponds to Rhodes' [Thes Rho] observation, but with cause and effect reversed! Huq and Tropper conclude that no correlation exists between particle motion and the current fluctuations. This observation may be evidence that when the particle oscillations had ceased, although most solid impurities had been removed from the gap, some particles remaining on the electrode could have given rise to enhanced field emission. Krasucki [Bd LD Kras] reported 'dark regions' growing from particles, and the picture produced by Thomas and Forster [Cond Bd Tho] show 'cavities' forming on the cathode at what might be particles or other rough features on the surface of the electrode.

The other possible method of particle induced breakdown, first

put forward by Sletten [Thes Slet] is that the charged particle approaching the electrode increases the local electric field strength and thus initiates breakdown. In considering the earlier postulation regarding space charge and shielding layers Sletten's theory may still apply. If such a shielding layer of space charge exists, the increase in the electric field will now occur between the space charge at the electrode and the shielding layer surrounding the particle. Thus the field will still increase on the approach of the particle and may lead to breakdown. The present author's measurements on the charge waveform prior to breakdown (see Section 10.4) are too few to discuss in detail, but the initial findings show that the transfer for charge is lower than that carried by a particle and the transit time is higher.

Although the charge acquired by an ideal particle according to classical electrostatics is less than the amount required by the approximate expression to cause high field emission from the surface of the particle [Bd LD Coel] (when it is not under the influence of the electrodes), for a natural particle with rough surface features, the field may be high enough to cause electrons to be emitted. If the particle possesses a shielding layer this would make the emission of electrons even more likely, as the shielding layer would create a high electric stress at the surface of the particle.

The formation of bridges in relation to dielectric failure seems more crucial in transformer oil than in the simple liquids. The reason for particle bridges causing breakdown in oil is almost certainly due to the adherence of water molecules to the particles which forms a conducting bridge (even if the particles are mainly

insulators). In purified hydrocarbons the water content will be much lower, usually in the order of a few tens of parts per million. Thus a bridge formed in a 'pure' liquid will not lead to a preferential breakdown path. Also the likelihood of metal particles is greater in transformer oil of industrial origin.

The 'memory' effect, which relates to the fall in breakdown strength with increasing numbers of breakdowns, has been reported in [Imp To Abg, Mem Dis Bom]. The effect is attributed to the increase of particle content, after each breakdown, which lowers the breakdown strength of the liquid. Unfortunately the mechanism of breakdown is not established. Thus either particles on the electrode enhancing the field emission or charged particles approaching an oppositely charged electrode are possible causes of breakdown. The fact that in both studies the liquid was in motion may make the former mechanism less likely.

The relevance of the shape of the pico Coulomb pulses (Fig. 11.2.1h) is difficult to gauge with so little data available. From the study performed, it would appear that each pulse represents a similar process which can be of varying duration. These pulses may indicate the temporary existence of preferred sites for electron emission, but further study will be necessary before any firm conclusions can be reached.

Comments in [Cond Bd ZaHa] relating to conditioning are contrary to an observation made by the present author. Zaky and Hawley state that there is general agreement that once the liquid and the

electrodes have been conditioned (by breakdowns) changing the liquid has no effect on the breakdown value. In the author's present study, changing the liquid (in an attempt to reduce the level of contamination) in the cell following a series of at least 200 breakdowns, reduced the electric strength of the liquid to approximately the values registered when the liquid was first placed in the test cell. Even changing a small quantity (approximately one quarter) of the liquid had the effect of increasing the current fluctuations. In this latter case the electrodes remained covered by liquid and were not exposed to vapour which may have contained impurities (i.e. oxygen). It may be that the conditioning process relates partly to the establishment of a static space charge on the insulating surfaces of the test cell.

SECTION 12

Measurements in other Fields.

12.1 Introduction

Since the subject of dielectric liquids poses measurement problems of a difficult nature, it is perhaps not surprising that in solving them one also provides solutions to experimental problems in apparently unconnected areas. Some of these measurements required the full power of the recorder, whilst others were made less tedious. In the following pages a few of the more interesting of these measurement problems are described, several of which demonstrate the power of the on-line recorder. One or two however, suggest limitations of the present system.

The first study, described in Section 12.2, deals with the recording and analysis of acoustic emissions from propagating cracks. The study, which was commissioned by the British Gas Council, was an examination of ways of detecting metal fatigue and failure due to small cracks occurring in pressurized containers.

Section 12.3 outlines a pilot study undertaken to record current waveforms associated with plasma formation and collapse in Ion Motors. At the time of writing, the Aeronautical Department at The City University was still engaged in this research.

Finally, in Section 12.4, three applications are described in which the transient recorder system has been utilized by co-workers of the author in the liquid dielectrics field.

One application of the transient recorder which is worth mentioning is its use in analysing timing problems and the erratic performance of digital circuits under development. The off-line transient recorder has frequently been used to detect race conditions and intermittencies in faulty or incorrectly designed circuits. Purely digital (with respect to the input signal)

12.1

versions of the recorder are available, but the analogue variety is quite capable of monitoring digital waveforms. In the cases of an intermittency in a digital waveform the pattern recognition software (see Section 5) could be used to detect the error if supplied with the expected waveform and thus allow the user to find the cause of the intermittency. Naturally, due to the incompatibility of the record mode with the programming mode, the one circuit that the recorder was unable to fault find was its own interface!

A short study of mains transients was made prior to the installation of the disc drive for the ICL1600B computer. The specifications of the disc drive required a mains supply of high integrity. The ordinary laboratory supply was subject to lost cycles and spikes; it was therefore considered to be unsuitable for the disc unit.

12.2 The Study of Acoustic Emissions

The research into the measurement of acoustic emissions from moving cracks was performed in the Department of Physics at The City University and at Imperial College [Thes Rav]. Domestic gas was to be stored, at high pressure, in cylindrical metal containers. Knowledge of the fatigue characteristics and the detection of moving cracks to indicate an impending failure was of particular importance.

Specimens of the metal to be used in the storage tanks (steel containing 9% nickel) were tested in a tensometer and the acoustic waves generated by the propagating cracks were detected by an

12.2

ultrasonic transducer mounted on the specimen. The signal from the transducer was fed, after amplification and filtering, to a modified video tape recorder (see Fig. 12.2.1).

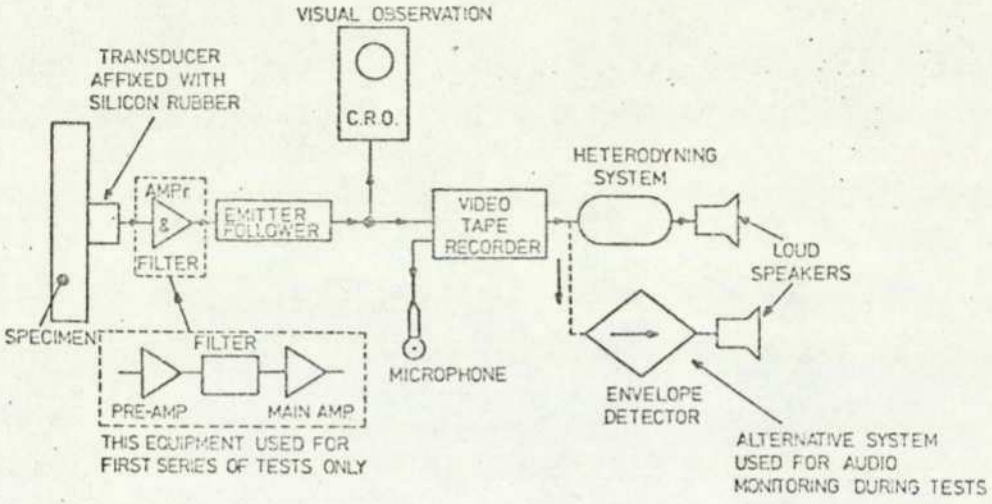

Fig. 12.2.1. The stress wave emission detecting system (after Thes Rav).

This video recorder has been reconfigured to allow continuous signals to be stored (as opposed to picture frames) on the tape. The passband of the device is approximately 0 - 1.2 x 10^6 Hz. The video recorder has a freeze frame facility and it is possible to stop the tape whilst leaving the play back heads in motion. This repeatedly outputs the same signal and allows single events to be monitored (in effect another form of transient recorder).

The data processing equipment was located at The City University while the tensile testing was performed at Imperial College London and at the British Gas Engineering Station Killingworth; thus the video tape recorder was used to link the constituent parts of the experiment. Fig. 12.2.2 shows the layout of the processing system which calculated the energy of each emission (E_c) and the emission activity (n_c).

12.2

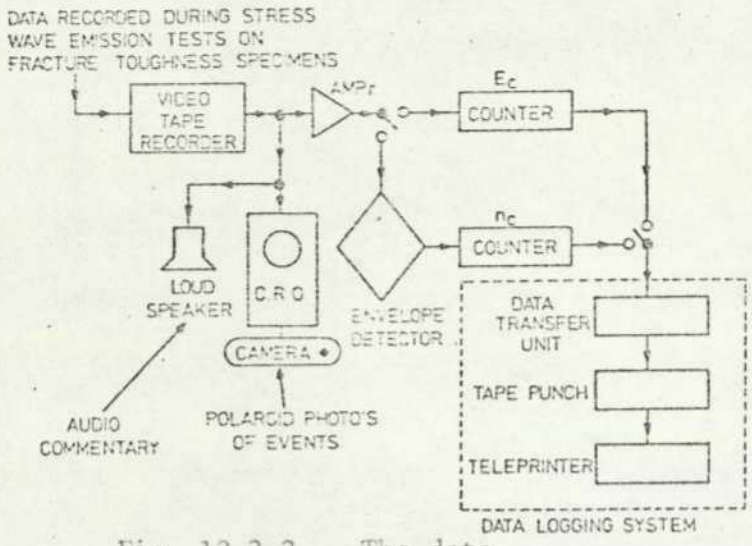

Fig. 12.2.2. The data processing system used for the evaluation of E_c and n_c (after Thes Rav).

The estimation of the energy in an acoustic emission is found by counting the number of oscillations of the transducer signal which exceed a preset threshold level; this is called ringdown counting and is demonstrated in Fig. 12.2.3 from which a count of 4 would be obtained. In practice counts in the order of 60 would be expected.

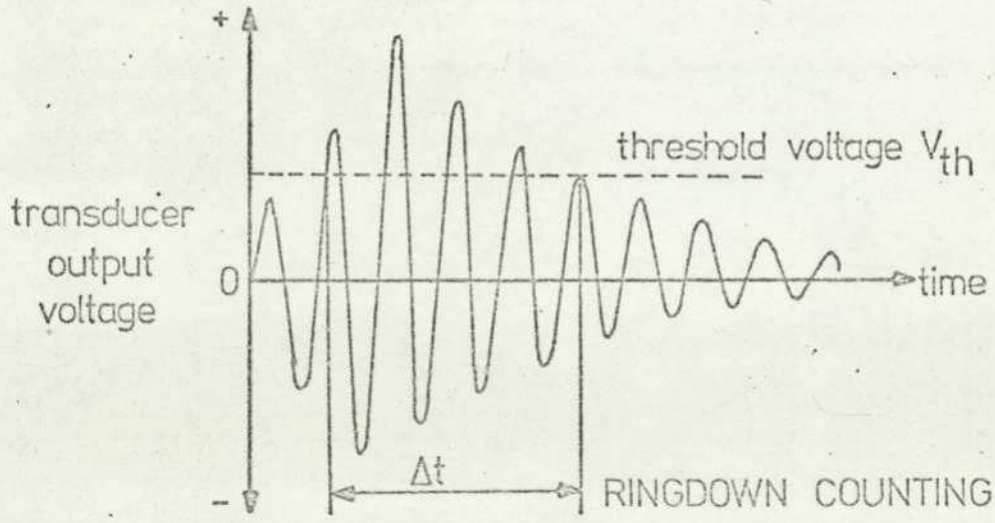

Fig. 12.2.3. The technique of ringdown counting (after Thes Rav).

12.2

The emission activity is measured by counting the number of acoustic waves occurring in a set period. The signal is passed through a low-pass filter and a differentiator before being applied to the n_c counter (see Fig. 12.2.2).

The author's on-line transient recorder system was considered for more detailed measurements (e.g. Fast Fourier Transforms) on the

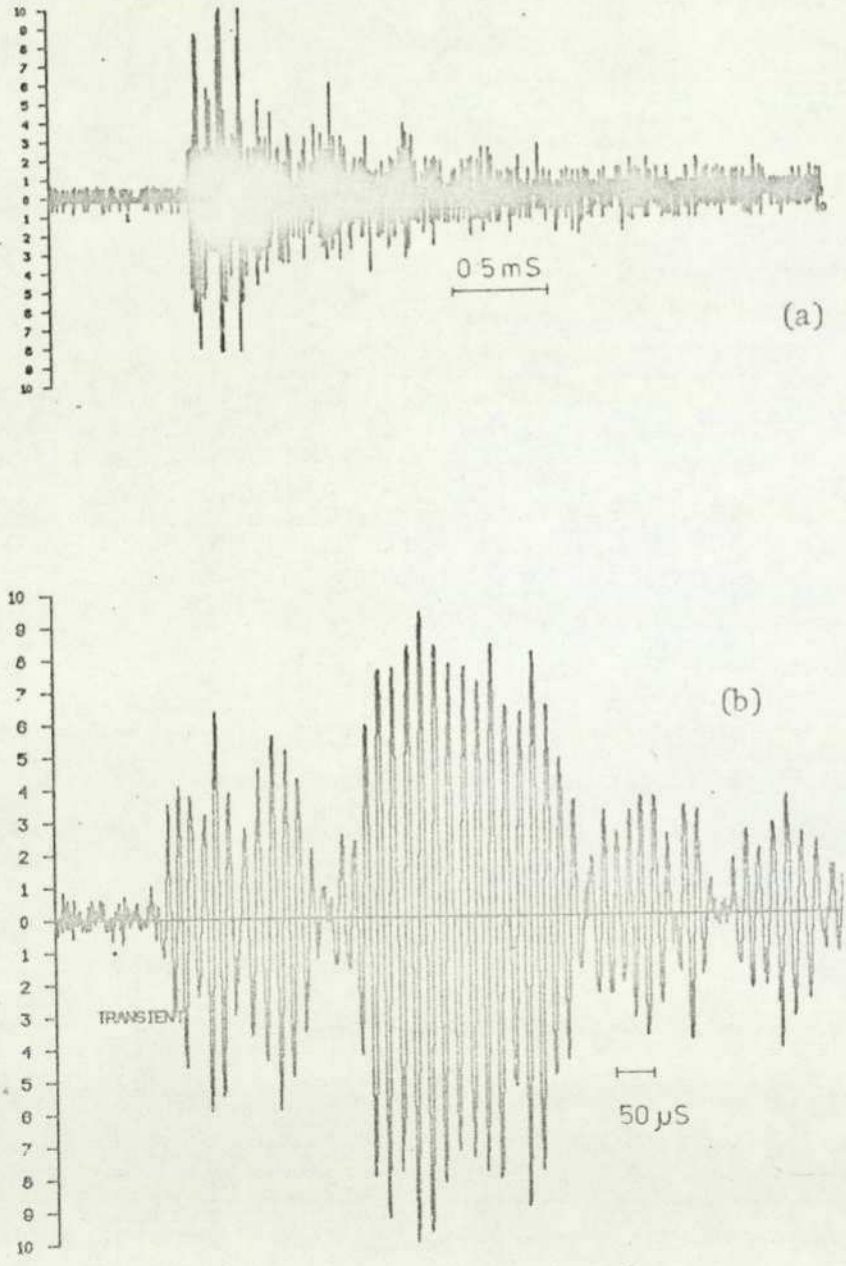

Fig. 12.2.4. A typical acoustic emission (a) captured by the on-line transient recorder. Waveform (b) shows the front of the emission in greater detail.

acoustic waveshapes than was possible with the simple counting system. The signal from the modified video tape recorder was fed to the transient recorder and a typical acoustic emission is shown in Fig. 12.2.4a and a more detailed plot of the front section of an emission is shown in Fig. 12.2.4b.

Owing to defects in the oxide coating on the magnetic recording tape waveforms such as that shown in Fig. 12.2.5 frequently triggered the transient recorder. These tape 'drop-out' waveforms had caused

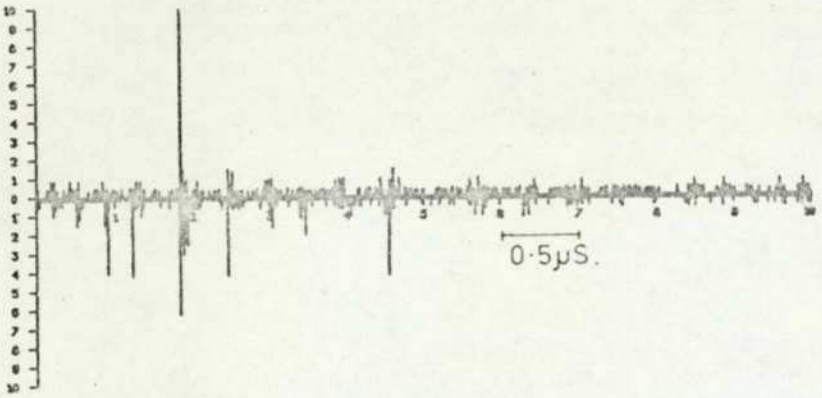

Fig. 12.2.5. A typical noise waveform from the video tape recorder.

problems in the system described by Ravenhall. The occurrence of a tape 'drop-out' did not seriously effect the value of the ringdown count but the event count could be considerably increased. However when the event count was high (i.e. just prior to failure) the tape noise was considered to be acceptable.

The advantage of using the on-line transient recorder arose from the fact that with a reasonably simple feature extracting program the acoustic emission could be distinguished from the spurious tape

noise. The test chosen for the pattern recognition system was a peak-picking routine (only positive peaks were detected by the program) which built up the shape of the envelope of the captured waveform. The resultant envelope was compared with a standard waveform which allowed the captured transients to be separated into two groups. A comparison of Fig. 12.2.4a and 12.2.5 reveals the dissimilarity in the envelopes of the two possible waveforms.

Computation of the energy of an event using the ringdown counting method can also be easily obtained by using a program to calculate the number of oscillations occurring above a preset reference level for a waveform defined (by pattern recognition) as being an acoustic emission. The event count can be accurately measured by utilizing the real time clock of the computer to note the time of capture of each waveform relative to the first application of stress. The distribution of events in time can then be studied. Before many measurements had been made, however, the video tape recorder was stolen; so the only result shown here is a fourier transform [FFT Pock] of an acoustic emission. Fig. 12.2.6a,b shows the Real and Imaginary parts from 0 Hz to the Nyquist Frequency [Sig Pro Beau].

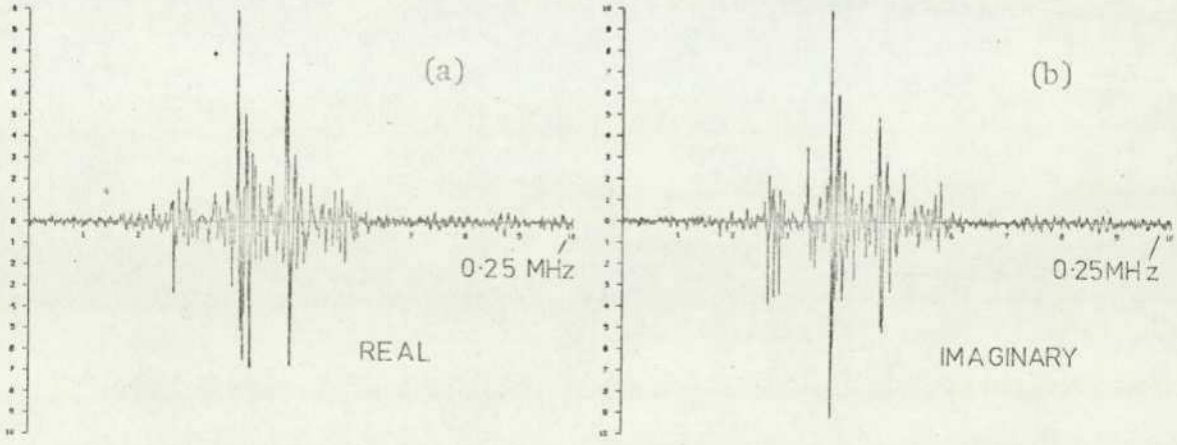

Fig. 12.2.6. The Real and Imaginary parts of a Fourier transform of an acoustic emission.

12.2

This study highlights the advantages of the 'intelligent' transient recorder with its capability of discarding unwanted waveshapes.

12.3 Current Transients in Ion Motors

A study of damage to Ion Motors is another area of research at The City University which utilized the transient recorder. Ion Motors or Ion Thrusters are being developed for use in space, where relatively small thrust levels are required for long periods of time. Several test satellites have already used such motors to maintain geostationary orbits. The diagram in Fig. 12.3.1 shows the cathode, anode and magnetic coil used to create and contain the plasma. The

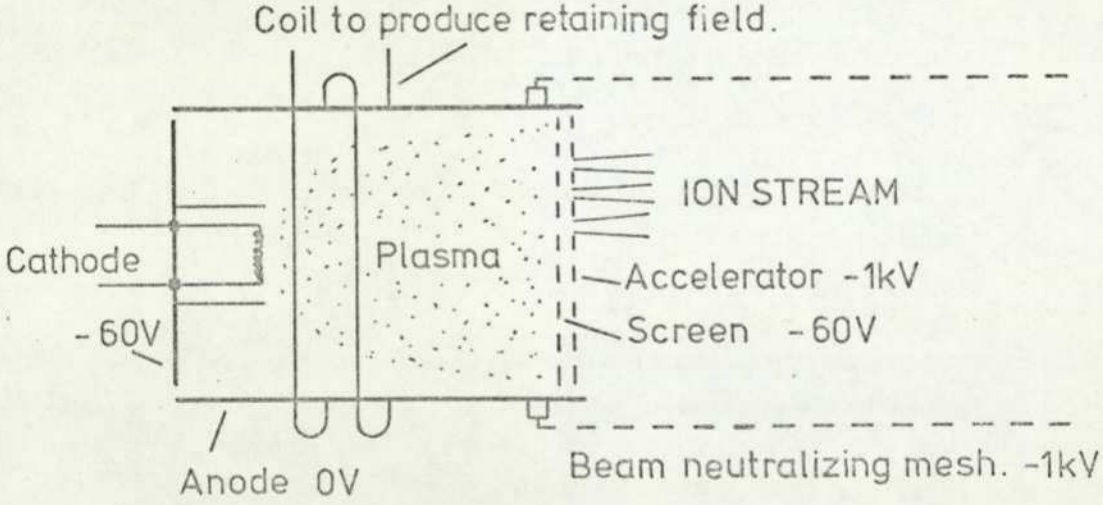

Fig. 12.3.1. A diagrammatic view of the ion thruster and test chamber.

thrust is generated by positive ions from the plasma being focussed and accelerated through the screen and accelerator electrodes out of the motor. A beam neutralizing mesh ensures that no overall charge build up occurs on the motor. One of the problems studied was the distribution of the currents which flowed when the motor was powered up or shut down. The currents are caused by the creation or

collapse of the plasma and an understanding of the damage to the screen electrode in particular is vital if such motors are to have long lives.

Owing to the location and immovable nature of the Ion Thrustor test rig the transient recorder had to be used off-line. An example of some of the waveforms captured is shown in Fig. 12.3.2. The three waveforms shown are the voltage (inverted) across the hot cathode (on start up) and the associated accelerator electrode current, which is measured via a 1 Ω resistor, and the screen electrode (inverted) measured with a current probe (hence the exponential decay).

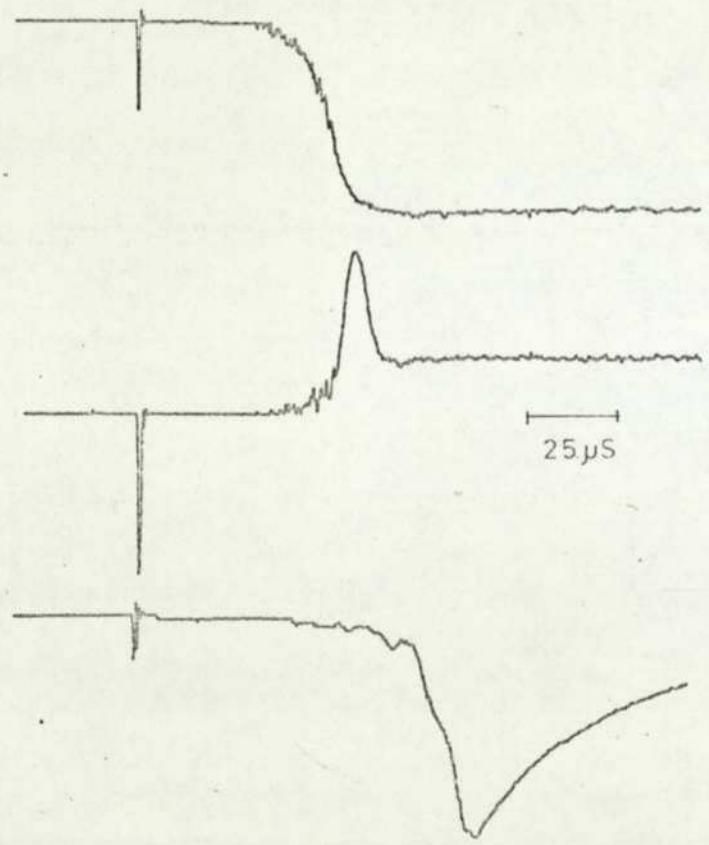

Fig. 12.3.2. Three waveforms captured during turn-on tests made on the ion motor.

More than 200 waveforms were plotted via the analogue output of the Biomation 8100. Spurious triggering was a considerable problem because of arcing in the mercury wetted contact used to control the motor, and also breakdowns between the electrodes within the motor.

12.3

The cathode voltage, input to channel A, was used as the trigger event. The electrode current to be examined was input to the second channel of the recorder.

This investigation would have benefited greatly had it been possible to link the Ion Thruster to the on-line system. The pattern recognition system could have been used to recognize the Channel A turn-on or turn-off transient and to store the associated waveform as being of interest. Spurious transients would have been ignored by the recognition program. Measurements of particular parameters and time delays for various values of cathode current and gas pressure in the motor could easily have been accomplished. The modified video tape recorder mentioned in the previous section (had it been available) would have been a convenient way of recording the slower transients (such as those shown in Fig. 12.3.2); it could not however have coped with the high frequency waveforms (up to 20 MHz) that were recorded directly. This problem of the immobility of the 'intelligent' transient recorder is referred to again in Section 13. An interesting comparison is that the capturing and plotting of the 200 waveforms off-line took three days to produce; the on-line system could have captured and stored the same number of waveforms in under four minutes. Even allowing for setting or changing experiment parameters the tests could be completed in three hours. One problem of taking the measurements over three days was the unrepeatability of certain results due to varying conditioning and stabilising processes in the Ion Motor. Over the reduced period of three hours these problems would have been greatly mitigated.

12.4 Other Measurements in Liquid Dielectrics

Several of the author's colleagues also working in the field of liquid insulant measurements have found the transient recorder beneficial. Evison and Hewish [Thes Ev, Phot Inj Hew] both used the recorder to measure movement of injected charge in liquid n-hexane under low electric stress conditions.

Evison found the recorder a convenient substitute for the FM1600B and its analogue to digital converter and plotter when the computer was not available owing to modifications being carried out by the manufacturer. Hewish used the two channels to capture a current pulse (caused by photo injection) and the resultant liquid disturbance measured with a schlieren system. The waveforms captured are shown in Fig. 12.4.1.

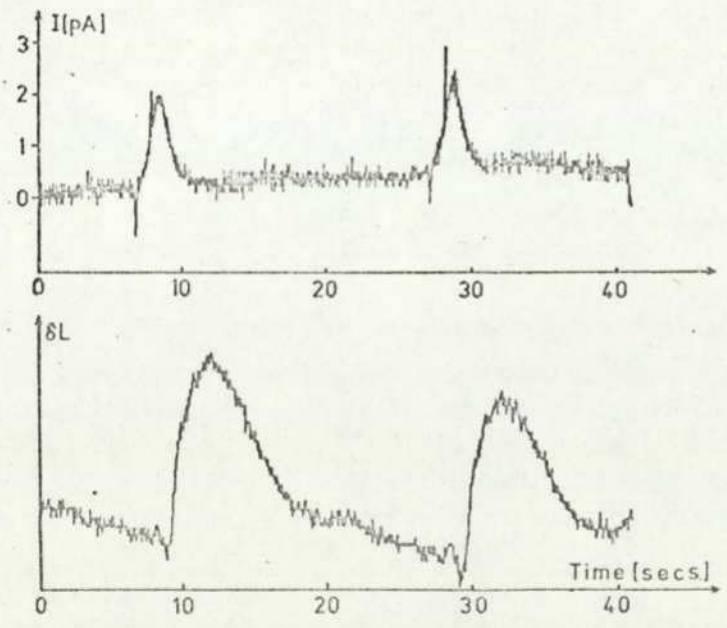

Upper Trace: Current response to 1-second pulses applied to the control grid.

Lower Trace: The corresponding schlieren disturbance signal from the diodes.

Fig. 12.4.1 (after Phot Inj Hew).

12.4

More recently Mears (private communication), using the on-line EHT unit (see Section 9.5.2), has generated a series of voltage ramps of varying rate of increase. The transient recorder was utilized to capture the average value of the alternating component of current flowing through the test cell as the applied voltage increased up to breakdown.

These waveforms were stored on disc and divided into classes according to their breakdown values. Thus waveforms associated with breakdowns in the range 5000 V to 5099 V were placed in class 1, those between 5100 and 5199 in class 2 and so on over the whole breakdown range. The waveforms in each class were then cumulatively averaged.

A typical average current waveform produced by low pass filtering the large noise bursts (see Section 10.3.1) is shown in Fig. 12.4.2, the breakdown range for this class is from 7555 Volts to 7645 Volts.

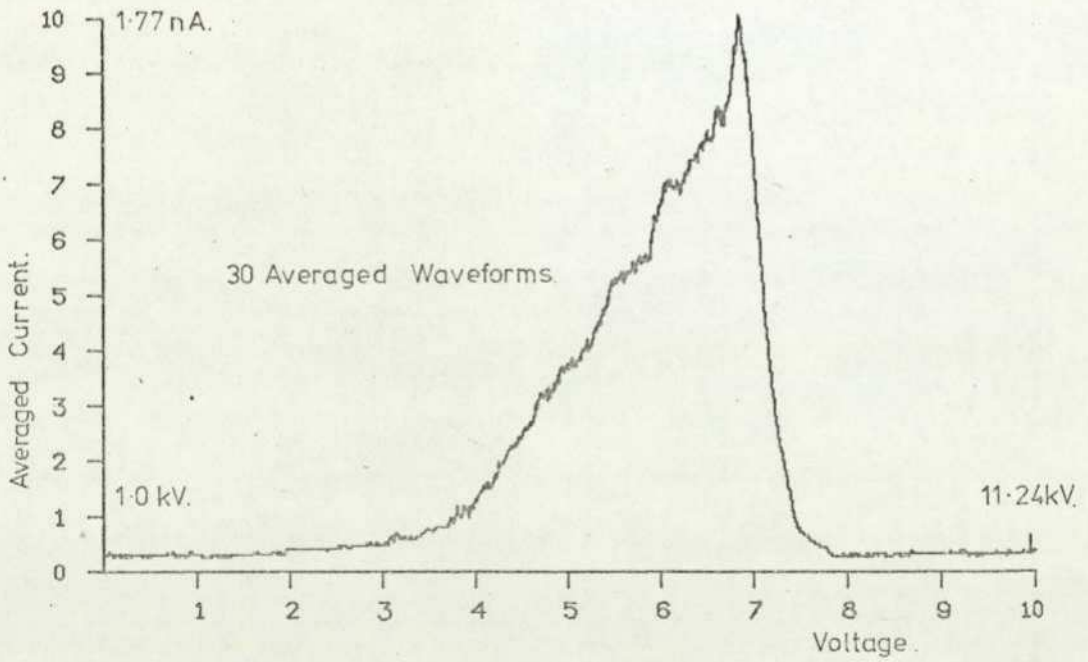

Fig. 12.4.2. The averaged current waveform for breakdowns ranging from 7.555 kV to 7.645 kV.

SECTION 13

Suggestions for Further Work.

13.1 Introduction

The following two sections contain proposals of developments of the present research that are considered worthwhile by the author. Section 13.2 deals with improvements that would increase the usefulness of the on-line transient recorder, whilst Section 13.3 outlines some possible extensions to the measurements already made in the area of liquid dielectrics.

13.2 Future Developments of the On-line Transient Recorder

The applications of the on-line transient recorder and waveform recognition system have been related in Sections 4, 5, 10 and 12. From these descriptions and some of the problems encountered by the author the following suggestions are made.

In Section 12.3 the difficulty of performing measurements at a remote site was reported. The partial solution to this problem (as given in Section 12.2) employed a modified Video taperecorder to link the experiment with the measuring apparatus. However, the ideal answer would be to take the 'intelligent' transient recorder to the experiment regardless of the location. A device under construction at the time of writing may be the solution to this problem of immobility. The device is called a Roving Slave Processor (RSP) and is being developed in the Computer Engineering Group at The City University by Messrs. R.A. Comley and R. Young (private communication). It comprises a 16 bit microprocessor, 4 or 8 k words of non-volatile random access memory, a digital cassette recorder and a data link to the main computer (FM1600B). The RSP does not possess any of the standard peripherals, such as reader, punch and teletype; instead it

uses those of the host computer. The RSP is programmed via the main computer to perform a certain measurement. It is then unplugged from the main machine and transferred to the experiment. The non-volatile memory is refreshed from a standby battery when the device is not connected to the mains supply, which ensures that the loaded program is not erased. The transient recorder once interfaced to an RSP programmed with a small version of the control software could, under microprocessor control, perform measurements aided by a simplified waveform classification system and store captured transients on the digital cassette recorder. When the experiment is completed the RSP can be returned to the host computer and pass the captured transients from the cassette to the backing store of the computer. Once recorded on disc the author's waveform recognition system can be used to classify the transients and perform the required measurements.

A useful software development would be the implementation of direct programming of the front panel registers of the transient recorder from the computer; at present all front panel functions are loaded via a parameter list supplied by the user. The additional facility would allow automatic range setting or trigger level adjustments. The necessary software could be incorporated into the overlay code (see Section 4.6 and Appendix I), which has over 900 words vacant. The length of the core resident software would only increase by a small amount in providing a simple user interface with this facility.

13.3 Further Studies in Liquid n-Hexane

Several experiments follow on from those described in Section 10 which would in the author's opinion be worthy of investigation.

The existing apparatus could be employed in an attempt to record the gap clearing effect mentioned by Rhodes [Thes Rho]. The photomultiplier would be masked from all but the central area of the inter electrode gap; the movement of particles out of this gap would cause a drop in the level of light scattered by the particles from the high intensity source. The light signal and charge signal could be captured by the transient recorder and a correlation performed in the computer.

The continuation of the studies of the pico Coulomb pulses may with the aid of the on-line transient recorder throw some light on their origin. In particular the use of anthracene [Lum D1 Gzo] to indicate the arrival of a particle at an electrode, by the emission of a light pulse, may, with the aid of the author's measurement system, enable a correlation to be established between particles (causing enhanced field emission at the electrode) and the pico Coulomb pulses. Once the test cell is filled with a mixture of purified n-hexane and anthracene the photomultiplier (described in Section 9.7.2) could be employed to monitor the light produced in the test-cell by the approach of a particle to an electrode. Note that the experiment described in Section 10.2.3 with slight modifications could be repeated to prove whether or not the flash of light coincided with the arrival of a charged particle. If at any time a large number of particles were in motion the average light output from the cell would be higher than if the particles were stationary.

The on-line transient recorder could again be used to monitor

13.3

both light and charge (or current) signals and perform a correlation between the two variables.

The study of the charge and current waveforms prior to breakdown could also be continued with the aid of the on-line FHT unit (see Section 9.5.2) to control the applied stress. The pattern recognition software could be utilized to discard waveforms that represented a breakdown during a burst of pico Coulomb charge pulses (see Section 10.4).

A more accurate study of the function $E(r_F \nabla E)^{-1}$ (see Section 8.4) based on the expansion derived by Thwaites [Elec Fie Th] may give a more reasonable prediction of the observed phenomena. The addition of known particulate impurities into the author's test cell might also allow a more useful application of the equations in Section 8.4 as the relative permittivity, density and size of the particles would then be known.

SECTION 14

Conclusions.

14.1 Conclusions

The realization of a novel measurement system has meant that many experiments involving formerly inaccessible transient phenomena can now be performed with relative ease. Not only can a large number of transients be captured, in their entirety, but also with the aid of simple metrics these waveforms can be sorted into various categories.

The application of this on-line transient recording system has enabled a detailed study to be undertaken of the role of natural impurity particles in liquid n-hexane under the influence of high electric fields.

A few experiments of earlier workers were repeated with the new measuring system (this enabled a greater number of events to be captured) and good agreement was found for the parameters measured. From the measured distribution of potentials on charged natural particles an average value of 11.1 volts was calculated. The value of mobility of the particles was estimated to be 0.45×10^{-6} $m^2 V^{-1} s^{-1}$.

For the first time the femto Coulomb charge pulses and the motion of the natural particles between the electrodes have been objectively related. In conjunction with the new technique the photomultiplier allowed the arrival and departure of a single particle to be monitored directly.

A study of the apparent dwell time of particles at the electrodes showed that, over the range of stresses examined, the dwell time is inversely proportional to the applied stress. A minimum value of 200 μS was recorded.

A brief off-line study of the shapes of the large charge

pulses and the charge waveform preceding breakdown have been performed. The former measurements revealed that the lengths of the pico Coulomb pulses are inversely proportional to the applied stress over the measured range. However, both the measurement of the large charge bursts and the prebreakdown charge waveform require further investigation.

The application of the on-line transient recorder, together with the waveform classification system, in other areas of research has been mentioned, and these examples demonstrate the urgent relevance of this form of instrument.

SECTION 15

Acknowledgements.

15.1 Acknowledgements

The provision of research facilities by the Head of the Electrical and Electronic Engineering Department [redacted], and the financial assistance of the [redacted] in providing an award for the three year period is gratefully acknowledged.

I would like to especially thank Dr. John Brignell for his continued encouragement and supervision throughout this project, and to all my colleagues who have contributed in some way to this study: [redacted]

The assistance of [redacted], with the computer and its operating system is also acknowledged.

My thanks also to [redacted] for his assistance with liquid preparation and the section headings for this Thesis, [redacted] for his work on the glass ware in the particle extracting system, [redacted] for the transient recorder trolley and the modifications to the test cell, [redacted] for his assistance with board wirings and for their help with the photographs in this work, [redacted].

I must also thank [redacted] for her patience and skill in the typing of this Thesis.

15.1

Finally my sincerest thanks to my parents [redacted], whose untiring support, encouragement and fruit cake enable this work to be completed; and also to [redacted] who, together with my parents, carried out the arduous task of proof reading the manuscript.

[redacted]

SECTION 16

References.

16.1 References

The following list gives the meaning of the more common mnemonics.

Bd	Breakdown
Comp	Computer
Cond	Conduction
Dl	Dielectric Liquids
Thes	Thesis
To	Transformer oil
Tran	Transient
Part	Particle
Pat	Pattern
Rec	Recognition/Recorder

Imp To Abg	Abgrall F., and Cardon J.M., 1975, Proc. Delft Conf.
Cond Bd Adam	Adamczewski I., 1969, 'Ionization, Conductivity and Breakdown in Dielectric Liquids', Taylor and Francis, London.
Mod Phys Be	Beiser A., 1963, 'Concepts in Modern Physics'. McGraw-Hill, London.
Sig Pro Beau	Beauchamp K.G., 1973, 'Signal Processing', George Allen and Unwin, London.
Part Calc Bir	Birlasekaran S., and Darveniza M., 1972, Proc. Dublin Conf.
Part Mov Bir	Birlasekaran S., and Darveniza M., 1972, Proc. Dublin Conf.
Pat Rec Bis	Bisignani W.T., 1975, IEEE Trans. on Instrumentation and Measurement. Vol. IM24 No. 1, March.
Mem Dis Bom	Bommeli B., Frei C., and Peter M., 1975, Proc. Delft Conf.
Liq Cir Boo	Boone W., and Vermeer J., 1972, Proc. Dublin Conf.
Lab Comp Brig	Brignell J.E., and Rhodes G.M., 1975, 'Laboratory on-line computing', Intertext, London.
Thes Brig	Brignell J.E., 1964, Ph.D. Thesis, University of London.
Spa Cha Cal	Calderwood J.H., and Scaife B.K.P., 1971, Royal Soc. Phil. Trans. A, 269.

16.1

Ind Cond Can — Cantril J.M., and Pohl H.A., 1968, J. Electrochem. Soc: Electrochemical Science, July, 700.

Spa Cha Cas — Cassidy E.C., and Cones H.N., 1969, Journal of Research of the Nat. Bureau of Standards. C, Eng and Inst, 73, 5.

Flo Liq Cen — Centurioni L., Delfino B., Molinai G., and Viviani A., 1975, Proc. Delft Conf.

Pre Phen Chad — Chadband W.G., and Wright G.T., 1965, Brit. J. Appl. Phys., 16, 305.

Bd LD Coel — Coelho R., and Gosse J.P., 1970, Annales de Physique, 5, 255.

Part Bd Cook — Cookson A.H., and Farish O., 1972, Proc. IEE Conf. on Gas Discharges.

Part Gas Cook — Cookson A.M., and Wootton R.E., 1974, Proc. IEE Conf. on Gas Discharges.

Photo Dev Dan — Dance J.B., 1969, 'Photoelectronic Devices' Iliffe, London.

Part To Dar — Darveniza M., 1969, Trans. Inst. Elec. Eng. Aust., September, 284.

Imp Part Den — Denegri G.B., Molinari G., and Viviani A., 1975, Proc. Delft Conf.

Inst Elec — Eleccion M., 1974, IEEE Spectrum, January.

Thes Ev — Evison J., 1975, Ph.D. Thesis, The City University.

Cond Part Fel — Felsenthal P., and Vonnegut B., 1967, Brit. J. Appl. Phys., 18, 1801.

Tran Rec Fow — Fowler C.W., 1974, IEE Electronics and Power, 14th November.

Si Dl Gall — Gallagher T.J., 1975, 'Simple Dielectric Liquids', Oxford University Press, Oxford.

Mag Fie Gall — Gallagher T.J., 1972, Proc. Dublin Conf.

Pot Dis Gar — Garton C.G., 1971, J. Phys. D: Appl. Phys., 4, 1785.

Cond Bd Good — Goodwin D.W., and Macfadyen K.A., 1953, Proc. Phys. Soc. B, 66, 85.

16.1

Spa Cha Good	Goodwin D.W., 1956, Proc. Phys. Soc., B69, 61.
Thes Gos	Gosling C.H., 1960, Ph.D. Thesis, University of London.
Imp Part Gosw	Goswami B.M., Angerer L., and Ward B.W., 1972, Proc. Dublin Conf.
Carb Part Gray	Gray E.W., 1976, IEEE Trans. Plasma Science, March, 4.
Part Cont Gray	Gray E.W., 1976, IEEE Trans. Parts, Hybrids and Packaging. March, 12.
Lum Dl Gzo	Gzowski O.A., Wlodarski R., Hesketh T.R., and Lewis T.J., 1966, Brit. J. Appl. Phys., 17, 1483.
Cont Elec Harp	Harper W.R., 1967, Contact and Frictional Electrification, Clarendon Press, Oxford.
Cros Wir Hes	Hesketh T.R., and Lewis T.T., 1969, Brit. J. Appl. Phys., 2, 557.
Thes Hew	Hewish T.R., 1975, Ph.D. Thesis, The City University.
Thes Hou	House H., 1955, Ph.D. Thesis, University of London.
Char Coll Hug	Hughes J.F., and Secker P.E., 1969, Brit. J. Appl. Phys., Ser. 2, 2.
Cond Puls Huq	Huq A.M.Z., and Tropper H., 1964, Brit. J. Appl. Phys., 15, 481.
Che Pur Ka	Kahan E., and Morant M.J., 1965, Brit. J. Appl. Phys., 16, 943.
Elec Mech Kao	Kao K.C., 1961, Brit. J. Appl. Phys., 12, 629.
Bd Liq Kok	Kok J.A., Poll J.W., and Van Vroonhoven G.E.G.M.M., 1962, App. Sci. Res. Sec B, 10.
Bd LD Kras	Krasucki Z., 1966, Proc. Roy. Soc., 294, 393.
Cond LD Kras	Krasucki Z., 1968, Proc. Grenoble Conf.
Part Imp Kras	Krasucki Z., 1972, Proc. Dublin Conf.
Bio Man	Service and Instruction Manual for the Biomation 8100 transient recorder.

16.1

FMB Comp Man	Ferranti FM1600B Programming Manual.
Rot Cond Mat 1	Matuszewski T., Terlecki J., and Sulocki J., 1972, Proc. Dublin Conf.
Rot Cond Mat 2	Matuszewski T., Terlecki J., and Sulocki J., 1975, Acta Physica Polonica, 48, 861.
Elec Mag Max	Maxwell J.C., 1904, Treatise on Electricity and Magnetism, Clarendon Press, Oxford.
Bd Phen Mear	Mears B.R., 1975, Proc. Delft Conf.
Cond Puls Meg	Megahead I., and Tropper H., 1971, J. Phys. D: Appl. Phys., 4, 446.
Liq Mot Mir	Mirza J.S., Smith C.W., and Calderwood J.H., 1970, J. Phys. D: Appl. Phys., 3, 580.
Tran Comp Miya	Miyamoto T., Takami T, Sakaguchi I., and Kawaguchi F., 1975, IEE Trans. Instr. and Meas. 24, 379.
Pola Dl Mor	Morant M.J., 1968, Brit. J. Appl. Phys., 1.
Part Air Mul	Mulcahy M.J., 1974, Proc. IEE Conf. on Gas Discharges.
Larg Elec Nel	Nelson J.K., Salvage B., and Sharpley W.A., 1971, Proc. IEE, February, 118.
Dis Gas Noss	Nosseir A., 1975, IEEE Trans on Elect. Insulation, June, 10.
Ref Ok	Okada S., 1964, IEEE Trans on Writing and Speech, December, 15.
Meas Inst Oli	Oliver B.M., and Cage J.M., 1971 'Electronic Measurements and Instrumentation', McGraw Hill, London.
FFT Pock	Pocknell K.J., 1955, Internal Report on 'The FFT and its uses'.
Die Phor Pohl	Pohl H.A., 1968, J. Electrochem. Soc., June, 115.
Fie Eff Pohl	Pohl H.A., 1960, J. Electrochem. Soc., May, 386.
Elec Mot Ram	Ramo S., 1939, Proc. IRE, September, 27, 584.

16.1

Tran Comp Rat	Ratcliffe C.A., and Felix W.D., 1973, Rev. Sci. Instrum., May, 44.
Thes Rav	Ravenhall F., 1975, Ph.D. Thesis, The City University.
Hi Volt Re	Reichert A.R., Rhodes G.M., and Brignell J.E., 1972, J. Phys. E., 5.
Part Cond Rho	Rhodes G.M., and Brignell J.E., 1972, Proc. Dublin Conf.
Thes Rho	Rhodes G.M., 1971, Ph.D. Thesis, The City University.
Comp Lab Ros	Rosner R.A., Penney B.K., and Clout P.N., 1976 'On-line Computing in the Laboratory', Advanced Publications Ltd., London.
Tran Rec Say	Saynajakangas S.J., and Sirkka I., 1975, IEEE Trans. on Communications, September, 23.
Dec Pro Seb	Sebestyen G.S., 1962, 'Decision-Making Processes in Pattern Recognition, MacMillan, New York.
Puls Gen Sha	Shammas N., Smith C.W., and Calderwood J.H., 1975, Proc. Delft Conf.
Mov Char Sho	Shockly W., 1938, J. Appl. Phys., 9, 635.
Dis Gas Slet	Sletten A.M., and Lewis T.J., 1963, Brit. J. Appl. Phys., 14, 883.
Thes Slet	Sletten A.M., 1960, Ph.D. Thesis, University of London.
Bd Dl Smi	Smith C.W., and Calderwood J.C., 1968, Proc. Grenoble Conf.
Bd To Spit	Spitzer F., 1975, Proc. IEE Conf. on Dielectric Materials, Cambridge.
Cond Part Sta	Stannett A.W., 1951, Brit. J. Appl. Phys., 2, 110.
Pat Rec Sto	Stockman G.C., Kanal L.N., and Kyle M.C., 1974, Proc. of Second International Joint Conference on Pattern Recognition, Denmark, (IEEE).
Elec Fie Th	Thwaites J.J., 1962, IEE Monograph, June.
Cond Bd Tho	Thomas W.R.L., and Forster E.O., 1975, Proc. Delft Conf.

16.1

Mol Stru Tho	Thomas W.R.L., 1975, Proc. IEE Conf. on Dielectric Materials, Cambridge.
Tran Cam Toro	Torok I., 1975, Nuclear Inst. and Methods, 126, 109,
Pat Rec Tech Ull	Ullman J.R., 1973, 'Pattern Recognition Techniques', Butterworths, London.
Ed Imp Viv	Viviani A., 1972, Proc. Dublin Conf.
Tran Therm Wied	Wieder H., Huth B.G., Koepcke R.W., and Juliana A., 1974, Rev. Sci. Instr., June, 45.
Cond To You	Young B., 1975, Proc. Delft Conf.
Cont To You	Young B., 1972 Proc. Dublin Conf.
Cond Bd ZaHa	Zaky A.A., and Hawley R., 1973, 'Conduction and Breakdown in Mineral Oil', Peter Peregrinus, London.

SECTION 17

Appendices.

APPENDIX I

A USER GUIDE TO THE CONTROL SOFTWARE FOR THE ON-LINE BIOMATION 8100 TRANSIENT RECORDER.

C.J. BUFFAM

CONTENTS

INTRODUCTION

This document is meant as a guide to the facilities provided by the on-line transient recorder software and should be read in conjunction with the manufacturers manual. The software is designed in such a way that the user need only familiarize himself with the specification of one program (which has 8 entry points), and need not consider the operation of other subroutines in the system.

The User's software interface is the Biomation Transient Recorder Control Program (BTR CP) subroutine S4510: which has various entry points that permit the user to load the front panel registers and to arm or trigger the recorder.

Incorporated into the BTR CP is a disc overlay which allows the main 2048 word data area to be used to hold either the front panel parameter input/output software or the 2048 x 8 bit transient waveform. The BTR CP supervises the overlay which should be transparent to the user.

Before using the transient recorder on-line the user should be reasonably familiar with the controls and modes of operation of the recorder off-line.

Before using the on-line transient recorder software ensure that all cables are connected and that the recorder and Interface Module are powered up. For details of the hardware refer to the document entitled Hardware Interface Description.

DESCRIPTION OF CONTROL PROGRAM

Fig. 1 shows the layout of the software to control the recorder. The user's program communicates only with the BTR CP. This in turn controls the operation of the User's Data Area (UDA), the Peripheral Data Area (PDA), the Active I/O and Passive I/O programs.

The software which deals with the loading of the front panel registers is termed the Passive Input/Output software and shares the

same core area as the transient waveform (see the Section on overlay). This software only changes the value of front panel registers in usurped control groups. Two data areas are associated with this software; the Users Data Area which is updated each time the user inputs any parameters and the Peripheral Data Area which is used to assemble the Operands and Operators prior to their transfer to the recorder.

The Active I/O software is the generator for commands such as Arm, Trigger, Plot, Reset, etc. which initiate some action on behalf of the recorder.

The operation of the system is best understood by reading through the following specifications and examples.

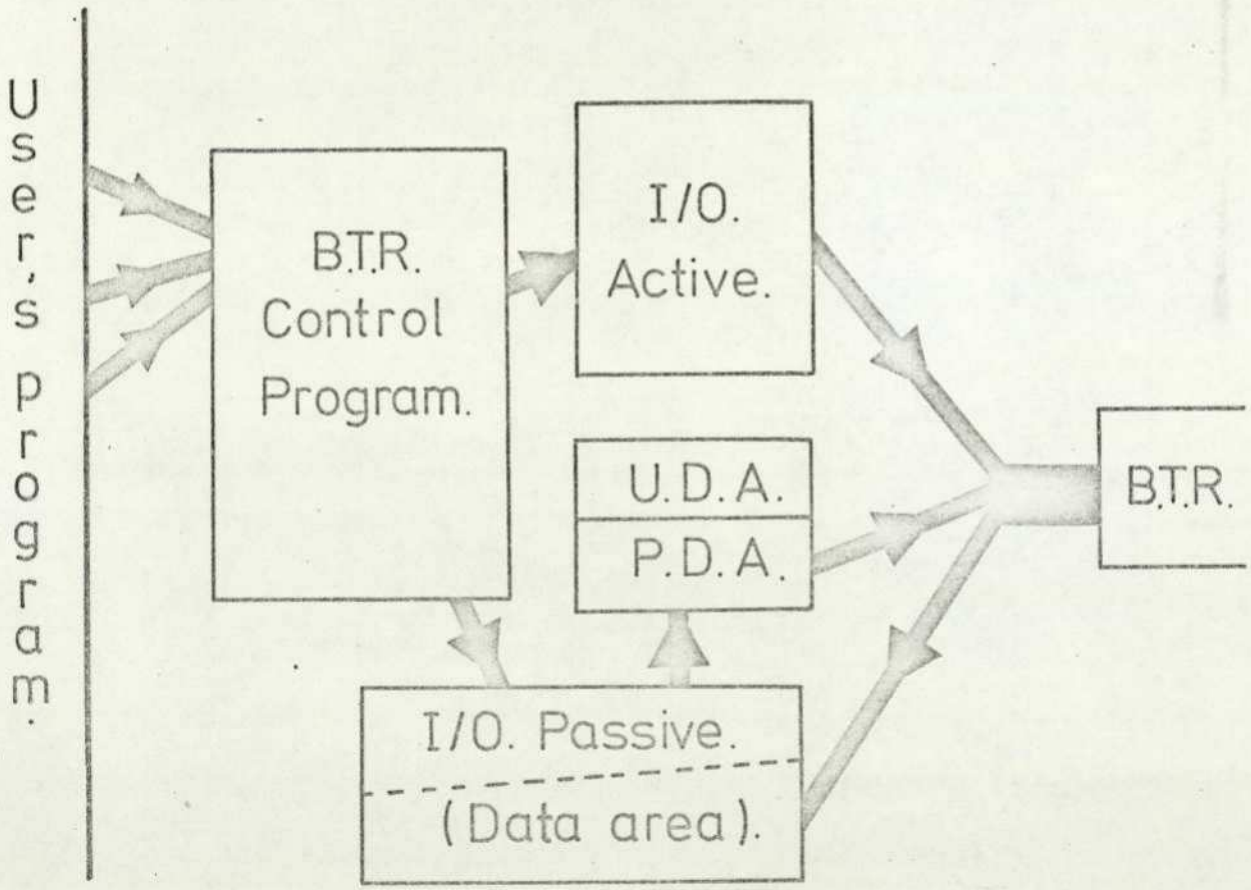

Fig. 1. Transient Recorder Control Program

ENTRY POINT 0 SET UP (S4510,0)

A call to S4510,0 is necessary before any other call to the BTR CP is made, this initializes the software flags and loads the Passive I/O software into file 0 of the disc pack. File 0 should be open before this entry is called (see User Guide to Magtape Simulator Control Program and example following).

Only on the first call to this entry will the overlay code be placed on disc. Subsequent calls to reset the software will only re-initialize the control program flags and send the RESET command to the recorder.

Should entry +1 be called before entry + 0 the BTR CP will make its own call to the set up entry (file 0 must be open), if however entry +2 were called before entry +0 STOP 1 30 18 will be produced.

ENTRY POINT 1 PARAMETER INPUT (S4510,1)

This entry point permits the loading of the front panel registers in control groups placed under computer control. The format of the input is

number/operand

where number = 0, 1, 2, ... 23

and operand = value to be loaded (see Table 1).

The parameter list comprises any number of these parameters separated by a new line and terminated by 24/.

The BTR CP always usurps the OUTPUT MODE, TIME BASE & RECORD MODE GROUP and places the recorder in the OUPTUT MODE AUTO. Thus the user must load the time base and record mode information when using the recorder on-line.

The parameter input is on stream 3 unless an error is found in the list, on reading the list terminator the user will be asked to re-enter the parameter in error on stream 5. The order in which the parameters are entered is irrelevant.

As an option on this entry point the user may request a copy of the UDA as it exists after the parameter input. This is output as 24

octal numbers on stream 2 and can be read on stream 3 via entry point + 1 (see following example).

Kernel register V20 bits 0 and 1 define the type of parameter input (normal or octal) and whether or not a copy of the UDA is to be generated. Thus on entry:-

```
V20[0] = 0          'NO COPY GENERATED'
V20[0] # 0          'COPY OF UDA OUTPUT ON STREAM 2'
V20[1] = 0          'NORMAL PARAMETER INPUT'
V20[1] # 0          'OCTAL PARAMETER INPUT'
```

Note on operation of software. Having received the list terminator (in the case of normal parameter input) the operands which have been partly decoded (by S4501) and placed in the UDA (S4530) are transferred (by S4502) with further decoding to the PDA (S4531). A copy of the UDA is generated (by S4505,1) if requested. The standard operators are overlayed into the PDA (by S4500 with a checksum S4506) and the instructions in the PDA to be transferred are packed together (by S4504) prior to output (by S4503). Flags are set in the BTR CP and cleared in the interrupt program (S4511) to check the satisfactory transfer of the parameter information.

Examples of parameter input.

```
(a)                 'Assume stream 3 is teletype input'.
    V20[1] = 0      'Normal parameter input'.
    V20[0] # 0      'Generate octal copy on stream 2 (Punch)'
    ←S4510,1        'Load front panel settings from teletype'.

(b)                 'Assume stream 3 is reader input'.
    V20[1] # 0      'Octal parameter input'
    V20[0] = 0      'No octal copy'
    ←S4510,1        'This will read the paper type generated in
                      example a'.
```

See also the example of parameter list.

ENTRY POINT 2 SET FUNCTIONS (S4510,2)

The following active commands can be sent via this entry point. The particular command being determined by a number in V20.

SET FUNCTION	VALUE OF V20 ON ENTRY
TRIGGER	0
ARM	1
RESET	2
READ STATUS	3
PLOT	4
ENABLE DATA	5

Thus:-

```
V20 = 1
←S4510,2                    'ARM'
```

will start the recorder sampling.

As it may be some time before a transient is captured control is returned from BTR CP to the User's program and it is up to the user to test for the arrival of the transient in core (see section on testing BNDP flag).

The TRIGGER command may be sent from the computer but the control program will check that the preceding command was ARM.

The ARM and TRIGGER commands will only be transmitted if their respective control groups are under computer control. Note the Arm button on the front panel must not be used when the device is under computer control and the Arm group is usurped.

Transmission of the RESET command is equivalent to depressing the Reset button on the Interface Module mounted under the transient recorder. This command does not reset the BTR CP flags.

If a request for STATUS is made the bottom 4 bits of V20 hold the recorders input channel overflow status on exit.

The recorders plotter output may be activated by the PLOT command.

Use of the ENABLE DATA command allows a transient held in the recorder to be transferred to the computer. Under normal circumstances this will not be used as transfer of transients to core is automatic.

ENTRY POINT 3 TEST FOR NEW DATA (S4510,3)

Once the recorder has been armed the user may periodically test if a transient has been captured (this allows other processing to be carried out whilst waiting for the next transient). On exit from the program V20 will be zero until the new data is in the main data area S4542.

Thus:-

```
[21] ←S4510,3
     ←21, V20 = 0        'loop until data available'
```

will loop until the next transient arrives.

This entry also checks the correct transfer of the last command (i.e. ARM) and re-sends the command if necessary.

ENTRY POINT 4 ABORT (S4510,4)

In case of a program crash this short piece of code may (if not corrupted) transfer the last transient to store. STOP 1 30 21 is output after the transfer. The program loops on handswitch 0 whilst awaiting data. Reset switch 3 on the front of the PCU may have to be used to initialize the transfer (the switch should be raised and returned to normal once the code has been entered).

ENTRY POINT 5 CLEAR NEW DATA PRESENT FLAG (S4510,5)

To protect the new transient in store the new data present flag (BNDP) must be cleared by the user before the transient recorder is re-activated (i.e. Armed). This is done by a call to this entry point of the control program.

```
←S4510,5          'Clear New Data Present Flag'.
```

ENTRY POINT 6 EXTRACT LAST STATUS WORD (S4510,6)

This allows the user to examine the overflow bits in the recorder status word which is transferred after the 2048 word waveform. On exit V20 bits 0 to 3 hold the overflow information as defined below.

```
V20[0] # 0          OFFSCALE CHB (-)
V20[1] # 0          OFFSCALE CHB (+)
V20[2] # 0          OFFSCALE CHA (-)
V20[3] # 0          OFFSCALE CHA (+)
```

Example of use:-

```
[2]  V20 = 1            'SELECT ARM COMMAND'
     ←S4510,2           'ARM RECORDER'
[1]  ←S4510,3           'TEST BNDP FLAG'
     ←1,V20=0           'LOOP UNTIL DATA AVAILABLE'
     ←S4510,6           'GET STATUS'
     ←S4510,5           'CLEAR  BNDP FLAG'
     ←2,V20#0           'RE-ARM IF ANY OVERFLOW BIT'
                        'IS SET'
     ←S6935             'PROCESS TRANSIENT'
```

This repeatedly re-arms the recorder until the captured waveform is within the input range.

ENTRY POINT 7 COPY AND DECODE DATA (S4510,7)

The main purpose of this entry is to decode the data when the recorder is in the dual channel mode. This entry uses a subroutine (S4591) which checks to see if CHA/B input modes are both ON (regardless of whether the input channels are under computer control). If the recorder is in the single channel mode the copy is straightforward (i.e. without any decoding), otherwise the two waveforms are unravelled; this results in the first 1024 words of the data area holding the channel A waveform and the second 1024 words holding the channel B waveform.

N1 holds the start address of the transient to be copied

N2 holds the start address of the data area into which the transient is to be copied.

Example

```
N1 = VNO
AS4542
N2 = VNO
AS4544
←S4510,7                'COPY'
```

EXAMPLES OF THE USE OF THE ON-LINE TRANSIENT RECORDER

Given below are two examples of code used to capture transients. The first example just sets up the recorder and captures 1 waveform. The second example processes 10 transients using a buffer to increase the turnround time between successive Arm instructions.

Example 1.

```
V20 = 0                 'FILE 0'
V21 = V20               'SET UP BOTL'
N1 = VNO                'SET N1 TO 10 WORD BLANK DATA AREA'
AS4548
←S4570,0                'OPEN FILE 0'
←S4510,0                'INITIALIZE SYSTEM AND OVERLAY'

V20 = 1
←S4510,1                'NORMAL INPUT WITH OCTAL COPY'
V20 = 1                 'SELECT ARM COMMAND'
←S4510,2                'ARM TRANSIENT RECORDER'

[1] ←S4510,3            'TEST BNDP FLAG'
←1,V20 = 0              'LOOP UNTIL DATA AVAILABLE'

←S6932                  'PROCESS TRANSIENT'
```

A suitable parameter list for input to S4510,1 is shown after example 2.

Example 2.

```
                    NUMBER
    V20 = 0         'FILE 0'
    V21 = V20       'SET UP BOTL'
    N1 = VNO        'SET N1 TO 10 WORD BLANK DATA AREA'
    AS4548
    ←S4570,0        'OPEN FILE 0'

    ←S4510,0        'INITIALIZE SYSTEM & OVERLAY'
    V20 = 1         'NORMAL INPUT WITH OCTAL COPY'
    ←S4510,1        'PARAMETER INPUT'
    V18 = 0         'ZERO COUNT'
    V20 = 1         'SELECT ARM COMMAND'
    ←S4510,2        'ARM TRANSIENT RECORDER'

[1] ←S4510,3        'LOOP UNTIL DATA AVAILABLE'
    ←1,V20 = 0

    N1 = VNO        'DATA TO BE COPIED'
    AS4542
    N2 = VNO        'AREA TO WHICH DATA IS COPIED'
    AS6930
    ←S4510,7        'COPY DATA'

    ←S4510,5        'CLEAR BNDP FLAG'
    V20 = 1
    ←S4510,2        'RE-ARM RECORDER'
    V18 = V18 + 1   'INCREMENT COUNT'
    ←S6931          'PROCESS LAST TRANSIENT'
    ←1, V18#9 = 0   'TEST NUMBER CAPTURED'
```

```
[2]  ←S4510,3          'WAIT FOR LAST WAVEFORM'
     ←2,V20 =0
     ←S4510,7          'COPY'
     ←S6931            'PROCESS 10TH TRANSIENT'
```

An example of the input parameter list that could be used is now given.

```
0/OCT 13               (USURP CHA, ARM & OUTPUT MODE, TIME BASE
                         & RECORD MODE GROUPS)
1/2                    (CHA DC COUPLED)
3/2.0                  (CHA RANGE ± 2 volts)
4/+.45                 (CHA OFFSET + .45 x RANGE)
5/1                    (CHA MODE ON)
13/1.45                (ARM GROUP DELAY 1.45 x 1000 x SAMPLE INTERVAL)
23/1                   (PRETRIGGER MODE)
20/5.0US               (MAIN TIME BASE SIMPLE INTERVAL 5.0 μS)
24/                    (LIST TERMINATOR)
```

This is read in on stream 3.

TABLE I

NUMBER	OPERATOR TITLE SPECIFICATION	EXAMPLE	DEFAULT
0/	USURP CONTROL GROUPS BITS 4 3 2 1 0 TRIGGER ARM CHB CHA T.B,O/P, REC. MODE	OCT 11	OCT 01
1/	CHA + INPUT COUPLING OFF AC D2 0 1 2	1	2
2/	CHA-INPUT COUPLING OFF AC D2 0 1 2	2	0
3/	CHA RANGE	0.5	5.0
4/	CHA INPUT OFFSET	-.42	+.00
5/	CHA MODE OFF ON 0 1	0	1
6/	OBSOLETE		
7/	CHB as 1		
8/	CHB as 2		
9/	CHB as 3		
10/	CHB as 4		
11/	CHB as 5		
12/	OBSOLETE		
13/	ARM DELAY MAGNITUDE	1.45	0.00
14/	ARM LEVEL MAGNITUDE	.56	.00
15/	ARM:-MODE, SOURCE, INT-SOURCE, SLOPE, COUPLING & LEVEL POLARITY This is a string of binary digits each separated by two spaces. MODE: INPUT 0, AUTO 1 — SOURCE: EXT 0, INT 1 — INT SOURCE: CHA 0, CHB 1 — SLOPE: -VE 0, +VE 1 — COUPLING: DC 0, AC 1 — LEVEL POLARITY: -VE 1, +VE 0		0 0 0 1 0 0 0
16/	TRIGGER as 13		
17/	TRIGGER as 14		
18/	TRIGGER as 15		
19/	MAIN TIME BASE SOURCE INTERNAL 0 — EXT <.25 mS 2 — EXT > 1 mS 1 — EXT .25 ms → 1 mS 3	3	0
20/	MAIN TIME BASE UNITS & RANGE Use MS for m Sec and US for u Sec	0.5 MS	.01 US
21/	ALTERNATIVE TIME BASE as 19		
22/	ALTERNATIVE TIME BASE as 20		
23/	RECORD MODE NORMAL MODE SINGLE TIME BASE 0 PRETRIGGER " " " " 1 NORMAL " DUAL " " 2 PRETRIGGER " " " " 3	1	0
24/	LIST TERMINATOR		

TRANSIENT RECORDER CONTROL PROGRAM

Although of little interest to the general user a list and description of the 17 Flags used by the BTR CP is given below. The flags are located in word 0 of black data area subroutine S4512.

BIT	FLAG	NAME
0	BIOT 0	B. INDICATION OF TRAIL 0.
1	BIOT 1	" " " 1
2	BIOT 2	" " " 2
3	BIOT 3	" " " 3
4	BIPSWCR	BIOMATION INPUT SOFTWARE CORE RESIDENT
5	BR	" RESET
6	BOO	" OPERATORS OVERLAYED
7	OOPUB	OCTAL OUTPUT OF USERS BLOCK (UDA) REQUESTED
8	OIPUB	" INPUT TO " " " "
9	BA	BIOMATION ACTIVATED
10	BDTI	" DATA TRANSFER IMMINENT
11	BSWSU	" SOFTWARE SET UP
12	BIOT 4	" INDICATION OF TRAIL 4
13	BNA	" NOT ACTIVATED
14	BIA	" INTERRUPT ABORT
15	BNDP	" NEW DATA PRESENT
16	BIPSWDR	" INPUT SOFTWARE DISC RESIDENT

The BIOT flags are used to check the order in which calls to the Control Program and interrupts occur. BIPSWCR and BIPSWDR are used to control the disc overlay. BA and BNA are set to indicate an ACTIVE or PASSIVE GROUP transfers respectively. BDTI inhibits use of the Control Program if a data transfer is expected. BIA is used by entry point 4 whilst waiting of the data transfer.

SUBROUTINES USED IN THE ON-LINE TRANSIENT RECORDER SYSTEM

Below is a list of the subroutines used by the BTR CP with a brief description of their function. Subroutines designated with the letter O are incorporated in the disc overlay.

SUBROUTINE AND VERSION NO.	DESCRIPTION
S4500 0 (O)	Loads the operators into the Peripheral Data Area.
S4501 0 (O)	Reads in parameter list and loads the User's Data Area.
S4502 0 (O)	Transfers with decoding the UDA data into the PDA.
S4503 0	Starts all Active and Passive transfers to the recorder.
S4504 0	Packs PDA prior to output.
S4505 0	UDA Octal Input and Output of parameters.
S4506 0	Checksum of operators.
S4510 0	BTR CP
S4511 0	Interrupt Program.
S4512 0	Flag Word.
S4526 0 (O)	Reset UDA & PDA
S4530 0	User's Data Area
S4531 0	Peripheral Data Area
S4532 0 (O)	Look up table
S4533 0 (O)	Look up table
S4534 0 (O)	Look up table

S4535 0 (0)	Look up table
S4536 0	Data Area containing all the Active Commands.
S4537 0	Blank Data Area for S4501 error flags and S4506 checksum values.
S4542 2	Main BTR Data Area for transient
S4548 0	Ten word Blank Data Area for disc overlay (see section on Overlay).
S4591 1	Copy routine for decoding transients.

THE DISC OVERLAY OF THE 1/O SOFTWARE

It has already been mentioned in this document that the on-line transient recorder software utilizes an overlay. The reduction in core used being in the order of 1100 words. Figure 2 shows the arrangement of the overlayed subroutines in the main 2048 word data area.

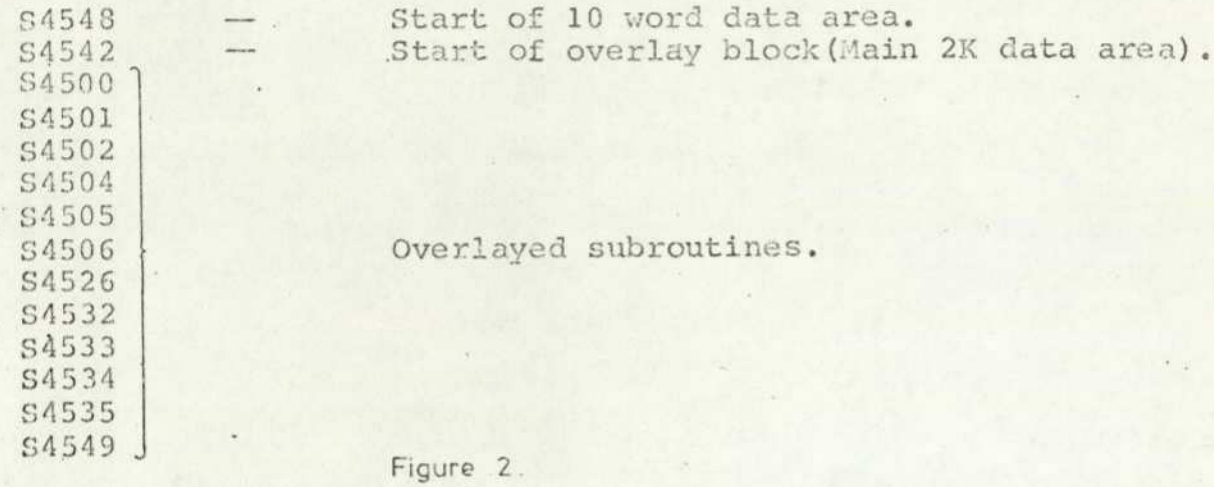

Figure 2.

It is important to note that the organization of the overlay takes place when the programs are assembled, thus the order of these subroutines is paramount.

Subroutine S4548 0 is a 10 word data area used by the Magtape Simulator (see User Guide to the Magtape Simulator Control Program) to load the overlayed subroutines to disc. S4542 2 is a zero word data area which denotes the start of the main data area.

Subroutine S4549 is assembled directly behind the Passive I/O software and makes up the remainder of the 2048 words for the main data area.

When the first call to the BTR Control Program set up entry (see entry point+0 details) is made the software in the main data area is written to the first 3 blocks on file 0 of the loaded disc pack. The blocks are written in the order 0, 1, 2 each having a 10 word data area at the beginning of the block. When parameter input is requested and the software is not present (i.e. a transient has been transferred to

core) the overlay blocks are read from disc to their respective positions in the order 2, 1, 0 as that block 1 overwrites the 10 word data area at the front of block 2 and similarly with blocks 0 and 1.

It must be emphasized that the order of the subroutines S4548 to S4549 should not be changed when the subroutines are transferred from one library to another.

Notes on Hardware and Push button commands

Before calling any of the BTR CP entries ensure that the data cable is plugged into the socket at the rear of the Interface Module (IM) and that the IM and the transient recorder are powered up. Also ensure that the reset switch on the front panel of the PCU is in the central position (Reset switch 3).

Three 'push button' commands have been incorporated into the interface circuit and are generated in the Interface Module. The commands are RESET, CLEAR FRONT PANEL MASK and SWITCH TO ALTERNATE TIME BASE (at the time of writing the last of the three has not been fully implemented).

Depressing the RESET button will cause the transient recorder to reset its internal registers; a change in the displayed waveshape may be observed.

The Clear Front Panel Mask button can be used to regain control over the usurped control groups. To re-program the front panel entry + 1 of the control program can be used. Note that if the same front panel settings are required requesting normal parameter input and entering just the terminator 24/ will initiate the transfer of the PDA as previously described.

APPENDIX II

BIOMATION TRANSIENT RECORDER HARDWARE INTERFACE DESCRIPTION

C.J. BUFFAM

This document outlines the operation of the digital circuitry which organises and controls the transfer of information between the FM1600B computer and the on-line Biomation transient recorder.

The circuits are constructed using Ferranti μ Nor II DTL logic elements (using a negative logic convention) and standard 7400 series TTL devices (using a positive logic convention).

For the DTL gates:-

Logic '0' is + 2.7 V to + 5.0 V

Logic '1' is 0 V to + 0.55 V

Thus for this negative logic a pulse '010' is denoted thus:- 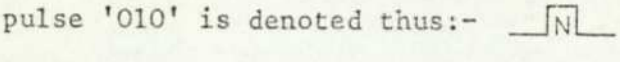

For the TTL gates

Logic '0' is 0V to + 0.4 V

Logic '1' is + 2.4 V to + 5.0 V

A positive logic '010' pulse is given by:- 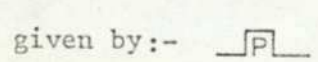

Fig. 1 shows the layout of the interface. The Computer Interrupt Equipment (CIE) is connected via the 24 way bidirectional data highway to the transient recorder Peripheral Control Unit (PCU). This in turn is linked via 20 metres of 24 way twisted pair line to the transient recorder Interface Module (IM). This module contains the line drivers and receivers and is mounted on the transient recorder trolley.

STRUCTURE OF DATA TRANSFERS

The interface caters for three groups of data transfer, these are:-

(1) variable length blocks of data sent to the transient recorder (i.e. Active and Passive transfers, see User Guide to the BTR Control Program).

(2) 2048 word x 8 bit blocks of transient waveform data transmitted, directly after capture, to the computer.

(3) transient recorder status information conveyed after each block transfer (i.e. groups 1 and 2).

OPERATION OF THE PCU

This section gives an example of the typical operation of the PCU. Continuous reference is made to the timing diagrams in Figs. 2 a, b, c and the circuit diagrams in Figs. 3 a, b, c, d. Table I defines the logic symbols used in these drawings. Grid references of gates used are given in square brackets.

The Peripheral Control Unit is mounted in the halfself module containing the EHT and FTU boards, and occupies the left hand 3 slots in the module. The PCU comprises a 177 PEC (Standard Interface with Register, 8 bits), a 115 PEC (Driver/Receiver with Register, 16 bits) and a handwired board containing the interface logic, line drivers and line receivers. The 16 bit register on the 115 PEC is wired for output (relative to the computer) only and the 8 bit 177 PEC register for input only. Fig. 2a shows the waveform sequence for a self-terminating. Passive data transfer to the recorder (refer also to the Information on Standard Interface with Register document by E.I. Richmond).

Subroutine S4503 loads the interface block and raises the S and M lines to initiate a transfer (see Fig. 2a). The MLe signal sets Q and D to '1' for the control word transfers (Active and Passive data sent to the recorder) [A5, B5, B2]. MLe also sets SET R to generate the first handshake (R, J, K) cycle [A8, B8, C2]. In acknowledgement of the cycle request the computer raises the J line; JLe is used to clock the 16 bit register on the 115 PEC board which holds the 13 bit operator/ operand and the three Control Bits [F11, E11]. The occurrence of K is used, via KLe, to generate a CMD Line signal which instructs the transient

recorder to obey the operator held in the 115 PEC register [C5, C8, B8, D5, F11, E11, C2, D2]. The transient recorder replies by dropping the Flag Line signal, this clears CMD Line [C2]. When the Recorder has dealt with the operator it raises Flag Line which generates Pseudo Flag Le (PsFLGLe) [H5, E11, D8, D5, F11, F5, H11, J5, B5]. Ps FLG Le is only generated when the last handshake cycle has finished and FLG, K and CMD have returned to their false states.

PsFLGLe is used to start the next RJK cycle by setting the SET R staticisers [B8, C2]. This cycle will be repeated providing all the Control Bits transmitted with each operator and operand are zero. The transfer of instructions is terminated by Control Bits 1 and 3. CB3 is passed to the PCU with the penultimate control word and CB1 with the last transfer just before status is returned. So that the status information is available during the PCU status cycle (just prior to the program interrupt) the last operator must be Read Status. JLe is used to clock the output register [F11, E11]. When the penultimate transfer occurs JLe clocks CB3 into the register; this sets the InM staticiser when it in turn is clocked by the combination of SET R, R and Ck [E8, E5, C5, J5, E11, F8]. Thus M is forced down after R goes true on the last transfer before the status cycle (this is M generated on PEC 177 not M line (True M)) [E8]. The JLe pulse for the last transfer clocks CB1 into the register. CB1 is used to inhibit KLe from generating a CMD Line signal during the status cycle. CB1 is clocked through the Inhibit CMD staticiser [D11] by the $\overline{\text{CMD*}}$ pulse associated with the request for status. This sets D11 and inhibits CMD Line. [F5, D11, F11, E11, C2].

After the status transfer the 16 bit register is cleared by KTra and a program interrupt is generated by the CIE. In the interrupt program M Line will be lowered, this will clear the InM staticiser to allow further transfers to start when requested [F5, E5].

The next example is an Active command group (Arm is shown in Fig. 2b). Once again the preceding sequence is followed except that in the interrupt program after the block transfer M Line is not lowered. This is to allow the InM staticiser to remain set until the transient recorder informs the PCU that it has captured a waveform. This is indicated by a pulse (REC Line) generated by the Interface Module at the end of the record cycle. The recorder also generates a 5 μS Flag at the end of the record cycle and this is used to clear the InM staticiser thus generating a MLe which sets Q and D to '1' to allow control word transfers [H5, C11, E8, F8, F5, E5, E8, A5, B2]. SET R is raised by the PsFLGLe pulse generated as the 5 μS FLG goes false. The command loaded into the 16 bit output register is Enable Data Out; CB2 is transferred with this instruction CB2 is combined (wired OR) with PsFLGLe to drop Q and D to '0' for the Data In cycles which transfer the 2048 x 8 bit transient waveform via the 8 bit register, in the 177 PEC board, to the computer [B5, A8, B2]. Note PsFLGLe is now FLGLe with K = 0 [F11, D5]. The 16 bit output register containing the EDO instruction is not clocked when D is '0' thus the command remains on the output highway whilst the 2048 words are strobed out of the recorder [F11, E11]. The input register is clocked by the R pulse which loads the data into the register so that it is transferred to the computer during the ensuing hankshake cycle [PIN 15 TO PIN 4].

The Data In cycles are counted by the CIE using the channel 7 status word to store the negative value of the number of transfers remaining. When this count reaches zero the computer drops M Line, after R has gone true. The next KTra pulse is used with M being false to set Q to '1' for the status cycle [A5, B2]. In order to request status from the recorder the JLe pulse from the last data transfer (determined by M being false) is used to set StPsRSO (Staticised Pseudo Read Status Operator) and to clear the output register [F8, E8, E5].

The effect of StPsRSO is to hardwire onto the data highway the Read Status command via the line drivers [J2 and A2] associated with this command. The CMD Line '0' to '1' transition instructs the recorder to give status which will be returned when FLG goes false. PsFLGLe generates the last RJK cycle which takes the status information into the computer prior to the interrupt. S is dropped in the interrupt program to ensure that all the staticisers are cleared.

The use of Control Bits to terminate or reverse the data flow was employed to give the interface flexibility at program level. An example of this flexibility is the Active Software Command Enable Data (see User's guide to the Control Software for the On-line Boimation transient recorder). This Active group comprises the following recorder instructions:-

Clear and Update Status Word.

Output Mode EDIT

Enable Data Out (CB2 is set).

This group firstly initializes the status register (in the Recorder) and programs the Output mode to EDIT. CB2 clears Q & D and the interface then follows the Data In sequence already described. Note the Control Program automatically reprograms the recorder Output Mode back to AUTO ready for the next ARM command. The output register inhibit gating circuitry is no longer used and is wired open.

Clock pulse distribution is by a power gate to three open collector nor gates giving Ck 1, 2 and 3 [A2, A5, A8]. The clock signal is inhibited by RESET. Two reset lines are used to initialize all staticisers, Rs1 and 2 [E11, H5].

THE OPERATION OF THE BIOMATION TRANSIENT RECORDER INTERFACE MODULE

The Interface Module is mounted below the Transient Recorder at the side of the trolley. It contains the DTL line drivers and receivers; all other logic circuitry in the IM is TTL.

The IM also contains circuits to modify the FLAG and RECORD signals the latter comes from a BNC socket mounted on the rear of the recorder. Push button commands are also generated within the IM; these are RESET, CLEAR FRONT PANEL MASK and SWITCH TO ALTERNATE TIME BASE. The buttons are mounted on the front panel of the Interface Module. Fig. 4 shows the timing diagrams and Figs. 5 a, b and c give the circuit configuration for the IM.

The COMMAND, FLAG and RECORD circuits are shown in Fig 5 a. The FLAG pulse from the Transient Recorder has a minimum width of 100 nS and so a monostable is used to lengthen the pulse to 1 μS [H2]. The output of the monostable is OR-ed with the input so that FLAGs of longer duration than 1 μS will be transmitted via the driver to the computer [H3, C8, F1, B6]. The CMD Line signal is received by gate B5 (lines are terminated by á 120 Ω resistor connected to + 3V) and passed to the Recorder by two TTL gates [C8].

In a similar manner to the extension of the FLAG signal the REC Line pulse is delayed if the recorder (working at a high sampling speed) becomes ready for the data transfer before the computer has loaded the status word in the interface block with -2048; otherwise the transfer will fail. For this reason the RECORD signal is extended to 100 μS by a monostable and the REC Line pulse is generated as the Extended RECORD signal goes false [G1, G2, C7, B6]. As a FLAG Line must be generated as Extended RECORD goes false, but not during the record cycle, a latch is used to inhibit the FLAG generated by the recorder when RECORD goes false [F1, F3, C8]. A FLAG signal is obtained from the REC Line monostable to simulate the normal operation of the recorder For record cycles longer than 100 μS the 5 μS FLAG will be sent to the PCU with the REC Line pulse [H3, H2, C8, F1, B6].

The REC signal from the recorder is displayed by a bulb mounted in the SWITCH TO ALTERNATE TIME BASE button on the front panel of the IM, REC is also available at the isolated BNC socket also on the front panel [C8, B8, C6]. Fig. 4 shows the waveforms for the two cases mentioned, firstly when REC is less than 100 μS and secondly when it is greater than 100 μS.

The 'push button' command circuit is shown in Fig. 5 b. Each button is de-bounced and fed to its respective command staticiser [E1, E2, E3]. Gate F2 acts as an OR gate so that pressing any button will trigger the monostable which sets the Pseudo (Ps) OPERATOR latch [B7, C6]. The generation of Ps OPERATOR forces a bit pattern onto the data highway defined by which command latch is set. The output from the first monostable going false fires the second monostable to generate Pseudo CMD [B7]. PsCMD is fed to the recorder input via [C8]. $\overline{\text{Ps OPERATOR}}$ is fed to the inhibit FLAG circuit so that the FLAG generated in response to the PsCMD does not leave the IM [F3]. The FLAG from the recorder triggers the circuit clear monostable as it goes false, this clears all the command latches and the Ps OPERATOR latch [C7, C6, E1, E2, E3]. The switch to ALTERNATE TIME BASE signal is enabled only during the record cycle.

The power supplies used in the IM are + 3 Volts for the line terminating resistors, + 4.5 Volts for the DTL logic and + 5 V for the TTL logic.

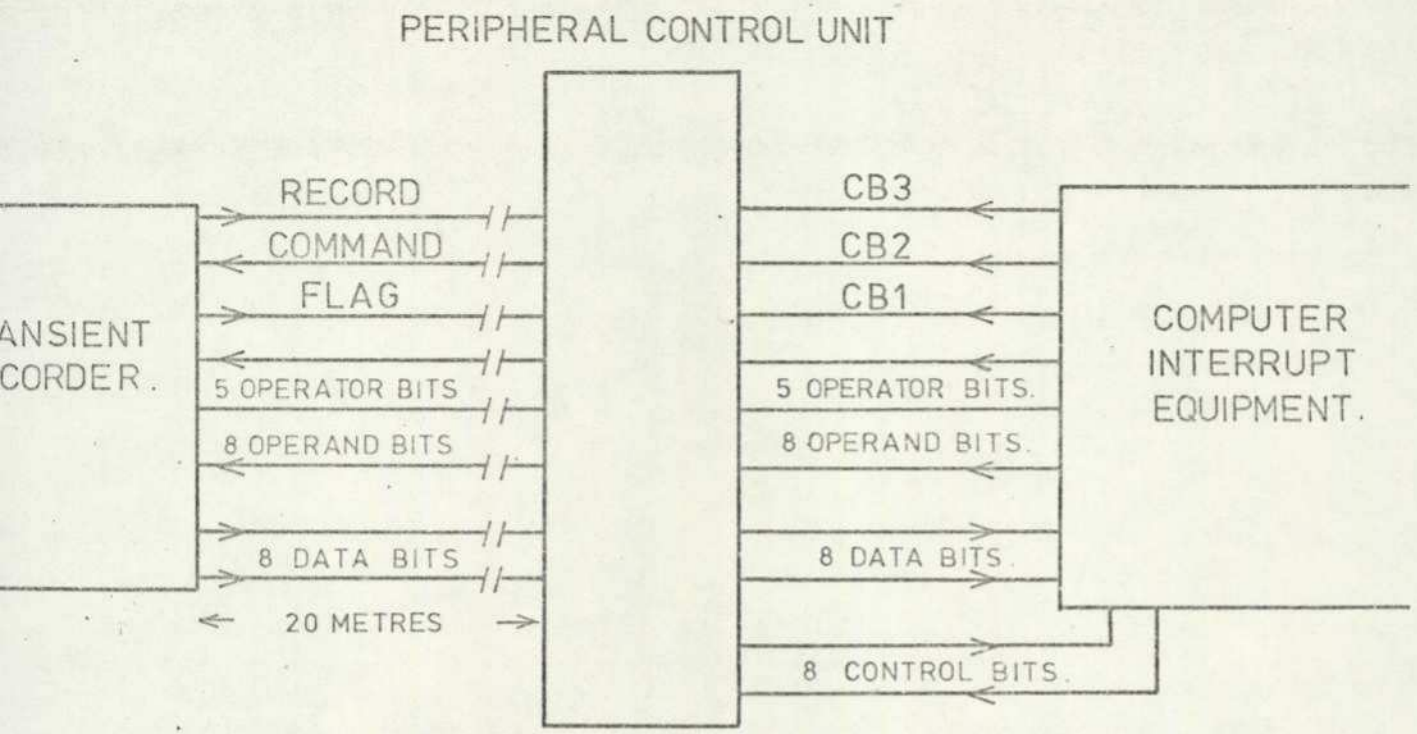
PERIPHERAL CONTROL UNIT
ANSIENT
CORDER.
RECORD
COMMAND
FLAG
5 OPERATOR BITS
8 OPERAND BITS
8 DATA BITS
20 METRES
CB3
CB2
CB1
5 OPERATOR BITS.
8 OPERAND BITS.
8 DATA BITS.
8 CONTROL BITS.
COMPUTER
INTERRUPT
EQUIPMENT.

Figure 1.

TABLE 1.

SYMBOL.	CONVENTION.	DESCRIPTION.
	Neg. Log.	Loaded OR
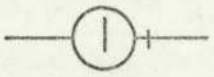	"	Un-loaded OR
	"	Power " "
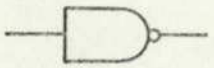	Pos. Log.	Loaded NAND
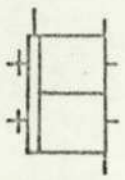	Neg. Log.	Staticizer.
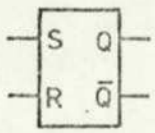	Pos. Log.	Latch.
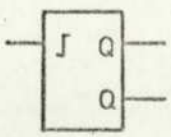	"	Monostable.

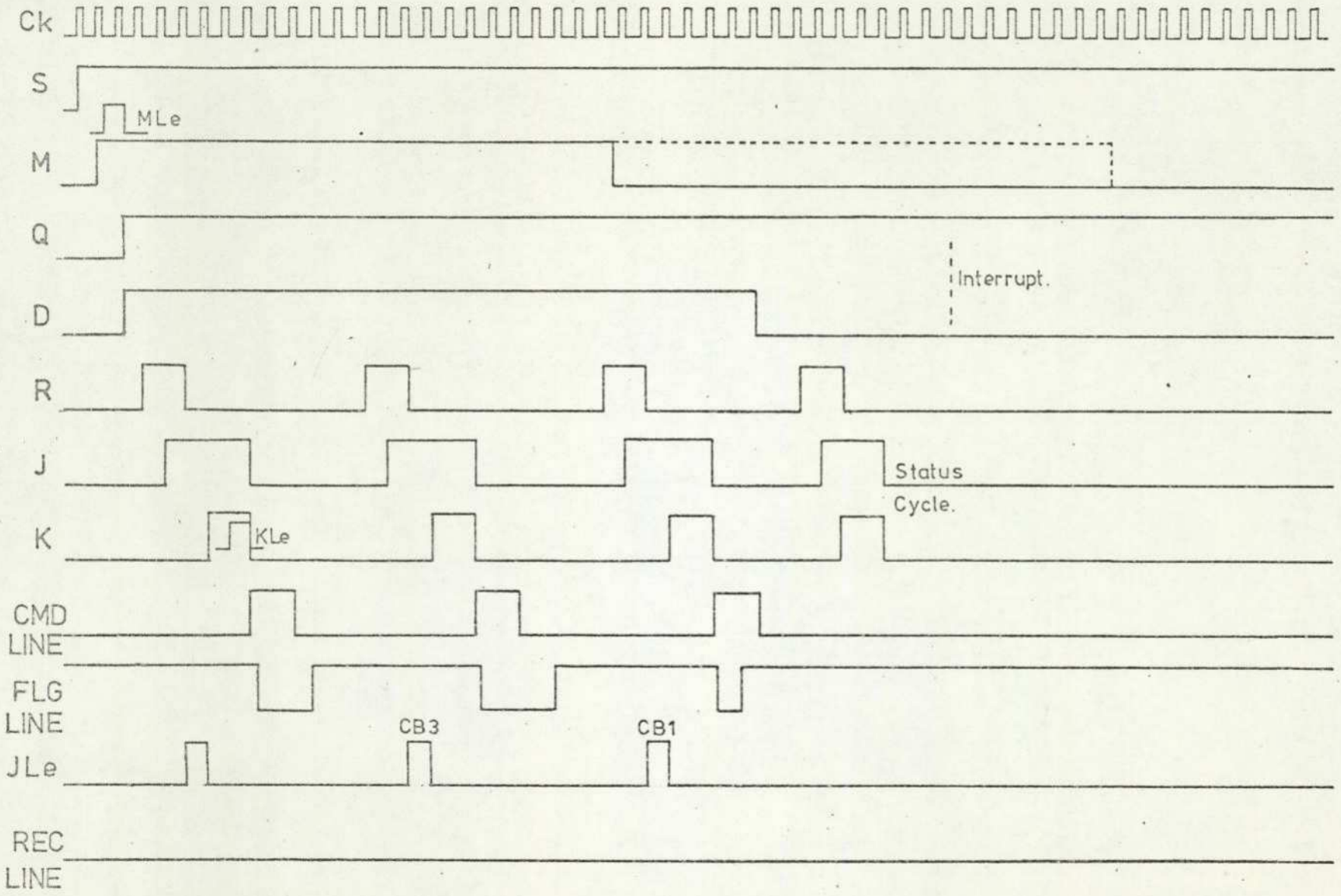
Ck
S
MLe
M
Q
Interrupt.
D
R
J
Status
Cycle.
K
KLe
CMD
LINE
FLG
LINE
CB3
CB1
JLe
REC
LINE

Fig. 2b

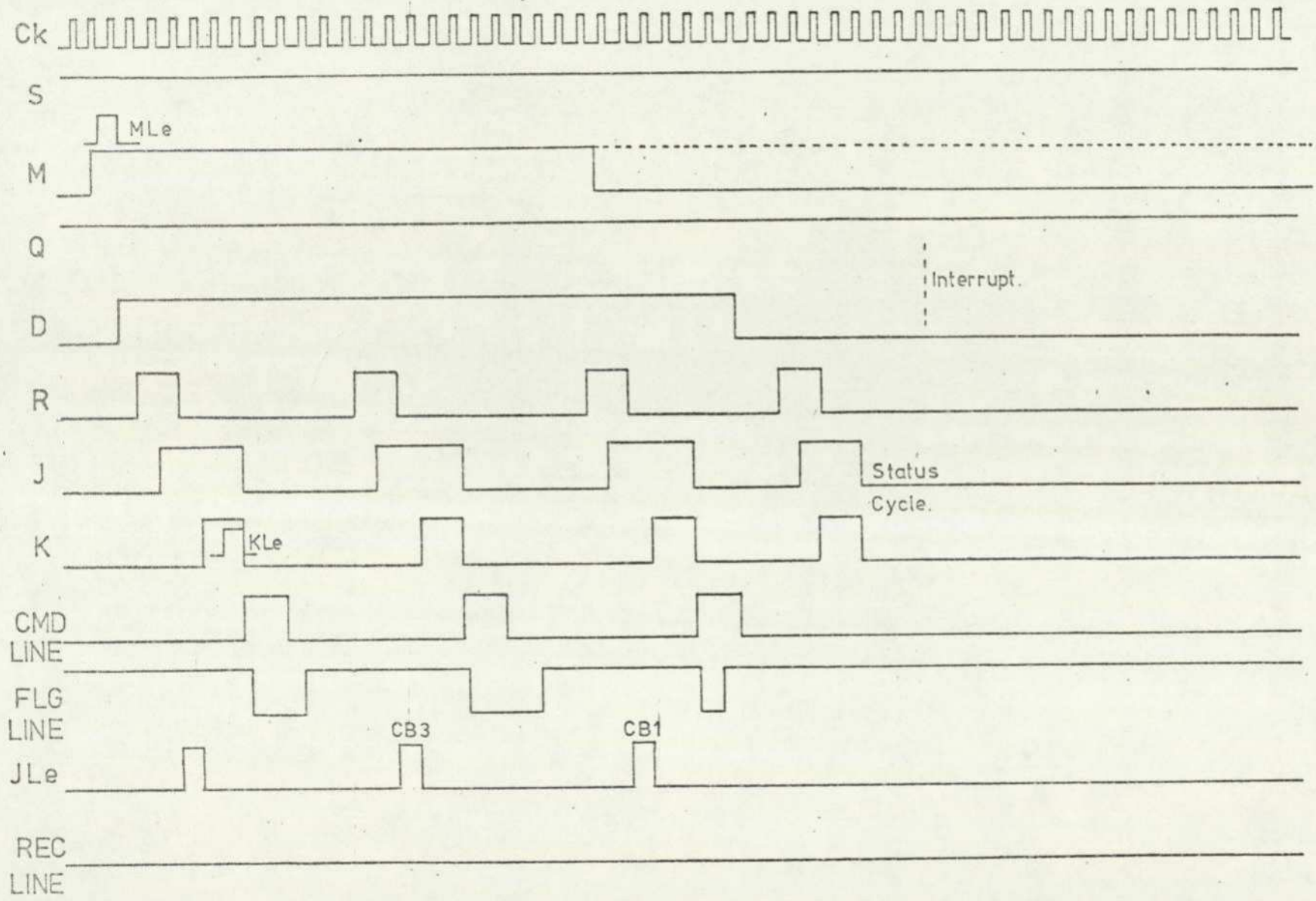
Ck
S
MLe
M
Q
Interrupt.
D
R
J
Status
Cycle.
K
KLe
CMD
LINE
FLG
LINE
CB3
CB1
JLe
REC
LINE

Fig. 2b.

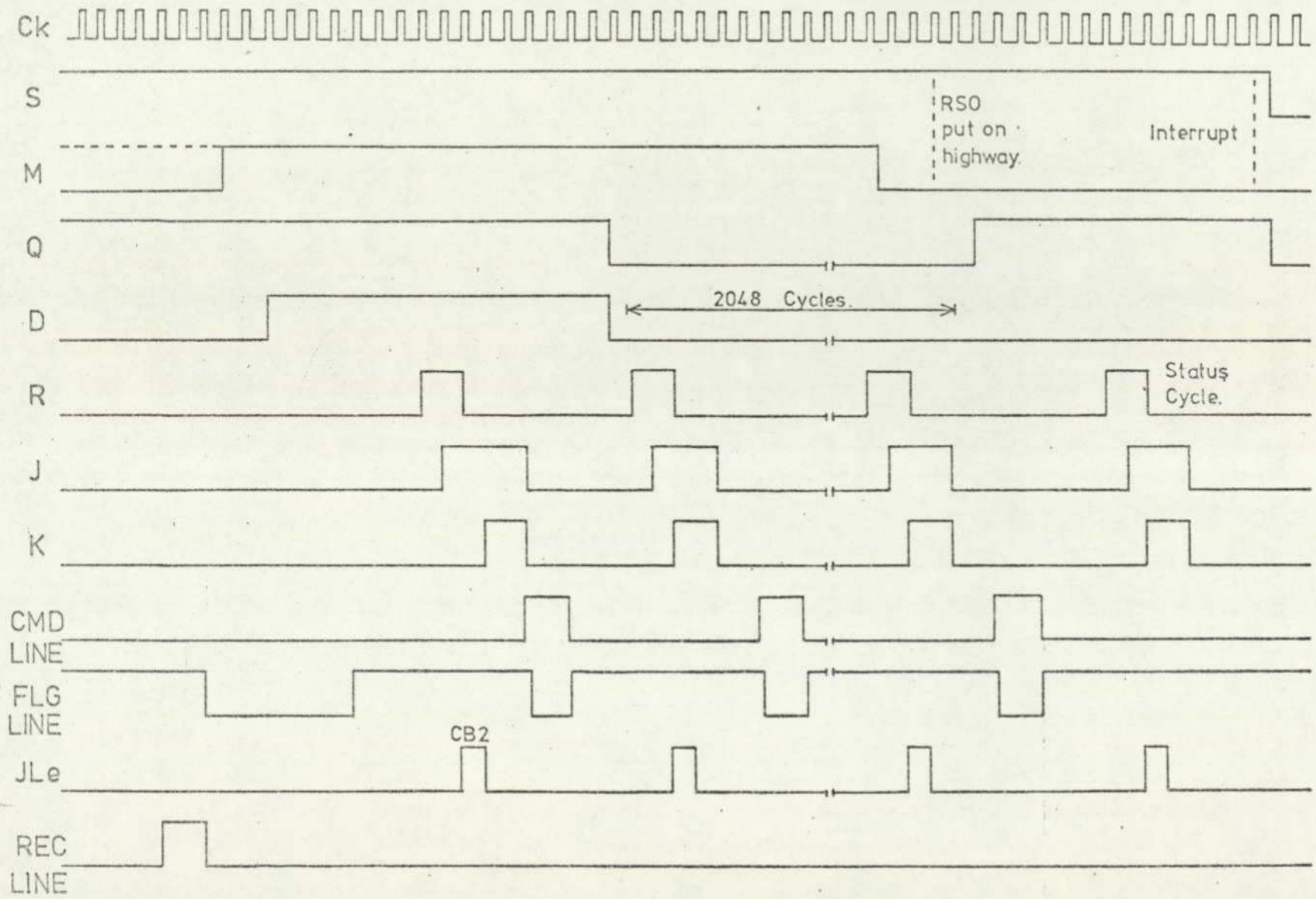
Ck
S
M
Q
D
R
J
K
CMD LINE
FLG LINE
JLe
REC LINE
RSO put on highway.
Interrupt
2048 Cycles.
Status Cycle.
CB2

Fig. 2c

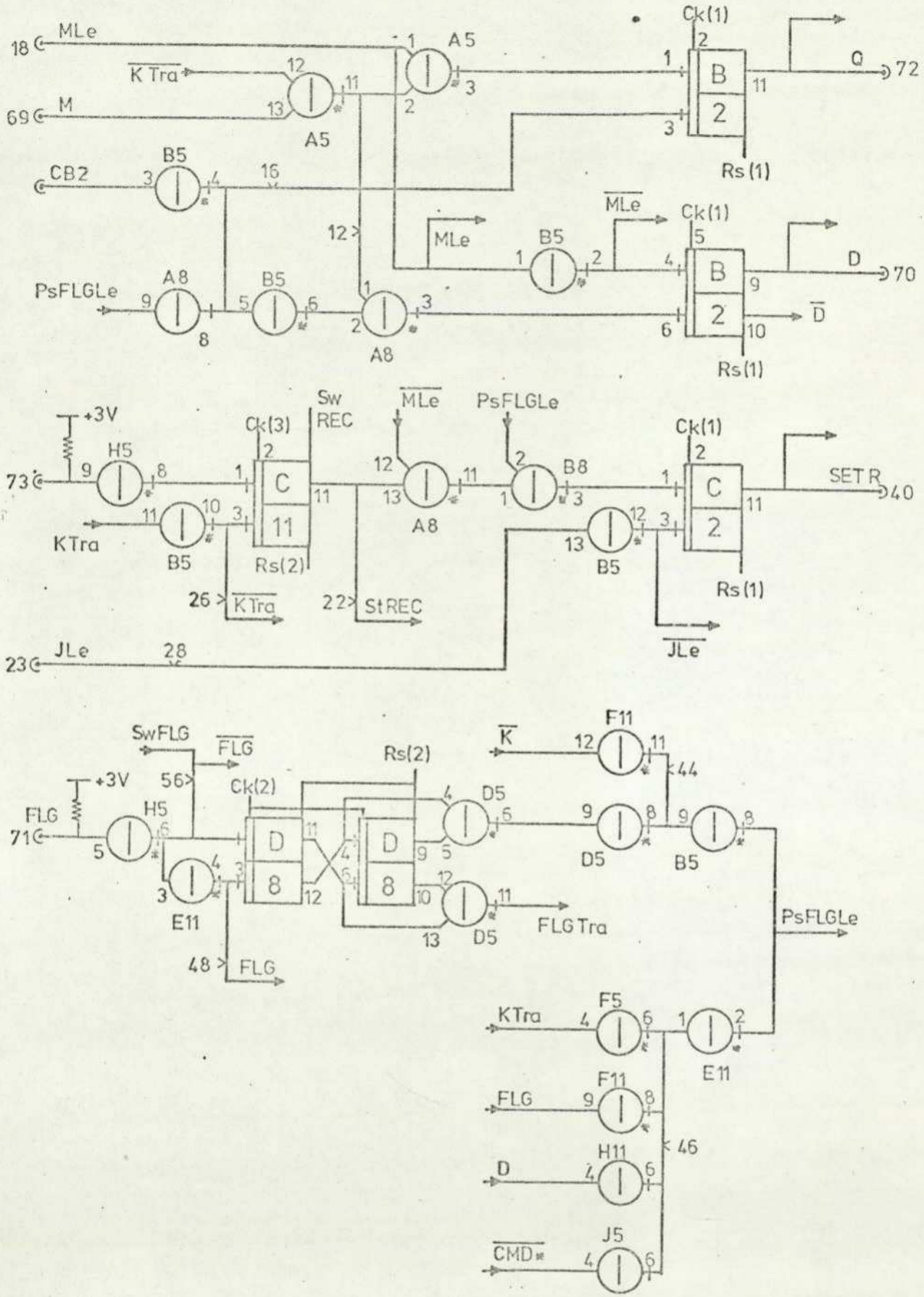
MLe
K Tra
M
A5
CB2
B5
PsFLGLe
A8
Ck(1)
B
2
Rs(1)
Q
72
D
70
Ck(3)
Sw REC
H5
+3V
73
KTra
Rs(2)
26
22
StREC
JLe
23
28
SwFLG
FLG
56
Ck(2)
D
8
E11
48
D5
FLG Tra
F11
K
44
F5
H11
D
J5
CMD
46

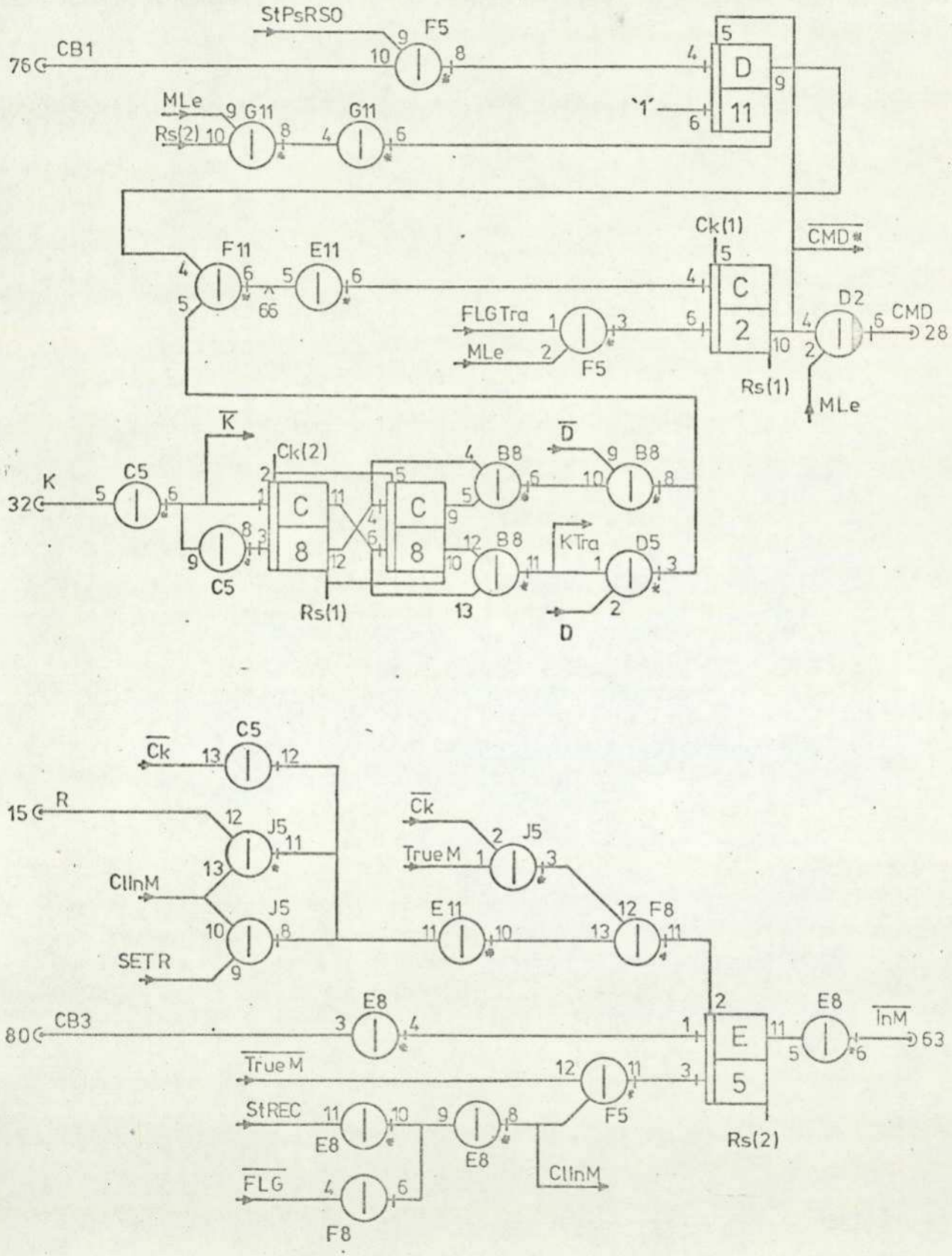
StPsRSO
F5
CB1
76
MLe
G11
Rs(2)
G11
'1'
D
11
F11
E11
66
Ck(1)
CMD
C
2
FLGTra
MLe
F5
D2
CMD
28
Rs(1)
MLe
K
32
C5
C
8
Ck(2)
B8
B8
KTra
D5
C5
Rs(1)
13
D
C5
Ck
R
15
J5
ClinM
J5
SETR
Ck
TrueM
J5
E11
F8
E8
CB3
80
TrueM
StREC
E8
E8
F5
E
5
E8
InM
63
Rs(2)
FLG
F8
ClinM

Fig. 3b

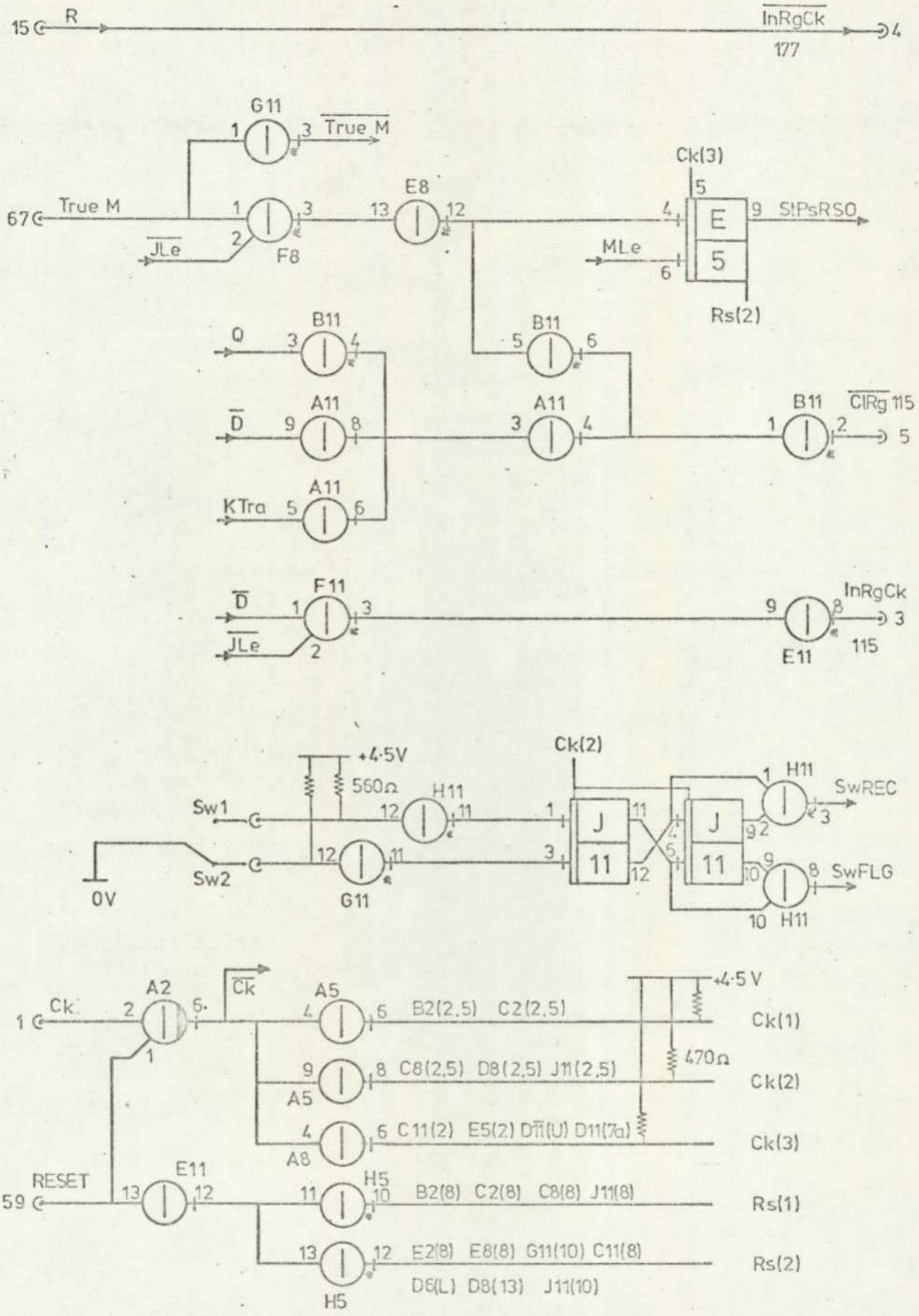
15 R
InRgCk
177
4
G11
True M
67 True M
JLe
F8
E8
Ck(3)
E
5
StPsRSO
MLe
Rs(2)
B11
Q
A11
D
KTra
CIRg 115
5
F11
InRgCk
E11
115
+4·5V
560Ω
Sw1
Sw2
0V
Ck(2)
H11
SwREC
SwFLG
J
11
Ck
A2
A5
A8
RESET
E11
H5
B2(2,5) C2(2,5)
C8(2,5) D8(2,5) J11(2,5)
C11(2) E5(2) D11(U) D11(7a)
B2(8) C2(8) C8(8) J11(8)
E2(8) E8(8) G11(10) C11(8)
D6(L) D8(13) J11(10)
470Ω
Ck(1)
Ck(2)
Ck(3)
Rs(1)
Rs(2)

Fig. 3c

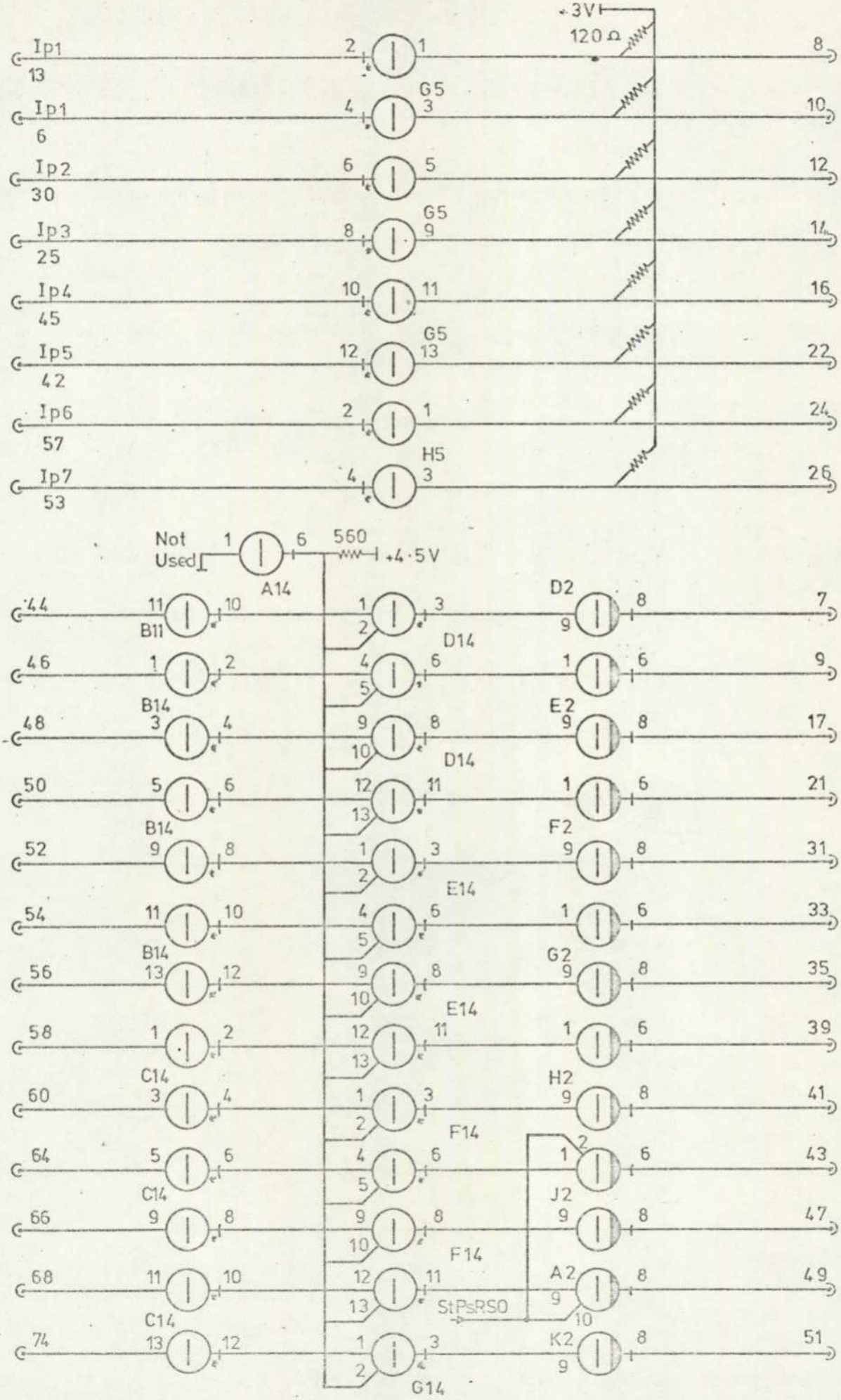
+3V
120Ω
Ip1
13
Ip1
6
Ip2
30
Ip3
25
Ip4
45
Ip5
42
Ip6
57
Ip7
53
G5
G5
G5
H5
Not
Used
560
+4·5V
A14
B11
B14
B14
B14
C14
C14
C14
D14
D14
E14
E14
F14
F14
G14
D2
E2
F2
G2
H2
J2
A2
K2
StPsRSO

Fig. 34

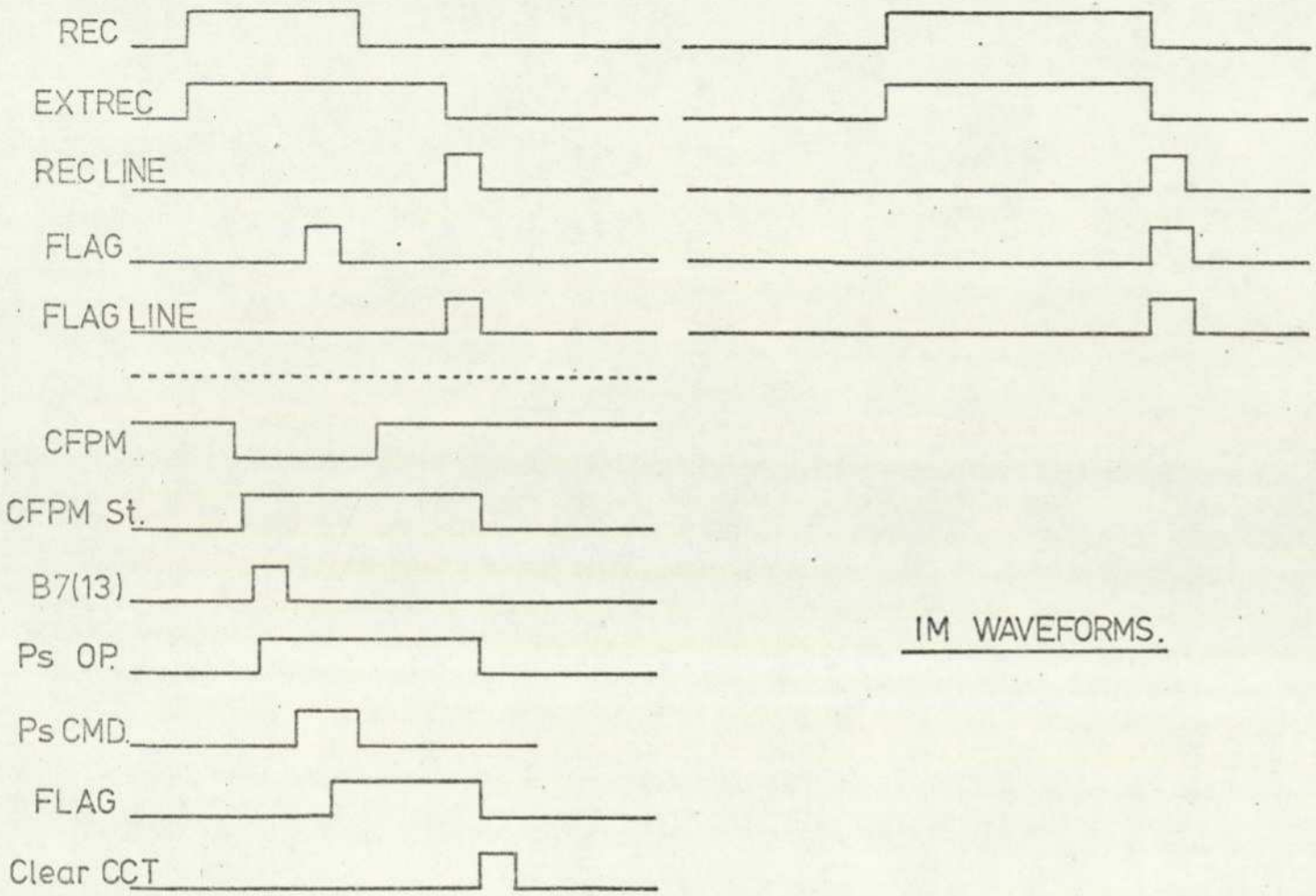

IM WAVEFORMS.

Figure 4.

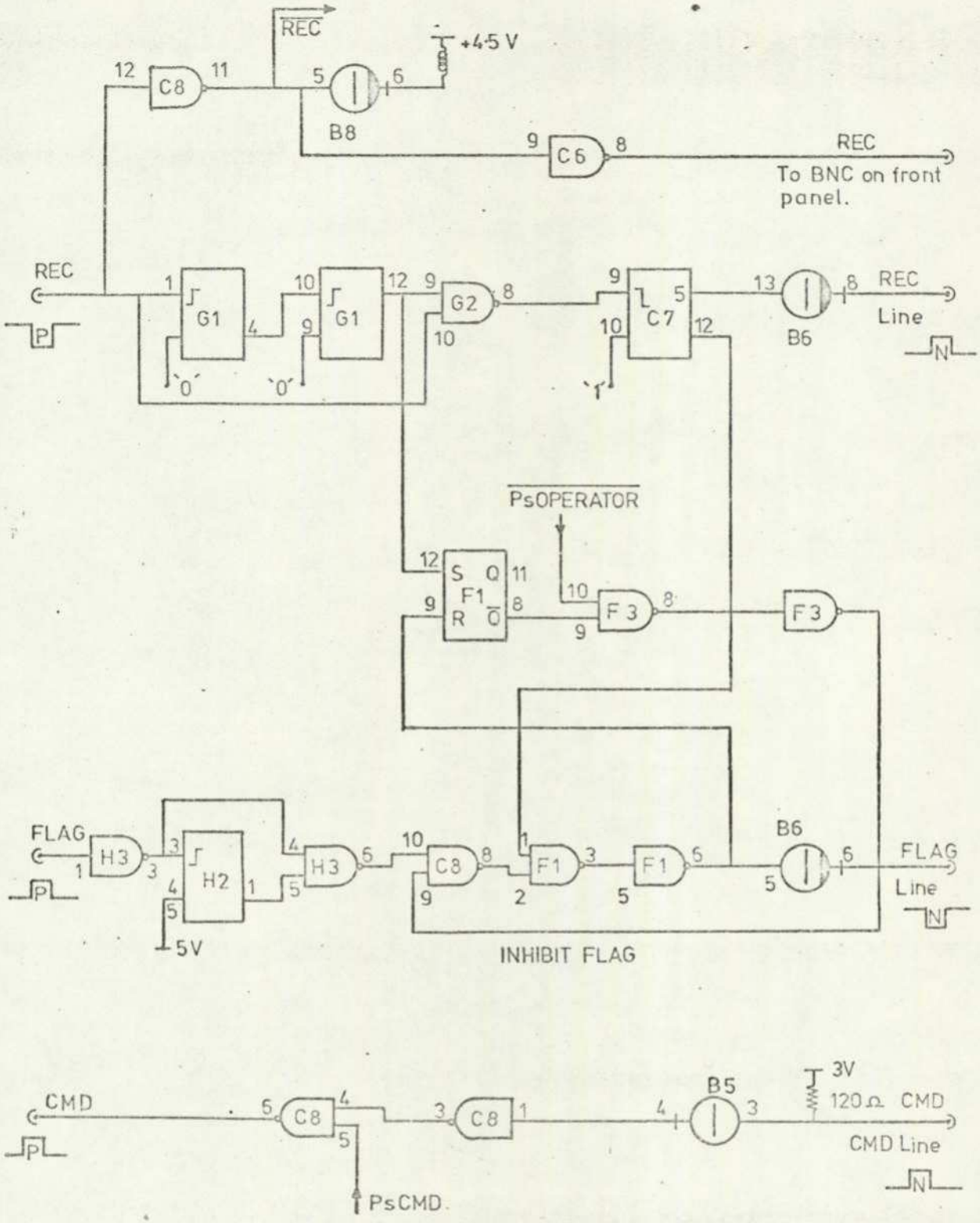
REC
+4·5 V
C8
B8
C6
REC
To BNC on front panel.
REC
G1
G1
G2
C7
B6
REC
Line
P
N
'0'
'0'
'1'
PsOPERATOR
S Q
F1
R Q̄
F3
F3
FLAG
H3
H2
H3
C8
F1
F1
B6
FLAG
Line
P
N
5V
INHIBIT FLAG
CMD
C8
C8
B5
3V
120Ω CMD
CMD Line
P
N
PsCMD

Fig. 5a

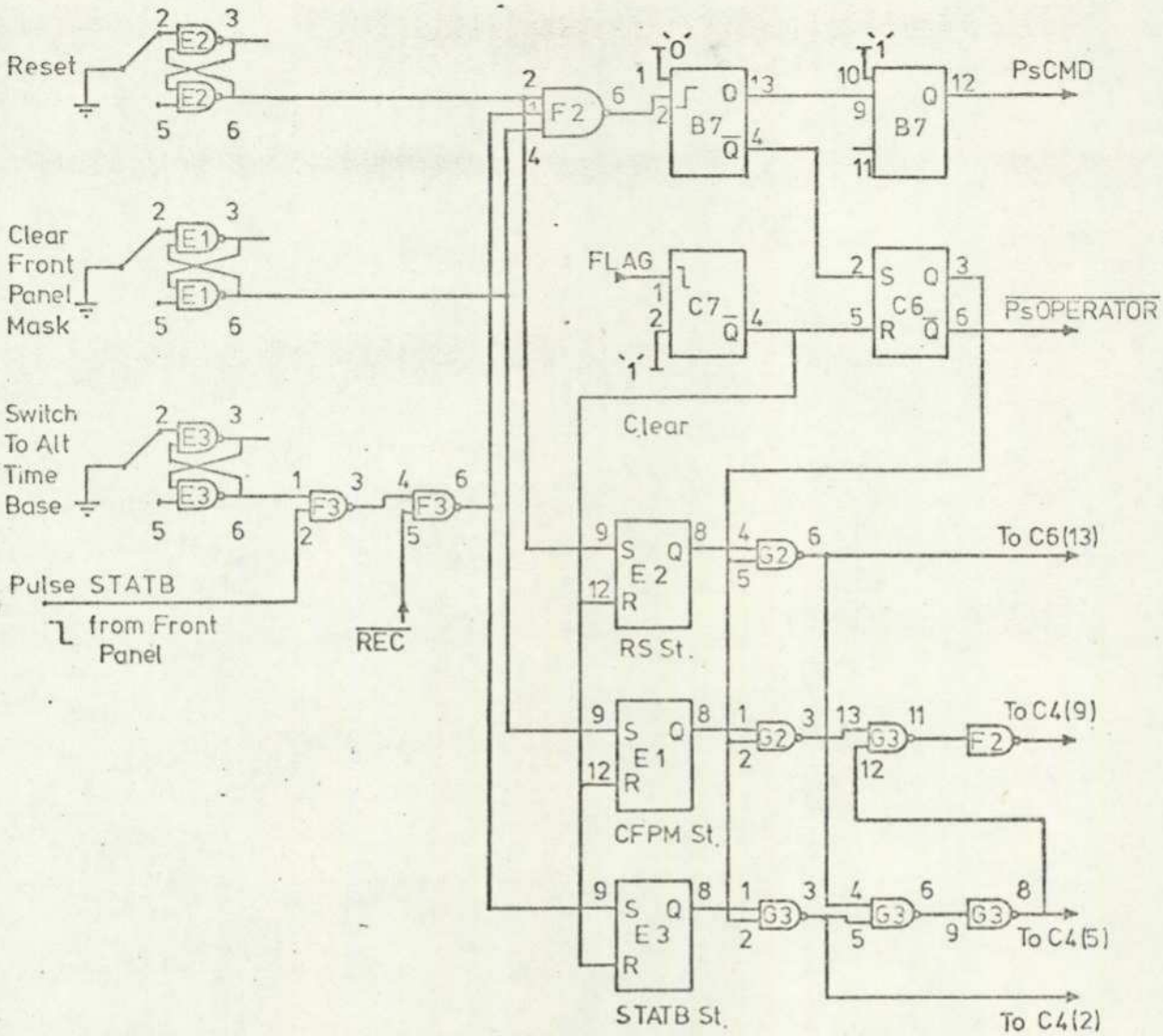
Reset
Clear Front Panel Mask
Switch To Alt Time Base
Pulse STATB
from Front Panel
REC
E2
E1
E3
F2
F3
B7
C7
C6
FLAG
Clear
PsCMD
PsOPERATOR
S Q
E 2
R
RS St.
E 1
CFPM St.
E 3
STATB St.
G2
G3
To C6(13)
To C4(9)
To C4(5)
To C4(2)

Fig. 5b

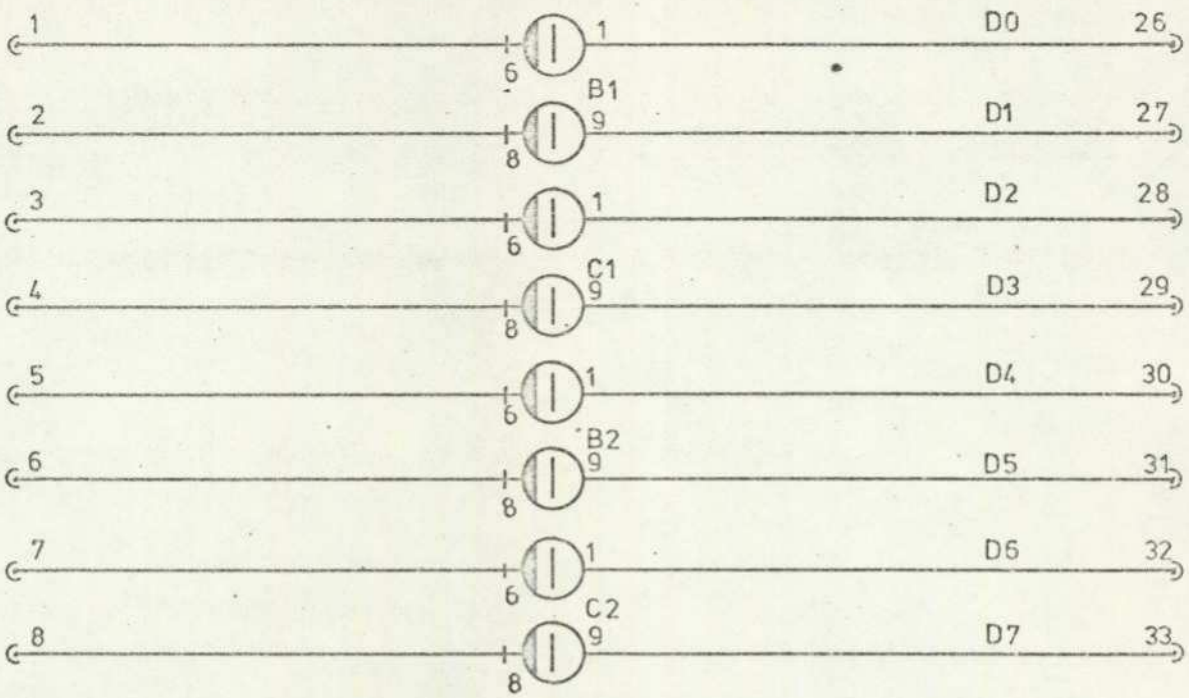
1
2
3
4
5
6
7
8
B1
B2
C1
C2
D0
D1
D2
D3
D4
D5
D6
D7
26
27
28
29
30
31
32
33

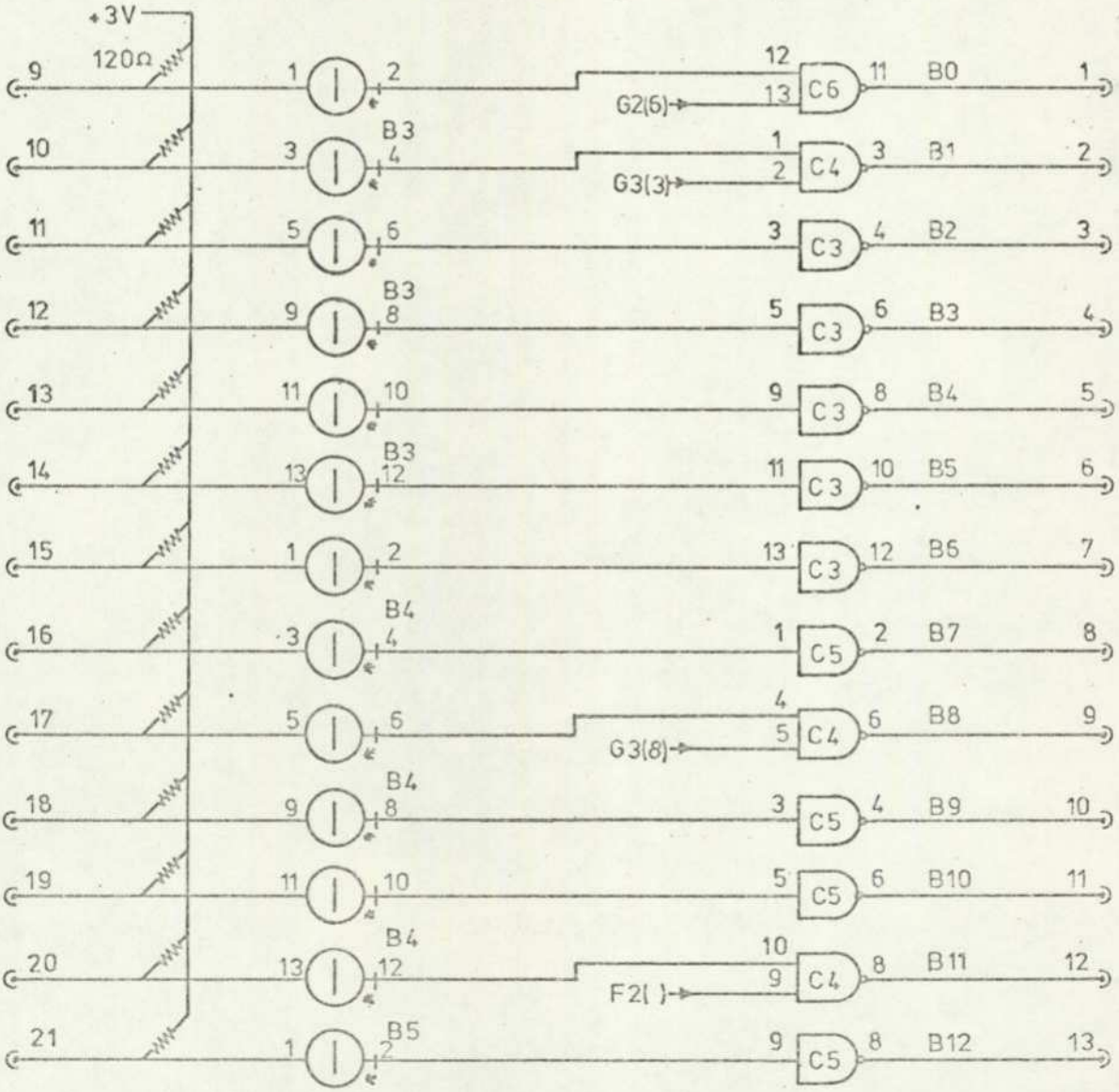
+3V
120Ω
B3
B4
B5
G2(6)
G3(3)
G3(8)
F2( )
C6
C4
C3
C5
B0
B1
B2
B3
B4
B5
B6
B7
B8
B9
B10
B11
B12

Fig. 5c

APPENDIX III

A User Guide to the Pattern Recognition Programs and Disc Handling associated with the On-line Transient Recorder. C.J. Buffam.

This document is divided into two sections. The first describes the organizing of transient waveforms on the disc via the Magtape Simulator Control Program (see the User Guide to the Magtape Simulator Control Program CJB). The second part deals with the Pattern Recognition Control Program.

The storing of transients on the disc

Transient waveforms are stored one to a 1000 word (each containing 24 bits) magtape block. The transient is packed 3 bytes to a word along with information such as the front panel settings of the transient recorder, status (i.e. input channel overflow information) and other user parameters. A total of 2000 blocks can be stored on a disc pack, provided the file allocation limit in the operating system is increased from 50% of the disc surface to approximately 90%. Transients are stored in file 4.

A map is held in file 3 and contains a two word entry for every transient (magtape block) on file 4. This map is in the form of 5 pages, each 1000 words long (once again a magtape block). The format of the entries in the map is shown in Fig. 1.

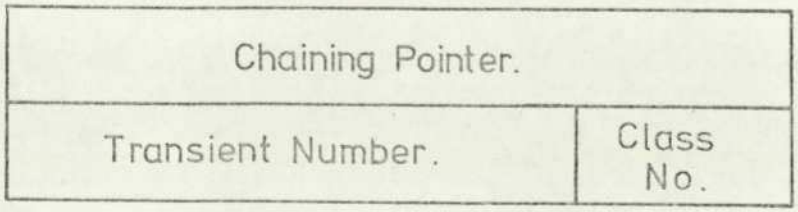

Figure. 1.

The first word contains the Class Number of the transient (in the associated block in file 4) in the lower 5 bits and the Transient Number (Tr. No.) in the top 19 bits. This is a number assigned to a transient, at capture time, by the user and is his reference to a particular waveform. The second word of the pair is a chaining pointer to the next transient captured (this may not always be in the next map entry; see section on chaining). The first two words of page 0 of the map (entry + 0) refer to the transient in block 0 on file 4, the second two words (entry + 1) refer to the transient in block 1 etc. From this point transients will be referred to by their block position i.e. Block Number (Bk. No.). Details of conversions between Bk. No. and Tr. No. are given later. Fig. 2 shows the layout of 3 transients on file 4 with their map entries on file 3.

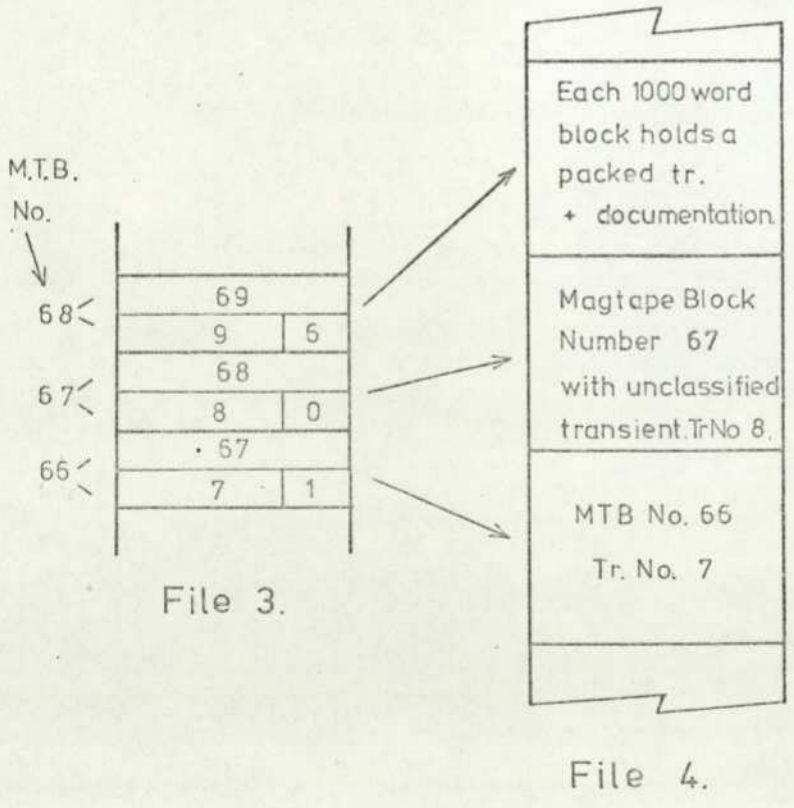

Figure 2.

Several subroutines control the passage of transients to and from the disc and the specification and use of these are given on the following pages. As a precaution against loss of filed data, due to failure to LOGOUT of the operating system, file 4 should be loaded with 2000 blank blocks each 1000 words long and file 2 with 2000 blocks, 34 words long, used to store the Match Factors (see section 2). File 3 is initialized by subroutine S4567 entry + 0 which sets all the Class Numbers in the map to 31 (i.e. block vacant) and loads the chaining pointers.

Data subroutine S4565 holds parameters pertaining to the map and the storing of transients. The entries in this data area are defined below.

+ 0	HIGHEST BLOCK NUMBER HOLDING A TRANSIENT
+ 1	NUMBER OF PAGES IN MAP (5 at present)
+ 2	NEXT BLOCK NUMBER IN CHAIN
+ 3	NEXT BLOCK NUMBER IN SAME CLASS AS CURRENT TRANSIENT
+ 4	NUMBER OF TRANSIENTS DELETED
+ 5	FIRST FREE BLOCK NO.
+ 6	-
+ 7	LAST STATUS WORD
+ 8	-
+ 9	TOTAL NUMBER OF WAVEFORMS STORED

Note: On entering a program that has just been loaded, the user must load S4546 with the parameters relating to the information stored on files 3 and 4.

S4566 Write transient to disc and unpack on return.

Entry + 0. This loads a transient (start address in N2 and Tr. No. in V21) to the first free block in file 4. This subroutine uses S4707,0 to pack the transient and loads the documentation with each waveform. The first two words of S4475 are copied to disc for user information. The assembled data is written to disc via S4554,6.

Entry + 1 of S4566 can be used to unpack a transient (start address in N2). It does not perform the read operation as this can take several forms which are controlled by S4554.

S4554 Transient Handling Program.

Entry Point + 0. This entry converts the Block Number of the transient in block V21 (on entry) to the associate Transient Number (held in V21 on exit). V17 holds the Class Number of the transient on exit.

Entry Point + 1. Similar to the previous entry point but converts a Tr. No. (in V21 on entry) to the associated Bk. No. (in V21 on exit) with V17 holding the Class No. (on exit).

Entry Point + 2. This reads from disc the transient in Block V21 and sets up the pointer (in S4565,2) to the next waveform. The transient is loaded into S4544 with S4545 acting as the 10 word blank data area at the front of the 2048 word transient data area.

Entry Point +3. This reads the transient in Block V21 into the data area as above but does not change the chaining pointer.

Entry Point +4. This obtains the Next Block Number from S4565,2 and reads the transient in that block into S4544. S4565,2 is then loaded with the new Next Block Number.

Entry Point +5. This entry is called by the Pattern Recognition software to load a waveform for a comparison test. The waveform is loaded into S4542 (see section 2).

Entry Point +6. This is used to load a packed transient to disc. V21 holds the number of the block into which the data is to be loaded. N1 holds the start address of the data and V16 holds the Tr. No. The program sets up the Next Vacant Block parameter in S4565 to the block pointed to by the chaining pointer held in the entry for block V21.

Note entry points +2, +3 and +4 all use S4568 to normalize the transient loaded from disc (see S4568 specification).

S4507 Pack and Unpack transients.

Entry Point +0. This entry packs a 2048 word transient (start address in N1) into the area whose start address is given by N2.

Entry Point +1. This is the complement of entry +0 and is used to unpack a transient brought down from disc. N2 holds the start address of the packed data and N1 holds the start address of the unpacked result.

Note that for both entries N1 and N2 may hold the same value.

S4564 Locate classified transients.

This subroutine is used to scan transients in one particular class.

Entry Point +0 reads to core the first transient in class V17 stored after Block Number V21. When the transient is found in the map the program scans ahead to locate the next waveform in the same class (V17) and loads the Block Number of the waveform into S4565,3.

Entry Point +1. This accesses S4565,3 to get the next block in the scanned class and reads it into store (via S4554). S4565,3 is updated in the same way as entry point +0.

S4568 Normalize waveform.

This subroutine is used to normalize a transient to a range of -0.999 to +0.999. On entry N1 holds the start address of the data and V16 holds the number of points in the waveform. On exit V14 holds the minimum value and V13 the maximum value (as a fraction of 257). When used by S4554 entries 2, 3 and 4, with the recorder front panel settings indicating dual channel operation, S4568 will be called twice at the time of capture, so that both the channel A and B waveforms become normalized with respect to their own range.
Note: the top two (or four for dual channel mode) locations of the 10 word data area in front of the transient data area store the maximum (, 9) and minimum (,8) values of the transient read to core.

The subroutines described above make extensive use of the file map. The map control subroutines are now described.

The map is stored in S4556, a 1000 word data area. The map is held in file 3 in 5 magtape blocks; each block represents 1 page of the map. The information for blocks 0 to 489 is situated in page 0 (block 0), blocks 490 to 979 are in page 1 and similarly for the remainder of the map. All references to the map (read or write) are made via S4553 which calculates in which page the entry is and reads that page into store; having previously written the page in store back to its place in file 3. Thus the map user is unaware that the map is ready in 5 sections as it appears to be 5000 contiguous words of store.

S4553 Locate page of map.

On entry V21 holds the Bk. No. to be accessed. The page containing this block is read to core (unless already present) and on exit N1 points to the first of the two word entry associated with block V21.

S4561 Load Class Number and restore page.

Entry Point +0. To assign a transient to a particular class the Class No. in the associated map entry must be updated. S4561 loads the Class No. in V17 into the map reference for block V21. The number in V17 must lie between 0 and 31 (see definitions of Class Numbers).

Entry Point +1. This restores the page of the map in core to its place in file 3. This is used after general updating of the map to ensure that the entries in the last page in store are copied to disc. Other pages will have been updated automatically as a new page is read to store. This does not apply to the Visual Recognition program S4550,3 which has its own call to S4561,1.

S4567 Map control program.

Entry Point +0. This entry point initializes the map stored in file 3. The chaining pointers are set up, all Tr. No.'s set to zero and all Class No.'s loaded with 31.

Entry point + 1. This entry is called to erase transients in class V17 and rechain all remaining waveforms. Fig. 3a shows a section of the map before class 11 waveforms have been deleted, and Fig. 3b the results of the call to S4567,1 with V17 hold + 11.

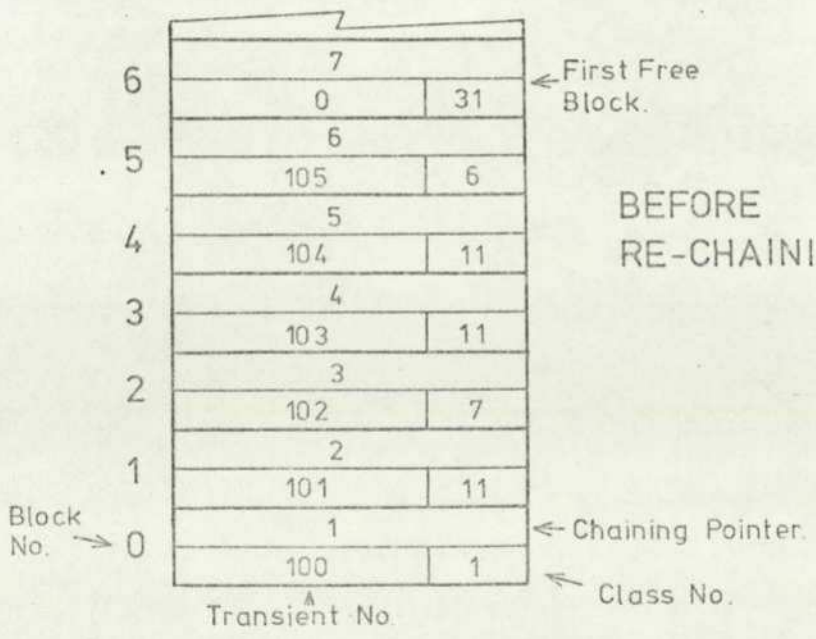

Figure 3a.

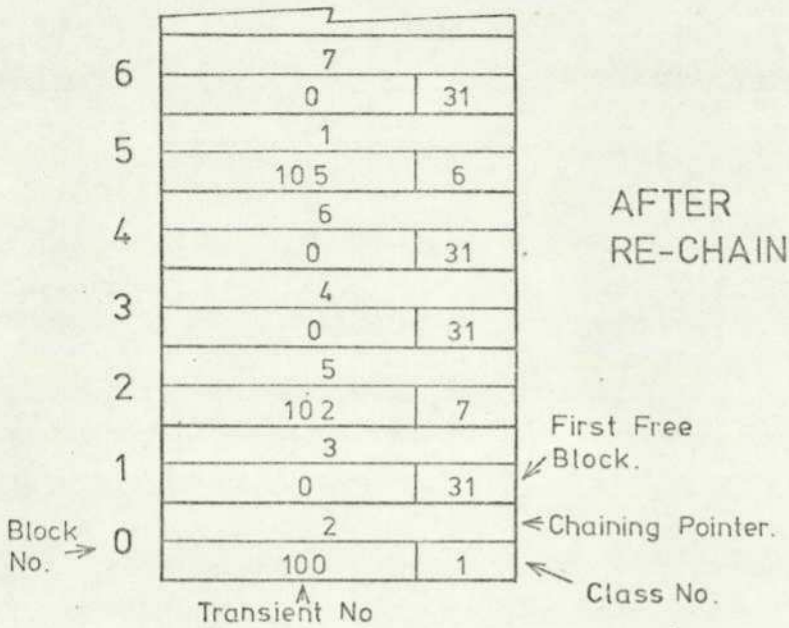

Figure 3b.

In the course of the rechaining, the First Free Block pointer in S4565 is updated along with the counts of the number of transients deleted and the total number of waveforms stored.

Pattern Recognition Control System

The Pattern Recognition system comprises a suite of programs which allow the user to define his own feature and waveform classifications. The software is really a hollow shell into which the user 'plugs in' his own subroutines or one of the standard ones to perform a particular test. The system is controlled by four data areas which are set up by the user (the specifications of these can be found later in this section).

The user can supply up to 24 subroutines which look for a particular feature in any section (or all) of a given set of waveforms. The output from the test routine must be in the form of a positive fraction (i.e. between + 0.0 and + 0.999). This fraction is called a Match Factor and is used to indicate the success of a test in recognizing a

particular feature. Thus a Match Factor of +0.999 indicates a positive match and a value of + 0.000 indicates a complete failure to locate the feature (i.e. the feature is not present at all).

The user has to define the level for the success or failure of a particular test to recognize a given feature. The Upper and Lower Decision levels are used to set the success and failure limits of a test. There are 48 decision levels, 2 for each test program.

The Match Factor can have one of three positions with respect to the two Decision Levels, these are:-

(1) the Match Factor is above the Upper and Lower Decision Levels (a match)

(2) the Match Factor is below the Upper and Lower Decision Levels (no match)

(3 the Match Factor is between the Upper and Lower Decision Levels (a Mis match).

Should the Match Factor fall between the two decision levels an uncertainty condition is defined and a Mis match is said to have occurred.

For each test, two bits are allocated to indicate which of the three conditions has resulted (i.e. Matched, Unmatched or Mis matched). The two bits are in two adjacent words (in S4558) and each pair refers to the test whose number is the same as the bit position of the two bits (i.e. test number 8 uses bit 8 in both S4558 +0 and +1). The bits in the first word of S4558 are set to indicate a matched result and clear for an unmatched result. The bits in the second word of S4588 are set to indicate an uncertainty in a result (i.e. a Mis match).

When the tests on a waveform are complete, providing no uncertainty bits are set, then the bit pattern in word +0 of S4558 is compared with the 10 bit patterns in the Class Definition Table S4557. The bit pattern in word +0 of S4557 defines Class Number 1's characteristics and in word +1, Class Number 2's features. If a match is not made the waveform is considered rubbish and placed in Class Number 11.

The table below defines the allocation of Class Numbers.

CLASS NO.	DEFINITION.
0	Unclassified (or Missmatched)
1 ⋮ 10	User defined
11	Rubbish
12 ⋮ 30	Comparison waveforms
31	Indication of a vacant Block

For any of the 24 tests the user may specify one waveform with which the data under test can be compared (e.g. by a least mean square difference test). This is done with the aid of the fourth data area which can be loaded with the block number of the comparison waveform; this waveform will have a Class Number between 12 and 30 in the map.

The specifications of the Pattern Recognition programs are given below.

S4550 Pattern Recognition Control Program

Entry Point +0. A call to this entry allows the user to find the best value for the Upper Decision Level, for a given class of waveform. The entry is given the Bk.No. of the first transient to be tested in V21, V22 holds the number of waveforms to be scanned, V18 holds the test number and V17 holds the Class No.

Thus the Visual Recognition (see entry +3) can be used to place several transients into a particular class and an estimate of the Upper Decision Level, necessary to recognize all the given waveforms as belonging to the given class, can be obtained using entry +0. The resulting estimate is stored in S4563, which holds the 48 decision levels.

Entry Point +1. This is the main entry point for pattern recognition. A parameter is passed in V13 to the subroutine and defines the modes of operation. The four possible modes are:-

1	V13=0	Normal pattern recognition.
2	V13[0]#0	Classification mode.
3	V13[1]#0	Real time pattern recognition.
4	V13[2]#0	Re-classify using Match Factors.

Normal mode (V13=0)

This operates in the non real time mode. The program reads a transient from disc (V21 holds Bk.No. of waveform on entry) and performs all the required tests and compares the Match Factors with the Decision Levels to obtain the Classification word. The Classification word is then compared with the Class list and the resulting class is loaded into the transient map entry for block V21. If an uncertainty bit is set then the waveform is put into Class 0.

Classification mode (V13[0]#0, V13=1)

This entry can be used to test the classification words given all the test subroutines and the waveform to be recognised. Alterations of the Decision Level values may be necessary to avoid uncertainties occurring.

Real time Pattern Recognition (V13[1]#0, V13=2)

Under certain conditions when the percentage of useful to useless data is small this entry can be used as a course filter, governing waveshapes transferred to disc. On exit, V17 holds the Class Number of the waveform. The user may then decide whether or not to write the waveform to disc.

Re-classify using Match Factors (V13[2]#0, V13=4)

This is used after all the normal mode tests have been made and the Match Factor blocks (each comprising up to 24 Match Factors) are stored in file 2 (see paragraph on Match Factors). The program uses the Match Factors stored on file 2 to assign the waveforms to their classes depending on the Decision Levels. Thus a change to a particular Decision Level does not require a complete re-run of the normal mode

entry.

Entry Point +3. This is the entry point for Visual Pattern Recognition. The program scans a given class of transients (Class No. in V17) and displays each waveform, on the VDU, so that the user may decide on the appropriate Class No. V21 holds the Block No. of the first transient to be viewed (the program locates the first transient in Class V17 after this if the Class No. is not the required one). V22 is loaded with the number of transients to be scanned. The Tr.No. of the waveform displayed on the VDU is output on stream 4 along with a request for the new Class Number, input on stream 5. The map is updated on exit from the subroutine.

S4562 Match Factor Data Area

This is arranged to work with the Magtape Simulator Control Program to write blocks of Match Factors (up to 24 for each waveform) to file 2; the first 10 words of this subroutine are thus left blank. The 24 Match Factors are located from word +10 to word +33 for tests 0 to 23 respectively. Match Factors read from disc by entry +1 of S4550 also use this data area.

The following four data areas are loaded by the user to drive the Pattern Recognition System: S4555, S4557, S4559 and S4563.

S4555 Comparison waveform data.

This 24 word blank data area is used to hold the block numbers for any of the 24 tests. Thus word +0 holds the comparison waveform required for test 0 etc. If no comparison waveform is needed for a test then the entry should be loaded with -1. S4554,5 is used to read the comparison waveform from disc by checking the comparison waveform data area.

S4557 Classification list.

This is a 10 word subroutine which is loaded with the classification

bit pattern that allows up to 24 different features to be defined and which place a waveform into 1 of 12 defined classes.

S4559 Test subroutine address list.

This 24 word blank data area holds the addresses of the user supplied test subroutines. The address stored in word +0 is for test 0 and in word +1 for test 1 etc. If less than 24 tests are required then the location after the last subroutine address in the list should be loaded with -1. Note there must be no blank words in the list before the terminating entry.

S4563 Decision Level data area.

This data area holds the 48 Decision Levels, two for each test. Words +0 and +1 hold the Upper and Lower Decision Levels for test 0; the following 23 pairs are stored consecutively. Subroutine S4552 compares the Match Factors with the Decision Levels and passes the result back to S4550.

The four subroutines described above must be loaded by the user before the Pattern Recognition is used although the Upper Decision Level can be estimated by using S4550,0.

There are several subroutines available which measure or compare various features in transient waveforms. Some of these subroutines are described below.

S4450 Compare waveforms using a Mean Square Difference Test.
This program compares the transient under test (in S4544) with a comparison waveform (in S4542) using a mean square difference test. On entry, V22 holds the number of points in the waveform. On exit, V16 holds the Match Factor which represents the 'distance' (or similarities) between the two waveforms.

S4451 Find the Number of zero crossings.
This subroutine scans the normalized waveform (V22 holds the number of points) in S4544 and counts the number of times the waveform passes through the zero level. The value obtained is compared with a number loaded in an

internal data area (entry point +31) and a high Match Factor is given if the two numbers are equal. A modified version of this program is planned in which the resulting Match Factor is a measure of the difference between the number of zero crossings measured and a number passed to the routine in a register.

APPENDIX IV

MACHINE CODE ('FIDS') EDITOR

The following commands are recognised by the editor.

Command	Meaning
M	Monitor a single location
MB	Monitor a block
C	Correct a single location
CB	Correct a block
LB	Load a block
L	Locate an instruction
MSK	Set locate instruction mask
LMK	Locate with instruction mask
MR	Monitor repeat
MBR	Monitor block repeat
CR	Correct repeat
CBR	Correct block repeat
LBR	Load block repeat
DTF	Convert decimal to FIDS A B C
FTD	Convert FIDS A B C to decimal
IBP	Insert breakpoint
DBP	Delete breakpoint
ZBPC	Zero breakpoint count
IBPR	Insert breakpoint repeat

These commands and their use is explained in further detail below. All commands are terminated by a newline. Entry to the editor dictionary is denoted by the text <EDIT CMD> Output on stream 4. Note that the output from monitor or monitor block is output on stream 6. In the following examples the user input has been underlined.

M Monitor a single location

```
EDIT CMD.
M
 ADDRESS 512  0110  19 0 4
EDIT CMD.
```

MB Monitor a block of code

```
EDIT CMD   .
MB
  START ADDRESS 512  LENGTH  4
512  0110 19 0 4
513  0110 20 12 0
514  0110 23 0 0
515  7000 10 0 0  10240      (Decimal of jump address)
EDIT CMD.
```

C Correct a single location

```
EDIT CMD.
C
 ADDRESS 512  TO  0110 19 0 6
EDIT CMD.
```

CB Correct a block of code

```
EDIT CMD.
CB
  START ADDRESS 516 LENGTH 2
516 0203 0 0 28
517 0000 5 8 23
EDIT CMD.
```

LB Load a block with one machine code instruction

```
EDIT CMD.
LB
  START ADDRESS 4096 END ADDRESS 5100
WITH FIDS 7317 31 31 31
EDIT CMD.
```

L Locate a machine code instruction

```
EDIT CMD.
L
INSTRUCTION 0116 21 12 2 BETWEEN WORD 512 AND WORD 2000

 LOCATED AT 560
     AND AT 700
     AND AT 1861
 EDIT CMD.
```

MSK Set up octal mask pattern for locate with mask

```
EDIT CMD.
MSK
 OCT01000037
EDIT CMD.
```

LMK Locate a machine code instruction with mask

This command masks the input instruction and each location of core scanned before making the comparison test.

```
EDIT CMD.
LMK
INSTRUCTION 0010 2 0 28 BETWEEN WORD 769 AND WORD 800

LOCATED AT 782
    AND AT 790
EDIT CMD.
```

NOTE: The 2 in the A field will be ignored in the comparison test.

Certain of the commands recognised by the FIDS editor do not require an address parameter (such commands end in 'R') but use the last address parameter entered.

MR Monitor repeat

```
EDIT CMD.
MR
  0203 0 0 28
EDIT CMD.
```

In this example the last address entered was 516 in the earlier CB example.

CR Correct repeat

```
EDIT CMD.
CR
  TO  0103 0 0 28
EDIT CMD.
```

MBR Monitor block repeat

```
EDIT CMD.
MBR
   LENGTH 3
516  0103  0  0  28
517  0000  5  8  23  5399
518  7212 21 21   8
EDIT CMD.
```

CBR Correct block repeat

This functions in a similar way to CB but with the repeat address used as the start address of the block to be corrected. Only the length of the block has to be entered.

LBR Load block repeat

This is the same as LB but only the END ADDRESS need be entered.

DTF Convert decimal to FIDS A B C

```
EDIT CMD.
DTF
514  0000 0 16 2
EDIT CMD.
```

FTD Converts FIDS A B C to decimal

Converse of DTF.

IBP Insert breakpoint

This allows a breakpoint to be inserted and designated.

```
EDIT CMD.
IBP
   ADDRESS  657  B/P  NO.  = 8  B/P TYPE ? E
INSERTED
EDIT CMD.
```

DBP Delete breakpoint

Deletes a previously inserted breakpoint.

```
EDIT CMD.
DBP
   B/P NO. = 8
DELETED
EDIT CMD.
```

ZBPC Zero break point count

Refer to the User Guide to Breakpoints by R. Young.

IBPR Insert breakpoint with repeat address

This is used to insert a breakpoint just after a location has been monitored.

```
EDIT CMD.
M
 ADDRESS  514  0110 23 0 0
EDIT CMD.
IBPR
 B/P NO. = 2  B/P TYPE ? E
INSERTED
EDIT CMD.
```

It is possible to monitor kernels 0 to 23 location 24 when monitored gives the state of the SCM software handswitches. Locations 27 & 28 can not be monitored. Locations 25, 26, 29, 30 and 31 may all be monitored.

NOTE. No locations between 0 and 31 inclusive may be monitored by the editor when it is called from a break-point.

Storage and Subroutine Requirements

A list of the subroutines which form CUPIDS (a combination of the FIDS Editor and Breakpoint programmes) are shown below:

S1020	44
S1021	94
S5814	586
S5815	50
S10050	346
S10051	64
S10052	128
S10053	380
S10054	32
Total	1724 words

It also calls the following standard subroutines

S1
S12
S15
S32
S100
S555

CUPIDS uses the SC Interface for all input/output operations.

CUPIDS is entered via a call to S5814.

Colin J. Buffam,
4th May 1976